TECHNISCHE UNIVERSITÄT MÜNCHEN
Integrative Research Center Campus Straubing für Biotechnologie und Nachhaltigkeit

Biotransformation of camphor-derivatives for the synthesis of bio-based polymers

Steffen Roth

Vollständiger Abdruck der von der promotionsführenden Einrichtung Campus Straubing für Biotechnologie und Nachhaltigkeit der Technischen Universität München zur Erlangung des akademischen Grades eines

Doktors der Naturwissenschaften (Dr. rer. nat.)

genehmigten Dissertation.

Vorsitzender:	Assoc. Prof. Dr. Magnus Fröhling
Prüfer der Dissertation:	1. Prof. Dr. Volker Sieber
	2. Prof. Dr. Bastian Blombach

Die Dissertation wurde am 19.07.2019 bei der Technischen Universität München eingereicht und von der promotionsführenden Einrichtung Campus Straubing für Biotechnologie und Nachhaltigkeit am 12.11.2019 angenommen.

Danksagung

Zunächst möchte ich mich bei meinem Doktorvater Herrn Prof. Dr. Volker Sieber bedanken, der es mir erst ermöglichte, meine Dissertation in Zusammenarbeit mit dem Institutsteil Straubing des Fraunhofer IGB anfertigen zu können. Vielen Dank Volker, für die spannende Themenstellung, die stets konstruktiven Diskussionen, die schnelle Aufnahme in einen tollen Arbeitskreis, aber auch für die unkomplizierte Zusammenarbeit und die Unterstützung zu jeder Zeit in den vergangenen Jahren.

Bei Herrn Prof. Dr. Bastian Blombach möchte ich mich ganz herzlich für die Übernahme der Zweitkorrektur bedanken.

Ein großes Dankeschön gebührt auch der Deutschen Bundesstiftung Umwelt (DBU) für die finanzielle Unterstützung meiner Dissertation im Rahmen eines Promotionsstipendiums. Insbesondere möchte ich mich bei meinem Betreuer von Seiten der DBU Herrn Dr. Hans-Christian Schäfer für die warmherzige Aufnahme in die DBU-Familie bedanken. Danke Hans-Christian, für die problemlose Zusammenarbeit über den gesamten Zeitraum des Stipendiums, die fachlichen Diskussionen und dass du es mir ermöglicht hast viele neue, tolle Leute an den Stipendienseminaren kennenzulernen. Außerdem gilt mein Dank Frau Sabine Dannhauer, die mir stets bei der Bewältigung der bürokratischen Aufgaben zur Seite stand.

Mein besonderer Dank gilt Herrn Dr. Michael Hofer für die Betreuung von Seiten des Fraunhofer IGB in Straubing. Lieber Michael, danke für alles, von einem Treffen in München woraus der Antrag für die DBU entstand, die Aufnahme in eine wahnsinnig tolle und aufgeschlossene Truppe am IGB, dein stets offenes Ohr für mich, die Betreuung vor Ort und die Zeit für das Korrekturlesen der Arbeit. Michael, danke für alles!

Meinen Studenten Lisa Bechtel und Julia Rehberger danke ich für ihre Mitarbeit an meinen Forschungsprojekten.

Außerdem möchte ich mich bei allen Mitarbeitern des Arbeitskreises Sieber für die schnelle Aufnahme und die gute Zusammenarbeit bedanken. Insbesondere gilt hier mein Dank meinen Mitdoktoranden am Fraunhofer-Institut Melli, Paul und meinem Isomer Sumanth. Danke für die tolle Zusammenarbeit, eure Hilfsbereitschaft bei jeglichen Problemen und vor allem die lustigen

Zeiten in den vergangen Jahren, während aber vor allem auch neben der Arbeit. Durch euch wurden so manche schwierige Phasen eindeutig erträglicher, danke euch!

Im gleichen Maße möchte ich mich bei allen Mitarbeitern am Fraunhofer IGB in Straubing für die äußerst warmherzige Aufnahme in eine, wie schon gesagt, wahnsinnig tolle Truppe bedanken. Besonders möchte ich mich beim biologischen Abteilung bedanken: Christina, Jonathan, Julia, Melli, Michael R, und Patricia, vielen Dank für eure Hilfsbereitschaft, die sehr gute Zusammenarbeit, die vielen guten Gespräche, die gemeinsamen Mittags- und Kaffeepausen, das beste Arbeitsklima, dass ich mir vorstellen kann und vor allem auch für die Zeit neben der Arbeit. Mein Dank gilt aber auch gleichermaßen der chemischen Abteilung für die zahlreichen Diskussionen, die reibungslose Zusammenarbeit und die Suche nach dem Molekül im Tanklaster. Danke Anette, Anton, Claudia, Harald, Lenard, Leonardo, Luciana, Manuela, Marion und Tobias. Außerdem möchte ich euch, Elisabeth und Sabine, für eure Hilfe in Verwaltungsangelegenheiten, eure Zeit für mich und die tollen Gespräche danken. Aus Kollegen wurden Freunde, danke dafür!

Ein großes Dankeschön gebührt auch meinen DBU'lern Andi, Beni und Jule für die durchwegs lustige Zeit bei den Seminaren, den Blödsinn den wir miteinander erleben durften und die guten Gespräche. Wenn mich jemand fragen würde „na, wie war et?", ihr kennt meine Antwort.

Besonders möchte ich mich bei all meinen Freunden bedanken, insbesondere bei euch, Toni, Udo, und Luk. Vielen Dank, dass ihr immer für mich da seid, mich permanent unterstützt, die zahlreichen Gespräche und lustigen Stunden. Vor allem aber auch dafür, dass es nicht abreißt, obwohl die gemeinsamen Zeiten leider kürzer wurden. Danke euch!

Mein größter Dank und zwar von ganzem Herzen gilt zuletzt meiner ganzen Familie, insbesondere aber meinen Eltern, meinem Bruder und meiner Freundin. Ich weiß, es war nicht immer leicht mit mir, aber genau aus diesem Grund bin ich zutiefst dankbar für eure Liebe, euren Rückhalt, eure Motivation, eure Ermutigung und eure Rücksicht. Danke, dass ihr mir ermöglicht habt, dass ich sein kann wer ich bin und tun kann was ich will. Ohne euch wäre das hier alles nicht möglich gewesen, danke, danke, danke!

“Ex nihilo nihil fit” – Aristoteles (384 – 322 v. Chr.)

Abstract

Since the middle of the 20th century the synthesis of polymers increased and nowadays could be found in nearly every sector of modern life. However, most of the polymers are still produced based on petrochemical resources which is in conflict with the demand of renewability and sustainability of today's society. As a consequence researchers focus on appropriate alternatives such as biopolymers which could be based on renewable resources. Terpenes are a versatile class of natural compounds and their use as biopolymer precursors was extensively investigated in the recent years.

Within this work the terpenoid camphor and camphor-derivatives such as borneol were analyzed for their use as monomers in order to obtain novel, bio-based polymers. Since both terpenoids could not directly be polymerized due to missing functionalities within their chemical structure, first of all these precursors had to be modified to yield appropriate monomers. Afterwards the production and isolation of the different monomers had been optimized and were consequently used for polymerization in a proof of concept.

Different strategies for the modification of camphor and borneol were pursued for the preparation of suitable monomers. For the biosynthesis of borneol based on glucose the expression of the (+)-bornyl diphosphate from *S. officinalis* was analyzed. However, the expression of the plant enzyme could not be realized in both bacterial organisms *P. putida* and *E. coli* wherefore it was focused on the biotransformation of borneol and camphor.

P. putida ATCC17453 was identified as a suitable host for the conversion of camphor and borneol due to its ability to use camphor as a single carbon source via the camphor degradation pathway encoded by the CAM plasmid. The metabolism should be interrupted at different stages yielding the polymer precursors 5-*exo*-hydroxyborneol, 2,5-diketocamphane and (+)-camphor lactone by the generation of several deletion strains. All of the desired mutants could be obtained and were analyzed depending on their conversion of camphor and borneol. The deletion of the *camD* gene should yield a strain able to hydroxylate borneol without further conversion. During the analysis of the Δ*camD* mutant a borneol dehydrogenase (Bdh) activity encoded by *orf16* (*bdh*) was found converting borneol into camphor. The Bdh was recombinantly expressed in *E. coli* and besides the conversion of (-)-borneol also the conversion of (+)-borneol, (±)-isoborneol and 5-*exo*-hydroxyborneol could be shown. As the conversion of borneol by the Bdh would result in a lower yield of 5-*exo*-hydroxyborneol also this gene was deleted. However, the resulting Δ*camD* Δ*bdh* mutant was not able to convert borneol towards 5-*exo*-hydroxyborneol. Next, the

2,5-DKCMO I and II (*camE*$_{25\text{-}1}$, *camE*$_{25\text{-}2}$) were deleted in *P. putida* ATCC17453 to give a strain which is able to convert camphor towards 2,5-diketocamphane. The analysis of this mutant grown on camphor as a single carbon source did show a small accumulation of 2,5-diketocamphane, but was still able to completely metabolize the substrate and therefore the desired monomer could not be obtained. For the production of 5-oxo-1,2-campholide the gene *camH* was deleted as its gene product is reported to be a putative lactone hydrolase which could be responsible for the cleavage of the 5-oxo-1,2-campholide. Growth analysis revealed that the mutant was still able to metabolize camphor and did not show any difference compared to the wt. In order to clarify the part of CamH in the camphor degradation pathway the gene was recombinantly expressed in *E. coli* and its activity towards (+)-camphor lactone and ε-caprolactone was analyzed. As it turned out both substrates were not recognized by the enzyme so the natural substrate 5-oxo-1,2-campholide should be produced by the biotransformation of (+)-camphor lactone using *P. putida* KT2440 pBBr122::*camDCAB*. Product analysis revealed that the 5-oxo-1,2-campholide is unstable under these conditions and the lactone ring spontaneously opens by an elimination reaction. Therefore CamH might not be responsible for the cleavage of the lactone 5-oxo-1,2-campholide.

As none of the desired mutants showed the expected behavior, the enzymes which could be responsible for the production 5-*exo*-hydroxyborneol ($P450_{cam}$, Pdr, Pdx) were recombinantly expressed in *P. putida* KT2440 under the control of the constitutive camphor promotor. The conditions for the biotransformation of (-)-borneol by $P450_{cam}$, Pdr and Pdx were optimized. Afterwards a semi-continuous batch process with cell recycling and direct product extraction was developed in order to obtain a higher amount of 5-*exo*-hydroxyborneol. Hence, 5-*exo*-hydroxyborneol could be produced with a concentration of 0.54 g L^{-1}. In a proof of concept 5-*exo*-hydroxyborneol was used for the copolymerization with succinic dimethyl ester. The terpene-based biopolymer showed a glass transition temperature of about 70 °C and a molecular weight in the range of 2,000 – 4,000 g mol^{-1}.

Within this work the production of terpene-based monomers as precursors for novel biopolymers via biotransformation could be shown. Deletion strains of *P. putida* ATCC17453 were not suitable for the production of the different intermediates of the camphor degradation pathway and therefore have to be further analyzed. Nevertheless, 5-*exo*-hydroxyborneol could be produced via biotransformation processes and its copolymerization with succinic dimethyl ester could be shown in a proof of concept. The resulting polymer could be an interesting starting point for a more detailed analysis of this monomer in order to obtain terpene-based biopolymers.

Table of contents

Abstract		**IV**
1	**Introduction**	**1**
1.1	**Polymers and "Biopolymers"**	**1**
1.2	**Terpenes**	**5**
1.2.1	Biosynthesis of terpenes	7
1.2.2	Degradation of terpenes by *Pseudomonas putida*	12
1.3	**Terpene-based monomers for polymers**	**15**
1.3.1	Chemical conversion of terpenes	16
1.3.2	Enzymatic conversion of terpenes	18
1.4	**Terpene-based polymers**	**24**
1.5	**Aim**	**27**
2	**Material and methods**	**29**
2.1	**Material**	**29**
2.1.1	Chemicals, media and buffers	29
2.1.2	Strains, plasmids, and oligonucleotides	38
2.1.3	Devices, software and consumables	43
2.2	**Methods**	**47**
2.2.1	Microbiological methods	47
2.2.1.1	Cultivation and storage of microorganisms	47
2.2.1.2	Preparation of competent cells for transformation	47
2.2.1.3	Growth curves of *P. putida* ATCC17453 and relating mutants	48
2.2.2	Molecular biological methods	49
2.2.2.1	Plasmid isolation	49
2.2.2.2	Isolation of the CAM plasmid	49
2.2.2.3	Restriction digestion according to Sambrook & Russel[150]	50
2.2.2.4	Ligation according to Sambrook & Russel[150]	50
2.2.2.5	Transformation according to Sambrook & Russel[150]	51

2.2.2.6	Polymerase Chain Reaction according to *Kleppe et al.*[151]	52
2.2.2.7	Gibson Assembly and ligase independent cloning	54
2.2.2.8	Agarose gel electrophoresis according to *Aaij et al.*[152]	55
2.2.2.9	Modification of the CAM plasmid using pEMG	56
2.2.2.10	UV/Vis spectroscopy	58
2.2.3	Biochemical methods	58
2.2.3.1	Protein expression	58
2.2.3.2	Cell disruption by sonication	59
2.2.3.3	Cell disruption by high-pressure homogenization	60
2.2.3.4	Protein purification by affinity chromatography	60
2.2.3.5	SDS-PAGE according to *Laemmli*[153]	61
2.2.3.6	Western blot according to *Towbin et al.*[154]	61
2.2.3.7	Glucose assay	62
2.2.3.8	Activity assay (+)-bornyl diphosphate synthase	63
2.2.3.9	Substrate screening $P450_{cam}$	63
2.2.3.10	Optimization of (-)-borneol conversion by $P450_{cam}$	63
2.2.3.11	Semi-continuous batch process for the conversion of (-)-borneol by $P450_{cam}$	64
2.2.3.12	Activity assay borneol dehydrogenase (Bdh)	65
2.2.3.13	Synthesis of 5-oxo-1,2-campholide	66
2.2.3.14	Activity assay CamH	66
2.2.4	Chemical methods	66
2.2.4.1	Purification 5-*exo*-hydroxyborneol	66
2.2.4.2	Polymerization of 5-*exo*-hydroxyborneol	67
2.2.5	Analytics	67
2.2.5.1	Gas chromatography-mass spectrometry (GC-MS)	67
2.2.5.2	High-performance liquid chromatography-mass spectrometry (HPLC-MS)	68
2.2.5.3	Differential scanning calorimetry (DSC)	68
2.2.5.4	Gel permeation chromatography (GPC)	68

2.2.5.5 Nuclear magnetic resonance spectroscopy (NMR) 69

3 Results 71

3.1 (+)-Bornyl diphosphate synthase 71

3.1.1 Cloning and expression 71

3.1.2 Activity assay 72

3.2 Modification of the CAM plasmid 73

3.2.1 Engineering molecular biological methods for *Pseudomonas* 73

3.2.2 Quantification of the CAM plasmid 75

3.3 Production of 5-*exo*-hydroxyborneol 77

3.3.1 Recombinant expression of $P450_{cam}$, Pdr and Pdx 78

3.3.2 Development of a semi-continuous batch process 81

3.3.3 Characterization of 5-*exo*-hydroxyborneol 84

3.3.4 Orf16 – a borneol dehydrogenase (Bdh) 87

3.3.5 Double mutant Δ*camD* Δ*bdh* 91

3.4 Polymerization of 5-*exo*-hydroxyborneol 95

3.5 Production of 2,5-diketocamphane 97

3.5.1 Double mutant Δ$camE_{25\text{-}2}$ Δ$camE_{25\text{-}1}$ 98

3.6 Production of lactones 100

3.6.1 Characterization of CamH 101

3.6.2 Mutant Δ*camH* 104

4 Discussion 107

4.1 (+)-Bornyl pyrophosphate synthase 107

4.2 Modification of the CAM plasmid 110

4.2.1 Engineering molecular biological methods for *Pseudomonas* 110

4.2.2 Quantification of the CAM plasmid 112

4.2.3 Seamless gene knock out on the CAM plasmid 113

4.3 Production of 5-*exo*-hydroxyborneol 115

4.3.1 The borneol dehydrogenase of *P. putida* ATCC17453 115

4.3.2	Mutant strains *P. putida* ATCC17453 Δ*camD* and Δ*camD* Δ*bdh*	119
4.3.3	Conversion of (-)-borneol by $P450_{cam}$, Pdr, Pdx	124
4.3.4	Semi-continuous batch process	126
4.4	**Polymerization of 5-*exo*-hydroxyborneol**	**127**
4.5	**Production of 2,5-diketocamphane**	**129**
4.6	**Production of lactones**	**131**
4.6.1	Characterization of CamH and the mutant *P. putida* ATCC17453 Δ*camH*	132
4.6.2	BVMOs of the CAM plasmid used in whole cell biotransformation	135
5	**Outlook**	**138**
6	**References**	**141**
7	**Appendix**	**151**
7.1	**NMR analysis of 5-*exo*-hydroxyborneol**	**151**
7.2	**Gel permeation chromatography**	**152**
7.3	**Glucose assay**	**153**
7.4	**HPLC-MS**	**154**
7.5	**Semi-continuous batch process**	**156**
7.6	**Gene sequences**	**157**
7.7	**Amino acid sequences**	**164**
Abbreviation and symbols		**167**
List of figures		**170**
List of tables		**176**

1 Introduction

1.1 Polymers and “Biopolymers”

Polymer-based materials can be found everywhere in modern life for example as clothes, paints, packaging or as a drug delivery material in medical applications.[1] Due to superior properties, polymers often replace common materials. Since the middle of the 20th century the primary plastic production worldwide increased constantly, with a total amount of 7,800 Mt produced resins and fibers until 2015 (Figure 1).[2] In the last 13 years half of the total amount (3,900 Mt) had been manufactured underlining the high demand and consumption of plastics worldwide.[2]

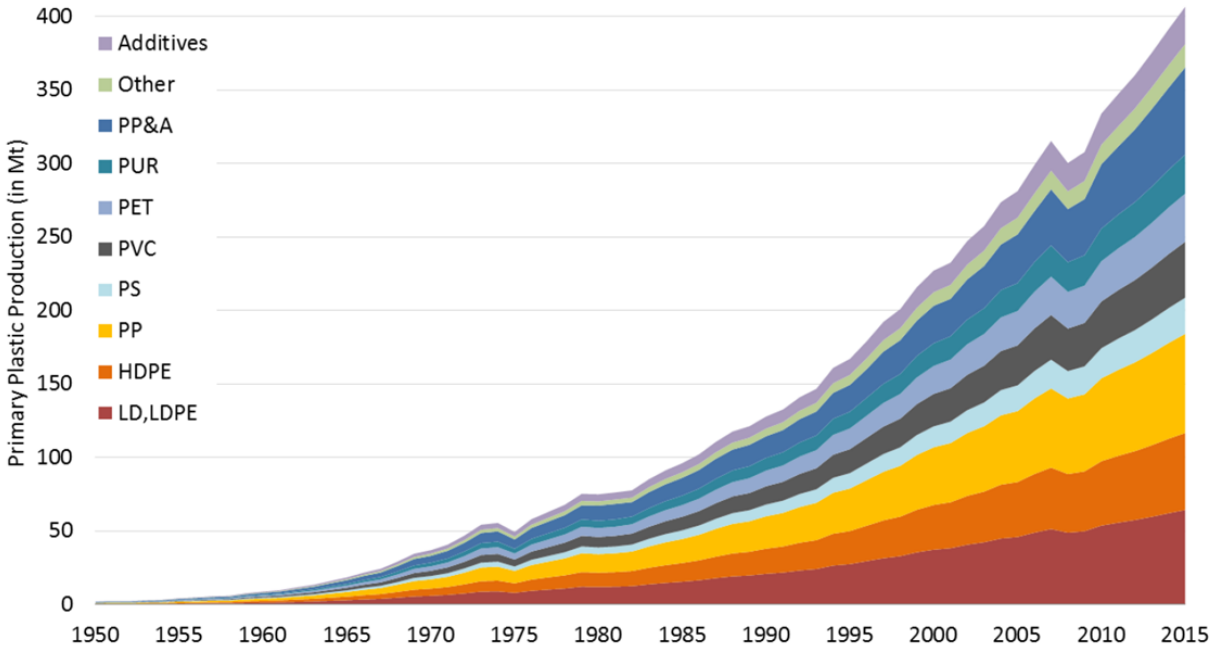

Figure 1: Global primary plastic production (in million metric tons) according to polymer type from 1950 to 2015. PP: polypropylene; PUR: poly urethane; PET: polyethylene terephthalate; PVC: polyvinyl chloride; PS: polystyrene; HDPE: high density polyethylene; LDPE: low density polyethylene (Source: *Geyer et al.*).[2]

Due to the low price of petroleum and its good utility, most of the common polymers are based on this fossil raw material. All in all 4 % of the total amount of petroleum is converted towards plastics and another 4 % is used to generate the energy, which is necessary for the plastic production processes.[3]

The high amount of plastics accompanies a high amount of plastic solid waste with an estimated increasing rate of 3.9 % per year.[4] In total, 299 million tons of plastic waste was globally generated in 2013, with more than 25.2 million tons in the European Union. Only 26 % of the waste within the European Union was recycled, another 36 % were utilized energetically by energy recovery processes like incineration and the remaining 38 % were stored at landfills.[4] The major challenge is to prevent the plastic waste entering the environment. The desired properties of polymer materials like durability and stability are also the drawbacks if it comes to biodegradation. The most common polymers will not degrade under normal environmental conditions for several years and therefore will remain in the landscape.[5] To counteract the environmental pollution caused by common polymers, researchers are looking for suitable and sustainable alternatives. What is more, petroleum as a raw material for polymers is a fossil resource of finite availability and its price is suggested to increase in the next decades.

Such an alternative could be biopolymers, which have recently moved into the focus of many researchers and companies due to the increasing awareness for sustainability of consumers and not at least because of the renewable energy debate of today. Furthermore, societal demands for bio-based products in combination with scientific research leads to commercialization of novel, sustainable and renewable biopolymers.[6] According to a market study carried out from the nova-Institute GmbH the worldwide production capacity of bio-based polymers is forecasted to increase from 6.6 million tons in 2016 to 8.5 million tons in 2021.[7] Compared to the total polymer capacity the global production of bioplastics currently only makes up 2 %, but this also means a turnover of about 13 billion € showing the high potential of bio-based polymers.[7]

Biopolymers are defined as “polymers produced partially or entirely from renewable natural resources other than petroleum” (*Hernández et al*).[8] Biodegradability often is closely connected to the term biopolymers. This might be one property of some biopolymers, such as polylactic acid (PLA),[9] but is not stringent. For example bio-based polyethylene is not biodegradable, but could be produced based on natural substances and therefore belongs to the class of biopolymers (Figure 2).[9]

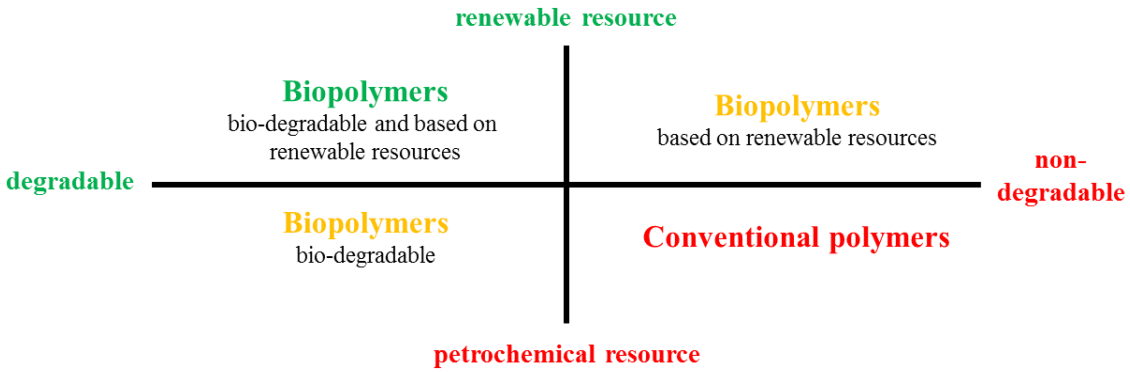

Figure 2: Classification of biopolymers and conventional polymers regarding degradability and resource. (Source: lfbb-Hannover)

The first ever man-made synthetic and commercial biopolymer was Bakelite produced by *Leo Hendrik Baekeland* in the early 20th century. The Belgian-American chemist obtained the polymeric material by combining formaldehyde and phenol.[10] Since then most of the biopolymers were replaced by the cheap petroleum-based polymers for a long time, but in recent years more and more attention has been paid to these materials.

Today's biopolymers are often classified depending on the way the material is obtained or produced into three different groups:[11] (i) natural polymers, such as starch or cellulose, (ii) synthetic polymers obtained from natural monomers, such as poly(lactic acid) (PLA) or poly(ethylene 2,5-furandicarboxylate) (PEF) and (iii) polymers from microbial fermentation, such as poly(hydroxybutyrate) (PHB) (Figure 3).[6, 11]

An example for the modification of natural polymers is cellulose acetate (CA) which could be obtained from cellulose. In nature cellulose is responsible for the structure and rigidity of cell walls and therefore the main component of many plants. By an acetylation reaction with acetic anhydride and acetic acid in the presence of sulfuric acid, cellulose could be converted to CA.[12] The degree of acetylation is one of the key factors for the properties of the resulting material, like solubility. High acetylated CA for example is soluble in dichloromethane, whereas CA with a lower degree of substitution is soluble in acetone or dioxane.[12] There are also reports on further conversion of CA to CA propionate (CAP) or CA butyrate (CAB), making the material suitable for different applications, such as film formation for photography or selective filtration in the medical field.[13]

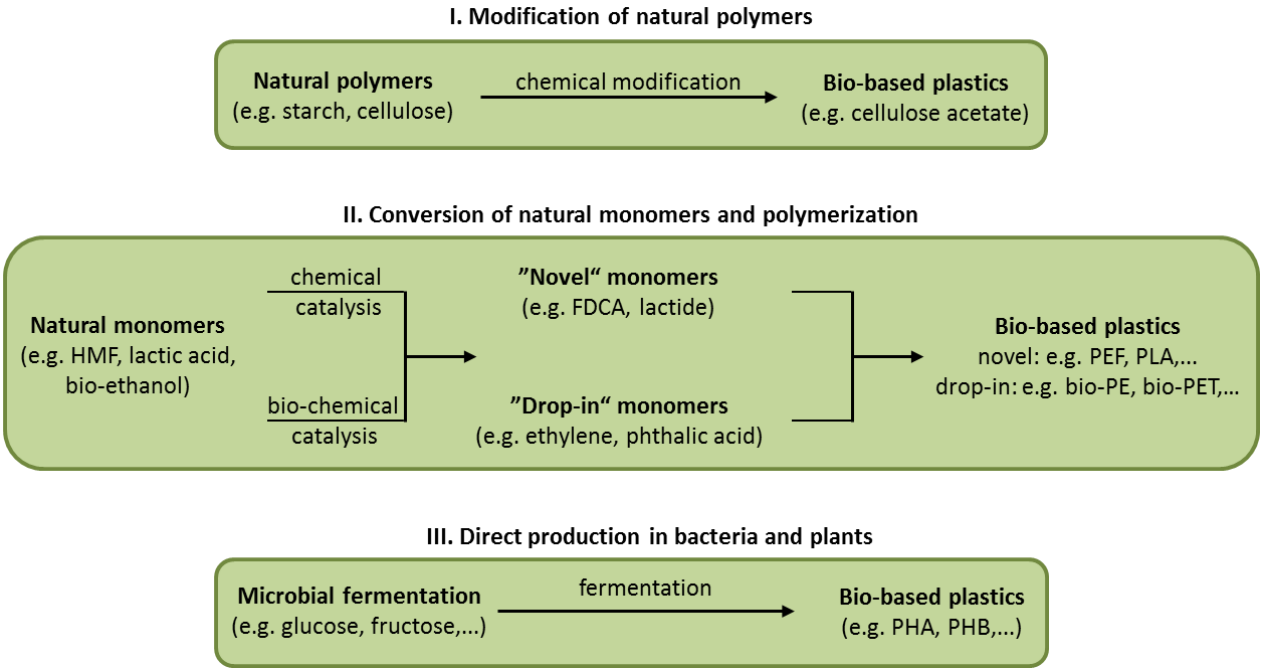

Figure 3: Principal routes to bio-based plastics according to *Storz et al.*[6] and *Flaris et al.*.[11]

The polymers of the second category are not directly produced by nature or fermentation, but the required monomers are obtained from bio-based substrates. By chemical or bio-chemical catalysis different types of monomers could be derived, "novel" and "drop-in monomers", respectively. The synthesis of drop-in monomers aims for the direct replacement of petroleum-based monomers. For example ethylene the monomer of polyethylene could be synthesized by dehydration of ethanol,[14] which in turn could be produced by sugar-based fermentation processes.[15] Drop-in monomers have exactly the same properties as their petroleum-based competitors, so the major challenge is the production at low costs. In contrast, "novel monomers" do not replace petroleum-based monomers, but rather are made for new applications or to replace established polymers in their application due to superior properties. In recent years poly(ethylene 2,5-furandicarboxylate) (PEF) made a great stir as it may have the potential to replace polyethylene terephthalate (PET),[16] the most widely used polyester.[17] The monomers of PEF are 2,5-furandicarboxylic acid (FDCA) and ethylene glycol,[17] both of which can be derived from bio-based substrates. For example, FDCA could be produced by chemical or biochemical conversion of 5-(hydroxymethyl)furfural (HMF).[16] The precursor HMF itself could be synthesized from glucose in a reductive amination reaction.[18] First studies showed that PEF has a higher barrier property towards H_2O, CO_2

and O_2 compared to PET, which is especially interesting for applications in the food and beverage sector.[17] Furthermore, FDCA could be produced in an economically feasible manner making it one of the most promising bio-based monomers.[17, 19]

In close relation to the first groups, polymers of the third group such as poly(hydroxyalkanoates) (PHA) are directly produced by sugar-based microbial fermentation and could be used without further modification. Naturally PHA serves as energy and carbon storage and is accumulated in many bacteria and plants. By optimization of fermentation parameters and recombinant expression of the responsible genes, the production level of PHA could be forced up to 80 % cell dry weight in fermentation processes using *Escherichia coli* (*E. coli*) as a host.[20] Especially PHB emerged to an attractive biopolymer as it shows similar physical and thermal properties compared to petroleum-based polypropylene (PP),[21] but the production of PHB – to date – is still more cost-intensive than PP.[22] Currently, the costs for PHB arise within the production method, as most bacterial fermentation processes need sugar from corn or cane sugar as a feedstock.[23] This feedstock represents up to 30 % of the total costs of PHB.[23] To overcome this issue, transgenic plants[24] are used increasingly for the production of PHA and PHB.[25] Instead of the comparable expensive sugars, CO_2 could be used as a feedstock for plant cultivation and PHA production.[26] Consequently, it could be possible to produce PHB at lower costs with the additional advantage of CO_2 fixation.

For the approach to obtain “novel” monomers terpenes might be another suitable source of natural products. This class has recently moved into the focus as a bio-based raw material for different applications due to the great structural diversity and abundance in nature.

1.2 Terpenes

Terpenes are a wide class of natural hydrocarbons synthesized by many plants, fungi, insects and microorganisms[27] and represent the largest class of natural products with more than 25,000 reported structures.[28] Naturally, terpenes build a big class of secondary plant metabolites and can be found as the main constituent of many essential oils.[29] Depending on the content of terpenes, many oils show antimicrobial,[30] anti-inflammatory and antifungal activity,[31] interesting properties for pharmaceutical applications. Other terpenes are

responsible for the typical flavor of different plants and fruits like peppermint ((-)-menthol), lemongrass or citrus fruits ((-)-limonene) and consequently can be used as flavors.[32] Higher terpenes such as carotenoids are essential for plants, where they act as energy transfer molecules to the chlorophylls,[33] but also can be used as coloring agents in the food industry.[34]

Chemically, all terpenes consist of isoprene units, which are usually joined in a head to tail manner during their biosynthesis (biogenic isoprene rule).[35] The classification is based on the number of isoprene units, which they consist of (Table 1).[36]

Hemiterpenes exhibit a linear (acyclic) structure, however already monoterpenes show mono- or bicyclic structures and higher terpenes are structurally even more diverse. Due to the unpolar character most of the terpenes are rather lipophilic and consequently cannot easily be dissolved under aqueous conditions.

Table 1: Classification of terpenes according to the number of isoprene units.[27, 36]

Class	Isoprene units	Molecular formula
Hemiterpenes	1	C_5H_8
Monoterpenes	2	$C_{10}H_{16}$
Sesquiterpenes	3	$C_{15}H_{24}$
Diterpenes	4	$C_{20}H_{32}$
Sesterterpenes	5	$C_{25}H_{40}$
Triterpenes	6	$C_{30}H_{48}$
Tetraterpenes	8	$C_{40}H_{64}$
Polyterpenes	>8	$(C_5H_8)_n$

In contrast, terpenoids carry different functional groups like hydroxyl or carbonyl groups and thus are slightly more water soluble than terpenes. One of the most popular terpenoid is camphor, which could be obtained by steam distillation of the wood, twigs or leaves of the camphor tree (*Cinnamomum camphora*). As a by-product of the pulp industry in China camphor could also be obtained in large amounts from already established industries. Furthermore the chemical synthesis of camphor based on pinene, which could be obtained from turpentine oil at low prices is known for more than 100 years.[37],[38] The structure of the bicyclic monoterpene formally derives from bornane; however, a single carbonyl group is

added to the backbone (Figure 4). In nature both enantiomers (+)- and (-)-camphor can be found in the camphor tree.

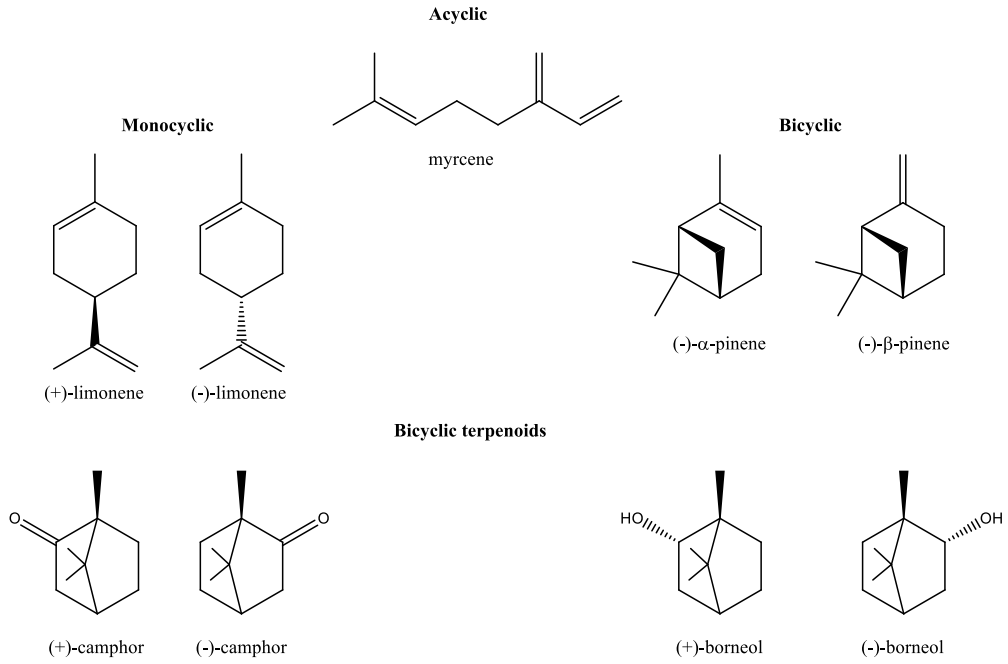

Figure 4: Common representatives for acyclic, monocyclic and bicyclic terpenes and terpenoids.

The incorporation of different functional groups is related with the great structural diversity of terpenes and is a result of the biosynthesis in many plants and bacteria.[39]

1.2.1 Biosynthesis of terpenes

All terpenes and terpenoids derive from the two activated isoprene precursors, isopentenyl pyrophosphate (IPP) and its allylic isomer dimethylallyl pyrophosphate (DMAPP).[40] The synthesis of these precursors is based on two independent pathways, the long known mevalonate pathway (MVA) and the non-mevalonate (non-MVA), deoxyxylulose phosphate (DOXP) or methylerythritol 4-phospahte pathway (MEP).[41] Eukaryotes other than plants use the MVA for the production of isoprene precursors.[42] In contrast prokaryotes, with some exceptions, use the MEP and plants use both pathways, the MVA in the cytosol and the MEP in the plastids.[43] The main difference between both pathways is the initial step in the biosynthesis. In the MVA the first step is the condensation of two acetyl-CoA, whereas in the MEP pyruvate and glyceraldehyde 3-phosphat serve as substrates for condensation.[44]

The mevalonate pathway (MVA) – a short overview

The MVA was revealed in the 1950s by *Lynen*, *Bloch* and *Cornforth* and for a long time it was considered to be the only pathway responsible for the formation of terpenes in plants, animals, fungi, archaea and some bacteria.[41] The initial step of the MVA is a thiolase-catalyzed Claisen condensation reaction of two molecules of acetyl-CoA to form acetoacetyl-CoA (Figure 5).[45]

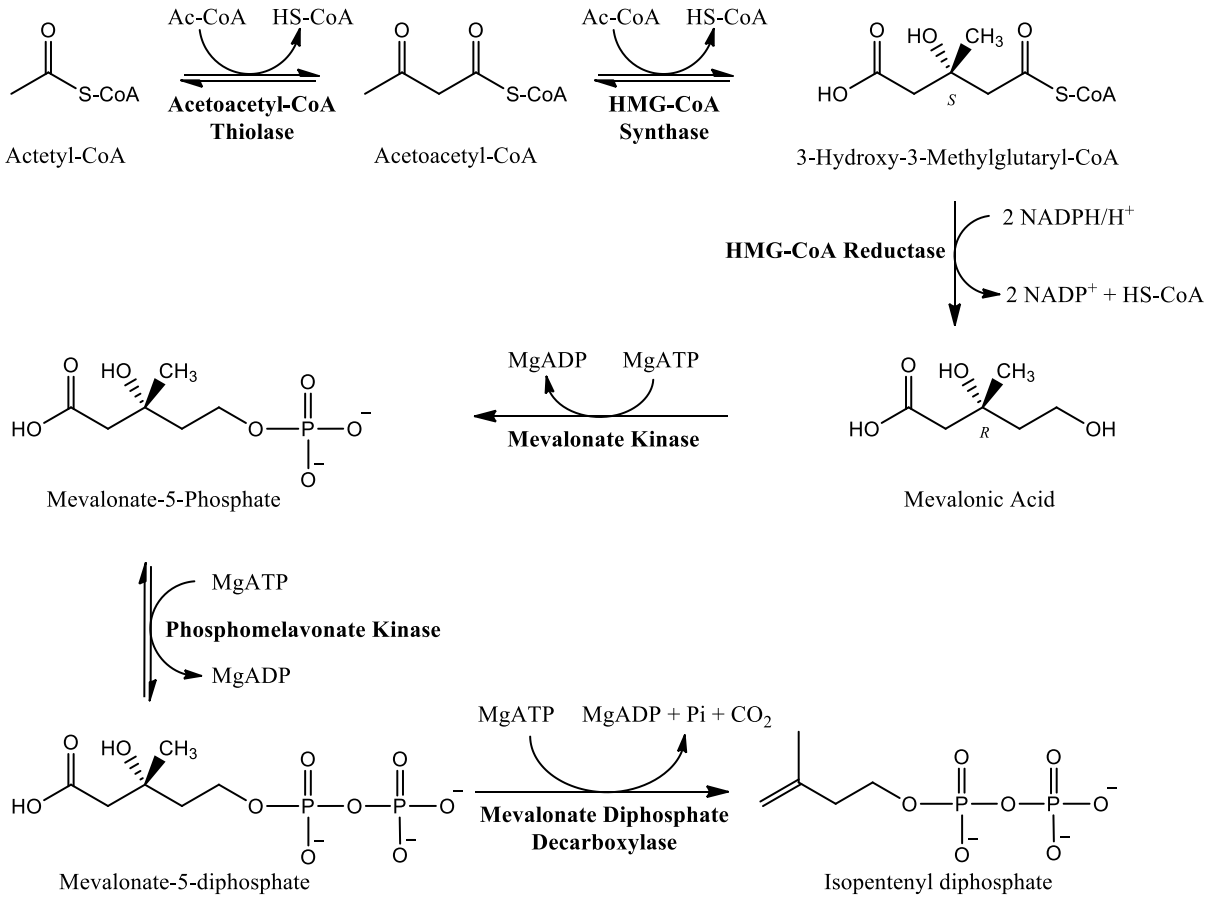

Figure 5: Biosynthesis of isopentenyl diphosphate as a precursor for terpenes via the MVA pathway. Involved enzymes are displayed in bold. Figure according to *Miziorko et al.*.[46]

Under consumption of another acetyl-CoA, acetoacetyl-CoA is converted to 3-hydroxy-3-methylglutaryl-CoA in a second condensation reaction, catalyzed by the HMG-CoA synthase.[47] After a two-step reduction catalyzed by HMG-CoA reductase, followed by a two-step phosphorylation catalyzed by mevalonate kinase and phosphomevalonate kinase

respectively, mevalonate-5-diphophate is formed.[46] In the last step, the mevalonate-5-diphosphate is converted by a decarboxylase and finally IPP is released.[46] An IPP isomerase converts IPP to DMAPP and vice versa to obtain both precursors.[45]

The methylerythritol 4-phosphate pathway (MEP) – a short overview

In the early 1990s an alternative route, the methylerythritol 4-phosphate pathway, towards IPP and DMAPP was discovered in bacteria (Figure 6).[48]

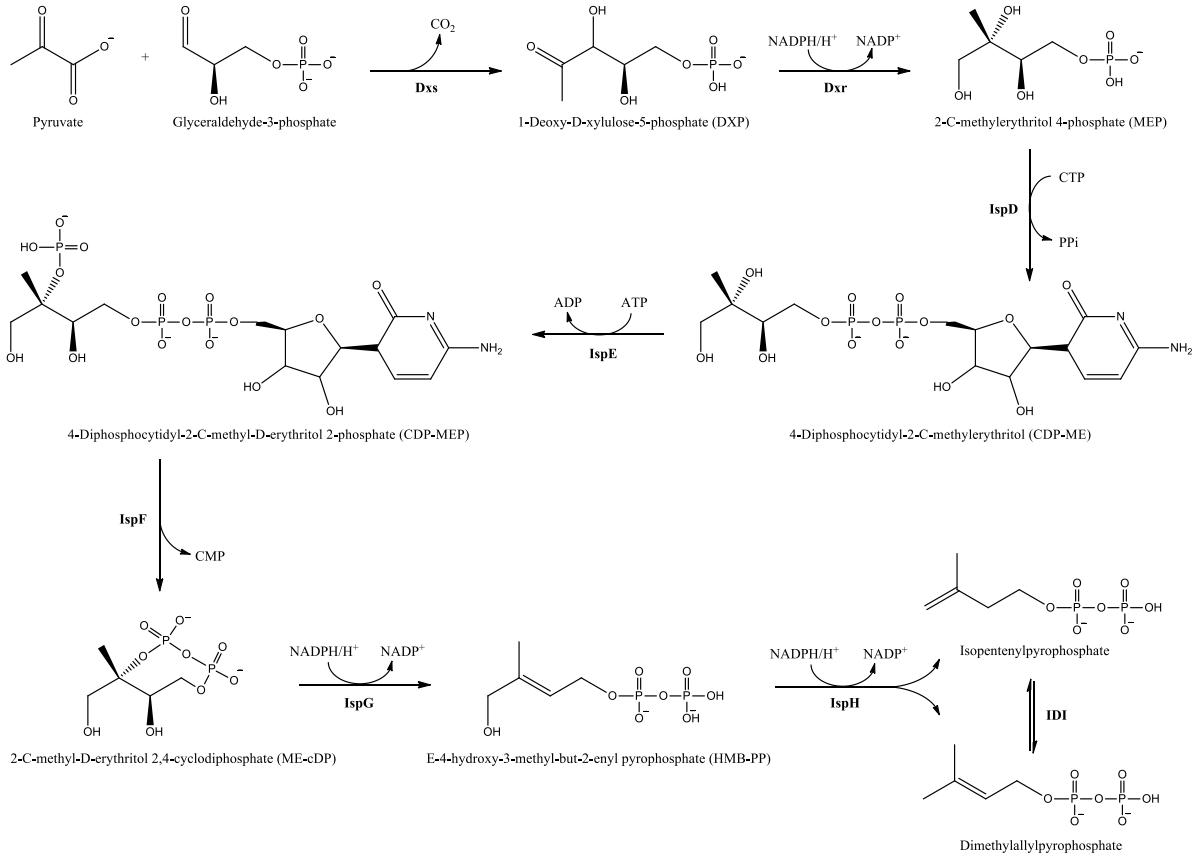

Figure 6: Biosynthesis of IPP and DMAPP as terpene precursors via the MEP pathway. Involved enzymes are displayed in bold. Dxs: 1-deoxy-D-xylulose-5-phosphate synthase; Dxr: 1-deoxy-D-xylulose-5-phosphate reductoisomerase; IspD: 4-diphosphocytidyl-2-C-methylerythritol synthase; IspE: 4-(cytidine-5´-diphospho)-2-C-methyl-D-erythritol kinase; IspF: 2-C-methyl-D-erythritol-2,4-cyclodiphosphate synthase; IspG: 4-hydroxy-3-methyl-but-2-enyl-diphosphate synthase; IspH: 4-hydroxy-3-methylbut-2-enyl-diphosphate reductase. (Source: *Banerjee et al*.[48], *Phillips et al.*[49])

In contrast to the MVA, the biosynthesis of isoprenoids via the MEP is initiated with the condensation of pyruvate and glyceraldehyde 3-phosphate,[48] catalyzed by the 1-deoxy-D-xylulose-5-phosphate synthase (Dxs).[50]In the next step, the typical branched-chain is introduced into the linear pentulose phosphate by the enzyme 1-deoxy-D-xylulose-5-phosphate reductoisomerase (Dxr). For the skeletal rearrangement two possible reactions are considered, followed by a reduction step. On the one hand there could be a sigmatropic rearrangement reaction caused by the 1,2-ketol function in combination with the enzyme,[51] but also a retro-aldol/aldol reaction could be responsible for the rearrangement.[50] Under consumption of ATP and CTP, three more enzymes (IspD, IspE and IspF)[52] convert the 2*C*-methyl-D-erythritol 4-phosphate into its cyclic diphosphate.[53] For the last step two more enzymes are required, namely IspG and IspH. First, IspG converts 2*C*-methyl-D-erythritol-2,4-cyclodiphosphate into 2-methyl-2-(*E*)-butenyl diphosphate in a two-electron reduction.[50] Afterwards IPP and some DMAPP (ratio 5 : 1) is released by IspH, the last enzyme of the MEP.[50] Similar to the MVA an IPP isomerase converts IPP to DMAPP.

Terpene synthases

For the biosynthesis of terpenes the IPP isomerase is a key factor as the enzyme adjusts the equilibrium of IPP and DMAPP, thus regulating the availability of the basic precursors.[44] These precursors are further converted by three prenyltransferases to form the linear substrates for terpene synthases (TPS), geranyl diphosphate (GPP, C_{10}), farnesyl diphosphate (FPP, C_{15}) and geranylgeranyl diphosphate (GGPP, C_{20}), respectively.[54] Based on these building blocks various TPSs build up the different terpenes in a “head-to-tail” or “head-to-head” reaction.[55]

All TPSs require divalent metal ions for activity and can be divided into different groups based on the released product (monoterpene, sesquiterpenes or diterpene synthases)[56] or based on the reaction mechanism (class I and class II).[54] The initial step of class I TPSs is the ionization of the diphosphate moiety stabilized by the divalent metal ions,[57] whereas class II TPSs catalyze a protonation-induced cyclization of the substrate.[54] Both mechanisms end up with the formation of a reactive carbocation intermediate, which then could undergo different reactions like rearrangements, hydride shifts or cyclization before the reaction is terminated by deprotonation or nucleophilic capture (often H_2O, Figure 7).[58] As

the reaction may be branched and could be terminated at different stages,[57] various TPSs release a mixture of different terpenes and therefore are considered as multi-product enzymes (Figure 7).[59]

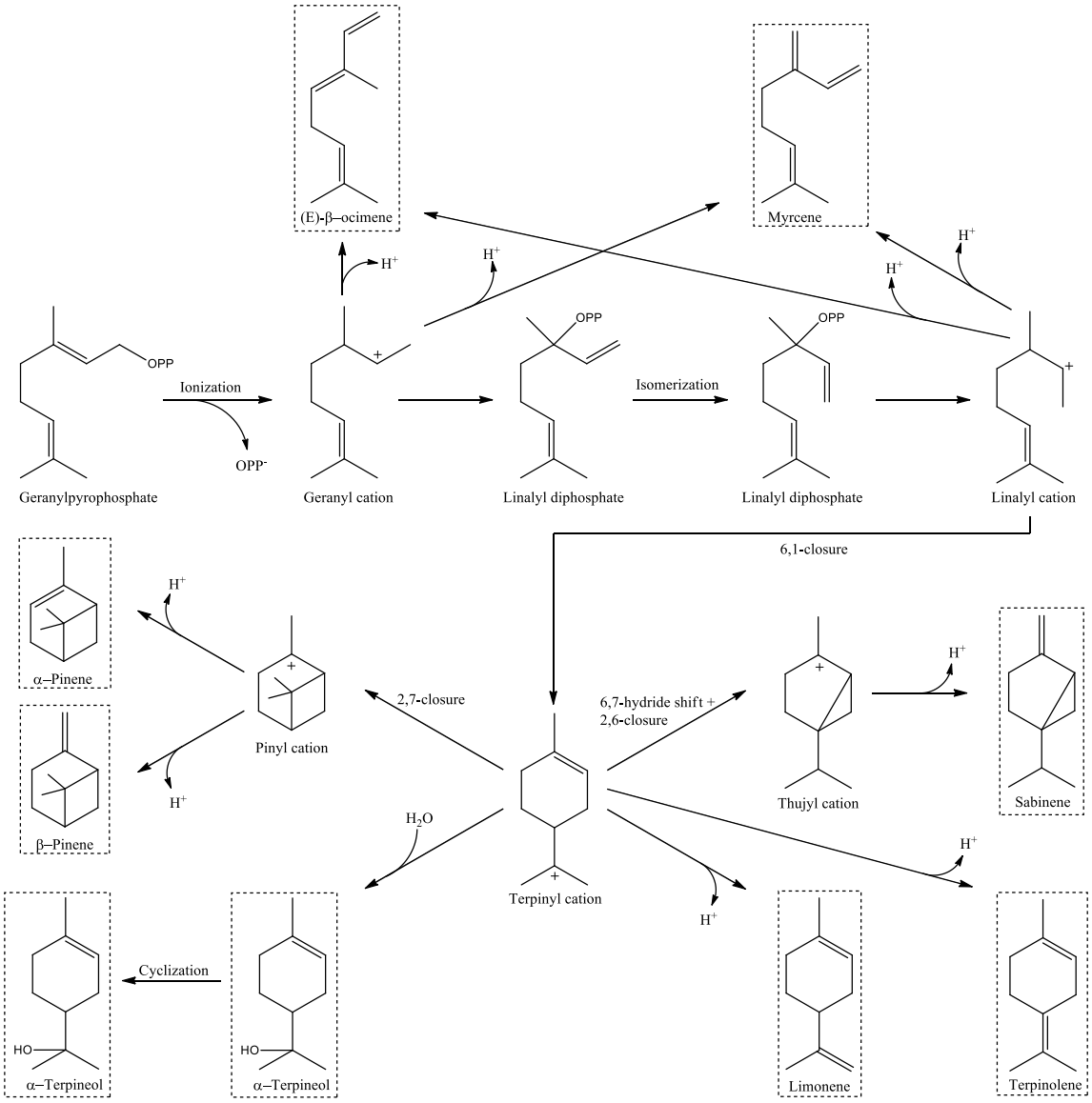

Figure 7: Reaction mechanism of the monoterpene synthase AtTPS-Cin from *Arabidopsis* as an example for a multi-product TPS. Different intermediates lead to various terpene products (in dashed boxes). Figure according *to Chen et al.*.[58]

Furthermore many TPSs also show a multi-substrate behavior and accept not only GPP as a substrate, but also FPP which consequently results in different products.[59]

The biosynthesis of some terpenes ends with their formation by TPSs, but others act as intermediates in the synthesis of higher terpenes. For example the synthesis of camphor is based on the formation of borneol, which is subsequently oxidized by a dehydrogenase.[60] Other terpenes such as menthol show even more complex biosynthesis pathways. Based on limonene six more enzymes convert the substrate in different hydroxylation, oxidation and isomerization reactions towards menthol.[61]

Due to the incorporation of different functional groups along the biosynthesis and the high structural diversity of terpenes, this class of natural substances has recently moved into the focus of various industries as raw material for novel applications, such as biopolymers.

1.2.2 Degradation of terpenes by *Pseudomonas putida*

Bacteria of the *Pseudomonas* species are ubiquitous Gram-negative rods with polar flagella and belong to the gamma subclass of the Proteobacteria.[62] These chemo-organotrophic aerobic bacteria colonize aerobic, semi-aerobic soil and water habitats and are known for their great metabolic diversity.[62] *Pseudomonas* is not able to metabolize C5 sugars by nature, but glucose could be consumed via the Entner-Doudoroff pathway generating glyceraldehyde 3-phosphate and pyruvate.[63],[64] However, in contrast to many other organisms, glucose is not the preferred carbon source, but rather glycerol or succinate and other intermediates of the tricarboxylic acid cycle are utilized.[63] Furthermore, it is reported that *Pseudomonas* species could accept more than 100 different organic compounds as carbon and energy sources.[62] Some of these compounds such like toluene or naphthalene are even toxic for other organisms. However, *Pseudomonas sp*. are able to utilize these aromatics by degradation operons mostly encoded on plasmids like the TOL plasmid (toluene degradation) or the NAH7 plasmid (naphthalene degradation).[62],[65] Often oxygenases introduce several hydroxyl groups to create aromatic polyols, which consequently undergo an enzyme catalyzed cleavage event for their complete degradation.[66],[67] These oxidation reactions require high redox capacity and NAD(P)H regeneration rate, which *Pseudomonas* overcome by two mechanisms.[68] On the one hand the glucose uptake rate is increased in the presence of such compounds and on the other hand biomass formation is reduced which both lead to an increased regeneration of NAD(P)H under laboratory conditions.[68],[69] It is worth

mentioning that even at high rates the degradation yields no by-products such as acetate or ethanol which are often observed by other industrial important organisms like *E. coli* or *Saccharomyces cerevisiae* underlining the high potential of *Pseudomonas* for industrial applications.[69] Another remarkable property of *Pseudomonas* is its high solvent tolerance due to several multidrug efflux systems such as ATP-binding cassettes (ABC-transporters) or other efflux pumps belonging to the resistance-nodulation-cell division (RND) family.[70] Because all these efflux systems require a high amount of energy *Pseudomonas* reacts with an overall upregulated metabolism for glucose conversion.[71] Another response to solvent penetration is the *cis* to *trans* isomerization of unsaturated fatty acids of the cell wall as well as the methylation of these fatty acids to produce cyclopropane derivatives.[71] Thus, the cell membranes show a higher density which consequently leads to a higher solvent resistance.[71] Besides the natural features of this organism, in the last years several attempts have been made with the goal to genetically modify *Pseudomonas*. As a result *Pseudomonas* became a host for gene expression often in combination with vectors based on the broad range expression vector pBBr.[72] Since the sequencing of some *Pseudomonas* strains in the recent years, several methods for genome editing were developed and their suitability has been proven by the deletion of some antibiotic resistance genes.[73] The availability of fast and easy methods for the genetic modification and gene expression is one of the key factors for development of *Pseudomonas* as a bacterial workhorse in the last years.

With this set of properties *Pseudomonas* also plays a relevant role for the environment in terms of bioremediation for example by element cycling or degradation and recycling of biogenic and xenobiotic pollutants in nature.[74] From an industrial point of view the combination of fast growth, high solvent tolerance and reducing power and especially the diverse genetic repertoire of the different plasmids in *Pseudomonas* is of high interest. Beside the already mentioned TOL and NAH7 plasmids another plasmid, the CAM plasmid is responsible for the biodegradation of the terpenoids (+)- and (-)-camphor. With regard to terpene-based monomers, the CAM plasmid of *Pseudomonas* offers both, interesting intermediates and enzymes.

The CAM plasmid

The initial steps for the biodegradation of camphor by the CAM plasmid have been known for more than 60 years, but it took a way longer to elucidate all steps of the pathway meanwhile the plasmid size was controversially discussed in the of range of 100 – 500 kbp.[75],[76],[77] Last reports in literature assume that the transmissible CAM plasmid is a linear piece of DNA with a size of about 530 – 553 kbp.[78],[79] The complete degradation of camphor yields on the one hand acetyl-CoA, which then enters the tricarboxylic acid (TCA) cycle and on the other hand isobutyryl-CoA. Isobutyryl-CoA serves as an intermediate within the valine biodegradation and could be further converted by the enzymes of the valine and leucine biodegradation pathway to acetyl-CoA, which subsequently enters the TCA.[80],[81] The first enzymes for the degradation pathway are encoded by the CAM operon *camDCAB*, which is negatively regulated by the CamR regulator (*camR*).[82],[83] The regulator binds the DNA between an overlapping promotor region of *camR* and *camDCAB* thereby hindering the transcription of the operon.[84] As a consequence the expression of *camR* is negatively controlled by its own product.[85] In the presence of camphor the binding of the regulator is inhibited and camphor biodegradation is initiated with the stereospecific hydroxylation of camphor to form hydroxycamphor by cytochrome $P450_{cam}$ (*camC*, Figure 8).[86]

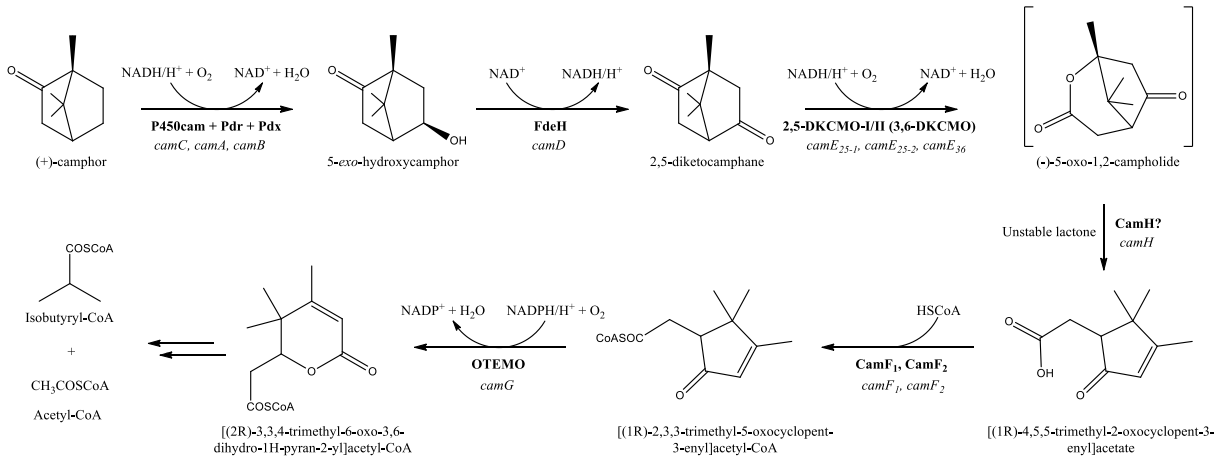

Figure 8: Biodegradation of (+)-camphor to isobutyryl-CoA and acetyl-CoA by the CAM plasmid of *P. putida* ATCC17453. Enzymes are displayed in bold, responsible genes in italic. Same enzymes are required for the degradation of (-)-camphor with one exception. Instead of the 2,5-DKCMO-I+II, the diketocamphane species of (-)-camphor is converted by 3,6-DKCMO (Source: *Iwaki et al.*).[79]

The electrons necessary for the hydroxylation are transferred from NADH via Pdr and Pdx towards the $P450_{cam}$ enzyme following the typical mechanism for class I monooxygenases as discussed above.[87],[88] Under consumption of another NADH the hydroxylated camphor is further oxidized by the hydroxycamphor dehydrogenase FdeH (*camD*) yielding diketocamphane.[89] This compound serves as a substrate for Baeyer-Villiger oxidation by different type II BVMOs.[90] Depending on the isomer of camphor the diketocamphane species is converted under the consumption of NADH by the 3,6-diketocamphane monooxygenase (3,6-DKCMO, $camE_{36}$) or two 2,5-diketocamphane monooxygenase (2,5-DKCMO, $camE_{25\text{-}1}$ and $camE_{25\text{-}2}$) resulting in the formation of a lactone.[91],[92] The lactone undergoes a spontaneous opening caused by its unstable structure (elimination/hydrolysis reaction). For this step also the enzyme CamH may be involved as it is supposed to be a putative lactone hydrolase, but this is not proven yet.[93] The cleavage of the lactone yields a carbonyl acid which is consequently modified by a CoA synthase under ATP consumption. Two enzymes are predicted to be responsible for this reaction ($CamF_1$ and $CamF_2$), but are also not proven yet.[79] Afterwards the FAD- and NADPH-dependent type I BVMO 2-oxo-Δ^3-4,5,5-trimethylcyclopentenylacetyl-CoA monooxygenase (OTEMO, *camG*) again forms a lactone.[94] After another elimination $\Delta^{2,5}$-3,4,4-trimethylpimeloyl-CoA is formed and consequently metabolized towards isobutyryl-CoA and acetyl-CoA, both of which are intermediates of the TCA.

Among the camphor degradation pathway there are some enzymes and intermediates which could be interesting as monomers for terpene-based polymers. On the one hand the $P450_{cam}$ introduces hydroxyl groups into terpene backbones leading to a higher functionality of the substrate. On the other hand three BVMOs release different lactones which may be capable for ROP. Furthermore the diketocamphane released via the conversion of hydroxycamphor by FdeH also displays an interesting intermediate as it could be further converted towards its diamine which represents a monomer for terpene-based polyamides.[95]

1.3 Terpene-based monomers for polymers

Although various structures of terpenes have been found in nature just few of them fulfill the criteria for direct usage as monomers in polymerization which are: (i) low molecular weight

reactive molecules; (ii) more than one double bond or functional group within their chemical structure; (iii) accessibility of the functional groups for the different polymerization procedures, such as polycondensation, cationic/anionic polymerization or ring-opening polymerization.

Acyclic monoterpenes with conjugated double bonds like myrcene or ocimenes as well as cyclic monoterpenes like limonene can be polymerized by radical, anionic or cationic procedures to obtain homopolymers.[96] Despite homopolymers, some terpenes are also used for polymerization of copolymers. One of the first terpene used for copolymerization was *β*-pinene.[97] *Lu et al*. carried out sequential living cationic polymerization of *β*-pinene and styrene or *p*-methylstyrene, respectively.[98] Another study showed the radical copolymerization of limonene and styrene.[99]

Beside these examples there might be some more terpenes, which can be directly used for polymerization, but the majority is not accessible for direct polymerization due to missing double bonds or other functional groups. To apply these raw materials for polymerization, single functional groups have to be modified or at least a second one has to be introduced. Thus, several strategies for chemical and also enzymatic conversion of terpenes were reported in recent years.

1.3.1 Chemical conversion of terpenes

The conversion of existing functional groups for example double bonds often is the first step in chemical functionalization of terpenes to obtain suitable monomers. The resulting monomers serve for different types of polymerization and consequently novel polymer materials for new applications could be created.

For example thiol-ene additions are a suitable tool to introduce different functional groups in a kind of click chemistry reaction to obtain different polymers such as polyurethanes (PU),[100] polyesters or polyamides (PA). *Firdaus et al.* showed the production of PU monomers from limonene by a thiol-ene addition reaction using cysteamine hydrochloride (Figure 9 A).[101] By varying the functionalization of the thiol substrate, it was also possible to build monomers for PAs and polyesters.[102]

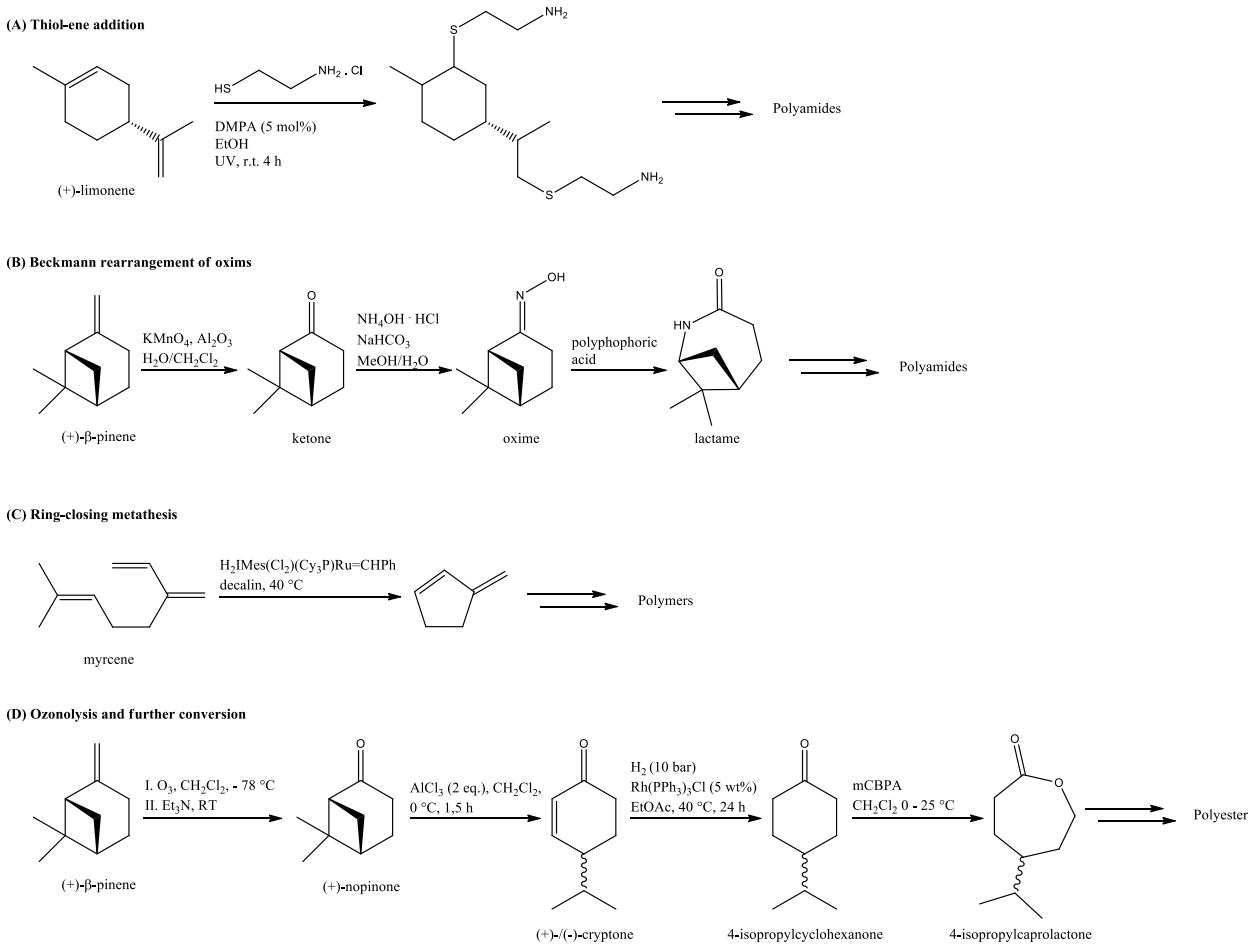

Figure 9: Different strategies to obtain terpene-based monomers for polymers by chemical modification of double bonds. A: Conversion of (+)-limonene via thiol-ene addition according to *Firdaus et al.* to obtain monomers for polyamides;[101] B: 2-Step conversion of *β*-pinene to the corresponding oxime and further conversion via Beckmann rearrangement. The resulting lactam serves as a monomer for polyamides (*Winnacker et al.*);[103] C: Ring-closing metathesis of myrcene leads to a terpene-based monomer for polymers (*Kobayashi et al.*);[104] D: Ozonolysis of *β*-pinene followed by hydrogenation with Wilkinsons's catalyst and lactonization. The resulting lactone could be a monomer for polyesters.

Other raw materials for polyesters are lactones, because they can be easily polymerized by ring opening polymerization (ROP) to obtain high molecular weight polymers. One approach to create lactones is the conversion of cyclic ketones by Baeyer-Villiger oxidation (BVO) with H_2O_2. In terms of terpenes *β*-pinene fulfills the criteria as a substrate for such oxidation.[105] By ozonolysis a carbonyl group is introduced into the terpene backbone followed by an isomerization step to obtain the monocyclic product cryptone.[106] After

hydrogenation with Wilkinsons's catalyst, the desired saturated ketone can be used for the production of the lactone.[106]

Besides lactones, lactams are an interesting class of monomers for ROP and the synthesis of PAs. *Winnacker et al.* for example showed the production of PAs also starting from *β*-pinene.[103] First, the double bond of the terpene is oxidized and further converted to the oxime, which then undergoes a Beckmann rearrangement to obtain the lactam and consequently could be used for ROP.[107] Apart from the synthesis based on double bonds changing the raw material towards a ketone substrate simplifies the synthesis of lactams. So, menthone, a terpene harboring a carbonyl group, could be directly converted to the lactam using hydroxylamine-O-sulfonic acid.[108]

Another approach for the synthesis of terpene-based monomers depends on the metathesis of double bonds. In general, metathesis is a reaction to exchange substituents in alkene or alkyne substrates. Often this method is used as ring closing metathesis to obtain different substance classes such as flavor compounds or other natural occurring substances. Although many terpenes contain double bonds metathesis was not the method of choice for a long time. A few years ago it was shown that the acyclic monoterpene *β*-myrcene could undergo a ring closing homometathesis which results in 3-methylenecyclopent-2-ene.[109] Afterwards the monomer could be polymerized under radical, anionic and cationic conditions to obtain a novel polymer.[104]

Besides double bonds and carbonyl groups, other functional groups such as hydroxyl, aldehyde, or esters in many terpenoids can be targets for the conversion into suitable monomers. In contrast, the modification of non-activated C–H bonds of terpenes is more challenging in chemical approaches, but could be achieved with enzymes.

1.3.2 Enzymatic conversion of terpenes

Many enzymes are known to modify terpenes by different types of reactions, including oxidation, reduction, isomerization, dehydrogenation, decarboxylation or hydroxylation.[110] Most of these enzymes are normally involved either in terpene synthesis or in terpene degradation pathways. For the production of terpene-based monomers especially two types of monooxygenases are of great interest because of their product spectrum. On the one hand

Baeyer-Villiger monooxygenases (BVMOs) convert ketones to lactones, which could directly serve as monomers. On the other hand cytochrome P450 enzymes are able to introduce molecular oxygen into allylic positions, double bonds or non-activated C-H bonds.[111] Especially the ability to hydroxylate non-activated C-H bonds is a great feature of P450 enzymes. Through higher functionalization of different organic substances novel raw materials could be formed opening them for different fields in industry. For that reason these two types of enzymes will be discussed in more detail depending on their occurrence, reaction mechanism and current use in industry.

Enzymes of the cytochrome P450 (also called CYP) family are known to release chiral molecules with a high regio- and enantioselectivity.[112] These monooxygenases can be found in nearly all organisms, bacteria, yeasts, insects, mammalian tissues and plants.[113] They play a major role in biosynthesis of steroids and secondary plant metabolites or in detoxification of poorly water-soluble compounds such as drugs or chemical pollutants.[111] Eukaryotic P450 enzymes are often membrane bound, whereas prokaryotic ones are mostly soluble. The name P450 is derived from their absorbance maximum at 450 nm when bound to carbon monoxide.[112] All P450s require NAD(P)H as cofactor and could be divided into four classes depending on the electron transfer to the catalytic cycle.[114] Class I enzymes require an FAD-containing reductase and an iron sulfur redoxin, whereas class II proteins only require an FAD/FMN-containing reductase for the transfer. In contrast, class III proteins are self-sufficient and do not require any electron donors. The P450s of class IV directly receive the electrons from the cofactor NAD(P)H.[114] Among these classes there is a high structural diversity except of three conserved regions:[114] (i) the heme-binding loop, located on the proximal side of the heme; (ii) the conserved Glu-X-X-Arg motif, which is probably responsible for stabilization of the core; and (iii) the central part of helix I, which forms the proton transfer groove on the distal side of the heme.[114] The heme (iron protoporphyrin IX) acts as prosthetic group within the enzyme where the ferric iron is ligated to six ligands (Figure 10).[115] Four of the ligands are represented by nitrogen atoms of the planar porphyrin ring, whereas the fifth ligand is a proximal thiolate anion from the side chain of the deprotonated cysteine residue located in the C-terminal region of the protein.[115]

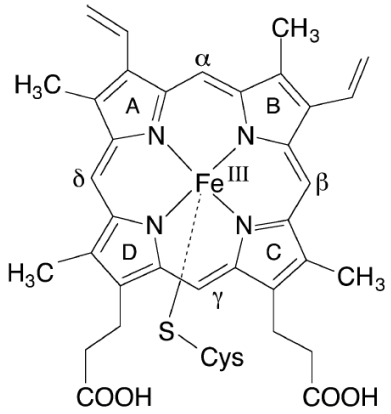

Figure 10: The prosthetic group of cysteinato-heme enzymes. The iron(III) is coordinated by four nitrogen atoms of the protoporphyrin IX and linked to the enzyme by a proximal cysteine ligand (*Meunier et al.*).[113]

In the resting state of the enzyme the sixth, distal ligand is a water molecule (Figure 11).[115] If the substrate enters the binding pocket of the enzyme, this water molecule consequently is replaced by the substrate (state **2**) and the catalytic cycle is initiated by increasing the redox potential of the heme.[116]

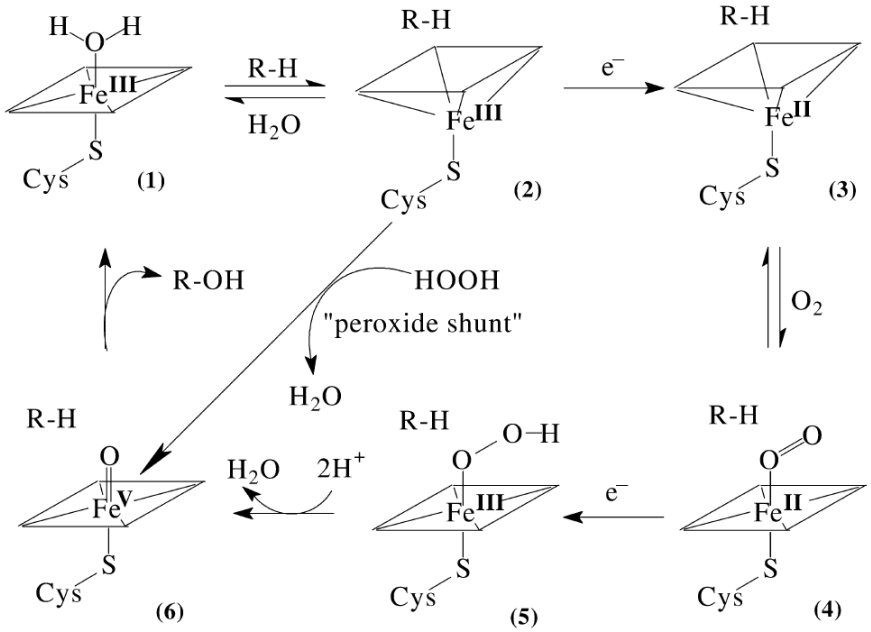

Figure 11: Hydroxylation mechanism for P450 enzymes. The heme of the enzyme is represented by squares. In the resting state of the enzyme the sixth ligand is a water molecule (1). The water molecule is released when the substrate enters the binding pocket (2). After two electron transfers and protonation events the enzyme forms a high-valent iron-oxo intermediate also known as compound I (6), where in the last step the substrate is hydroxylated. Figure according to *Urlacher et al.*.[111]

Consequently, an associated reductase reduces the heme to the Fe^{II} state **3** which then could bind molecular oxygen to yield the ferric superoxide complex **4**.[116] After a second electron transfer and the formation of an iron-peroxo intermediate the heme is protonated to give an iron-hydroperoxy species **5**.[116] Another protonation event is responsible for the cleavage of the oxygen bond while water is released and a high-valent iron-oxo intermediate **6** is formed (also known as compound I).[111] In hydroxylation reactions, thus a hydrogen molecule is abstracted from the substrate to give two radicals, which immediately recombine to produce the hydroxylated product and the enzyme in the resting state.[116] Beside this reaction mechanism a side-pathway called the peroxide shunt is known. There, it has been demonstrated that hydrogen peroxide also can serve as a source of electrons and oxygen for the catalytic cycle and directly produces the iron-oxo species (compound I, Figure 11).[111],[117]

As already mentioned above the selective hydroxylation of non-activated C-H bonds at low pressure and temperature without side-product make P450 enzymes an outstanding biocatalyst. In the meantime over 4,000 members of this family are known with a broad range of substrates[118] and P450 enzymes find use in different enzymatic hydroxylation reactions and whole cell biotransformations.[119] For that reasons and the ability to introduce chiral moieties into carbon backbones, various fine chemicals such as pharmaceuticals or flavors were produced by P450 enzymes.[120],[121]

The chemical BVO to produce lactones out of ketone substrates was discovered in 1899 by *Adolf Baeyer* and *Victor Villiger*.[122] The mechanism is based on the nucleophilic attack of a carbonyl group by a peroxo species which results in the formation of the tetrahedral *Criegee* intermediate.[123] Consequently the *Criegee* intermediate undergoes a rearrangement to the corresponding ester or lactone, respectively (Figure 12).[123]

Common oxidants for the reaction are different acids such as *m*-chloroperoxybenzoic acid, trifluoroperoxyacetic acid, peroxyacetic acid or hydrogen peroxide.[124] The use of toxic and halogenated oxidants and solvents as well as limited regioselectivity are some of the disadvantages of the chemical synthesis of lactones by BVO.[125] These drawbacks lead to a detailed investigation of Baeyer-Villiger monooxygenases (BVMOs) in the recent years.

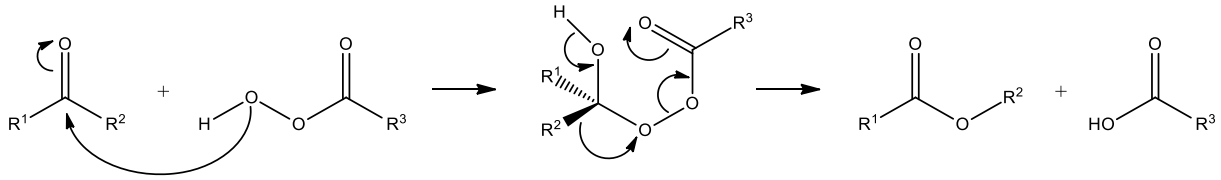

Figure 12: Reaction mechanism for chemical Baeyer-Villiger oxidation. The carbonyl group of the ketone substrate is attacked by a peroxyacid and consequently the tetrahedral *Criegee* intermediate is formed. The intermediate rearranges to form the corresponding ester or lactone (*Roberts et al.*).[124]

BVMOs are monooxygenases catalyzing BVO, sulfoxidation, phosphoxidation, amine oxidation, boron oxidation and selenoxidation by introducing molecular oxygen with a high regio-, enantio- and stereoselectivity.[124],[125] These enzymes can be found in nearly every organism as they catalyze different key steps, for example in the biosynthesis of sesquiterpenoids, aflatoxins or steroids, but are also involved in different degradation pathways, for example of bulky cyclic aliphatic or linear ketones.[126] All BVMOs contain flavin as a prosthetic group which is essential for their activity and could be subdivided into three groups.[127] Type I BVMOs contain a tightly bound FAD as cofactor, are NADPH-dependent and harbor a BVMO fingerprint motif (FXGXXXHXXXWP).[128] In contrast, the BVMO fingerprint motif is absent in type II BVMOs.[129] Type II BVMOs consist of two components, a reductase and an oxygenase, which together form the active BVMO.[129] These enzymes use the reduced FMN (generated by the reductase) as a cofactor and can use NAD(P)H. The third group, namely the type O BVMOs bind FAD on the surface, are NAD(P)H dependent and share a structural relationship to FAD-dependent hydrolases.[129] All BVMOs share one common reaction mechanism which is based on the investigation of the cyclohexanone monooxygenase (CHMO) from *Acinetobacter calcoaceticus* NCIMB 9871.[123] The catalytic cycle is initiated by the reduction of FAD by NADPH, which rapidly binds molecular oxygen to give the flavin 4a-peroxide anion **2** (Figure 13).[130] The flavin 4a-peroxide anion is stabilized by $NADP^+$ and exists in equilibrium with its protonated form **3** in the absence of a substrate.[131],[132] When the substrate enters the binding pocket, the flavin 4a-peroxide anion, but not the protonated one, is able to form the classical tetrahedral *Criegee* intermediate **4** by a nucleophilic attack at the carbonyl group of the substrate.[123],[131] The rearrangement of the intermediate is responsible for the lactone formation and the 4a-hydroxyflavin **5**.[133],[134] In the next step water is eliminated to form FAD and the product

and cofactor are released.[134]

BVMOs can be used for the synthesis of a wide range of chiral and/or biological active compounds, for example steroids. Up to date the main challenges for BVMOs in industrial applications are low thermostability, poor solvent tolerance, substrate and/or product inhibition as well as the dependence on their expensive cofactors NAD(P)H.[125],[135] To overcome these drawbacks a lot of work was done to improve the activity and stability of BVMOs by enzyme engineering and process optimization, such as cofactor regeneration or the use in whole cell biotransformations.[136]

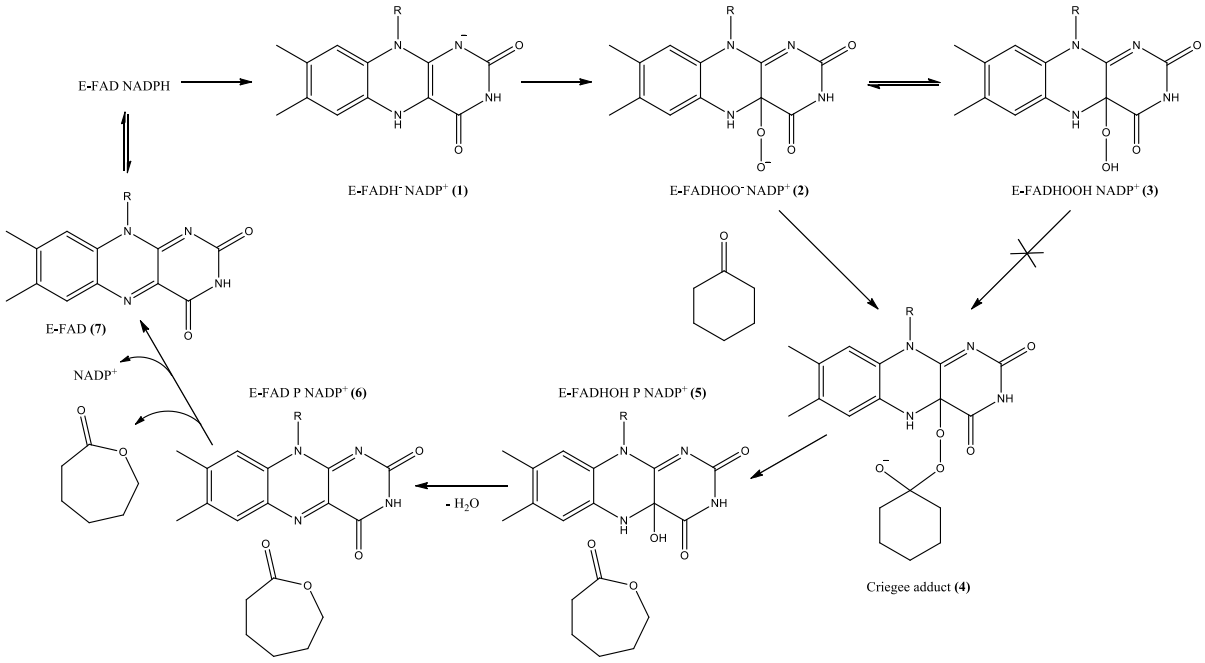

Figure 13: Reaction mechanism for enzyme-catalyzed Baeyer-Villiger oxidation. The mechanism is based on the investigation of the cyclohexanone monooxygenase (CHMO) from *Acinetobacter calcoaceticus* NCIMB 9871 according to *Mihovilovic et al*..[124]

Both types of enzymes could be found in nearly every organism, but in terms of terpene modification the species *Pseudomonas* is of special interest as some strains can grow on the terpenoid camphor as a single carbon source.[78]

1.4 Terpene-based polymers

Since the middle of the last century, efforts have been made to use terpenes for the production of polymers as the main constituent (polyterpenes) or as a polymer conjugate to preserve the properties such as bioactivity.[96] Already in 1937 *Carmody et al.* reported the polymerization of pinene using different solvents (e. g. toluene, benzene, and hexane).[137] The interest in terpenes as monomers for polymers arises from different reasons. As already mentioned many terpenes harbor different functionalities, which can be used for different types of polymerization[96] and furthermore terpenes represent a renewable resources, which meet the criteria for the need of a sustainable development, especially in the last decades. Additionally, some terpenes show properties such as biodegradability, lipophilicity or bioactivity, which are also of high interest for the resulting polymers or polymer conjugates.[96]

One of the first commercial applications of terpenes as polymers was the use as terpenic resin in adhesives, sealants or wax coatings.[138] The term "terpenic resin" describes low molecular weight polymers obtained by cationic polymerization of terpenes.[139] Dipentene as well as α- and β-pinene represent the most commonly used monomers to obtain terpenic resins.[138] The high softening points and compatibility with a broad range of polymers made terpenic resins an ideal tackifying agent.[139],[140] Beside terpenic resins, camphor is also used as an additive in the polymer industry for the production of celluloid (Figure 14).[141] As a mixture of ~ 75 % of cellulose nitrate and ~ 25 % camphor, celluloid represents the oldest thermoplastic polymer made from cellulose and it is still used for the production of table tennis balls.[141]

The most known polymer solely made of terpenes is polyisoprene, which naturally occurs in two forms. Depending on its linkage within the polymer structure it is known as *natural rubber* (*cis*-1,4) or *gutta-percha* (*trans*-1,4).[142] The technical production of *cis*-1,4-polyisoprene is based on the polymerization of isoprene using $TiCl_4/Al(C_2H_5)$ as a catalyst.[142] The worldwide consume of *natural rubber* was about 9.7 x 10^6 t/a and another 1.3 x 10^7 t were technically produced in 2007. Typically, *cis*-1,4-polyisoprene is used as a material for car tires and seals.[142]

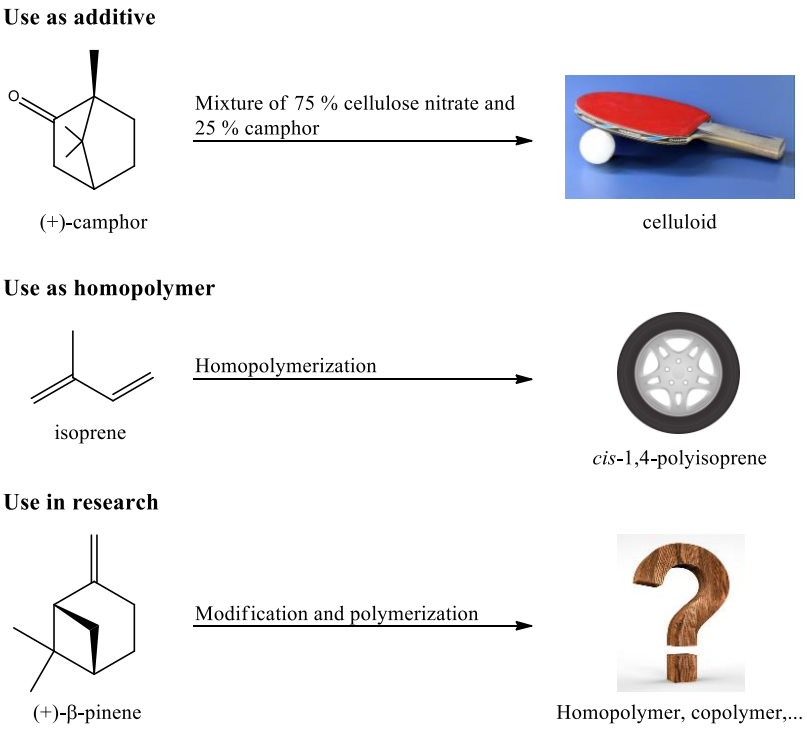

Figure 14: Terpenes in the polymer industry. For example, camphor is used as an additive for the production of table tennis balls, whereas the homopolymers of isoprene, *cis*-1,4-polyisoprene is used in the automobile industry. (+)-*β*-Pinene currently represents one of the most investigated terpene for terpene-based biopolymers. A suitable polymerization technique for the industry as well as its potential application is still to be figured out.

In recent years the demand of a bio-based alternative for common polymers, not only to replace them but also to find new materials with new properties is more and more in the focus. Nevertheless, different challenges still have to be overcome for terpene-based polymers compared to petroleum-based polymers, especially the high production costs and the often relative low molecular weights.[143] Thus, in the last few years chemical modification and polymerization procedures were enhanced to enable terpenes as raw material for biopolymers.[144] As a consequence *β*-pinene, one of the most extensively studied terpene for polymerization, could be used in homopolymerization yielding poly(*β*-pinene) with relatively high molar masses ($M_n \leq 14.0$ kDa) under mild conditions (room temperature, low catalyst loading), which is especially interesting for the production at an industrial scale.[145] Another polymerization approach for poly(*β*-pinene) resulted in higher molecular weights (up to M_n = 40,000 g mol^{-1}), but the conditions to achieve these weights such as low temperatures (- 80 °C), very dilute solutions and high initiator concentrations are not suitable

for an industrial scale.[146] There are more reports for the polymerization of different terpenes such as myrcene or limonene and limonene oxide respectively using different polymerization techniques like emulsion polymerization or copolymerization with CO_2, but up to now none of these monomers combined with the polymerization method is suitable for an industrial scale.[147],[148],[149]

However, as already mentioned terpenes are still in the focus of research because of their properties and sustainable production. What is more, some terpenes arise from already established industries as a cheap by-product and therefore display an attractive source of natural compounds. Thus, in these days and the future researchers will keep on searching for suitable modification and polymerization methods to open these materials for different fields of industries.

1.5 Aim

Terpenes and terpenoids are a wide class of natural substances, which often find use in the medical or flavor industry. In the recent years it has also been shown that some terpenes could be monomers for the production of novel bio-based polymers. Prior to polymerization most of these terpenes have to be modified to build a feedstock for the polymer industry. These modifications include chemical procedures such as *Baeyer-Villiger* oxidation, which make use of functional groups within the terpene backbone. Often these procedures depend on the use of toxic or halogenated chemicals. In contrast, some enzymes are also able to convert these terpenes into monomers under milder conditions. For example *Baeyer-Villiger* monooxygenases (BVMOs) are responsible for the lactonization of carbonyl substrates without the use of toxic chemicals. Other enzymes such as cytochrome P450 enzymes could perform stereo specific hydroxylation reactions of non-activated C-H bonds which is more challenging under chemical conditions. One source for these enzymes is the CAM plasmid of *Pseudomonas putida* ATCC17453 which is responsible for the degradation of the terpenoid camphor.

Within this work different camphor-derived monomers should be produced via biotransformation using *P. putida* and the ability to polymerize the resulting monomers should be analyzed. For the preparation of these monomers three approaches should be investigated: (i) *de novo* synthesis and modification of the terpenoid borneol using the bornyl diphosphate synthase and $P450_{cam}$; (ii) different mutant strains of *P. putida* ATCC17453 where the metabolism of camphor ends at the desired monomer; (iii) biotransformation of different substrates using *P. putida* KT2440 and recombinant expression of $P450_{cam}$ and BVMOs (Figure 15). The most promising approach should be further optimized regarding the yield of the monomer. Following this, a suitable process should be implemented in order to produce grams of monomer in an automatic system. Furthermore an appropriate polymerization procedure for the monomer should be developed and the resulting biopolymer should be analyzed regarding its molecular weight and thermal properties.

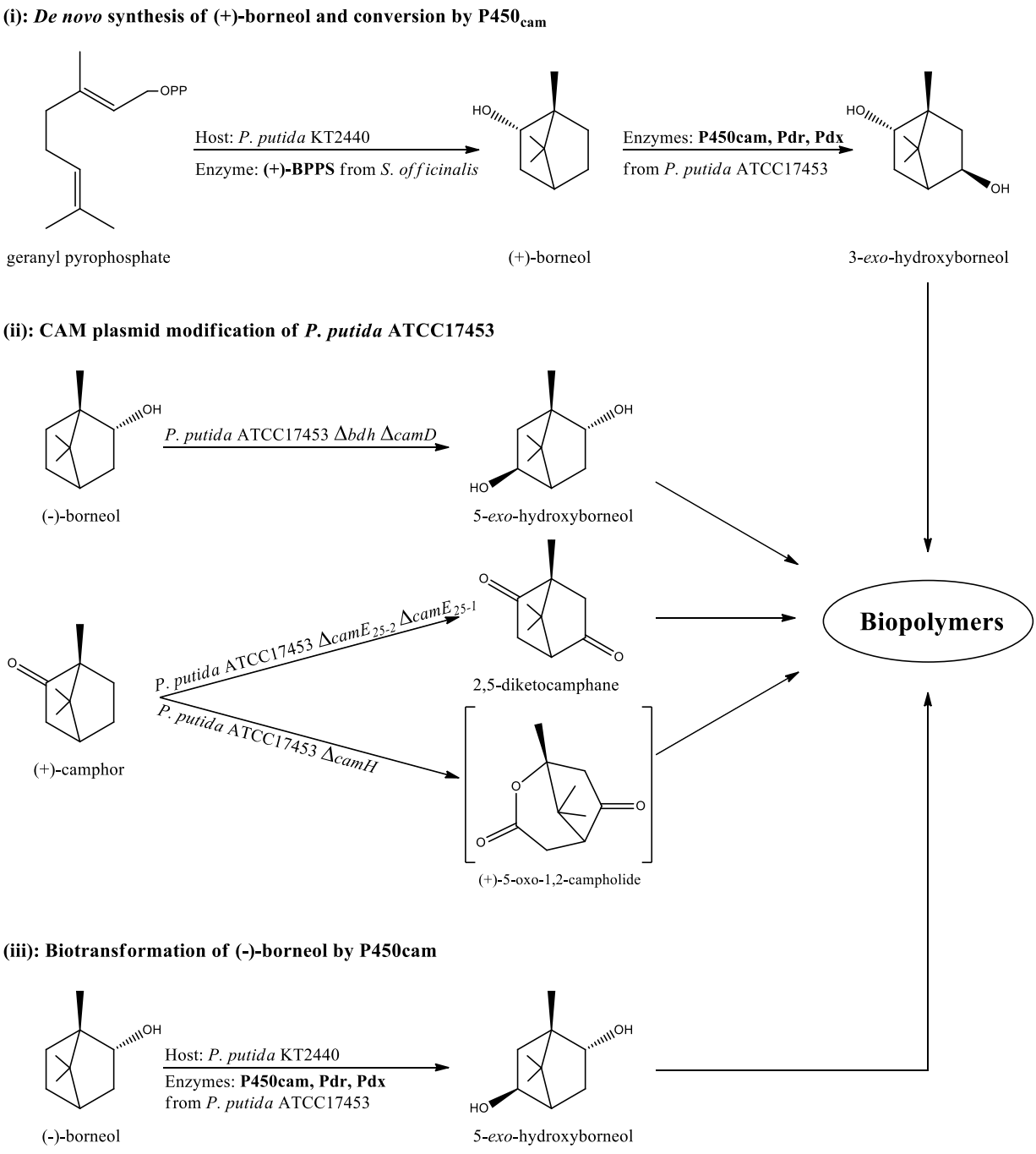

Figure 15: Different strategies to obtain terpene-based monomers for novel biopolymers. (i): Recombinant expression of (+)-BPPS from *S. officinalis* and $P450_{cam}$, Pdr, Pdx from *P. putida* ATCC17453 for the *de novo* synthesis of hydroxyborneol using *P. putida* KT2440 as a host organism. (ii): Deletion of different genes on the CAM plasmid of *P. putida* ATCC17453 yield different mutant strains for the production of different terpene-based monomers. (iii): Biotransformation of (-)-borneol by recombinant expression of P450cam, Pdr and Pdx from *P. putida* ATCC17453 using *P. putida* KT2440 as a host organism.

2 Material and methods

2.1 Material

2.1.1 Chemicals, media and buffers

All enzymes and chemicals were purchased from the following companies as listed (Table 2).

Table 2: List of the chemicals used within this work and their supplier.

Chemical	Supplier
(-)-Borneol	Sigma Aldrich, St. Louis, USA
(-)-Camphor	Alfa Aesar, Ward Hill, USA
(+)-Borneol	Sigma Aldrich, St. Louis, USA
(+)-Camphor	Sigma Aldrich, St. Louis, USA
(±)-Isoborneol	Sigma Aldrich, St. Louis, USA
Acetic acid	VWR International LLC, Radnor, USA
Acetonitrile	Th. Geyer GmbH & Co. KG, Renningen, Germany
Acrylamide-, bis-acrylamide stock solution [30 % (w/v), 37.5:1]	VWR International LLC, Radnor, USA
Agar Kobe I	Carl Roth GmbH, Karlsruhe, Germany
Agarose basic	AppliChem GmbH, Darmstadt, Germany
Ammonium formate	Sigma Aldrich, St. Louis, USA
Ammonium persulfate [10 % (w/v)]	AppliChem GmbH, Darmstadt, Germany
Ammonium sulfate	AppliChem GmbH, Darmstadt, Germany
Ampicillin sodium salt	AppliChem GmbH, Darmstadt, Germany
ABTS	Sigma Aldrich, St. Louis, USA
BCIP	AppliChem GmbH, Darmstadt, Germany

Bromphenol blue	AppliChem GmbH, Darmstadt, Germany
BSA	AppliChem GmbH, Darmstadt, Germany
$CaCl_2$	VWR International LLC, Radnor, USA
$CaCO_3$	Sigma Aldrich, St. Louis, USA
Cetrimide agar	Sigma Aldrich, St. Louis, USA
Chloramphenicol	AppliChem GmbH, Darmstadt, Germany
Chloroform : isoamyl alcohol (24 : 1)	AppliChem GmbH, Darmstadt, Germany
Coomassie Brilliant blue G250	VWR International LLC, Radnor, USA
Coomassie Brilliant blue R250	VWR International LLC, Radnor, USA
$CoSO_4$	Sigma Aldrich, St. Louis, USA
$CuSO_4$	VWR International LLC, Radnor, USA
Deuterated formic acid	Sigma Aldrich, St. Louis, USA
DMSO	Sigma Aldrich, St. Louis, USA
dNTPs	Rapidozym GmbH, Berlin, Germany
Dodecane	Sigma Aldrich, St. Louis, USA
DTT	VWR International LLC, Radnor, USA
ε-Caprolactone	Sigma Aldrich, St. Louis, USA
EDTA	VWR International LLC, Radnor, USA
Ethanol	Carl Roth GmbH, Karlsruhe, Germany
Ethidiumbromide	VWR International LLC, Radnor, USA
$FeSO_4$	Sigma Aldrich, St. Louis, USA
Gentamycin sulfate	AppliChem GmbH, Darmstadt, Germany
Geranyl diphosphate	Sigma Aldrich, St. Louis, USA
Glucose	VWR International LLC, Radnor, USA

Glycerol	Carl Roth GmbH, Karlsruhe, Germany
H_3BO_3	VWR International LLC, Radnor, USA
HCl (37 %)	VWR International LLC, Radnor, USA
HEPES	AppliChem GmbH, Darmstadt, Germany
HFIP	Sigma Aldrich, St. Louis, USA
Imidazole	VWR International LLC, Radnor, USA
IPTG	Carl Roth GmbH, Karlsruhe, Germany
K_2HPO_4	VWR International LLC, Radnor, USA
Kanamycin sulfate	AppliChem GmbH, Darmstadt, Germany
KCl	VWR International LLC, Radnor, USA
KH_2PO_4	Carl Roth GmbH, Karlsruhe, Germany
L-Rhamnose	Sigma Aldrich, St. Louis, USA
Methanol	VWR International LLC, Radnor, USA
$MgCl_2$	Carl Roth GmbH, Karlsruhe, Germany
$MgCl_2$, for PCR	Rapidozym GmbH, Berlin, Germany
MgO	Sigma Aldrich, St. Louis, USA
$MnCl_2$	Merck KGaA, Darmstadt, Germany
$MnSO_4$	VWR International LLC, Radnor, USA
MOPSO	Carl Roth GmbH, Karlsruhe, Germany
Na_2HPO_4	AppliChem GmbH, Darmstadt, Germany
NaAc	AppliChem GmbH, Darmstadt, Germany
NaCl	VWR International LLC, Radnor, USA
NAD	VWR International LLC, Radnor, USA
NADH di sodium salt	Carl Roth GmbH, Karlsruhe, Germany

NADP	Carl Roth GmbH, Karlsruhe, Germany
NADPH di sodium salt	Carl Roth GmbH, Karlsruhe, Germany
NaH_2PO_4	VWR International LLC, Radnor, USA
NaOH granulate	Sigma Aldrich, St. Louis, USA
NaTFA	Sigma Aldrich, St. Louis, USA
NBT	Sigma Aldrich, St. Louis, USA
n-Hexane	Th. Geyer GmbH & Co. KG, Renningen, Germany
Potassium formate	Sigma Aldrich, St. Louis, USA
SDS 20 % solution	Sigma Aldrich, St. Louis, USA
Succinic acid dimethyl ester	Sigma Aldrich, St. Louis, USA
Taq polymerase buffer	Rapidozym GmbH, Berlin, Germany
Tetracycline HCl	AppliChem GmbH, Darmstadt, Germany
Tetramethylethylenediamine	VWR International LLC, Radnor, USA
Tin(II) acetate	Alfa Aesar, Ward Hill, USA
Tris	VWR International LLC, Radnor, USA
Tris base	VWR International LLC, Radnor, USA
Triton X-100	VWR International LLC, Radnor, USA
Tween20	VWR International LLC, Radnor, USA
Yeast extract	Carl Roth GmbH, Karlsruhe, Germany
$ZnCl_2$	VWR International LLC, Radnor, USA
$ZnSO_4$	Alfa Aesar, Ward Hill, USA
β-Mercaptoethanol	Sigma Aldrich, St. Louis, USA

The different enzymes, which were used in this work are listed in Table 3.

Table 3: List of the enzymes used within this work and their supplier.

Enzyme	Supplier
BamHI HF	New England Biolabs, Ipswich, USA
BbsI	New England Biolabs, Ipswich, USA
BglII	New England Biolabs, Ipswich, USA
BsaI HF	New England Biolabs, Ipswich, USA
BsmBI	New England Biolabs, Ipswich, USA
DNase I	AppliChem GmbH, Darmstadt, Germany
DpnI	New England Biolabs, Ipswich, USA
EcoRI HF	New England Biolabs, Ipswich, USA
Formate dehydrogenase from *Candida boidinii*	VWR International LCC., Radnor, USA
Glucose oxidase from *Aspergillus niger*	Sigma Aldrich, St. Louis, USA
HindIII	New England Biolabs, Ipswich, USA
Lysozyme	Carl Roth GmbH, Karlsruhe, Germany
NcoI	New England Biolabs, Ipswich, USA
NdeI	New England Biolabs, Ipswich, USA
NotI	New England Biolabs, Ipswich, USA
Pfu polymerase	New England Biolabs, Ipswich, USA
Phusion polymerase	New England Biolabs, Ipswich, USA
Peroxidase from horseradish	Sigma Aldrich, St. Louis, USA
Q5 polymerase	New England Biolabs, Ipswich, USA
Taq polymerase	Rapidozym, Berlin, Germany
XhoI	New England Biolabs, Ipswich, USA

All media were autoclaved at 121 °C and 2 bar for 20 min. All heat-labile solutions were sterilized by filtration (0.2 µm) and added to the corresponding medium at RT. For agar plates 1.5 % (w/v) agar-agar was added to the corresponding medium. Antibiotics for selective media were sterilized by filtration (0.2 µm) and added after the media were allowed to cool down at RT. The composition of the different media is shown in Table 4.

Table 4: Composition of the different media.

Medium	Components
Lysogeny Broth (LB) medium pH 7.0 adj. with HCl	5 g L^{-1} Yeast extract 10 g L^{-1} NaCl 10 g L^{-1} Tryptone
LB-low salt medium pH 7.0 adj. with HCl	5 g L^{-1} Yeast extract 5 g L^{-1} NaCl 10 g L^{-1} Tryptone
SOC medium pH 7.0 adj. with HCl	5 g L^{-1} Yeast extract 0.5 g L^{-1} NaCl 0.3 g L^{-1} KCl 20 g L^{-1} Tryptone Ad 10 mM $MgCl_2$ and 20 mM glucose after autoclaving
Terrific Broth (TB) medium pH 7.0 adj. with HCl	24 g L^{-1} Yeast extract 12 g L^{-1} Tryptone 8 mL L^{-1} glycerol 2.2 g L^{-1} KH_2PO_4 2.2 g L^{-1} K_2HPO_4
P-medium pH 7.0 adj. with H_3PO_4	2 g L^{-1} KH_2PO_4 4 g L^{-1} Na_2HPO_4 1 g L^{-1} $(NH_4)_2SO_4$ 2.5 g L^{-1} glucose 0.4 % TMS

Cetrimide agar pH 7.2	46.6 g L^{-1} Cetrimide
adj. with HCl	10 mL L^{-1} glycerol

The composition of buffers, staining solutions and antibiotics is shown in Table 5.

Table 5: Composition of buffers, staining solutions and antibiotics.

Buffers/staining solutions/antibiotics	Components
Lysis buffer for Gram negative bacteria	5 mL L^{-1} acetic acid
pH 7.8, adj. with HCl	240 g L^{-1} Tris
	1.64 g L^{-1} NaAc
	0.37 g L^{-1} EDTA
	100 mL L^{-1} SDS
50x TAE buffer pH 8.0 for agarose gel	242.3 g L^{-1} Tris
electrophoresis	16.41 g L^{-1} EDTA
	57.1 mL L^{-1} acetic acid
Ethidium bromide staining solution for agarose gel electrophoresis	5 drops ethidiumbromide in 1x TAE buffer
10x SDS running buffer pH 8.3	30.29 g L^{-1} Tris base
adj. with HCl	144.13 g L^{-1} glycine
	50 mL L^{-1} SDS solution [20 % (w/v)]
2x SDS sample buffer pH 6.8 adj. with HCl	100 mL L^{-1} Tris (stock solution 1.5 M) 150 mL L^{-1} β-mercaptoethanol
	300 mL L^{-1} glycine
	60 mL L^{-1} SDS solution [20 % (w/v)]
	20 mg L^{-1} bromophenol blue
Coomassie staining solution for SDS-PAGE analysis	50 % (v/v) methanol
	10 % (v/v) acetic acid
	0.2 % (w/v) Coomassie Brilliant blue R250
	0.2 % (w/v) Coomassie Brilliant blue G250
TBS buffer pH 7.5 for western blot analysis, adj. with NaOH	10 mM Tris-HCl
	150 mM NaCl

TBST buffer pH 7.5 for western blot analysis, adj. with NaOH	20 mM Tris-HCl 500 mM NaCl 0.05 % (v/v) Tween20 0.2 % (v/v) Triton X-100
Semi-dry buffer pH 8.3 for western blot analysis, adj. with HCl	25 mM Tris-base 150 mM glycine 10 % (v/v) methanol
Blocking buffer pH 7.5 for western blot analysis	0.3 % (w/v) BSA in TBS buffer
Antibody solution (primary and secondary) for western blot analysis	0.2 mg mL^{-1} antibody in H_2O
Staining solution pH 9.5 for western blot analysis, adj. with NaOH	100 mM Tris-HCl 100 mM NaCl 5 mM $MgCl_2$ 66 µL of 5 % NBT (70 % in DMF) per 10 mL 33 µL of 5 % BCIP (100 % in DMF) per 10 mL
Lysis buffer pH 7.5 for his-tagged protein purification of CamH adj. with NaOH	50 mM Tris-HCl 100 mM NaCl 5 mM DTT 10 % (v/v) glycerol 1 mM $ZnCl_2$
Elution buffer pH 7.5 for his-tagged protein purification of CamH adj. with NaOH	50 mM Tris-HCl 100 mM NaCl 5 mM DTT 10 % (v/v) glycerol 1 mM $ZnCl_2$ 500 mM imidazole
Desalting buffer pH 7.5 for CamH adj. with NaOH	50 mM Tris-HCl 1 mM $ZnCl_2$
Lysis buffer pH 8.0 for his-tagged protein purification of Bdh, adj. with HCl	50 mM Na_3PO_4 500 mM NaCl 20 mM imidazole

Elution buffer pH 8.0 for his-tagged protein purification of Bdh, adj. with HCl	50 mM Na_2PO_4 500 mM NaCl 500 mM imidazole
Desalting buffer pH 8.0 for Bdh	50 mM Na_3PO_4
Activity assay buffer pH 8.0 (+)-BPPS	
TB buffer pH 6.7 for heat shock transformation, adj. with HCl	10 mM HEPES 15 mM $CaCl_2$ 55 mM $MnCl_2$ 250 mM KCl
1000x Ampicillin stock solution	100 mg mL^{-1} ampicillin sodium salt in H_2O
1000x Chloramphenicol stock solution	34 mg mL^{-1} chloramphenicol in ethanol
1000x Gentamycin stock solution	10 mg mL^{-1} gentamycin sulfate in H_2O
1000x Kanamycin stock solution	30 mg mL^{-1} kanamycin sulfate in H_2O
1000x Tetracycline stock solution	12.5 mg mL^{-1} tetracycline HCl in ethanol

2.1.2 Strains, plasmids, and oligonucleotides

In Table 6 the different strains used in this work are listed.

Table 6: Different microorganisms used in this work.

Microorganism	Strain	Genotype	Source
E. coli	DH10B	F^- mcrA Δ(mrr-hsdRMS-mcrBC) φ80lacZΔM15 ΔlacX74 recA1 endA1 araD139 Δ(ara, leu)7697 galU galK λ^- rpsL nupG /pMON14272 / pMON7124	Invitrogen
	BL21(DE3)	F^- ompT gal dcm lon hsdSB(rB- mB^-) λ(DE3 [lacI lacUV5-T7 gene 1 ind1 sam7 nin5])	Novagen
	DH5α λpir	sup E44, ΔlacU169 (ΦlacZΔM15), recA1, endA1, hsdR17, thi-1, gyrA96, relA1, λpir phage lysogen	
	HB101 pRK2013	upE44, ΔlacU169(ΦlacZΔM15), recA1, endA1, hsdR17, thi-1, gyrA96, relA1, pRK2013 (Km^R oriColE1 RK2-Mob^+ RK2-Tra^+)	
P. putida	KT2440	rmo- mod+	DSMZ
	ATCC17453		DSMZ

All constructs of plasmids used in this work are listed in Table 7.

Table 7: Constructed plasmids used in this work.

Plasmid	Properties
pET28a	Km^R, expression vector
pET28a::*bpps*	Km^R, expression (+)-bornyl diphosphate synthase from *S. officinalis*
pET28a::*bpps-N-his*	Km^R, expression (+)-bornyl diphosphate synthase with N-terminal his tag from *S. officinalis*
pET28a::*bpps-C-his*	Km^R, expression (+)-bornyl diphosphate synthase with C-terminal his tag from *S. officinalis*
pET28a::*bpps-E50*	Km^R, expression of a truncated (+)-bornyl diphosphate synthase missing the first 50 aa from *S. officinalis*
pET28a::*bpps-E50-C-his*	Km^R, expression (+)-bornyl diphosphate synthase with C-terminal his tag from *S. officinalis*

pET28a::*camH*	Km^R, expression native *camH*
pET28a::*camH-N-his*	Km^R, expression *camH* with N-terminal his tag
pET28a::*camH-C-his*	Km^R, expression *camH* with C-terminal his tag
pET28a::*bdh*	Km^R, expression native borneol dehydrogenase from *P. putida* ATCC17453
pET28a::*bdh-N-his*	Km^R, expression borneol dehydrogenase from *P. putida* ATCC17453 with N-terminal his tag
pET28a::*bdh-C-his*	Km^R, expression borneol dehydrogenase from *P. putida* ATCC17453 with C-terminal his tag
pJH14	Km^R, vector encoding for the biosynthesis of zeaxanthin
pJH14::*bpps-E50*	Km^R, vector encoding for a truncated (+)-bornyl diphosphate synthase from *S. officinalis* together with dxs and idi from *E. coli*
pBBr122	Km^R, expression vector
pBBr122::*camDCAB*	Km^R, expression of the cam operon *camDCAB* from *P. putida* ATCC17453 under control of the constitutive camphor promoter
pBBr122::*camCAB*	Km^R, expression of the cam operon *camCAB* from *P. putida* ATCC17453 under control of the constitutive camphor promoter
pBBr122::*bpps*	Km^R, expression (+)-bornyl diphosphate synthase from *S. officinalis*
pBBr122:*bpps-N-his*	Km^R, expression (+)-bornyl diphosphate synthase with N-terminal his tag from *S. officinalis*
pBBr122:*bpps-C-his*	Km^R, expression (+)-bornyl diphosphate synthase with C-terminal his tag from *S. officinalis*
pBBr122:*bpps-E50*	Km^R, expression of a truncated (+)-bornyl diphosphate synthase missing the first 50 aa from *S. officinalis*
pBBr122::$camE_{25\text{-}1}$	Km^R, expression of 2,5-DKCMO-1 from *P. putida* ATCC17453 under control of the constitutive camphor promoter
pBBr122::$camE_{36}$	Km^R, expression of 3.6-DKCMO from *P. putida* ATCC17453 under control of the constitutive camphor promoter
pBBr122::*camG*	Km^R, expression of OTEMO from *P. putida* ATCC17453 under control of the constitutive camphor promoter
pSW-II	$Genta^R$, expression of I-SceI nuclease under control of a 3-methyl-benzoate inducible promoter
pEMG	Km^R, does only replicate in λpir strains, harbors two SceI sites, host vector for the deletion in *P. putida* ATCC17453
pEMG::Δ*camD*	Km^R, harbors two SceI sites and 1000 bp down- and upstream of *camD* for the genome integration in *P. putida* ATCC17453

pEMG::Δ*bdh*	Km^R, harbors two SceI sites and 1000 bp down- and upstream of *bdh* for the genome integration in *P. putida* ATCC17453
pEMG::Δ*camE*$_{25-1}$	Km^R, harbors two SceI sites and 1000 bp down- and upstream of *camE*$_{25-1}$ for the genome integration in *P. putida* ATCC17453
pEMG::Δ*camE*$_{25-2}$	Km^R, harbors two SceI sites and 1000 bp down- and upstream of *camE*$_{25-2}$ for the genome integration in *P. putida* ATCC17453
pEMG::Δ*camH*	Km^R, harbors two SceI sites and 1000 bp down- and upstream of *camG* for the genome integration in *P. putida* ATCC17453

All oligonucleotides are listed in 5'-3' direction in the following tables and were obtained from Eurofins Genomics GmbH (Ebersberg).

Table 8: Oligonucleotides used for the cloning of (+)-BPPS. Sequences are listed in 5'-3' direction.

Oligonucleotide	Sequence
bpps fwd	AGCGACTTCTTCCAGGACGAAATC
bpps rev	CAGTAGCACAGCTGCATGTAG
bppshisfwd	ATCGGAATTCATGCACCACCACCACCACCACTCGATCATCTCGATGAATG
bppsrev	GGCCAGATCTTCAGGCGTAG
bppsfwd	GAGCGACGCGATGAGAATTCATGTCGATCATCTC
bppshisrev	GATCAGATCTTCAGTGGTGGTGGTGGTGGTGGGCGTAGGGCTCAAAG
bpps_nco_fwd	GCATCGCCATGGATGTCGATCATCTCGATGAATG
bpps_hind_rev	GCTGAAGCTTTCAGGCGTAGGGCTC
bpps_ov_fwd	CAAGGTCCTCTTGTTGTTGTATGTCGATCATCTC
bpps_bglII_rev	GATCAGATCTTCAGGCGTAG
pJH14_crtZ_fwd	GATCGAAGACCGGGAAGTAAGTTTAAACTGTACAAG
pJH14_crtE_rev1	TAAACGGATACATTCGGGCTGT
pJH14_crtE_rev2	GATCGAAGACCATTCGGGCTGTCCTTATAAAC
bpps_pJH14_fwd	GATCGAAGACCCCGAATGTCGATCATCTCGATG
bpps_pJH14_rev	GATCGAAGACCATTCCTCAGGCGTAGGGCTC
zea_crte_fwd	TTATAAGGACAGCCCGAATG
zea_crtz_rev	CTTTCTGTACCGCGATCTC
zea_crtz_fwd	GAAAGACATGGCGCTAGAG
zea_crte_rev	ATTCGGGCTGTCCTTATAAAC
bpps_fwd_blunt	ATGTCGATCATCTCGATGAATG

crte_rev_blunt	TCGGGCTGTCCTTATAAACCCC
bpps_seq_fwd_1	GCGCCAACATGGCTTC
bpps_seq_fwd_2	TACGGGACGCTGGATG
bpps_seq_rev	CTGGATGCGCCAGTG
pJH14_seq_fwd	CAGACAAGCCCGTCAG
pJH14_seq_rev	TTCCGGCTCGTATGTTG
bpps_E50_EcoRI_fwd	GATCGAATTCATGGAGGCTCACCAGATCCG
bpps_E50_BglII_rev	ATCGCCCACAGATCTTCAG
bpps_E50_blunt_fwd	ATGGAGGCTCACCAGATCCG
bpps_E50_NcoI_fwd	GATCCCATGGATGGAGGCTCACCAGATCCG
bpps_E50_His_HindIII_rev	GATAAGCTTTTAGTGGTGGTGGTGGTGGTGGGCGT AGGGCTCAAA
pJH14_LIC_fwd	GTTTAAACTGTACAAGTAAGCTTAC
pJH14_LIC_rev	TTCGGGCTGTCCTTATAAAC
bpps_LIC_fwd	GGCATAATGTTTGGGGTTTATAAGGACAGCCCGAA TGTCGATCATCTCGATGAATG
bpps_LIC_E50_fwd	GGCATAATGTTTGGGGTTTATAAGGACAGCCCGAA TGGAGGCTCACCAGATCCG
bpps_LIC_rev	CAATAAACCGGTAAGCTTACTTGTACAGTTTAAAC TCAGGCGTAGGGCTC
bpps_LIC_His_rev	CAATAAACCGGTAAGCTTACTTGTACAGTTTAAAC TCAGTGGTGGTGGTGGTG
bpps_pat_LIC_fwd	GGCATAATGTTTGGGGTTTATAAGGACAGCCCGAA TGCGTCGTTCGGGTAACTAC

Table 9: Oligonucleotides used for the cloning of 2,5-DKCMO-I, 3,6 DKCMO, OTEMO, CamH and Bdh. Sequences are listed in 5'-3' direction.

Oligonucleotide	Sequence
25BVMO_pME_fwd	GATCGGTCTCTAATTATGAAATGCGGATTTTTCCATAC
25BVMO_pME_rev	GATCGGTCTCGTCGATCAGCCCATTCGAACCTTC
36BVMO_pME_fwd	GATCCGTCTCTAATTATGGCAATGGAAACTGGTTTG
36BVMO_pME_rev	GATCCGTCTCGTCGATCAACGCTTAGGCAGGAG
oxoBVMO_pME_fwd	GATCCGTCTCTAATTATGAGCAATAGAGCAAAAAG
oxoBVMO_pME_rev	GATCCGTCTCGTCGATTAGGCGAGTTCAAATCCG
camH-pET-fwd	GATCCCATGGATGCGCAAGTTCAGATCCTTCG
camH-pET-rev	GATAGCGGCCGCTCAGGGGTGGTCTCCAACTG
camH-pET-His-fwd	GATCCCATGGATGCACCACCACCACCACCACCGCAAGTT CAGATCCTTCG
camH-pET-His-rev	GATAGCGGCCGCTCAGTGGTGGTGGTGGTGGTGGGGGTG GTCTCCAACTG
Bdh-NcoI-fwd	GATCCCATGGATGAAACCGCTAGCAGG

Bdh-NotI-rev	GATAGCGGCCGCTCAACCAGACAATCGATTG
Bdh-NcoI-His-fwd	GATCCCATGGATGCACCACCACCACCACCACAAACCGCTAGCAGGTAAAAG
Bdh-NotI-His-rev	GATAGCGGCCGCTCAGTGGTGGTGGTGGTGGTGACCAGACAATCGATTGCC

Table 10: Oligonucleotides used for the knockout of *camD*, *camH*, *bdh*, $camE_{25\text{-}1}$ and $camE_{25\text{-}2}$. Sequences are listed in 5'-3' direction.

Oligonucleotide	Sequence
camD-CPCR-fwd	CGGTTATCAGGTAGAACAAGTG
camD-CPCR-rev	CTGGGGTTCTCAGGTACAG
camD-LF-fwd	ATCTACCCTTTCCCGGGCTTG
camD-LF-rev	GATCCGTCTCTGCATTACCTCGTTCTTATTGTGTTGTGG
camD-RF-fwd	GATCGGTCTCAATGCCCAACCCGCGTTCCAGG
camD-RF-rev	ATCTGCGGTAGCAGGATCTGG
camD-Seq-fwd	CTCAAGCCTGAGGGTAAAC
camD-Seq-rev	CCGTTGCAGCGAGTCC
camH-CPCR-fwd	ATAGCATGTTCACCAGCATCGC
camH-CPCR-rev	TTGCACTACGACGGTGTCATC
camH-LF-fwd	TACAACATTAGACGCAGCAC
camH-LF-rev	GATCGGTCTCAGAGTGATTCTCTGTAACGAACTG
camH-RF-fwd	GATCCGTCTCAACTCAACAAACTCGGCACGAACCC
camH-RF-rev	ACCAGTGCCCCACCTGG
camH-Seq-fwd	AATCGAGCTTGAAGTAGACTCC
camH-Seq-rev	GATTTAGCCCAGTTCCATGC
LF camH BbsI fwd	GATCGAAGACAGAATTCCCGACGACTCTACAACATTAGACGC
LF camH rev	CGAGTTTGTTGAGTGATTCTCTGTAACGAACTGTTTTCGC
RF camH fwd	AGAATCACTCAACAAACTCGGCACGAACCCG
RF camH BamHI rev	GATCGGATCCCTAGCACCACGCGTACCAGTG
CPCR orf16 fwd	ATGGCGACCTTACCCGACAATC
CPCR orf16 rev	CCTCGCTGGTTCTGGTGGC
LF-orf16-EcoRI-fwd	TCAGGAATTCGTCCATGCAGGAGACGATGGATC
LF-orf16-rev	CGAGGCCAGCAGCTGCCTTCCTATTGTCTGTC
RF-orf16-fwd	GAAGGCAGCTGCTGGCCTCGGCCATGGAAC
RF-orf16-BsaI-rev	GATCGGTCTCCGATCTGCGCGGCCTGCACATCC
Seq orf16 fwd	TGCGTGCAGTTGATGG
Seq orf16 rev	TAAGCTGCCGGGATTGC
CPCR 2,5-BVMO-II-fwd	GGCCTGTTTCACATCGAGCG
CPCR 2,5-BVMO-II-rev	TGAGCTGTATCAGCGGTTTCTGG

LF 2,5-BVMO-II-EcoRI-fwd	GATCGAATTCAACAGGGAGTGATAGCCCCAG
LF 2,5-BVMO-II-rev	GGAAATGACTGGAGACGTGCCCGGGAC
RF 2,5-BVMO-II-fwd	GCACGTCTCCAGTCATTTCCTCTCATTTTTGTTCTAG
RF 2,5-BVMO-II-BamHI-rev	GATCGGATCCTCGGTTTGCACTCCAAGC
2,5-BVMO-II-Seq-fwd	TTACCGGCAACGGAAAAC
2,5-BVMO-II-Seq-rev	TAGGCTTCAACGAACTGTTC
CPCR 2,5-BVMO-I-fwd	TCGCATGCCTGACATCAAG
CPCR 2,5-BVMO-I-rev	CATCAATTGCATGGGCTTCGTCG
LF 2,5-BVMO-I-EcoRI-fwd	GATCGAATTCACCATCCTCGAGTATGTG
LF 2,5-BVMO-I-rev	TGGTGTTCCCAGTGTGTCCTCTTATCGGTC
RF 2,5-BVMO-I fwd	AGGACACACTGGGAACACCAATTCGGGAGAGG
RF 2,5-BVMO-I-BbsI-rev	GATCGAAGACTCGATCCATCTCCTCGCTCAGTTCAACAGC
2,5-BVMO-I-Seq-fwd	AATGCCTGGTGGGTCAAG
2,5-BVMO-I-Seq-rev	TATAGGGCGGTGCGTTG

Table 11: Oligonucleotides used for the quantification of the CAM plasmid. Sequences are listed in 5'-3' direction.

Oligonucleotide	Sequence
qPCR camD fwd	CGACGTGCACATCGTATC
qPCR camD rev	TTTCGATGCGGCCAATG
qPCR camA fwd	CCTATGCAGCGCAGAAC
qPCR camA rev	ATACCAGCCGGTCGTAATC
qPCR camC fwd	CAGTGCAACTTCACCGAG
qPCR camC rev	CGGGTCATCTGATCCGTTAG

2.1.3 Devices, software and consumables

Mostly used devices:

Fluorescence-UV/VIS-spectral photometer

Infinite 200 pro	Tecan Group Ltd., Männedorf, Schweiz
ECM630 Electro Cell Manipulator	Havard Apparatus, Holliston MA, USA
ÄKTA™ purifier	GE Healthcare Europe GmbH, Freiburg
GC-MS QP 2010 Plus	Shimadzu Corporation, Kyoto, Japan

Freezer (- 20 °C) GGU 1500	Liebherr-International Deutschland GmbH, Biberach an der Riß
Freezer (- 80 °C)	GFL Gesellschaft für Labortechnik mbH, Burgwedel
Agarose gel chamber GH100 Series	Biostep GmbH, Jahnsdorf
DH-40 Felix 6020 documentation system	Biostep GmbH, Jahnsdorf
Hamilton syringe 50 µL	Hamilton AG, Bonaduz, Schweiz
High-pressure homogenizer	Constant Systems LTD, Daventry, GB
Incubator and shaker (Innova42 and Innova40 Incubator Shaker Series)	New Brunswick Co., Inc.
Thermomixer Comfort	Eppendorf AG, Hamburg
TiMix 5 control	Edmund Bühler GmbH, Hechingen
Refrigerator FKEX 1800	Liebherr-International Deutschland GmbH, Biberach an der Riß
FLUOstar Omega	BMG Labtech, Ortenberg
PCR Thermocycler peqSTAR 2X	VWR International LLC, Radnor, USA
pH meter pHenomenal	VWR International LLC, Radnor, USA
Milli Q ultra pure system	Merck KGaA, Darmstadt
Sonicator Q700 Microplate Horn	Qsonica LLC., Newtown CT, USA
UV/VIS-spectral photometer UV 1800	Shimadzu Corporation, Kyoto, Japan
Cubis MSA balance	Sartorius AG, Göttingen
P-40 02 balance	Sartorius AG, Göttingen
Water bath	LAUDA Dr. R. Wobser GmbH & CO. KG, Lauda-Königshofen
Ultraspec 10	GE Healthcare Europe GmbH, Freiburg
Centrifuge 1-14	Sigma Laborzentrifugen GmbH, Osterode

Centrifuge 1-15 PK	Sigma Laborzentrifugen GmbH
Avanti J-E Centrifuge	Beckmann Coulter GmbH, Brea, USA
Peristaltic pump LA-900	Landgraf Laborsysteme HLL GmbH
Safe 2020 sterile workbench	Thermo Fisher Scientific GmbH

Software and databases:

Basic Local Alignment Search Tool (BLAST)	National Centre for Biotechnology Information (http://blast.ncbi.nlm.nih.gov/)
BioEdit 7.2.5	Isis Pharmaceutical, Carlsbad, USA
Braunschweig Enzyme Database (BRENDA)	Technische Universität Braunschweig, Institut für Biochemie und Biotechnologie (http://brenda-enzymes.info/)
Clone Manager 9	Scientific & Educational Software, Cary, USA
National Centre for Biotechnology Information (NCBI)	http://ncbi.nlm.nih.gov/
SWISS-MODEL	Universität Basel, Schweiz, Swiss Institute of Bioinformatics, Protein Structure, Bioinformatics Group (http://swissmodel.expasy.org/)
Argus 1.0	Biostep GmbH, Jahnsdorf
Omega 1.3	BMG Labtech, Ortenberg
Omega Data-Analysis 210R3	BMG Labtech, Ortenberg
GCMS Real Time Analysis	Shimadzu Corporation, Kyoto, Japan
GCMS Postrun Analysis	Shimadzu Corporation, Kyoto, Japan
GCMS Analysis Editor	Shimadzu Corporation, Kyoto, Japan

Other consumables:

GeneJet Plasmid MiniPrep	Thermo Fisher Scientific GmbH
GeneJet PCR Purification KIT	Thermo Fisher Scientific GmbH
GeneJet Gel Extraction KIT	Thermo Fisher Scientific GmbH
Gibson Assembly Master Mix	New England Biolabs, Ipswich, USA
SsoAdvanced™ Universal SYBR Green Supermix	Bio-Rad Laboratories, Inc., Hercules, USA

2.2 Methods

2.2.1 Microbiological methods

2.2.1.1 Cultivation and storage of microorganisms

For the cultivation of the different *E. coli* strains 5 mL of LB-medium containing the corresponding antibiotics were inoculated with a single colony from selective agar plates. After incubation over night at 37 °C and 135 rpm this preculture was used to inoculate cultures up to a volume of 250 mL in Erlenmeyer flasks which were further cultivated under the same conditions. If not mentioned otherwise the cultivation of *Pseudomonas* strains was according to *E. coli* in LB-medium, but the temperature was set to 30 °C.

For the long-term storage of microorganisms 500 µL of a preculture were mixed with 500 µL of 60 % (v/v) glycerol and incubated for 30 min at RT. Afterwards the cells were stored at - 80 °C.

2.2.1.2 Preparation of competent cells for transformation

Preparation of cells for electroporation:

A preculture of *E. coli* or *P. putida* was incubated over night with the corresponding antibiotics in LB-low salt medium at 135 rpm and 37 °C or 30 °C respectively. This culture was used to inoculate 400 mL of LB-low salt medium with an OD_{600} of 0.2. The culture was allowed to grow to an OD_{600} of 0.5 – 0.6 at the corresponding temperature and consequently incubated on ice for 30 min. Afterwards the cells were split into 50 mL portions and centrifuged (15 min, 4,000 rpm, 4 °C). The resulting cell pellets were resuspended in 50 mL sterile H_2O and centrifuged under the same conditions. Next, the pellets were resuspended in 50 mL of 10 % (v/v) glycerol and again centrifuged under the same conditions. This step was repeated one more time and after each centrifugation step always two of the resuspended cells were combined. The cell pellet of the last centrifugation step was resuspended in 10 % (v/v) glycerol to give an OD_{600} of 50. Afterwards 70 µL of the cells were frozen in liquid nitrogen and stored at – 80 °C.

Preparation of cells for heat shock:

A preculture of *P. putida* in LB-medium containing the corresponding antibiotics was incubated over night at 30 °C and 135 rpm. With this culture 250 mL of LB-medium were inoculated with an OD_{600} of 0.2 and allowed to grow to an OD_{600} of 0.5 – 0.8 at 30 °C and 150 rpm. Afterwards the cells were incubated on ice for 10 min, split into 50 mL portions and centrifuged (10 min, 4,100 xg, 4 °C). The cell pellets were resuspended in 10 mL of TB buffer and combined. After incubation on ice for 10 min the cells were centrifuged under the same conditions. Next, the pellet was resuspended in 10 mL TB buffer containing 7 % DMSO and again incubated on ice for 10 min. Afterwards 600 µL of the cells were frozen in liquid nitrogen and stored at – 80 °C.

2.2.1.3 Growth curves of *P. putida* ATCC17453 and relating mutants

A preculture of *P. putida* ATCC17453 and all confirmed mutants in P-medium containing the corresponding antibiotics were incubated over night at 30 °C and 135 rpm. With these cultures 25 mL of P-medium containing glucose (2.5 g L^{-1}) or (+)- or (-)-borneol and (+)- or (-)-camphor (0.5 g L^{-1}) respectively were inoculated with an OD_{600} of 0.2 in independent triplicates and incubated at 30 °C and 135 rpm. Every hour the OD_{600} values of each culture were measured. In order to analyze stationary cells the overnight cultures were directly used for conversion tests by the addition of 0.5 g L^{-1} substrate.

For the analysis of the intermediates using (+)- or (-)-borneol and (+)- or (-)-camphor respectively as single carbon source samples for GC-MS analysis were taken every two hours.

For the analysis of the consumption of glucose every hour a sample of 500 µL culture was centrifuged (13,000 rpm, 2 min, 25 °C) and the supernatant was stored at – 20 °C until its analysis.

2.2.2 Molecular biological methods

2.2.2.1 Plasmid isolation

For the isolation of plasmid DNA a 5 mL preculture in LB medium including the corresponding antibiotic was inoculated with a single colony of an *E. coli* clone carrying the desired plasmid and incubated at 37 °C and 135 rpm over night. Next, 4 mL of the culture was centrifuged (13,800 rpm, 2 min), the supernatant was discarded and the pellet was used according the handbook of the GeneJet Plasmid MiniPrep kit. For the elution of the DNA 30 µL of sterile ultrapure water was used.

Concentration of the DNA was measured by UV/Vis spectroscopy (chapter 2.2.2.10).

2.2.2.2 Isolation of the CAM plasmid

For the isolation of the CAM plasmid a 5 mL preculture in LB medium including the corresponding antibiotic was inoculated with a single colony of a *P. putida* ATCC17453 or a mutant of it and incubated at 30 °C and 135 rpm over night. Next, 2 mL of the culture was centrifuged (13,800 rpm, 2 min), the supernatant was discarded and the pellet was resuspended in 200 µL of lysis buffer (40 mM Tris-acetate, 20 mM sodium acetate, 1 mM EDTA, 1 mM SDS, pH 7.8) by vigorously pipetting up and down. After the addition of 66 µL of 5 M NaCl the resuspended pellet was centrifuged (12,000 rpm, 4 °C, 10 min) and the supernatant was transferred into a fresh vessel. Afterwards, 200 µL of a mixture of chloroform and isoamyl alcohol (24:1) were added and gently mixed by inverting the vessel. The milky, turbid mixture was centrifuged (12,000 rpm, 4 °C, 3 min) and the DNA was precipitated by the addition of 400 µL of ice cold EtOH abs. following the next centrifugation step (12,000 rpm, 4 °C, 3 min). The supernatant was discarded and the pellet was washed two times with 200 µL of ice cold 70 % EtOH (12,000 rpm, 4 °C, 3 min). After the washing the supernatant was discarded and the pellet was air dried for 5 – 10 min. Afterwards the pellet was gently resuspended in 100 – 200 µL of sterile ultrapure water and the concentration of the DNA was measured by UV/Vis spectroscopy (chapter 2.2.2.10).

2.2.2.3 Restriction digestion according to Sambrook & Russel[150]

For the restriction digestion of plasmid DNA or PCR fragments the amount of the corresponding restriction endonuclease was calculated according to the following equation (Equation 1).

[Eq. (1)] $$U_{restriction} = m_{DNA}\ [\mu g] \times t\ [h] \times \frac{\text{recognition site (sample)} \times N\text{(assay)}}{\text{recognition site (assay)} \times N\text{(sample)}}$$

m_{DNA}: amount of DNA [µg]
t: time of incubation [h]
recognition site (sample): amount of recognition sites within the sample DNA
N (assay): amount of base pairs within the assay DNA
recognition site (assay): amount of recognition sites within the assay DNA
N (assay): amount of base pairs within the sample DNA

The assay DNA for the determination of the activity of the corresponding restriction endonuclease is reported by the supplier. Incubation time, temperatures and buffers for the different restriction endonucleases were set according to the manuals of the enzymes. If plasmids were used for ligation afterwards, the plasmids were dephosphorylated by the addition of antarctic phosphatase according to the manual of the enzyme. The resulting fragments of the restriction digestion were analyzed by agarose gel electrophoresis (chapter 2.2.2.8) and if necessary isolated from the gel (chapter 2.2.2.8).

2.2.2.4 Ligation according to Sambrook & Russel[150]

For the ligation the amount of vector and insert DNA was calculated under the consideration of the amount of base pairs. On average one bp is equal to a molecular mass of 6.6 x 10^{-4} ng fmol^{-1} (660 g mol^{-1}). The ratio of vector and insert DNA for the ligation was set to 1:3 (100 fmol vector : 300 fmol insert DNA) and the corresponding amount of substance was calculated according to the following equation (Equation 2).

[Eq. (2)] $$c_{DNA}\ [\text{fmol}\ \mu L^{-1}] = \frac{c\ (\text{DNA} / \text{ng}\ \mu L^{-1})}{6{,}6\ 10^{-4}\ \text{ng fmol}^{-1} \times \text{base pairs}}$$

The calculated amount of DNA for the vector and the insert were mixed together with the T4 DNA ligase and the corresponding buffer from the supplier. The total volume for the ligation was set to 20 µL and if necessary sterile ultrapure water was added. Ligation was performed by incubation at 16 °C for 16 h following an inactivation at 60 °C for 20 min.

Afterwards the ligation was used for transformation (chapter 2.2.2.5).

2.2.2.5 Transformation according to Sambrook & Russel[150]

Transformation was performed either by electroporation or by heat shock. For electroporation 70 µL of the prepared cells were thawed on ice and 1 µL of vector DNA or 2 µL of the ligation mixture were added and incubated for 1 min on ice (chapter 2.2.1.2). Afterwards the cells were transferred into an electroporation cuvette and electroporation was performed under the conditions in Table 12 for the different *E. coli* and *P. putida* strains.

Immediately after electroporation for 4 – 5 ms 700 µL of pre-warmed SOC medium (30 °C for *Pseudomonas*, 37 °C for *E. coli*) were added to the cells and incubated for 1 h at 30 °C and 37 °C respectively. Afterwards 100 µL were plated on selective agar plates and incubated over night at 30 °C and 37 °C, respectively.

Table 12: Setup for the transformation by electroporation of *P. putida* KT2440, *E. coli* DH10B and *E. coli* BL21(DE3) respectively.

Strain	Setup
P. putida KT2440	1.2 kV, 200 Ω, 25 µF
E. coli DH10B	2.0 kV, 200 Ω, 25 µF
E. coli BL21(DE3)	1.38 kV, 125 Ω, 50 µF

For the transformation using heat shock, 200 µL of cells were thawed on ice and 1 – 2 µL of vector DNA or 1 – 10 µL of the ligation mixture were added (chapter 2.2.1.2). The cells were incubated for 30 min on ice and heat shock was performed for 30 s at 42 °C following an incubation for additional 2 min on ice. After the addition of 700 µL of pre-warmed SOC medium (30 °C for *Pseudomonas*, 37 °C for *E. coli*) the cells were incubated for 1 h at 30 °C and 37 °C respectively. Afterwards 100 µL were plated on selective agar plates and incubated over night at 30 °C and 37 °C respectively.

For the determination of the transformation efficiency 10 pg of pUC18 (*E. coli*) or 10 pg of pET28a (*Pseudomonas*) were used for electroporation and heat shock respectively. Afterwards 100 µL of a dilution series was plated on selective agar plates and incubated over night at 30 °C and 37 °C respectively. On the next day the colonies on the plates were counted and transformation efficiency (T_E) was calculated according to the following equation (Equation 3).

[Eq. (3)] $$T_E = \frac{N\,(\text{colonies}) \times d_f}{m\,(\text{DNA})}$$

N: number of colonies
d_f: dilution factor
m: amount of DNA [µg]

2.2.2.6 Polymerase Chain Reaction according to *Kleppe et al.*[151]

Different variants of PCR were used depending on the aim of the PCR.

For the cloning of target genes, the addition of tags or restriction site, for sequencing or cloning procedures for the deletion on the CAM plasmid the phusion polymerase was used due to its proofreading ability. The composition for a PCR reaction using the phusion HF polymerase or Q5 HF polymerase and the program of the PCR is shown in Table 13. The annealing temperature (T_A) was 3 °C higher than the melting temperature of the lower primer.

Table 13: Composition and program for the PCR reaction using the phusion HF polymerase.

Composition		Program			
Template	0.1 - 100 ng		T [°C]	Time	Cycles
Primer I (10 µM)	1.25 µL	Initial denaturation	98	30 s	1
Primer II (10 µM)	1.25 µL	Denaturation	98	10 s	
dNTPs (10 mM)	1 µL	Annealing	T_A	20 s	x30
Buffer (5x)	10 µL	Extension	72	30 s/kb	
Polymerase (2 U µL^{-1})	0.5 µL	Final extension	72	10 min	1
Sterile ultrapure water	ad 50 µL				
Total	50 µL				

For the screening of positive clones derived either from ligation of vector and insert or the deletion of genes on the CAM plasmid a colony PCR was performed using Taq polymerase. As a template a single colony was resuspended in 20 µL of sterile ultrapure water and 2 µL were used for the PCR. In order to identify successful gene deletion on the CAM plasmid, the CAM plasmid was isolated and 0.1 – 10 ng were used for the PCR (chapter 2.2.2.2). The composition for a PCR reaction using the Taq polymerase and the program of the PCR is shown in Table 14. The annealing temperature (T_A) was 5 °C below the melting temperature of the lower primer.

Table 14: Composition and program for the PCR reaction using the Taq polymerase.

Composition		Program			
Template	0.1 - 10 ng		*T* [°C]	Time	Cycles
Primer I (10 µM)	0.1 µL	Initial denaturation	95	5 min	1
Primer II (10 µM)	0.1 µL	Denaturation	95	30 s	x30
dNTPs (10 mM)	0.5 µL	Annealing	T_A	30 s	
Buffer (5x)	4 µL	Extension	72	1 min/kb	
Polymerase (5 U μL^{-1})	0.2 µL	Final extension	72	10 min	1
Sterile ultrapure water	ad 20 µL				
Total	20 µL				

For the quantification of the CAM plasmid a qPCR was performed using the Q5 HF polymerase and the isolated CAM plasmid (chapter 2.2.2.2). For the calibration curve different concentrations of the plasmid pBBr122::*camDCAB* were used as standards.

Table 15: Composition and program for the qPCR reaction using the Q5 HF polymerase.

Composition		Program			
Template	0.01 - 1 ng		*T* [°C]	Time	Cycles
Primer I (10 µM)	0.2 µL	Initial denaturation	95	2 min	1
Primer II (10 µM)	0.2 µL	Denaturation	95	15 s	x40
Syber Green Mix (2x)	5 µL	Annealing / Extension	61	15 s	
Sterile ultrapure water	ad 10 µL	Denaturation	95	10 s	Melt curve
Total	10 µL	Heat	65 - 95	0.5 °C / 5 s	

For the combination of two PCR fragments, specific overlaps (20 nt) were added in a first PCR. The fragments were analyzed by agarose gel electrophoresis and extracted from the gel (chapter 2.2.2.8). Next, an equal amount of both fragments (100 – 200 fmol) were used for a PCR with the forward primer of the upstream fragment and the reverse primer of the downstream fragment. Afterwards the PCR was analyzed by agarose gel electrophoresis and the desired band was extracted from the gel (chapter 2.2.2.8) and used for further cloning steps.

If vector DNA was the template for a PCR, the background vector DNA was digested by the addition of 1 µL of DpnI followed by incubation for 2 h at 37 °C following an inactivation step by the incubation at 80 °C for 20 min. All PCRs were analyzed by agarose gel electrophoresis (chapter 2.2.2.8). For sequencing the PCRs were purified according to the manual of the GeneJet PCR Purification KIT. For the elution of the DNA 30 µL of sterile ultrapure water was used. The samples for sequencing were performed according to the standards from Eurofins Genomic Germany GmbH and consequently sent to the company.

2.2.2.7 Gibson Assembly and ligase independent cloning

Gibson Assembly was performed according to the manual from New England Biolabs. In Table 16 the composition of a typical Gibson Assembly is shown. The templates were obtained by PCR adding specific overlaps for the assembly (chapter 2.2.2.6). The Gibson Assembly was incubated at 50 °C for up to 60 min. Every 15 min 1 µL of the assembly was directly used for transformation (chapter 2.2.2.5). Furthermore, the assembly was analyzed by agarose gel electrophoresis (chapter 2.2.2.8).

Table 16: Composition of a Gibson Assembly.

	Volume
PCR fragment I	0.03 - 0.3 pmol
PCR fragment II	0.03 - 0.3 pmol
Gibson Assembly Master Mix (2x)	10 µL
Sterile ultrapure water	ad 20 µL
Total	20 µL

For the ligase independent cloning specific overlaps (35 nt) were added by PCR (chapter 2.2.2.6), analyzed by agarose gel electrophoresis and extracted from the gel (chapter 2.2.2.8). Next, 1 µg of both PCR fragments were incubated separately at 22 °C with 0.5 U of T4 DNA polymerase which harbors a 3'-5' exonuclease activity (20 nt / 30 min). After 52 min 30 s the reaction was stopped by the addition of 2 µL of 10 mM dXTP (X ≙ the nucleotide, which represents the end of the single strand area). Afterwards ligation was performed by the incubation of 100 fmol of vector DNA and 300 fmol of insert DNA for 30 min at 37 °C and 2 µL were used for transformation (chapter 2.2.2.5). In order to improve the cloning procedure 1 µL of T4 DNA ligase was added and incubated at 16 °C for 16 h. Another 2 µL were used for transformation (chapter 2.2.2.5).

2.2.2.8 Agarose gel electrophoresis according to *Aaij et al.*[152]

For agarose gel electrophoresis of DNA fragments with a size of 500 – 4,000 bp 1 % of agarose was heated in TAE buffer until a clear solution was obtained, filled in a camber equipped with a comb and allowed to harden at RT. For DNA fragments < 500 bp a 2 % agarose gel and for fragments > 4,000 bp a 0.8 % agarose gel was prepared.

For analytical agarose gel electrophoresis 2 – 5 µL of sample were mixed with 1 µL of loading dye (6x) and filled into the pockets. As a reference 6 µL of 1 kb DNA ladder or 100 bp DNA ladder from New England Biolabs were used. Separation of the DNA fragments was performed at 110 V for 35 min.

For preparative agarose gel electrophoresis the whole sample was mixed with the loading dye (6x) and filled into the pockets. As a reference 6 µL of 1 kb DNA ladder or 100 bp DNA ladder from New England Biolabs were used. Separation of the DNA fragments was performed at 100 V for 45 min.

After the run the agarose gels were incubated in the ethidium bromide staining solution for 10 min at RT (chapter 2.1.1). For minimizing the background the gel was destained in TAE buffer for 10 min at RT and analyzed with the DH-40 Felix 6020 documentation system.

If the fragments were needed for further cloning steps, the bands were cut off the gel and extracted according to the manual of the GeneJet Gel Extraction Kit. For the elution of the

DNA 30 µL of sterile ultrapure water were used.

2.2.2.9 Modification of the CAM plasmid using pEMG

The method for the seamless gene deletion on the CAM plasmid was adopted from *Martinez-Garcia et al*..[73] In the first step a 800 – 1,000 bp flanking region upstream of the start codon and downstream the stop codon of the gene to be deleted was amplified by PCR (chapter 2.2.2.6) using the isolated CAM plasmid as a template (chapter 2.2.2.2). Both PCR fragments were combined by overlap extension PCR (chapter 2.2.2.6) and restriction site for the digestion with EcoRI and BamHI were added. If the flanking region also harbors an EcoRI or BamHI restriction site, the specific overhang was created by the digestion with BsaI HF, BsmBI or BbsI. The pEMG vector was digested with EcoRI and BamHI (chapter 2.2.2.3) and consequently both fragments were ligated (chapter 2.2.2.4). The pEMG vector harbors two SceI restriction sites and a R6K origin for replication and therefore was transferred into *E. coli* DH5α λpir. Positive clones were analyzed by colony PCR (chapter 2.2.2.6) and transfer into the target organism *P. putida* ATCC17453 was performed by mating. Therefore the *E. coli* DH5α λpir strain containing the pEMG plasmid for the desired gene deletion was mixed with *P. putida* ATCC17453 and *E. coli* HB101 pRK2013 (helper strain) on a non-selective LB agar plate and incubated over night at 30 °C. Next, a full inoculation loop of the mixed organisms was spread onto cetrimide agar plates (selective for *Pseudomonas*) supplemented with kanamycin (selective for pEMG). As the pEMG vector could not replicate in *Pseudomonas* the resulting clones should have integrated the vector in the CAM plasmid. This was confirmed by colony PCR or a PCR using the isolated CAM plasmid in combination with primers which bind on the CAM plasmid and on the pEMG plasmid (chapter 2.2.2.6). The vector integrates by homologous recombination and therefore two integration sites are possible, upstream and downstream of the gene to be deleted. Consequently, two primer pairs were used to cover both integration sites. Next, the pSW-II plasmid which encodes for the I-SceI nuclease was transferred to a positive clone either by electroporation (chapter 2.2.2.5) or another mating using *E. coli* DH5α pSW-II and the helper strain *E. coli* HB101 pRK2013 on a non-selective LB agar plate. If mating was used for the transfer of the pSW-II plasmid a full inoculation loop was spread on cetrimide (selective for

Pseudomonas) agar supplemented with kanamycin (selective for pEMG) and gentamycin (selective for pSW-II) in order to isolate the desired *P. putida* ATCC17453 pEMG pSW-II. A single colony was used for the inoculation of 25 mL of LB medium supplemented with gentamycin and incubation over night at 30 °C and 135 rpm. On the next day 100 mL of LB medium supplemented with gentamycin were inoculated with an OD_{600} of 0.2 and incubated at 30 °C and 135 rpm. At an OD_{600} of 0.8 – 1.0 the expression of the I-SceI nuclease was induced by the addition of 10 mM 3-methyl benzoate (final concentration, solvent DMSO) and further incubated at 30 °C and 135 rpm. In the range of 2 – 6 h 100 µL samples were taken and spread onto LB agar plates supplemented with gentamycin and incubated over night at 30 °C. The I-SceI nuclease generates a double strand break within the pEMG vector sequence which is integrated in the CAM plasmid. The double strand break is repaired by homologous recombination whereby the wt or the desired mutant strain is generated and the kanamycin resistance is lost in both cases. Consequently, single colonies were screened for kanamycin sensitivity by plating on LB agar plates supplemented with gentamycin and LB agar plates supplemented with kanamycin and incubated over night at 30 °C. Next, the CAM plasmid of kanamycin sensitive clones was isolated (chapter 2.2.2.2) and used for PCR using primers which bind upstream and downstream of the deleted gene in order to differentiate between wt and the strains harboring the desired gene deletion (chapter 2.2.2.6). PCR fragments with the size of the desired gene deletion were extracted from the gel and sequenced to confirm the seamless gene deletion (chapter 2.2.2.8). In order to get rid of the pSW-II plasmid the knock out strain was cultivated in LB medium without gentamycin at 30 °C and 135 rpm. The culture was used to inoculate fresh LB medium every day and screened for gentamycin sensitive clones. Typically the gentamycin resistance was lost between 3 – 5 days. In order to generate double mutants the pSW-II plasmid was first cured and afterwards the single mutant strains were used for the gene deletion according to the same procedure.

2.2.2.10 UV/Vis spectroscopy

For the determination of DNA the absorbance was measured at 260 nm. An absorbance of 1 is equal to 50 ng μL^{-1} of dsDNA. The DNA concentration was calculated under the consideration of the dilution factor according to the following equation (Equation 4).

[Eq. (4)] c_{dsDNA} [ng μL^{-1}] = A_{260nm} x 50 ng μL^{-1} x d_f

A_{260nm}: absorbance at 260 nm
d_f: dilution factor

The protein concentration was measure at 280 nm and calculated according to the *Lambert-Beer* law under the consideration of the dilution factor (Equation 5).

[Eq. (5)] $A_{280nm} = \varepsilon$ x c x d x d_f

A_{280nm}: absorbance at 280 nm
ε: molar attenuation coefficient [L mol^{-1} cm^{-1}]
c: concentration
d: thickness of the cuvette [cm]
d_f: dilution factor

The molar attenuation coefficients were calculated for each protein using the ProtParam tool from https://web.expasy.org.

2.2.3 Biochemical methods

2.2.3.1 Protein expression

For protein expression using *E. coli* BL21(DE3) and the pET28a vector the optimal conditions were determined by a test expression. Hence, 100 mL of LB containing kanamycin were inoculated from an overnight culture of *E. coli* BL21(DE3) harboring the pET28a vector with or without the desired gene (negative control) with an OD_{600} of 0.2 and incubated at 37 °C and 135 rpm. When the culture reached an OD_{600} of 0.5 – 0.6 it was divided, induced with different concentrations of IPTG (0.1 mM, 0.5 mM and 1.0 mM) and incubated at different temperature (16 °C, 30 °C, 37 °C) and 135 rpm. Samples for

SDS-PAGE analysis were taken after different time points ending after 4 h (chapter 2.2.3.5).

The optimal conditions were then used for the expression of a higher amount of enzyme. Consequently, 500 mL or 1 L of LB medium containing kanamycin were inoculated with an OD_{600} of 0.2 and incubated at 37 °C and 135 rpm. At an OD_{600} of 0.5 – 0.6 the cells were induced with the optimal IPTG concentration and incubated at the optimal temperature and 135 rpm. Protein expression at 16 °C was performed overnight, whereas protein expression at 30 and 37 °C was performed for 4 h. Afterwards the cells were harvested (4,100 xg, 4 °C, 20 min), the supernatant was discarded and the cell pellets stored at – 20 °C until protein purification (chapter 2.2.3.2).

The protein expression using *P. putida* KT2440 and the pJH14 vector was according to the method described here, however 0.2 % (w/v) L-rhamnose were used for the induction of the cells.

If protein expression was performed using *P. putida* KT2440 and the pBBr122::*cam* plasmid no induction of the expression was necessary as the protein expression was regulated by the constitutive camphor promoter. The cells were incubated at the optimal temperature and samples for SDS-PAGE analysis were taken after different time points (chapter 2.2.3.2).

All samples for SDS-PAGE analysis were normalized by the following equation (Equation 6) and if necessary also used for western blot analysis (chapter 2.2.3.6).

[Eq. (6)] $$V\,[\mu L] = \frac{500}{OD_{600}}$$

OD_{600}: optical density at 600 nm

2.2.3.2 Cell disruption by sonication

The cell disruption of samples with a small volume was performed using sonication. Therefore, the cell pellets were resuspended in assay buffer to give an OD_{600} of 10. Next, the samples were sonicated three times for 1 min with an amplitude of 60 % (UIS250L, VialTweeter sonotrode). Between each sonication step the samples were incubated for 2 min on ice. Afterwards the samples were centrifuged (13,800 rpm, 4 °C, 30 min), the supernatant removed and the cell pellets resuspended in the same volume of buffer and consequently used for SDS-PAGE analysis (chapter 2.2.3.5).

2.2.3.3 Cell disruption by high-pressure homogenization

The cell pellets from the protein expression (chapter 2.2.3.1) were resuspended by the addition of 5 mL of lysis buffer to each gram of pellet. Afterwards 0.1 mg mL^{-1} of DNase I and lysozyme were added and the mixture was incubated on ice for 30 min. The cell disruption was performed by high-pressure homogenization (1.38 kbar) in intervals of 5 mL at 4 °C. The whole sample was homogenized two times and consequently centrifuged (30,000 xg, 4 °C, 35 min). The cell pellet was resuspended in the same volume of lysis buffer for SDS-PAGE analysis (chapter 2.2.3.5) and the supernatant was filtered (0.2 µm) before purification (chapter 2.2.3.4).

2.2.3.4 Protein purification by affinity chromatography

For the purification of his-tagged proteins the Äkta purifier was used in combination with a HisTrap™ FF column (1 mL or 5 mL) and the whole system was equilibrated using 20 CV of lysis buffer. Afterwards the whole protein solution was loaded with a flow rate of 3 mL min^{-1}. After the washing step (5 CV lysis buffer) the protein was eluted from the column by a gradient of elution buffer. Starting with 5 CV of 10 % elution buffer weakly bound substances were washed from the column. Typically the protein was eluted by increasing the elution buffer concentration to 60 % for 10 CV. In order to remove any tightly bound substances in the last step of the gradient 5 CV of 100 % elution buffer were used. The run was followed by the absorbance at 280 nm and the fraction size was set to 0.5 mL for each step. The fractions of the resulting peaks from the elution were analyzed by SDS-PAGE (chapter 2.2.3.5) and fractions containing the target protein were combined.

Before the proteins were used for any activity tests the buffer was exchanged to the corresponding assay buffer. Therefore, a PD-10 Desalting column was equilibrated with 10 CV of the assay buffer. Next, 2.5 mL of the protein solution were loaded, the flow-through discarded and the protein eluted by the addition of 3.5 mL of assay buffer. If the sample volume was greater than 2.5 mL the procedure was repeated starting with the equilibration of the column.

During the purification different samples were taken for SDS-PAGE analysis (chapter 2.2.3.5).

2.2.3.5 SDS-PAGE according to *Laemmli*[153]

For the discontinuous SDS-PAGE electrophoresis a 12 % separating gel was casted and overlaid with a 5 % stacking gel. The composition of both gels is shown in Table 17.

To 20 µL of sample 20 µL of SDS sample buffer (2x) were added, the mixtures were boiled for 5 min at 95 °C and centrifuged (13,800 rpm, 10 s). Afterwards 5 – 15 µL of sample were loaded on the gel and 15 µL of 250 kDa protein ladder from New England Biolabs were used as a reference standard. Protein separation was performed at a constant current strength of 25 mA for 45 – 60 min. Afterwards the gels were colored using Coomassie staining solution (chapter 2.1.1) at RT for 20 – 40 min. In order to reduce the background color the gels were boiled in ddH_2O for several times and analyzed with the DH-40 Felix 6020 documentation system.

If SDS gels were used for western blot analysis a prestained protein ladder was used and the gels were not stained (chapter 2.2.3.6).

Table 17: Composition of the separating and stacking gel for SDS-PAGE analysis for two gels.

	Separating gel (10 mL, 12 %)	Stacking gel (5 mL, 5 %)
Acrylamide-, bis-acrylamide stock solution [30 % (w/v), 37.5:1]	3 mL	0.65 mL
ddH_2O	4.29 mL	3 mL
Buffer (4x, separating and stacking gel)	2.5 mL	1.25 mL
SDS [10 % (w/v)]	100 µL	50 µL
Ammonium persulfate [10 % (w/v)]	100 µL	50 µL
Tetramethylethylenediamine	10 µL	5 µL

2.2.3.6 Western blot according to *Towbin et al.*[154]

For the western blot transfer four Whatman paper and a nitrocellulose membrane were cut to the size of the SDS gel. The membrane was equilibrated in methanol for 20 min whereas the Whatman papers were equilibrated in semi-dry buffer for 20 min. Afterwards the membrane was washed with semi-dry buffer and the blot was set up in the following order: two Whatman paper, membrane, SDS gel, two Whatman paper. The protein transfer was performed by a constant voltage of 25 V for 20 – 30 min using the Trans-Blot SD semi-dry

transfer cell (Biorad). After the transfer was completed the membrane was washed twice with TBS buffer for 10 min at RT. Next, the membrane was blocked with blocking buffer at 4 °C overnight. On the next day the membrane was washed twice with TBST buffer for 10 min at RT. After another washing step for 10 min at RT using TBS buffer the membrane was incubated for 1 h at RT with the primary antibody solution. Then the membrane was washed twice with TBST buffer for 10 min at RT following a washing step for 10 min at RT using TBS buffer. For the binding of the secondary antibody the membrane was then incubated for 1 h at RT in the secondary antibody solution. Afterwards the membrane was washed four times for 10 min at RT using TBST buffer. Staining was performed by the incubation of the membrane in the staining solution for 5 – 15 min at RT and stopped by the addition of ddH_2O.

2.2.3.7 Glucose assay

In order to determine the glucose concentration an enzymatic color assay was performed using the glucose oxidase from *Aspergillus niger* and the peroxidase from horseradish. Within the assay glucose is oxidized in the presence of oxygen whereby glucono lactone and H_2O_2 are released. The H_2O_2 consequently oxidizes the dye ABTS and the color change could be detected at 418 nm. The composition for the master mix of the assay is shown in Table 18.

Table 18: Composition of the master mix for the glucose oxidase assay.

	Concentration
ABTS	750 µM
Glucose oxidase from *Aspergillus niger*	2 U mL^{-1}
Peroxidase from horseradish	0.1 U mL^{-1}
Potassium phosphate buffer pH 6,0	20 mM

For the calibration curve glucose stock solutions in the range of 0 – 90 mg L^{-1} were prepared. To 50 µL of master mix 50 µL of sample or standard were added and the absorbance at 470 nm was measured as a reference. After incubation at 30 °C for 30 min and 500 rpm the absorbance was measured at 418 nm. For the evaluation the absorbance at 470 nm was

subtracted from the absorbance at 418 nm for each sample and standard ($A = A_{418\ nm} - A_{470\ nm}$). All samples and standards were used in triplicates.

2.2.3.8 Activity assay (+)-bornyl diphosphate synthase

For the activity assay of the (+)-BPPS the cell pellets from the protein expression were resuspended in 50 mM MOPSO 10 mM $MgCl_2$, 5 mM DTT, 10 % (v/v) glycerol, pH 6.1 and treated by sonication (chapter 2.2.3.2). As a negative control cells without the coding sequence of (+)-BPPS were used and treated the same way. Next, 900 µL of crude extract were incubated with 100 µL of geranyl diphosphate and overlaid with 100 µL of ethyl acetate. The assay mixture was incubated at 30 °C and 120 rpm for 5 h – 4 d. Samples of the aqueous phase were prepared for GC-MS analysis (chapter 2.2.5.1) as well as 50 µL of the organic phase. The remaining aqueous phase was acidified by the addition of five drops of 1 M HCl and incubated for additional 5 h at 30 °C and 120 rpm. Afterwards samples of the aqueous phase were prepared for GC-MS analysis again (chapter 2.2.5.1).

2.2.3.9 Substrate screening $P450_{cam}$

Single *P. putida* clones were used for inoculation of 25 mL of P-medium. The cells were incubated in Erlenmeyer flasks overnight (30 °C, 150 rpm). This preculture was then used to inoculate 1 L fresh media with an OD_{600} of 0.2. The cells were then further incubated (30 °C, 150 rpm) for 24 h. Afterwards (-)-borneol, (+)-borneol or (+/-)-isoborneol was dissolved in dodecane or ethyl acetate and added to the cell broth in a final concentration of 3 – 5 mM. Cells were further incubated (30 °C, 150 rpm) and samples were taken at different time intervals and analyzed by GC-MS (chapter 2.2.5.1).

2.2.3.10 Optimization of (-)-borneol conversion by $P450_{cam}$

P. putida cells containing the pBBR122::*camCAB* plasmid were incubated (2 d, 30 °C, 120 rpm) in shake flasks. To check whether different buffers at different pH affect conversion, cells were harvested by centrifugation (4,000 xg, 30 min, 4 °C), washed twice with the corresponding buffer (pH 6.0 – 8.0) and set to an OD_{600} of 1.0. All buffers (20 mM)

contained equal amounts of glucose (2.5 g L^{-1}) and TMS (0.4 %) as the P-medium. Cells were treated with 1 mM of (-)-borneol (100 mM stock solution, solvent ethyl acetate), further incubated (30 °C, 120 rpm) and samples for GC-MS analysis were taken after 0 h and 6 h (chapter 2.2.5.1). For the conversion at different temperatures (T = 23 °C – 40 °C), cells were produced as above and also incubated (30 °C, 120 rpm) with 1 mM (-)-borneol at different temperatures (23, 30, 37, 40 °C). Samples for GC-MS were taken at regular time intervals (chapter 2.2.5.1). The conversion in a two phase system was performed using n-hexane and n-dodecane as solvents (each 20 % (v/v)) containing (-)-borneol (50 mM). Cells were incubated (30 °C, 120 rpm), samples for GC-MS were taken at different time intervals and space-time yields (*STY*) were calculated (Equation 7 and 8).

[Eq. (7)] $$STY\ [\text{g L}^{-1}\ \text{h}^{-1}] = \frac{m\ (\text{obtained product [g]})}{V\ (\text{obtained volume [L]})\ t\ (\text{time [h]})}$$

[Eq. (8)] $$STY\ [\text{g g}^{-1}\ \text{h}^{-1}] = \frac{m\ (\text{obtained product [g]})}{m\ (\text{wer biomass [g]})\ t\ (\text{time [h]})}$$

For the toxicity tests of substrate, product or the corresponding solvent, the cells were incubated (30 °C and 120 rpm) with (-)-borneol, 5-*exo*-hydroxyborneol (each 2 mM) or ethyl acetate either for 48 h and OD_{600} values were measured with the Ultraspec 10 cell density meter (Amersham Biosciences) at different time intervals and compared to a control.

2.2.3.11 Semi-continuous batch process for the conversion of (-)-borneol by $P450_{cam}$

For the biotransformation of borneol to the corresponding diol, cells were produced as described above and (-)-borneol was used as the substrate. The OD_{600} of the main culture was set to 1.0 and 1 L of the culture broth was then transferred to a stirred tank reactor with a total volume of 1.5 L. The broth was incubated (30 °C, 215 rpm, air flow of 2.75 L L^{-1} min^{-1}) and 3 – 5 mM of (-)-borneol was added as substrate. Samples withdrawn at regular time intervals were analyzed by GC-MS (chapter 2.2.5.1). After full conversion of (-)-borneol, the weight of wet biomass was determined and the product was separated from the cells by cross flow filtration with a Vivaflow 200 membrane (MWCO = 30 kDa, Sartorius). In addition, the

reactor was filled up with fresh P-medium and substrate. This step was repeated three more times. The aqueous product was extracted with the same amount of ethyl acetate and the organic solvent was removed by evaporation.

2.2.3.12 Activity assay borneol dehydrogenase (Bdh)

The activity of the Bdh towards (-)-borneol was confirmed by the addition of 1 mM substrate (100 mM stock solution, solvent ethyl acetate) to the induced cells followed by GC-MS analysis after 4 h of incubation at 30 °C and 135 rpm (chapter 2.2.5.1). The sequencing results revealed the incorporation of a stop codon at the C-terminus wherefore only the N-terminal his-tagged variant was purified and used for the activity assay (chapter 2.2.3.4). A typical assay contained 1 mL of purified enzyme (100 – 200 µg), 1 mM of substrate (100 mM stock solution, solvent ethyl acetate), 1 mM of cofactor (100 mM stock solution of NAD^+ or $NADH/H^+$ in ddH_2O) and was incubated at 30 °C and 170 rpm for up to 4 d. The activity of the purified enzyme was confirmed by the increase of $NADH/H^+$ measured at 340 nm in a photometric assay.

For the analysis of the oxidation activity of the Bdh (-)-borneol, (+)-borneol, (±)-isoborneol and 5-*exo*-hydroxyborneol were used as substrate (cofactor NAD^+) whereas (-)-camphor and (+)-camphor were used for the examination of the reduction activity ($NADH/H^+$). The formation of the corresponding products was analyzed by GC-MS (chapter 2.2.5.1).

In order to shift the equilibrium of the reduction reaction of the Bdh 1 mg of the Fdh of *Candida boidinii* and 12.5 mM of potassium formate (100 mM stock solution, solvent H_2O) were added to the assay mixture. The effect of different amounts of cofactor was analyzed by the addition of 10, 100 and 200 µM $NADH/H^+$ respectively. The assay was incubated at 30 °C and 170 rpm for 1 d. The formation of the corresponding products was analyzed by GC-MS (chapter 2.2.5.1).

2.2.3.13 Synthesis of 5-oxo-1,2-campholide

For the synthesis of 5-oxo-1,2-campholide the strain *P. putida* KT2440 pBBr122::*camDCAB* was grown in 100 mL P-medium at 30 °C and 135 rpm overnight. The culture was centrifuged (4,100 xg, 4 °C, 10 min) and resuspended in 50 mL P-medium. For a negative control the strain *P. putida* KT2440 pBBr122 was treated the same way. Both cultures were incubated with 2 mM of (+)-camphor lactone (100 mM stock solution, solvent ethyl acetate) for 6 h at 30 °C and 135 rpm. Samples for GC-MS (chapter 2.2.5.1) and HPLC-MS analysis (chapter 2.2.5.2) were taken after different time points.

2.2.3.14 Activity assay CamH

For the activity assay of CamH the purified enzyme as well as the crude extract, flow-through and the elution peaks which did not contain the enzyme were analyzed. Furthermore, as a negative control the pellet and supernatant of *E. coli* BL21(DE3) pET28a treated the same way as the CamH expression was used. The sample volume was 1 mL of each (equal to 30 – 900 µg of protein). (+)-Camphor lactone and ε-caprolactone were used as substrates with a final concentration of 1 mM (10 mM stock solution, solvent ethyl acetate). The assay mixture was incubated at 30 °C and 125 rpm for 3 d. Samples for GC-MS (chapter 2.2.5.1) and HPLC-MS analysis (chapter 2.2.5.2) were taken after different time points.

2.2.4 Chemical methods

2.2.4.1 Purification 5-*exo*-hydroxyborneol

To each gram of 5-*exo*-hydroxyborneol 6.2 g of ethyl acetate were added and heated to 77 °C. After 2 –3 min the clear reaction mixture was allowed to cool down to RT, whereby white crystals precipitated. The suspension was incubated for 24 h at RT, following an incubation of another 24 h at 4 °C. After an additional incubation for 30 h at – 20 °C the suspension was vacuum filtered and white crystals were obtained. The resulting filtrate was purified once more with the same procedure.

2.2.4.2 Polymerization of 5-*exo*-hydroxyborneol

For the transesterification of succinic acid dimethyl ester (1.29 g, 8.8 mmol) with 5-*exo*-hydroxyborneol (1.05 g, 6.2 mmol) in the presence of 0.5 mol-% tin(II) acetate (7.1 mg, 0.029 mmol, on 5-exo-hydroxyborneol), a two-necked round bottom flask equipped with a magnetic glass stirrer and a reflux condenser with a distillation bridge were used and heated to 105 °C for 16 h to remove any residual moisture. The educts were added under an atmosphere of nitrogen and transesterification was conducted for 2 h at 190 °C under a nitrogen atmosphere without the use of any solvent. In the second step the reaction mixture was heated to 245 °C under reduced pressure (p = 90 mbar) in order to remove the excess of succinic acid dimethyl ester. After 4 h the reaction mixture was cooled down to RT.

For the removal of residual monomers polymer samples (200 – 250 mg) were pulverized and then stirred in 10 mL of methanol for 16 h at RT. After filtration followed by a washing step with 5 mL methanol, the solvent was removed by evaporation and the filter was dried.

2.2.5 Analytics

2.2.5.1 Gas chromatography-mass spectrometry (GC-MS)

Cell samples were mixed with an equimolar volume of ethyl acetate and centrifuged after vigorous mixing. A sample of the upper organic phase (150 µL) was mixed with ethyl acetate (350 µL) and GC-MS was performed using auto-injector AOC-5000, the Shimadzu GC-2010 Plus and a SGE BPX-column (30 m x 0.25 mm inner diameter). Separation of the substances on the GC-MS was achieved at an oven-temperature of 50 °C followed by a temperature programming from 50 °C to 120 °C (15 °C min^{-1}), then to 170 °C (5 °C min^{-1}), finally to 200 °C (20 °C min^{-1}) and holding this temperature for 10 min under the constant flow of 1.69 mL helium min^{-1}. The resultant chromatograms were analyzed with the Shimadzu GCMSsolution software.

2.2.5.2 High-performance liquid chromatography-mass spectrometry (HPLC-MS)

Cell samples were centrifuged (13,800 rpm, 2 min), the supernatant was filtrated (0.2 µm) and directly used for HPLC-MS analysis using a LUNA HILIC column (150 mm x 4.6 mm, particle size 3 µm, porosity 200 Å) in combination with a HPLC system from Shimadzu (LC-30AD pumps, SIL-30AC auto sampler, CTO-20AC oven, CBM-20A controller) and the mass spectrometer LTQ XL from ThermoScientific. As eluents a 10 mM ammonium formate solution pH 3 (eluent A) and acetonitrile (eluent B) were used. 5 µL of sample were applied to the system at a temperature of 20 °C and a flow rate of 1 mL min^{-1}. For the run a gradient of eluent B was applied over 20 min as follows: 0 – 2.5 min 95 % eluent B, 2.5 – 10 min 80 % eluent B, 10 – 17.5 min 50 % eluent B, 17.5 – 20 min 95 % eluent B. The absorbance was measured in the range of 190 – 260 nm in wavelength steps of 1 nm. Fragmentation of the samples was performed using electrospray ionization and masses in the range of 110 – 600 (m/z) were analyzed by the detection of M-H fragments. The resulting chromatograms were analyzed using the Xcalibur™ software.

2.2.5.3 Differential scanning calorimetry (DSC)

Thermal properties of polymer materials (e. g. glass transition temperature (*T*g)) were recorded with differential scanning calorimetry using the METTLER Toledo DSC 1 Star system. Samples of solid polymer (10 – 15 mg) were heated from 50 °C to 300 °C (25 °C min^{-1}), held for 2 min and then cooled down to – 20 °C (- 25 °C min^{-1}) and held for 5 min. Next, the samples were heated to 100 °C (10 °C min^{-1}), then to 400 °C (30 °C min^{-1}) and finally cooled down to 50 °C (- 30 °C min^{-1}). The heating program was performed under constant flow of 50 mL nitrogen min^{-1}. The DSC curves obtained were analyzed with the METTLER STARe SW 13.00 software and all *T*g values were obtained from the second scan, after removing the thermal history.

2.2.5.4 Gel permeation chromatography (GPC)

Sample preparation was performed by drying (4 h at 80 °C) the solid polymer samples (5 – 15 mg) under vacuum. Dried samples were dissolved in appropriate volume of HFIP

containing NaTFA (0.05 mol L^{-1}). For the calibration curve polymer standards of the ReadyCal-Kit Poly(methyl methacrylate) low were dissolved in HFIP (1.5 mL) containing NaTFA (0.05 mol L^{-1}). Samples and polymer standards were stored for two days at RT protected from light. Samples were then filtered (0.2 µm) and GPC analysis was performed using the SECcurity GPC System (Inline degaser and oven TCC600 (Polymer Standards Service), 1260 Infinity pump, 1260 Infinity auto-sampler, 1260 Infinity RI-detector (Agilent Technologies)), a PSS PFG pre-column (50 mm x 8 mm, particle size 7 µm) and two PSS PFG columns (300 mm x 8 mm, particle size 7 µm, porosity 100 Å and 1000 Å). The GPC curves obtained were analyzed using PSS WinGPC UniChrom software (Polymer Standards Service).

2.2.5.5 Nuclear magnetic resonance spectroscopy (NMR)

Sample preparation for NMR analysis was performed dissolving 5 – 15 mg of sample in 600 µL of deuterated formic acid for 2 h at RT. After filtration (0.2 µm) the samples were used for NMR analysis. NMR-spectra were measured on a JNM-ECA 400 MHz spectrometer from JOEL at 25 °C with the application of standard pulse programs. The chemicals shifts (δ) are reported in ppm with reference to tetramethylsilane. Coupling constants J are reported in Hertz (Hz). For determining CH2-signals, the DEPT135°-technique was used. For correct assignment of the signals, 2D NMR methods, like COSY, HSQC and HMBC.

3 Results

The first part of the work relates to the *de novo* biosynthesis of borneol in *Pseudomonas* starting from glucose. For that reason the (+)-bornyl diphosphate synthase [(+)-Bpps], which is responsible for the formation of borneol should be expressed in *P. putida* KT2440. The resulting borneol could be a precursor for terpene-based polymers after further modification (Figure 16).

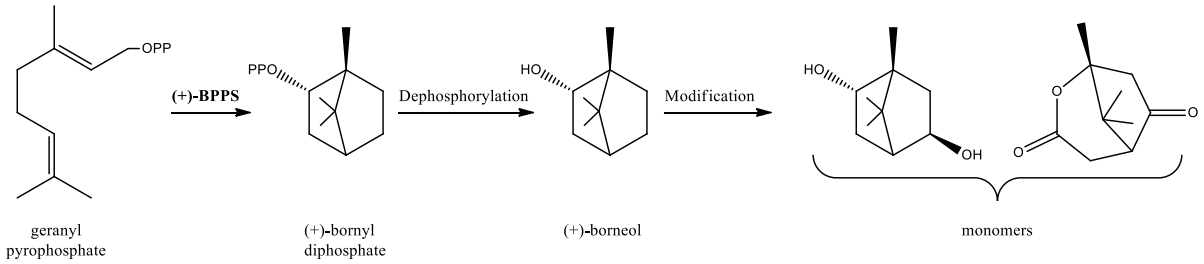

Figure 16: Formation of (+)-borneol diphosphate by recombinant expression of (+)-BPPS in *P. putida* KT2440. After dephosphorylation and further modification suitable monomers for terpene-based biopolymers are obtained.

3.1 (+)-Bornyl diphosphate synthase

The plant enzyme (+)-bornyl diphosphate synthase ((+)-Bpps) is responsible for the formation of (+)-bornyl diphosphate based on geranyl pyrophosphate (GPP) in *S. officinalis*. To test the expression and activity of the enzyme, a synthetic gene codon-optimized for *Pseudomonas* was cloned into different expression vectors and expressed in *P. putida* KT2440 and *E. coli* BL21(DE3).

3.1.1 Cloning and expression

The native version of the enzyme and two his-tag variants (N-/C-terminal) were cloned into the expression vector pBBrDuet and the correct insertion of the gene was confirmed by sequencing (chapter 2.2.2.3). Expression tests using *P. putida* KT2440 did not show a visible expression of the enzyme and also western blot analysis targeting the his-tagged variants was negative (chapter 2.2.3.1). Furthermore, borneol formation could not be detected by GC-MS analysis of the cell extracts and the supernatant.

It is known that the enzyme carries an N-terminal signal peptide responsible for the transfer towards the chloroplasts in *S. officinalis*.[155] As this signal peptide might hinder the correct expression in prokaryotes, a truncated version of (+)-Bpps missing the first 50 amino acids (E50), which encode for the transit sequence was cloned into the expression vectors pBBrDuet and pET28a according to *Whittington et al.*.[155] Furthermore, variants of the enzyme harboring N- and C-terminal his-tags were cloned as well and all constructs were checked by sequencing. Successful expression using *P. putida* KT2440 and *E. coli* BL21(DE3) could not be confirmed by SDS-PAGE (chapter 2.2.3.5) and western blot analysis (chapter 2.2.3.6). Also GC-MS analysis did not reveal the formation of borneol.

Next, the same truncated version (E50) of the (+)-Bpps was cloned into the vector pJH14 (chapter 2.2.2.7). This vector also expresses enzymes responsible for the formation of GPP which should enhance the formation of (+)-borneol if the enzyme was active. Successful cloning was confirmed by sequencing, but the expression and activity of the enzyme in *P. putida* KT2440 could neither be confirmed by SDS-PAGE nor a product formation by GC-MS analysis.

3.1.2 Activity assay

To exclude false negative results based on borneol formation under the limit of detection during the expression tests, crude extracts in combination with a high amount of GPP as a substrate were used for activity assays (chapter 2.2.3.8). The aqueous assay was overlaid with ethyl acetate in order to trap any volatile products. GC-MS analysis of acidified aqueous samples as well as samples of the organic phase did not show any borneol formation.

Taken these results together the heterologous expression of the (+)-Bpps in different organisms (*P. putida* KT2440, *E. coli* BL21(DE3)) using different expression vectors (pBBrDuet, pET28a, pJH14) and variants of the enzyme was not possible. Furthermore, the activity of the enzyme could not be confirmed during the expression or in activity assays using crude cell extracts. For that reason it was focused on the biotransformation of camphor-derived raw materials by whole cell biotransformation using recombinantly expressed enzymes or the genetically modified *P. putida* ATCC17453 instead of the biosynthesis of borneol.

3.2 Modification of the CAM plasmid

As the formation of (+)-borneol and its further modification in order to obtain different monomers was not successful by the expression of (+)-BPPS in *P. putida* KT2440, the CAM plasmid of *P. putida* ATCC17453 was investigated in more detail to produce the desired monomers via biotransformation. The plasmid carries the genes responsible for the biodegradation of camphor. Along the degradation pathway there are interesting intermediates as well as enzymes in terms of terpene-based monomers for biopolymers. Consequently, different camphor-based monomers should be produced via two different approaches: (i) gene deletion on the CAM plasmid in order to interrupt the metabolism at different stages to produce the desired monomers; (ii) recombinant expression of several enzymes in *P. putida* KT2440 in order to obtain a whole cell biocatalyst for the biotransformation of camphor-derived substrates.

For the interruption of the metabolism it was necessary to clarify if it is principally possible to knock out different genes on a natural plasmid and if the resulting mutants are suitable for the production of terpene-based monomers using camphor or borneol as substrates.

3.2.1 Engineering molecular biological methods for *Pseudomonas*

For this purpose it was necessary to screen and optimize molecular biological methods for the modification of *P. putida* ATCC17453 because standard protocols for PCR and transformation failed. For each PCR it was necessary to isolate chromosomal and plasmid DNA from the strain because any approach using cells resulted in no product formation (chapter 2.2.2.2). Even PCR with the isolated DNA as a template did not result in constant signals. Consequently, different parameters of the PCR namely template concentrations (0.2 – 100 ng μL^{-1}), kind of polymerase (Taq, Phusion, Pfu and Q5 polymerase), annealing temperature (± 10 °C of the primer with the lower melting temperature), elongation time (standard up to two times of the standard) and additional ingredients (± 5 % DMSO) were varied in order to optimize the PCR setup. As a result an optimized PCR method was developed using the Q5 polymerase in combination with 0.2 ng μL^{-1} of template DNA and an annealing temperature of + 3 °C of the primer with the lower melting temperature (Table 19).

Next, several transformation methods were investigated in order to transfer plasmids into

P. putida ATCC17453. For that reason different kinds of competent cells were prepared and used for electroporation and heat shock. In the end reliable results were obtained by conjugation according to *Martinez-Garcia et al*.[73] using *E. coli* DH5α with the desired plasmid as a donor and *E. coli* DH5α pRK2013 as a helper strain (chapter 2.2.2.9).

Table 19: Screening for suitable PCR conditions targeting the CAM plasmid of *P. putida* ATCC17453. For standard protocol see chapter 2.2.2.6. The results for the confirmation of the successful knockout of *camD* and $camE_{25\text{-}1}$ together with the wt control are shown exemplarily.

Polymerase	c_{DNA} [ng µL^{-1}]	Deviation to standard protocol	Signal target gene		
			wt	Δ*camD*	Δ$camE_{25\text{-}1}$
Taq	10	-	-	-	-
	1 - 50	-	-	-	-
	1 - 50	Denaturation 10 min, 95 °C	-	-	-
	1 - 100	Gradient ± 10 °C	-	-	-
	5	Double time elongation	+	-	-
	0.2 - 10	Gradient ± 10 °C + 5 % DMSO	±, weak	-	-
Phusion	10	-	-	-	-
	5 - 10	-	+	-	-
	1 - 350	Gradient ± 10 °C + 5 % DMSO	-	-	-
Pfu	5 - 10	-	+	-	-
	5 - 10	Gradient ± 10 °C	+	-	-
	5 - 10	Denaturation 10 min, 95 °C	+	-	-
Q5	5 - 10	-	weak	weak	weak
	0.2	-	+	+	+

3.2.2 Quantification of the CAM plasmid

After the molecular biological methods were established, the copy number of the CAM plasmid was analyzed by qPCR in order to clarify if a single gene or more than one had to be deleted. For the quantification of the CAM plasmid the vector pBBr122::*camDCAB* and specific primers targeting *camC* were used for a calibration curve (chapter 2.2.2.6). Samples were prepared by different dilutions of the CAM plasmid and the corresponding cell number per mL was determined. In the first approach the amplification curves of the standards and samples were not constant and a high variation in signal strength was observed. Consequently, the resulting calibration curve showed an efficiency of 115 %, which is out of the tolerable range (90 – 110 %). Melt peak analysis revealed the formation of side-products, which might be due to unspecific binding of the primers. The main product of the PCR had a melting temperature of about 84 °C, but there was also a significant amount of PCR products around the temperature of 88 – 92 °C.

In order to avoid any side-product formation the template DNA, standard DNA and primer concentrations were reduced for the next experiment. This time the efficiency and coefficient of determination of the standard curve were in an expected range and also constant PCR signals were obtained (Figure 17).

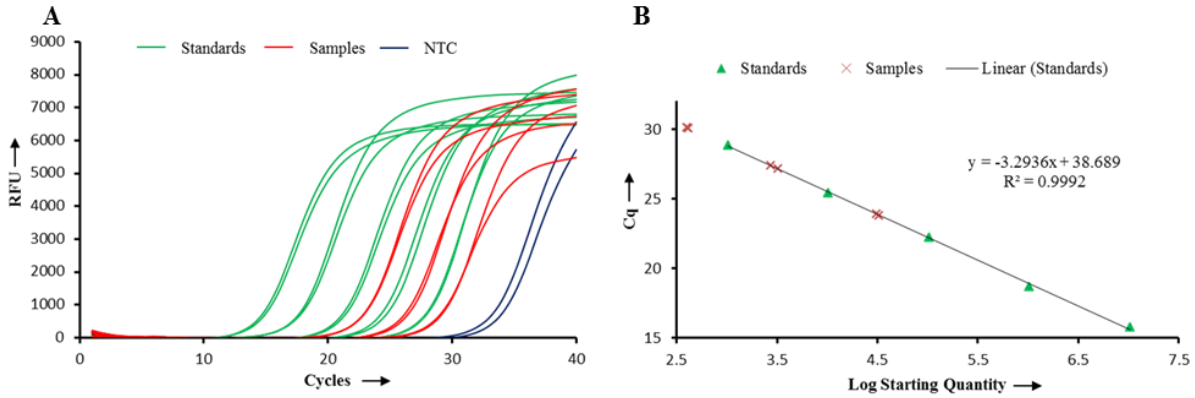

Figure 17: Results of the qPCR for the quantification of the copy number of the CAM plasmid. A: Amplification chromatogram. Y-axis: reaction forming units; x-axis: cycles of the PCR; green: standards in the range of 1.03 x 10^3 – 1.03 x 10^7 copies in double determination; red: 0.01, 0.1 and 1 ng of sample DNA in double determination; blue: no template control in double determination. B: Standard curve for the quantification. Y-axis: c_q-value; x-axis: starting quantity in logarithmic scale; triangle: standards; X: samples.

Melt peak analysis revealed a major peak for the main product of the PCR at the same temperature as in the first experiment of about 84 °C (Figure 18 B). Additionally, side-product formation could be reduced by the optimized parameters for the qPCR and were lower than the c_t-value. As expected the negative control without template showed a peak with a lower melting temperature than the samples and standards (Figure 18 B).

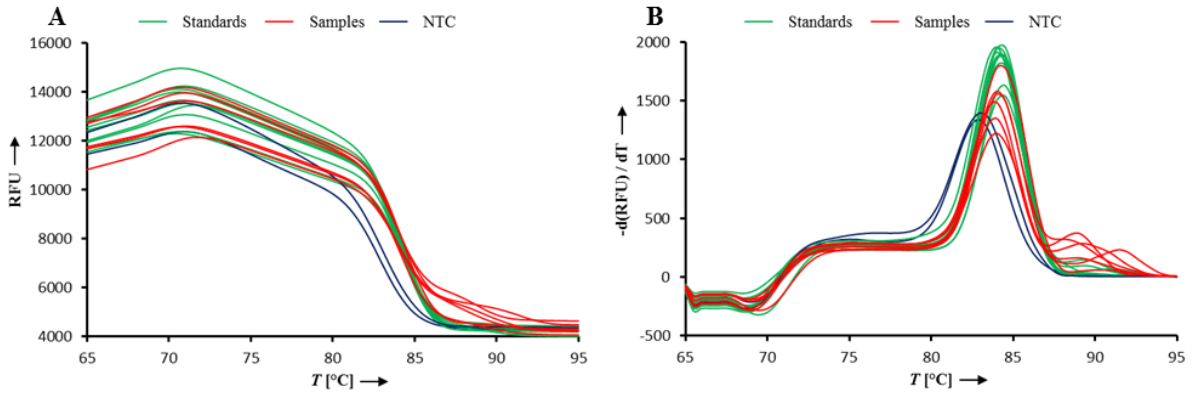

Figure 18: Melt curve and melt peak analysis of the PCR products obtained by qPCR of the CAM plasmid. A: Melt curve of the PCR products. Y-axis: reaction forming units; x-axis: temperature [°C]; B: Melt peak analysis of the PCR products. Y-axis: derivative reaction forming units on temperature; x-axis: temperature [°C]; green: standards in the range of 1.03 x 10^6 – 1.03 x 10^8 copies in double determination; red: 0.1, 1.0 and 10 ng of sample DNA in double determination; blue: no template control in double determination.

For the calculation of the copy number the lowest dilution was excluded because the data points were not within the calibration curve. Based on the starting quantity and the cell number, the copy number per cell of the CAM plasmid was calculated for both experiments and finally 4 – 6 copies of the CAM plasmid per cell were determined (Table 20).

The results of the second experiment are more reliable than the results of the first experiment due to the lower side-product formation and the consistent standard curve. In conclusion, the qPCR revealed that *P. putida* ATCC17453 harbors more than one CAM plasmid per cell. As a consequence, the genes for the desired deletions had to be deleted on all plasmids in order to obtain positive mutant strains.

Table 20: The copy number of the CAM plasmid per cell was calculated based on the qPCR results. The quantity per mL was calculated based on the amount of the sample DNA and the starting quantity. Referred to the cells per mL the quantity per cell and the mean quantity per cell were calculated.

Experiment	Cells per mL	Sample DNA [ng]	Starting quantity	Quantity per mL	Quantity per cell	Mean Quantity per cell
1	1.05×10^8	60	9.19×10^8	4.59×10^8	4.17	4.31 ± 0.13
		10	9.56×10^8	4.78×10^8	4.34	
		10	9.72×10^8	4.86×10^8	4.42	
2	1.05×10^8	1	1.35×10^9	6.73×10^8	6.12	6.07 ± 0.49
		1	1.42×10^9	7.10×10^8	6.46	
		0.1	1.39×10^9	6.97×10^8	6.34	
		0.1	1.18×10^9	5.90×10^8	5.37	

3.3 Production of 5-*exo*-hydroxyborneol

After a suitable method for the modification of the CAM plasmid was established the bifunctional 5-*exo*-hydroxyborneol should be produced. For that reason the biotransformation of borneol was on the one hand analyzed by the recombinant expression of the $P450_{cam}$ operon in *P. putida* KT2440 and on the other hand the deletion of the *camD* gene (FdH) on the CAM plasmid should yield a mutant, which stops the degradation of camphor at the level of 5-*exo*-hydroxyborneol. During the analysis of the Δ*camD* mutant strain a short chain dehydrogenase encoded by the open reading frame 16 (*orf16*) was found, which showed a dehydrogenase activity towards borneol (Figure 19).

Consequently, this enzyme was characterized regarding its activity towards different borneol-derived substrates. Finally, the double mutant strain *P. putida* ATCC17453 Δ*camD* Δ*bdh* was generated and its capability for the conversion of borneol to 5-*exo*-hydroxyborneol was analyzed.

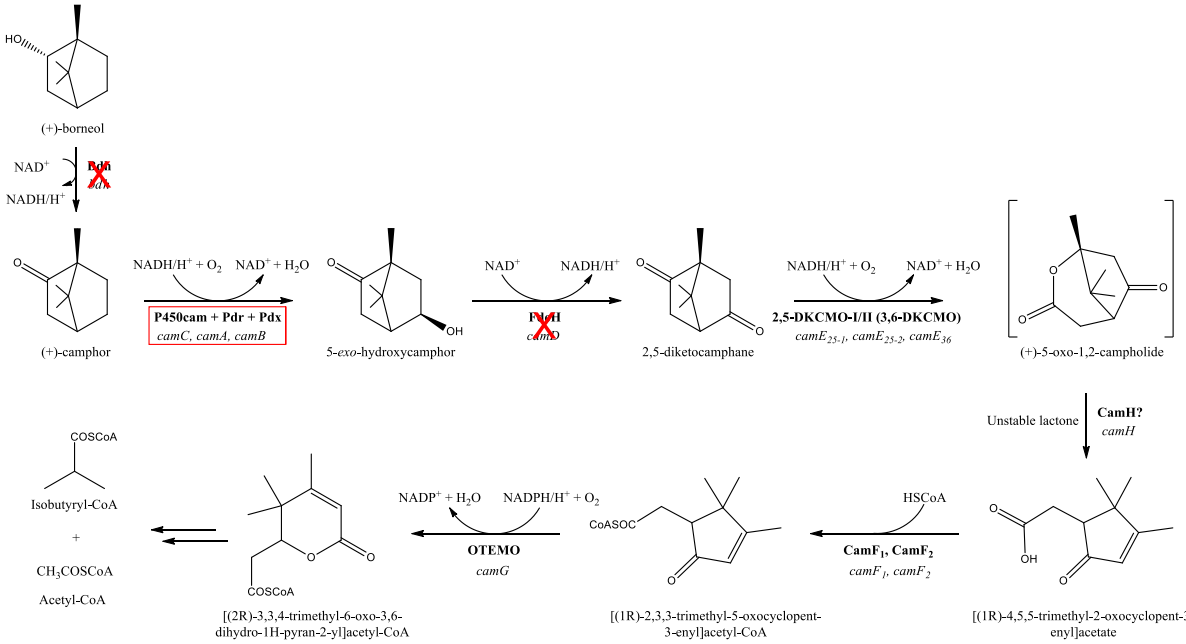

Figure 19: Biodegradation of (+)-borneol to isobutyryl-CoA and acetyl-CoA by the CAM plasmid of *P. putida* ATCC17453. *Orf16* was found to be a borneol dehydrogenase (*bdh*). Two strategies for the conversion of (-)-borneol towards 5-*exo*-hydroxyborneol were analyzed: (i) recombinant expression of $P450_{cam}$, Pdr and Pdx in *P. putida* KT2440 (red box); (ii) deletion of Orf16 (*bdh*) and FdH (*camD*) to interrupt the metabolism after hydroxylation by $P450_{cam}$, Pdr and Pdx (red cross). Enzymes are displayed in bold, responsible genes in italic.

3.3.1 Recombinant expression of $P450_{cam}$, Pdr and Pdx

In previous works a synthetic operon (*camCAB*) harboring the enzymes $P450_{cam}$, Pdr and Pdx, which are responsible for the hydroxylation of camphor was designed and cloned into the broad host vector pBBr122. The operon also includes the native promotor region without the regulator gene *camR*. Thus, the expression of the synthetic operon is under the control of the constitutive camphor promoter. Successful cloning was confirmed by sequencing, which showed two mutations at the DNA level: T465C and T681C. As it turned out both mutations were silent mutations and the plasmid was transferred to *P. putida* KT2440 yielding a whole-cell catalytic system.

Expression of the synthetic operon and the activity of the three enzymes were confirmed by the biotransformation of different substrates using *P. putida* KT2440 pBBr122::*camCAB* as a whole cell catalyst (chapter 2.2.3.9). For the first activity tests both enantiomers (+)- and (-)-borneol were used and GC-MS analysis of the different biotransformations revealed that

both substrates were completely converted over time yielding the corresponding hydroxyborneols. Thus, it could be shown that the novel created strain *P. putida* KT2440 pBBr122::*camCAB* is able to produce a borneol-diol.

Consequently, the biotransformation process of (-)-borneol was optimized in order to increase the yield of 5-*exo*-hydoxyborneol by varying parameters such as temperature, buffer and pH value (chapter 2.2.3.10). The range of pH 6.0 – 8.0 was covered using sodium-potassium-phosphate (S/P), Tris-HCl and MOPS buffers because the activity of $P450_{cam}$ is influenced by the pH value as well as the buffer substance itself. The conversion rate of (-)-borneol as well as the yield of 5-*exo*-hydroxyborneol decreased in all buffers at alkaline pH values (Table 21). In contrast, the selectivity increased at alkaline pH values using S/P and Tris-HCl buffers, whereas it remains nearly constant in MOPS buffer. Based on the results shown in Table 21 the preferred buffer system for the conversion of (-)-borneol is S/P at pH 6, because it showed a fast substrate conversion in combination with a high product yield.

Table 21: (-)-Borneol substrate consumption and 5-*exo*-hydroxyborneol product formation depending on different buffer systems and pH values after 6 h at 30 °C. Selectivity is calculated based on conversion and yield.

	Conversion [%]	Yield [%]	Selectivity [%]
S/P buffer pH 6	100 ± 0.0	78.6 ± 11.1	78.6
S/P buffer pH 7	76.3 ± 2.0	69.8 ± 3.8	92.6
S/P buffer pH 8	63.0 ± 1.5	63.6 ± 1.6	100
Tris-HCl buffer pH 7	100 ± 0.0	70.2 ± 2.8	70.2
Tris-HCl buffer pH 8	74.9 ± 5.4	70.7 ± 3.7	94.4
MOPS buffer pH 6	100 ± 0.0	64.8 ± 1.7	64.8
MOPS buffer pH 7	100 ± 0.0	67.1 ± 0.9	67.1
MOPS buffer pH 8	76.6 ± 1.9	51.9 ± 4.0	67.8

Substrate conversion as well as microbial growth is strongly linked to the temperatures in the surrounding. Hence, the biotransformation process of (-)-borneol by *P. putida* KT2440 pBBr122::*camCAB* was analyzed at different temperatures (Figure 20). Conversion rates were similar in the range of 30 – 40 °C and decreased at lower temperatures. On the contrary, product yields decreased at higher temperatures reaching their maximum at 30 °C. The

optimal temperature for the biotransformation was observed at 30 °C as a high conversion rate in combination with the highest product yield was obtained. This temperature also represents the optimal growth temperature for *P. putida* KT2440. Both experiments showed the formation of side-products, such as hydroxycamphor and diketocamphane.

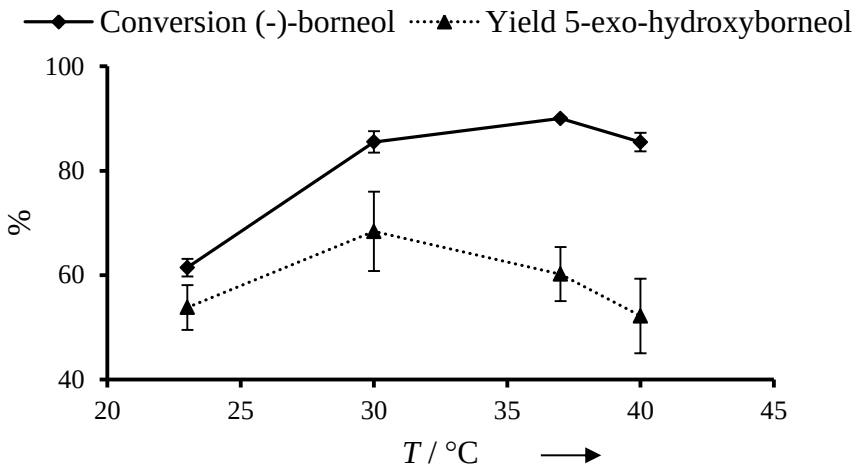

Figure 20: Conversion of (-)-borneol and yield of 5-*exo*-hydroxyborneol at different temperatures after 5 h of reaction time using $P450_{cam}$ enzymes in recombinant *P. putida* KT2440 as a whole-cell catalytic system. Error bars represent standard deviation of triplicates.

In addition, the biotransformation using a two phase system with *n*-hexane and *n*-dodecane as an organic phase was analyzed. With this approach the high volatility as well as insolubility of the substrate should be circumvented. Space-time yields (*STY*) were calculated accordingly. *STY*s for both two phase systems were similar ($STY_{\text{two phase}}$ ~ 32 mg L^{-1} h^{-1}) and also comparable to the conversion without an organic phase (STY_{aqueous} ~ 34 mg L^{-1} h^{-1}). To determine any toxicity of (-)-borneol or 5-*exo*-hydroxyborneol towards *P. putida* KT2440, which would affect the conversion rates, a toxicity test was performed using 2 mM of substrate or product respectively. Bacterial growth was analyzed over 24 h, but neither (-)-borneol nor 5-*exo*-hydroxyborneol showed any toxic effect towards the cells.

These results indicate that the optimal parameters for the conversion of (-)-borneol are a S/P buffer pH 6 based medium without a second organic layer (high product yields) and a conversion temperature of 30 °C (fastest conversion with highest yield).

3.3.2 Development of a semi-continuous batch process

In order to produce a higher amount of 5-*exo*-hydroxyborneol a process was developed for the conversion of (-)-borneol by *P. putida* KT2440 pBBr122::*camCAB* (chapter 2.2.3.11). The substrate itself is hardly water soluble due to its unpolar character, so a continuous substrate feed would result in precipitation of the substrate, which would decrease the conversion rate. In a simple batch process the cells have to be separated after complete substrate conversion as they form an interphase during the extraction with an organic solvent, which would result in a lower product yield. To avoid this, the cells could be separated from the product by centrifugation, but this step would be very time-consuming. To solve these challenges a semi-continuous batch process was developed where the product was separated from the cells and extracted within the process.

The biotransformation of (-)-borneol by *P. putida* KT2440 pBBr122::*camCAB* was performed in a 1.5 L stirred tank reactor which was inoculated with 1.0 L of a culture with an OD_{600} of ~ 1.0. For aeration, a ring sparger with a constant flow of 2.7 L min^{-1} of compressed air in combination with a stirrer were used (Figure 21).

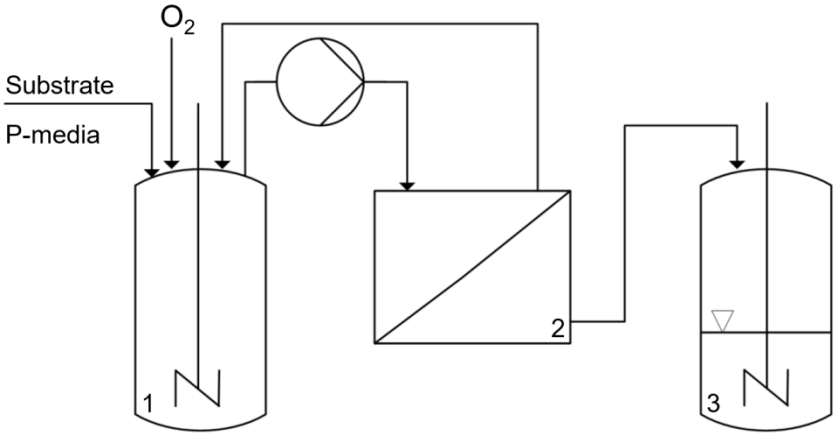

Figure 21: Flow chart of the biotransformation process of (-)-borneol. Biotransformation was performed in a 1.5 L air-flushed stirred tank reactor (1). After complete conversion, the product is separated from the cells by cross-flow filtration (2) and subsequently extracted with an organic solvent (3), whereas the cells were returned to the reactor and used for further biotransformations after addition of fresh media and substrate.

The substrate conversion and product formation was followed by GC-MS analysis and after complete conversion of the substrate the fermentation broth was pumped over a membrane

with a molecular weight cut off of 30 kDa. Thus, the cells were separated from the broth and the product and removed into the reactor. For the product extraction, the resulting filtrate was directly trickled into a stirred tank filled with ethyl acetate. During the separation the cells were concentrated caused by the decrease of the reactor volume. In order to avoid any shear stress only 80 – 90 % of the total reactor volume were used for the separation. Afterwards fresh medium and substrate were added to the cells for further conversion of (-)-borneol.

With this setup it was possible to reuse the cells as a catalyst up to four times without an intermediate centrifugation step whereby the cells grew to a final OD_{600} of 2.8 during the process. The first conversion of (-)-borneol was completed after 8 h, but with each substrate addition the time for complete conversion towards 5-*exo*-hydroxyborneol increased and for the last conversion 40 h were necessary for the complete substrate conversion (Figure 22).

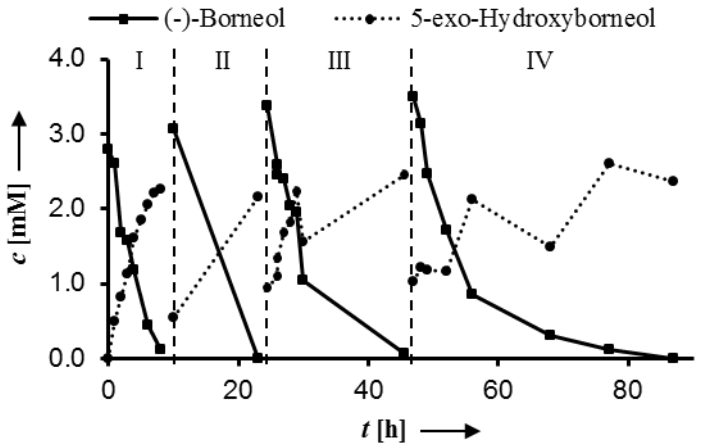

Figure 22: Substrate conversion and product formation during the biotransformation of (-)-borneol by *P. putida* KT2440 pBBr122::*camCAB* with cell recycling. Each dotted vertical line indicates the addition of fresh substrate and medium. Overall cells could be used up to four times for the conversion of (-)-borneol (Phase I - IV). Figure according to *Roth et al.*.[156] Experiments were carried out together with Irina Funk. For conversion of 5 mM (-)-borneol see chapter 7.5.

In every batch process the substrate could completely converted (Table 22), which confirmed that the cells were reusable as a catalyst for the conversion of (-)-borneol. As mentioned above only 80 – 90 % of the total volume was extracted. Thus, the yield of every batch process remained at approximately 80 %. Besides the advantage of direct product extraction within the process also no side-product formation was observed compared to the shake flask

experiments, which is most likely due to the controlled lower oxygen level in the medium by the aeration. Finally, 5-*exo*-hydroxyborneol could be produced with a concentration of 0.54 g L^{-1}.

Table 22: Parameters obtained during the biotransformation of (-)-borneol by *P. putida* KT2440 pBBr122::*camCAB*. *STY*s refer to wet biomass, for calculation see experimental section. Table according to *Roth et al.*.[156] Experiments were carried out together with Irina Funk. For conversion of 5 mM (-)-borneol see chapter 7.5.

	Phase I	Phase II	Phase III	Phase IV
t [h]	8	13	21	40
Conversion [%]	99.8	99.6	98.0	98.8
Yield [%]	80.9	75.3	81.7	83.3
STY [mg L^{-1} h^{-1}]	48	28	20	11
STY [mg mg^{-1} h^{-1}]	12	6.0	4.0	2.0

3.3.3 Characterization of 5-*exo*-hydroxyborneol

After further purification by recrystallization 5-*exo*-hydroxyborneol was obtained as a white powder with a melting point of T_m = 130 – 140 °C (chapter 2.2.4.1). The site-specific hydroxylation of camphor to 5-*exo*-hydroxycamphor by the $P450_{cam}$ enzyme is reported in literature.[157] GC-MS and NMR analysis were carried out in order to verify that hydroxylation of (-)-borneol resulted in an enantiomeric pure product. As there is no 5-*endo*-hydroxyborneol available, the effect of the stereochemistry of the hydroxyl group was investigated with (-)-borneol and its isomer (-)-*iso*-borneol. GC-MS analysis of a mixture of both diastereoisomers revealed a clear separation of both substances with the used method (Figure 23).

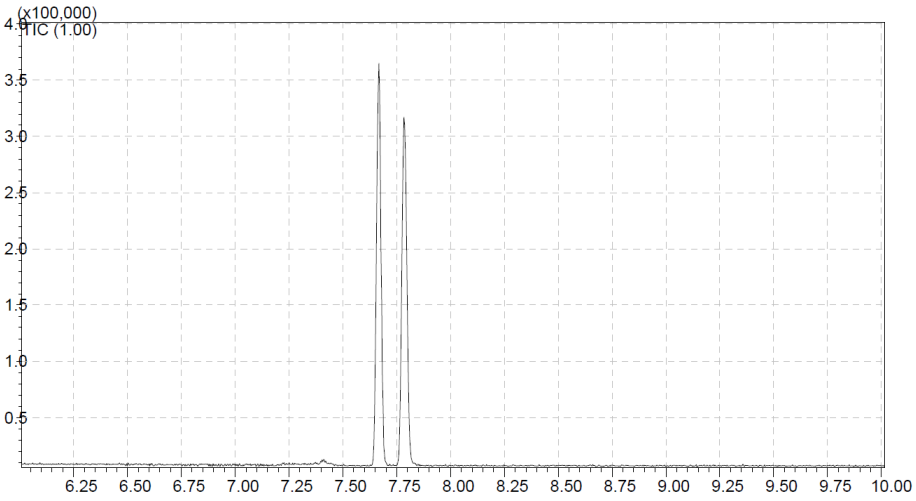

Figure 23: GC-MS analysis of a mixture of (-)-borneol and (-)-*iso*-borneol in ethyl acetate. Y-axis: intensity; x-axis: retention time [min]; t_r((-)-*iso*-borneol) ~ 7.65 min; t_r((-)-borneol) ~ 7.80 min.

If the hydroxylation of (-)-borneol would result in a mixture of 5-*exo*- and 5-*endo*-hydroxyborneol two peaks would be detectable, but GC-MS analysis revealed one clear peak, which was a first indication for the production of only one enantiomer.

Furthermore, these results were confirmed by NMR spectroscopy analyzing (-)-borneol, (-)-*iso*-borneol and a mixture of both (Figure 24, chapter 2.2.5.5). The H-atoms of the hydroxyl group of (-)-borneol as well as of (-)-*iso*-borneol showed a certain chemical shift in ^{1}H NMR analysis. The analysis of the mixture of both also revealed these two chemical

shifts, whereby both diastereoisomers could be clearly identified and differentiated by the orientation of their hydroxyl group (Figure 24).

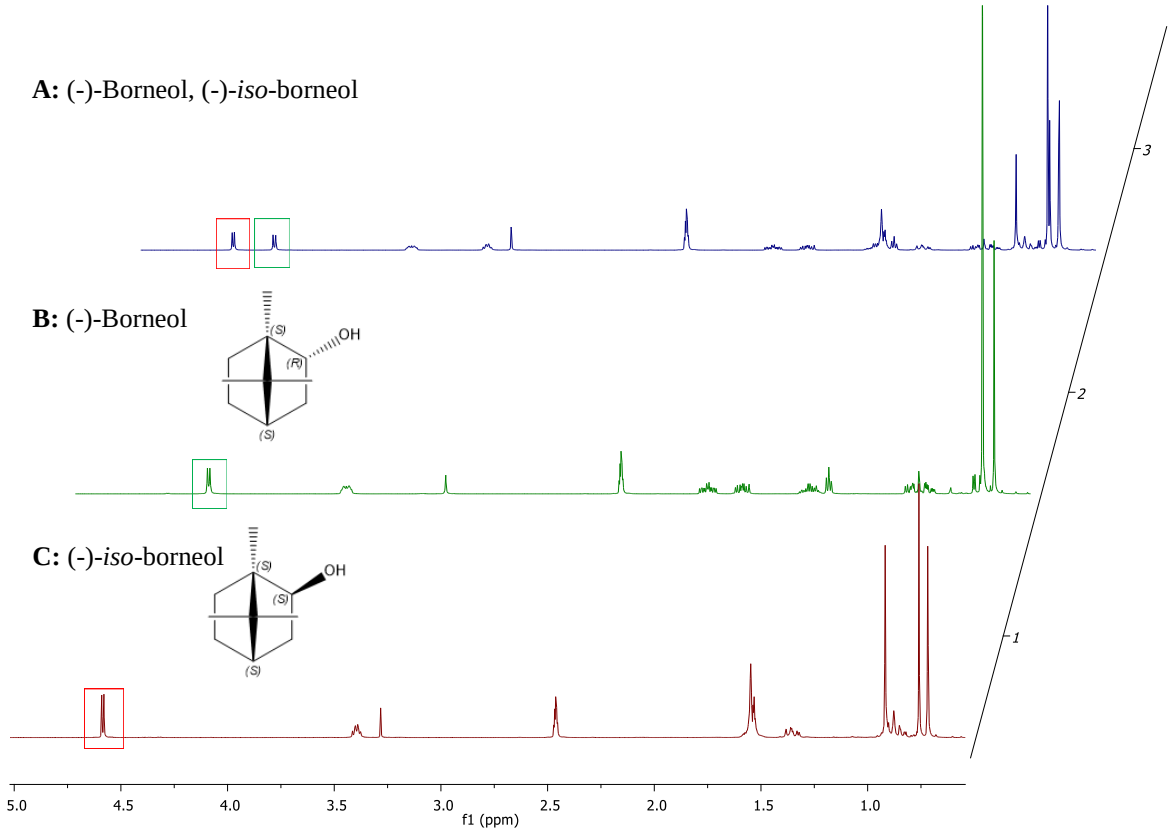

Figure 24: ^{1}H NMR chromatogram of (-)-borneol (B), (-)-*iso*-borneol (C) and a mixture of both in *d*-DMSO. Y-axis: The different ^{1}H NMR chromatograms; x-axis: Chemical shifts with reference to tetramethylsilane [ppm]. The peak for the hydroxyl group of (-)-borneol is highlighted in a green box, the one for (-)-iso-borneol in a red box. In the mixture both diastereoisomers could be separately detected.

All chemical shifts of the ^{1}H NMR analysis of 5-*exo*-hydroxyborneol could be assigned to the corresponding H-atoms in the structure of 5-*exo*-hydroxyborneol according to an NMR analysis of *Gunawardana et al.* (Figure 25).[158] Similar shifts compared to the analysis of (-)-borneol and (-)-*iso*-borneol could also be observed for both hydroxyl groups present in 5-*exo*-hydroxyborneol. Integration of these signals revealed that the H-atoms of the hydroxyl groups are at a ratio of 1:1, which is a strong evidence for the presence of two hydroxyl groups with different orientations. Otherwise if the hydroxylation of (-)-borneol would result in a mixture of 5-*exo*- and 5-*endo*-hydroxyborneol the ratio of these signals would not be balanced. Furthermore, if only the 5-*endo*-hydroxyborneol would be produced by the cells,

only one signal with a higher intensity would be obtained. Additionally, hydroxylation of camphor by $P450_{cam}$, Pdr and Pdx of *P. putida* ATCC17453 is reported to be highly site-specific and only 5-*exo*-hydroxycamphor is formed.[157]

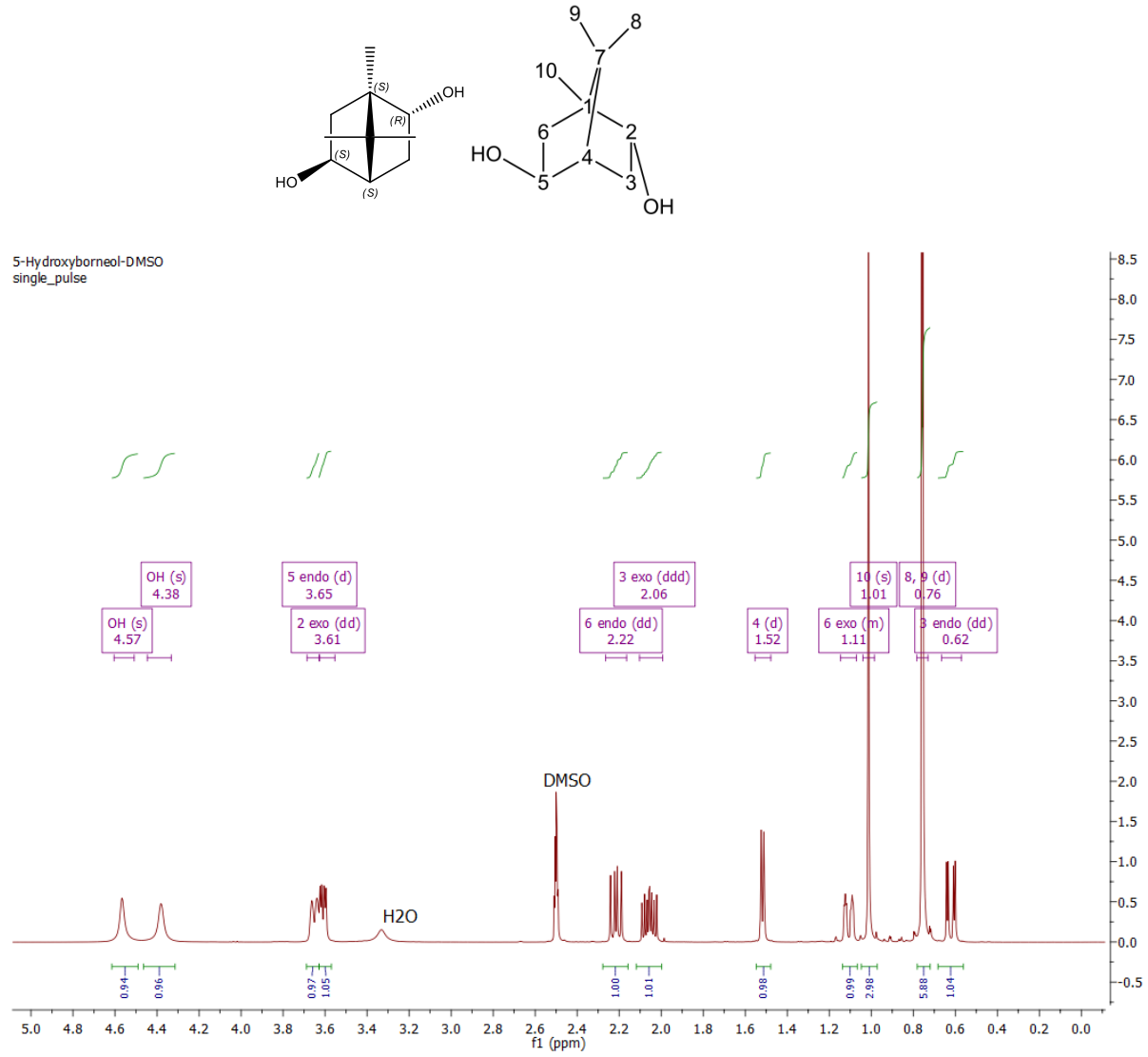

Figure 25: ^{1}H NMR chromatogram of 5-*exo*-hydroxyborneol in *d*-DMSO. Y-axis: intensity; x-axis: Chemical shifts with reference to tetramethylsilane [ppm]. Above: structure of 5-*exo*-hydroxyborneol (left); the different C-atoms were numerated from 1 – 10 according to *Gunawardana et al.* (right).[158] All peaks were assigned to the corresponding H-atoms. ^{1}H NMR (400 MHz) δ 4.57 (s, 1H), 4.38 (s, 1H), 3.65 (d, J = 9.4 Hz, 1H), 3.61 (dd, J = 8.0, 3.3 Hz, 1H), 2.22 (dd, J = 12.9, 8.0 Hz, 1H), 2.06 (ddd, J = 13.3, 9.7, 5.2 Hz, 1H), 1.52 (d, J = 5.1 Hz, 1H), 1.15 – 1.07 (m, 1H), 1.01 (s, 3H), 0.76 (2s, overlap, 6H), 0.62 (dd, J = 13.2, 3.2 Hz, 1H). Two chemical shifts for the *endo*- and *exo*-hydroxyl group of 5-*exo*-hydroxyborneol were obtained at the same ratio.

Taken these results together, GC-MS and NMR analysis revealed the enantiomeric pure production of 5-*exo*-hydroxyborneol by the conversion of (-)-borneol by *P. putida* KT2440 pBBr122::*camCAB*.

3.3.4 Orf16 – a borneol dehydrogenase (Bdh)

In order to provide a *P. putida* ATCC17543 mutant strain for the production of 5-*exo*-hydroxyborneol the activity of the wt against (-)-borneol was analyzed. A growth test revealed that the wt was able to grow using (-)-borneol as a single carbon source. Recently, a borneol dehydrogenase was found in *Pseudomonas* TCU-HL1 and sequence alignment showed an identity of 82 % on the protein level with an open reading frame (*orf16*) in *P. putida* ATCC17453 located on the CAM plasmid.[159] The conversion of (-)-borneol towards camphor would result in a strain, which could not be used for the production of 5-*exo*-hydroxyborneol. Hence, the enzyme encoded by the *orf16* was characterized in more detail. The gene sequence of Orf16 is located on the CAM plasmid between different enzymes for the camphor degradation. Chromosomal and plasmid DNA were isolated from *P. putida* ATCC17453 cultivated with camphor as a sole carbon source (chapter 2.2.2.2) and the gene was amplified using specific primers to add restriction sites (NotI, NcoI) as well as an N- and C-terminal his-tag, respectively (chapter 2.2.2.6, 2.2.2.3). The expression vector pET28a was digested with the same enzymes and after ligation the successful cloning was confirmed by sequencing. Both his-tag variants showed a deletion at bp 737, which resulted in the expression of a truncated version of the enzyme (260 amino acids instead of 285).

As all PCRs were performed independently and showed the same deletion, one could suggest that the PCR itself was not the reason for the deletion but rather the native DNA sequence could be reported erroneously. For the first analysis and in order to clarify if even the truncated enzymes are active, the constructs were transferred into *E. coli* BL21(DE3) and used for an expression test by varying the temperatures and the amount of inductor (Figure 26, chapter 2.2.3.1).

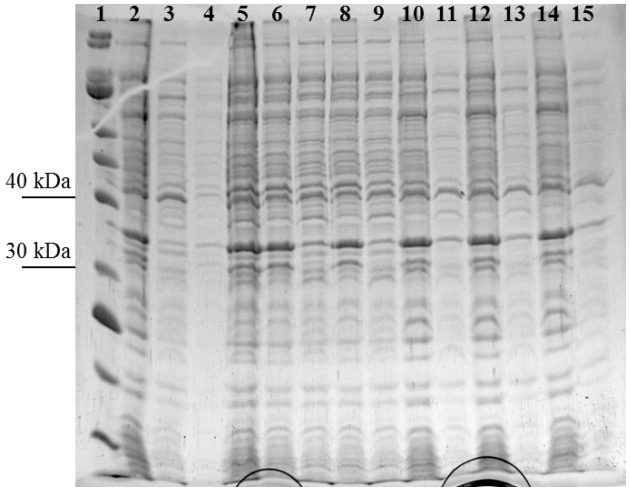

Figure 26: SDS-PAGE analysis of *E. coli* BL21(DE3) pET28a::*orf16* expression test after 16 h of induction at 16 °C (lane 4 – 9) and after 4 h at 30 °C (lane 10 – 15). Lane 1: protein standard; lane 2: before induction, pellet; lane 3: before induction, supernatant; lane 4: 0.1 mM IPTG, pellet; lane 5: 0.1 mM IPTG, supernatant; lane 6: 0.5 mM IPTG, pellet; lane 7: 0.5 mM IPTG, supernatant; lane 8: 1.0 mM IPTG; pellet; lane 9: 1.0 mM IPTG, supernatant; lane 10: 0.1 mM IPTG, pellet; lane 11: 0.1 mM IPTG, supernatant; lane 12: 0.5 mM IPTG, pellet; lane 13: 0.5 mM IPTG, supernatant; lane 14: 1.0 mM IPTG; pellet; lane 15: 1.0 mM IPTG, supernatant.

The expected size for the protein Orf16 is about 33 kDa and the expression at 16 °C as well as at 30 °C resulted in a clear band in the pellet fraction and a weak band in the supernatant at the expected height. Compared to the cells before the induction with IPTG the expression cultures showed the same behavior in the SDS-PAGE analysis, thus a clear expression of the enzyme could not be confirmed. Also an additionally western blot analysis did not provide clear evidence whether the enzyme was expressed or not.

Hence, (-)-borneol was added to the already induced cells as a substrate in order to obtain any activity and GC-MS analysis confirmed the nearly complete conversion of (-)-borneol towards camphor after already 1 h, whereas the negative control (*E. coli* BL21(DE3) pET28a) showed no conversion (Figure 27). These results strongly indicate that the enzyme encoded by *orf16* on the CAM plasmid has a borneol dehydrogenase activity.

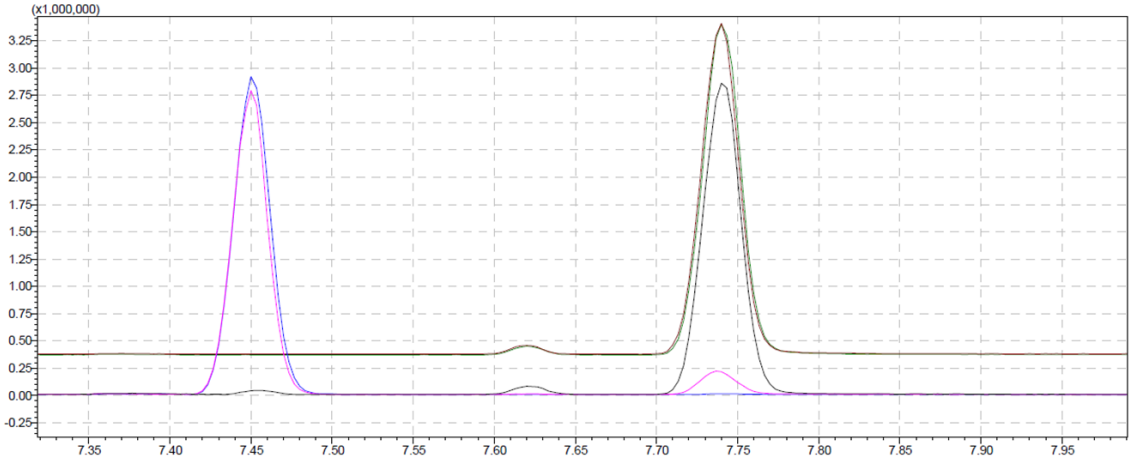

Figure 27: GC-MS analysis of the conversion of (-)-borneol by *E. coli* BL21(DE) pET28a::*orf16* after 0, 1 and 2 h of incubation. Y-axis: intensity; x-axis: retention time [min]; black: after 0 h; pink: after 1 h; blue: after 2 h; brown: negative control after 0 h; green: negative control after 1 h; t_r(camphor) ~ 7.45 min; t_r((-)-borneol) ~ 7.75 min.

Next, the his-tagged enzyme was purified and used for activity tests with different substrates. SDS-PAGE analysis of the different fractions during the purification showed that the enzyme has a slightly lower size (< 30 kDa) than expected (~ 33 kDa, Figure 28).

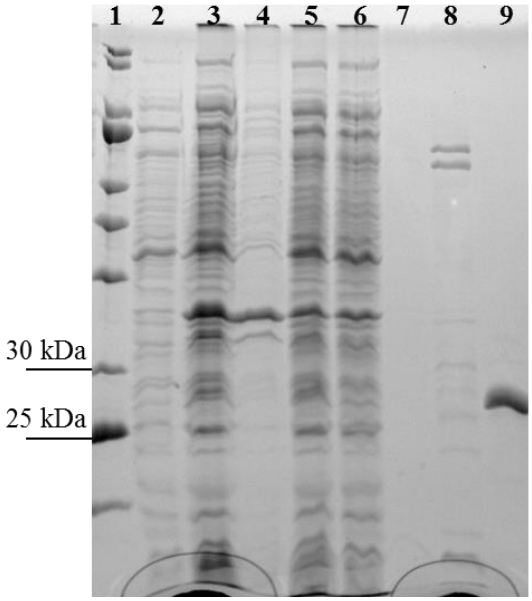

Figure 28: SDS-PAGE analysis of the purification of Orf16-N-his expressed in *E. coli* BL21(DE3) for 4 h at 30 °C using 1.0 mM IPTG. Lane 1: protein standard; lane 2: before induction, supernatant; lane 3: crude extract; lane 4: pellet; lane 5: supernatant; lane 6: flow-through; lane 7: washing step; lane 8: elution peak 1 (10 % elution buffer); lane 9: elution peak 2 (60 % elution buffer).

Most probably the lower size of the enzyme is the result of the expression of the truncated version of the enzyme. Most of the enzyme is present in the soluble fraction of the crude extract (lane 5) and no enzyme was lost during the washing step (lane 7). Analysis of the elution peaks revealed that the enzyme completely elutes within peak 2 at a high purity (chapter 2.2.3.4).

In total 2.36 mg of protein could be purified which is equivalent to 0.16 $mg_{protein}/g_{pellet}$. Activity of the purified enzyme was confirmed in a photometric assay using (-)-borneol as a substrate and following the formation of $NADH/H^+$ at 340 nm. Based on the conversion of (-)-borneol the enzyme was renamed as borneol dehydrogenase (Bdh).

Next, the conversion of different borneol-derived substrates was investigated. GC-MS analysis revealed that besides (-)-borneol also (+)-borneol, (±)-*iso*-borneol and 5-*exo*-hydroxyborneol were converted into the corresponding ketones by the Bdh (chapter 2.2.3.12). Interestingly, 5-*exo*-hydroxyborneol was completely converted to 5-*exo*-hydroxycamphor without further conversion to 2,5-diketocamphane. Furthermore, the back reaction of the enzyme was analyzed using (-)- and (+)-camphor as substrate and $NADH/H^+$ as a cofactor, but after incubation overnight only small amounts of borneol were formed. In order to shift the equilibrium towards the carbonyl product, a coupled enzyme reaction cascade was developed using the formate dehydrogenase (Fdh) from *Candida boidinii* converting formate to CO_2 while the consumption of NAD^+ (Figure 29, chapter 2.2.3.12).

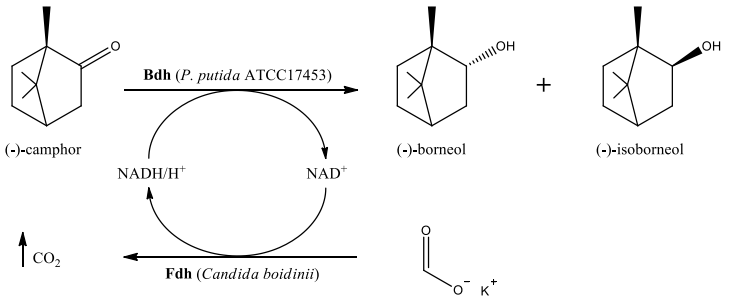

Figure 29: The equilibrium for the reduction of (-)-camphor by the Bdh could be shifted towards the borneol product side by a coupled enzyme reaction using the Fdh of *Candida boidinii* and potassium formate as a substrate. CO_2 is released as a product and could not be used for the back reaction due to its volatile nature. Enzymes are displayed in bold.

Fdh and its substrate were used in excess, so that any NAD^+ which is formed during the reaction by the conversion of (+)- or (-)-camphor is immediately converted to $NADH/H^+$. Substrate consumption and product formation was analyzed by GC-MS (Figure 30).

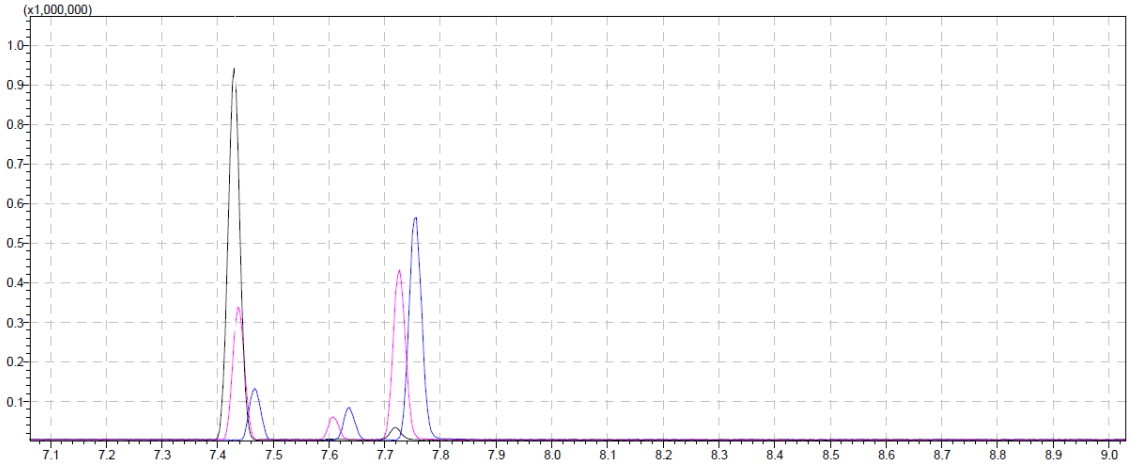

Figure 30: GC-MS analysis of the conversion of (-)-camphor by the purified Bdh (N-His) after 1 h, 1 d and 2 d of incubation. Y-axis: intensity; x-axis: retention time [min]; black: after 1 h; pink: after 1 d; blue: after 2 d; t_r((-)-camphor) ~ 7.45 min; t_r(isoborneol) ~ 7.65 min; t_r(borneol) ~ 7.75 min.

Besides borneol also small amounts of isoborneol were formed by the Bdh in the regeneration system. With the combination of low amounts of $NADH/H^+$ and a high excess of Fdh and formate, it was possible to shift the equilibrium. This setup allowed the complete conversion of camphor by the Bdh within 2 – 3 d whereby borneol was obtained as the major product.

3.3.5 Double mutant Δ*camD* Δ*bdh*

After characterization of Bdh the double mutant strain *P. putida* ATCC17453 Δ*camD* Δ*bdh* should be generated and used for the production of 5-*exo*-hydroxyborneol by the conversion of (-)-borneol. First the *camD* gene was deleted using the method according to *Martinez-Garcia et al.*[73] and the resulting mutant strain was used for the sequential knockout of the *bdh* gene (chapter 2.2.2.9). The desired size for the PCR product of both mutants was confirmed by agarose gel electrophoresis (Δ*camD* ~ 3.0 kbp, Δ*camD* Δ*bdh* ~ 2.4 kbp) and sequencing of PCR products confirmed the seamless knockout of both genes (Figure 31).

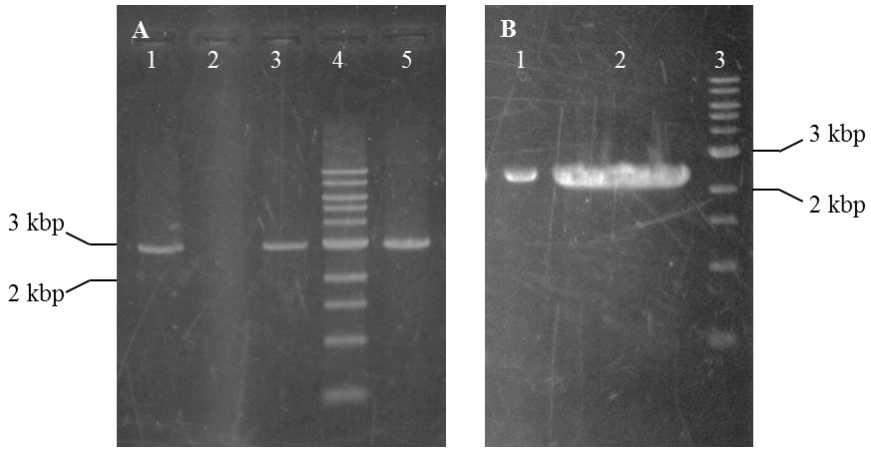

Figure 31: Phusion PCR using isolated DNA of the mutant strains *P. putida* ATCC17453 Δ*camD* (A) and *P. putida* ATCC17453 Δ*camD* Δ*bdh* (B). Size of the expected PCR products: Δ*camD* mutant ~ 3.0 kbp; Δ*camD* Δ*bdh* mutant ~ 2.4 kbp. A: Lane 1, 2, 3 and 5: different mutants of *P. putida* ATCC17453 Δ*camD*; lane 4: DNA standard; B: Lane 1 and 2: different mutants of *P. putida* ATCC17453 Δ*camD* Δ*bdh*; lane 3: DNA standard.

The growth behavior of both mutant strains depending on the different substrates (-)- and (+)-camphor, (-)- and (+)-borneol was analyzed and compared to the wt (Figure 32, chapter 2.2.1.3). The *P. putida* ATCC17453 wt showed the expected growth behavior in the presence of (+)-camphor as a single carbon source and entered the stationary phase after complete consumption of the carbon source with an OD_{600} ~ 1.2 after 4 h (Figure 32 A and B). In contrast, neither of the mutants grew in the presence of (+)-camphor. Only a small amount of 5-*exo*-hydroxycamphor for the Δ*camD* mutant and no conversion of (+)-camphor for the Δ*camD* Δ*bdh* mutant could be detected by GC-MS analysis. Growth curves and GC-MS results for the cultivation using (-)-camphor as single carbon source were similar and are not shown here.

Next, both mutants and the wt were cultivated using glucose and (-)-camphor as carbon source (Figure 32 C and D). Again, the wt showed an expected growth behavior and due to the higher amount of the carbon source, the stationary phase was entered at higher OD_{600} values compared to the first experiment (OD_{600} ~ 1.8, after 7 h). This time also both mutant strains were able to grow, but entered the stationary phase a lot earlier (4 h) with a lower OD_{600} (OD_{600} ~ 1.0) compared to the wt. An enzymatic glucose assay of the samples during the cultivation revealed that the glucose was completely consumed after 3 h by the wt and both mutant strains (chapter 7.3).

At this time both mutant strains entered the stationary phase while the wt was able to grow further by metabolizing camphor. GC-MS results were similar compared to the first experiment and only a small amount of 5-*exo*-hydroxycamphor was formed by the Δ*camD* mutant and no formation of any intermediates was observed for the Δ*camD* Δ*bdh* mutant.

Similar results for the cultivation using (-)-borneol compared to the cultivation using (+)-camphor were observed for the wt and both mutant strains. The wt showed the expected growth behavior and reached the stationary phase after 8 – 9 h with an OD_{600} of 1.5 (Figure 32 E and F). In contrast, both mutant strains were not able to metabolize (-)-borneol and showed no growth. GC-MS analysis during the cultivation showed the formation of a high amount of camphor and a small amount of 5-*exo*-hydroxycamphor by the Δ*camD* mutant. This result was expected as the borneol dehydrogenase is still active in this mutant strain. The Δ*camD* Δ*bdh* mutant did not show the formation of camphor as expected, but also no 5-*exo*-hydroxyborneol formation could be observed by GC-MS analysis.

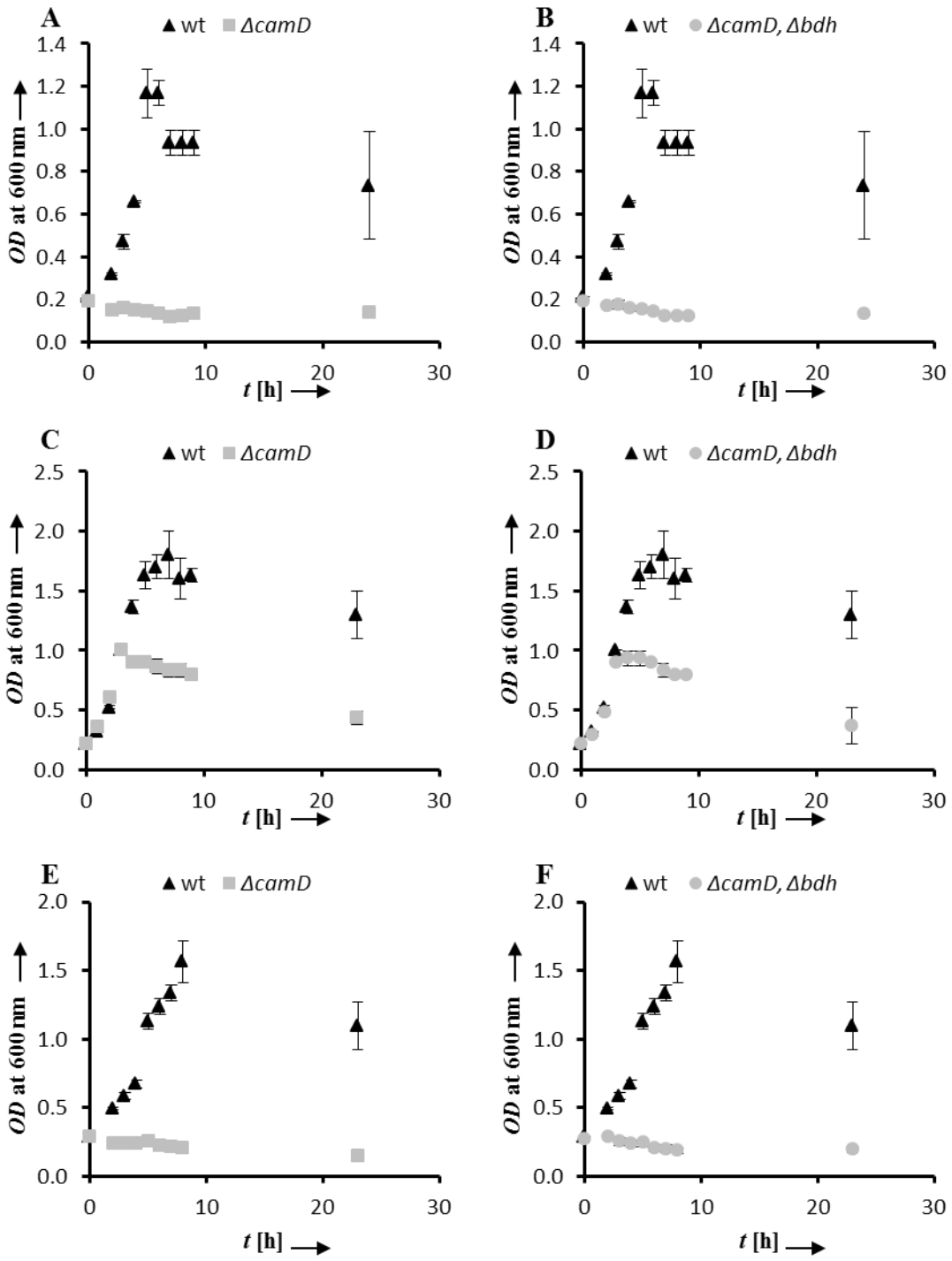

Figure 32: Growth curves of *P. putida* ATCC17453 wt, *P. putida* ATCC17453 Δ*camD* and *P. putida* ATCC17453 Δ*camD* Δ*bdh* in minimal medium using 0.5 g L^{-1} of (+)-camphor (A and B), (+)-camphor and glucose (each 0.5 g L^{-1}, C and D) or (-)-borneol (E and F) as carbon source, respectively. Y-axis: *OD*-values at 600 nm; x-axis: time [h]; black triangle: wt; grey square: Δ*camD* mutant; grey dots: Δ*camD* Δ*bdh* mutant. Error bars represent the standard deviation of triplicates.

In order to increase the amount of catalyst, stationary cells grown with glucose were incubated with the substrates (-)- and (+)-camphor and (-)-and (+)-borneol respectively (chapter 2.2.1.3). GC-MS analysis revealed a similar behavior of the wt and all mutants compared to the growth tests (Figure 33). (+)-Borneol was converted towards camphor and a small amount of 2,5-diketocamphane by the wt. The Δ*camD* mutant strain also converted (+)-borneol to camphor, but as expected no further conversion was detected by GC-MS analysis. In contrast, no conversion of (+)-borneol was observed by the double mutant Δ*camD* Δ*bdh*.

Taken these results together it could be confirmed that the borneol dehydrogenase (Bdh) is responsible for the oxidation of (-)- and (+)-borneol to the corresponding camphor isomer as the ability for the conversion was completely lost by the deletion of the *bdh* gene. The single mutant Δ*camD* as well as the double mutant Δ*camD* Δ*bdh* were not able to hydroxylate any of the substrates (-)- and (+)-camphor and (-)-and (+)-borneol, respectively.

Figure 33: GC-MS chromatogram using (+)-borneol as a substrate and stationary grown cells of *P. putida* ATCC17453 wt (brown), Δ*camD* mutant (pink) and Δ*camD* Δ*bdh* mutant (blue). Y-axis: intensity; x-axis: retention time [min]; t_r(camphor) ~ 7.8 min; t_r((+)-borneol) ~ 8.1 min; t_r(2,5-diketocamphane) ~ 9.8 min.

3.4 Polymerization of 5-*exo*-hydroxyborneol

The purified 5-*exo*-hydroxyborneol from the biotransformation (chapter 3.3.2) was used for a proof of principle to clarify whether camphor-derived monomers represent suitable building blocks for bio-based polyesters (chapter 2.2.4.2). As a comonomer succinic dimethyl ester, which also could be produced based on renewable resources was chosen to obtain a completely bio-based polyester. The procedure for the polycondensation was adapted from

the polymerization of polybutylene terephthalate (PBT), one of the most commercially produced polyesters. The first step of the polymerization, the oligomerization, was carried out at reaction temperatures (T = 190 °C) above the melting point of 5-*exo*-hydroxyborneol (T_m = 130 – 140 °C) and slightly below the boiling point of succinic acid dimethyl ester (T_b = 196 °C). Methanol was released and used as a marker to follow the reaction process. After the expected amount of methanol was released, the second step of the polycondensation was carried out at higher temperatures (T = 210 °C) and reduced pressure (p = 90 mbar) in order to remove residual succinic acid dimethyl ester. This first attempts of the solvent-free polycondensation resulted in viscous, glutinous reaction mixtures. Consequently, the reaction temperature (T = 250 °C) and also time (from 3 h to 5 h) for the second step of the polycondensation were increased and an amber-colored, transparent solid was obtained (Figure 34). The polycondensation was repeated three times whereby optically similar products were obtained.

Figure 34: The novel terpene-based biopolymer (left) in comparison to polybutylene terephthalate (right). The amber-colored biopolymer showed a high transparency compared to the white PBT.

For a first characterization of the novel polyester the thermal properties and molecular mass distribution were investigated by differential scanning calorimetry (chapter 2.2.5.3) and gel-permeation chromatography (chapter 2.2.5.4). The samples of the crude biopolymer showed a glass transition temperature in a range of 35 – 55 °C. After the removal of the residual monomers, the glass transition temperature increased to about 70 °C (Figure 35), which is higher compared to the structural related polybutylene terephthalate.

The molecular weight of the terpene-based copolymer was in the range of 2,000 – 4,000 g mol^{-1} (*PDI* = 1.9, chapter 7.1), which is much lower compared to the industrial PBT (~ 55,000 g mol^{-1}). The difference in the molecular weights might be attributed to the non-optimized polymerization procedure and the purity of the monomers.

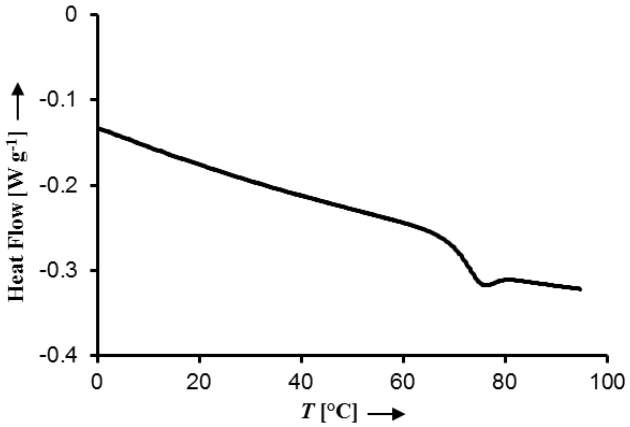

Figure 35: Differential scanning calorimetry of the terpene-based biopolymer after removal of the residual monomers. Y-axis: Heat flow [W g^{-1}]; x-axis: temperature [°C]. The second scan of the sample is shown and glass transition temperature was calculated by integration.

3.5 Production of 2,5-diketocamphane

The production of 2,5-diketocamphane could already be demonstrated by the recombinant expression of the *camDCAB* operon in *P. putida* KT2440 using camphor as a substrate. The resulting product itself is not suitable for polymerization, but could be further modified to build a precursor for polyamides. For that reason, the suitability of the mutant strain *P. putida* ATCC17453 Δ*camE*$_{25\text{-}1}$ Δ*camE*$_{25\text{-}2}$ for the production of 2,5-diketocamphane was investigated in this work (Figure 36).

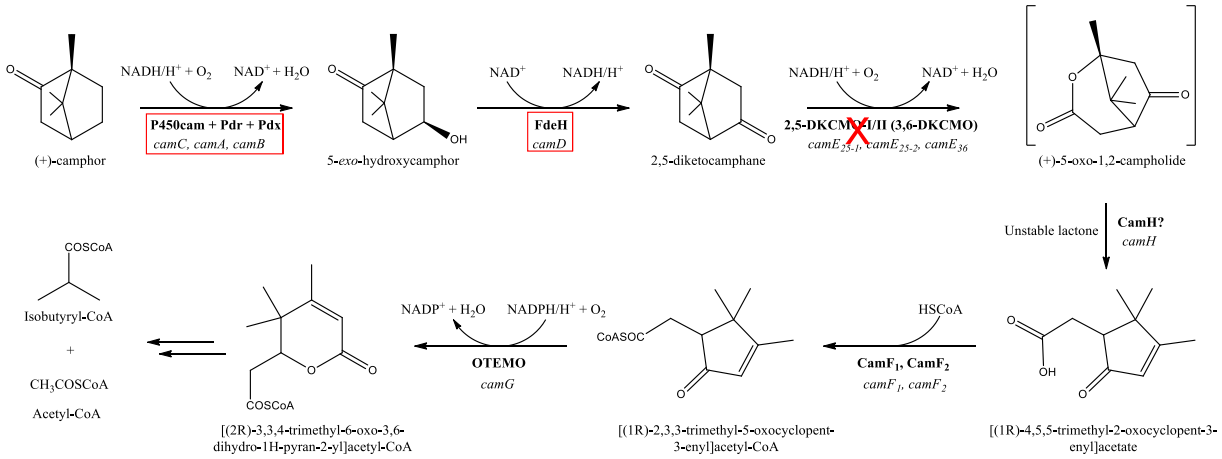

Figure 36: Biodegradation of (+)-camphor to isobutyryl-CoA and acetyl-CoA by the CAM plasmid of *P. putida* ATCC17453. Two strategies for the conversion of (+)-camphor towards 2,5-diketocamphane were analyzed: (i) recombinant expression of $P450_{cam}$, Pdr, Pdx and FdH in *P. putida* KT2440 (red box); (ii) deletion of 2,5 DKCMO-I and -II (*camE*$_{25\text{-}1}$, *camE*$_{25\text{-}2}$) to interrupt the metabolism (red cross). Enzymes are displayed in bold, corresponding genes in italic.

3.5.1 Double mutant Δ*camE*$_{25-2}$ Δ*camE*$_{25-1}$

The sequential gene knockout of both genes was performed using the method according to *Martinez-Garcia et al.*[73] (chapter 2.2.2.9). The desired size of the PCR product of the Δ*camE*$_{25-2}$ mutant was confirmed by agarose gel electrophoresis (Δ*camE*$_{25-2}$ ~ 2.2 kbp, Figure 37).

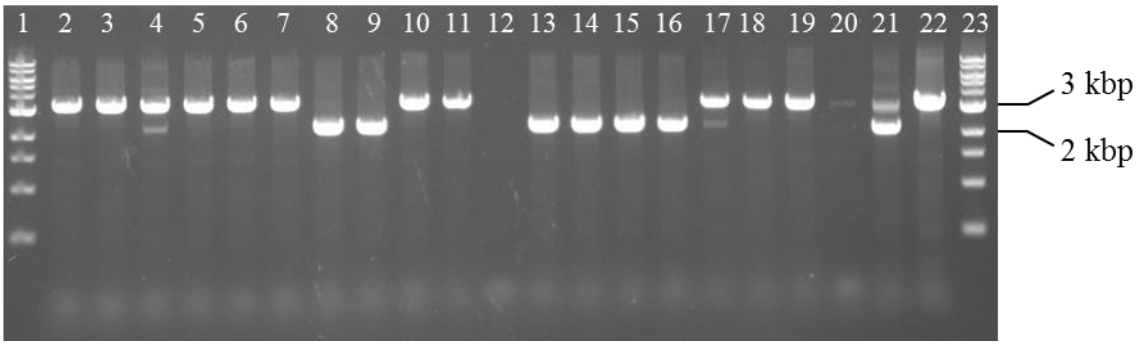

Figure 37: Phusion PCR using isolated DNA of the *P. putida* ATCC17453 wt and Δ*camE*$_{25-2}$ mutant. Size of the expected PCR products: wt ~ 3.3 kbps; Δ*camE*$_{25-2}$ mutant ~ 2.2 kbp. Lane 1 and 23: DNA standard; lane 2: wt control; lane 3 – 22: different clones for the gene knockout.

The wt showed the expected size of 3.3 kbp (lane 2) and six of the 20 tested clones showed the desired size of 2.2 kbp for the knockout mutants. Furthermore, three of the analyzed clones showed both a band for the wt and the mutant. This confirmed the results of the qPCR that more than one CAM plasmid is present in each cell of *P. putida* ATCC17453. The sequential knockout of the second 2,5-DKCMO-1 was also analyzed by agarose gel electrophoresis and the seamless knockout of both genes was confirmed by sequencing.

Next, the growth of the resulting double mutant Δ*camE*$_{25-2}$ Δ*camE*$_{25-1}$ was analyzed in presence of (+)-camphor and (+)-borneol as a single carbon source or in combination with glucose and compared to the wt (Figure 38, chapter 2.2.1.3).

The wt and Δ*camE*$_{25-2}$ Δ*camE*$_{25-1}$ mutant showed nearly the same growth behavior in the presence of (+)-camphor, (+)-camphor with glucose and (+)-borneol. A slightly faster growth was obtained for the wt in the presence of (+)-camphor and (+)-camphor with glucose than the Δ*camE*$_{25-2}$ Δ*camE*$_{25-1}$ mutant, but both reached the stationary phase after 5 – 6 h with nearly the same optical densities. GC-MS analysis of samples during the cultivation showed

an accumulation of 2,5-diketocamphane for the Δ*camE*$_{25\text{-}2}$ Δ*camE*$_{25\text{-}1}$ mutant compared to the wt. The accumulation is the result of the knockout of both 2,5-DKCMOs, but as the mutant strain still showed growth on camphor, the 2,5-diketocamphane somehow was still further metabolized. In contrast, growth on (+)-borneol as a single carbon source revealed no difference between the wt and the mutant strain.

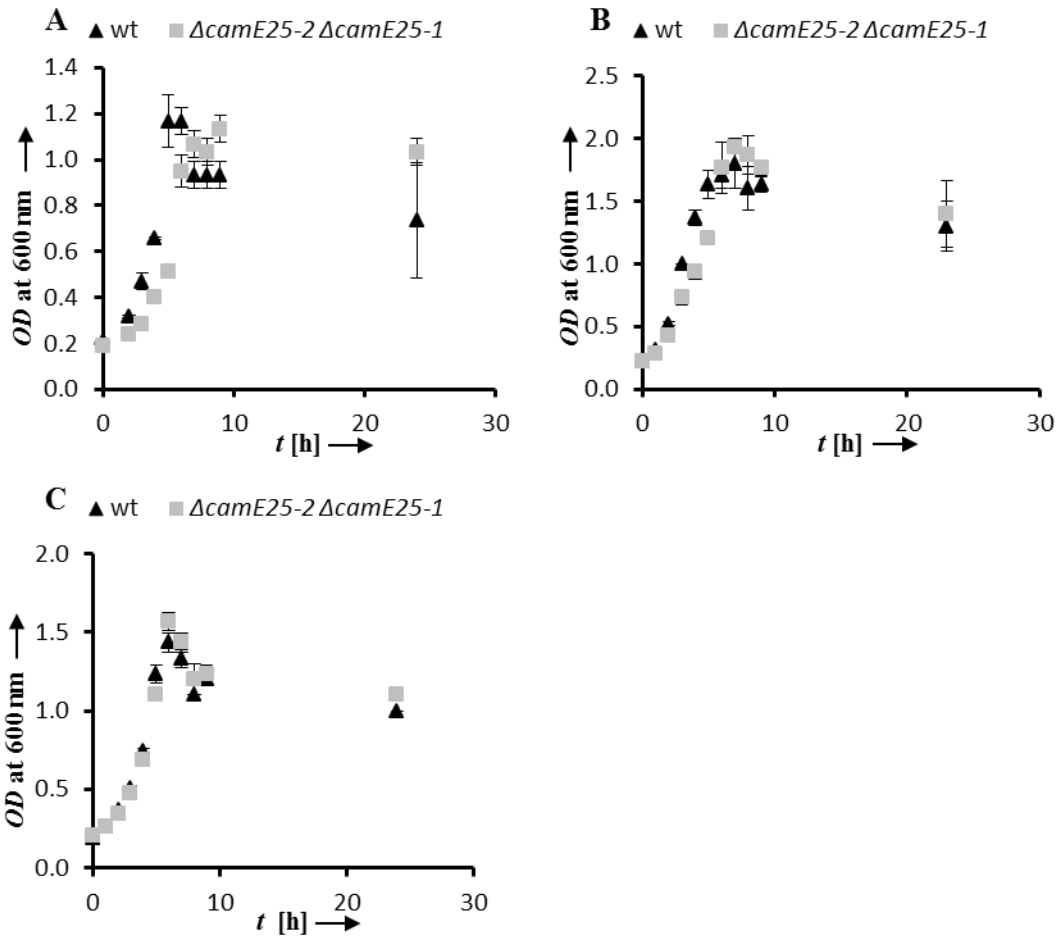

Figure 38: Growth curves of *P. putida* ATCC17453 wt (same data Figure 32) and *P. putida* ATCC17453 Δ*camE*$_{25\text{-}2}$ Δ*camE*$_{25\text{-}1}$ in minimal medium using 0.5 g L^{-1} of (+)-camphor (A), (+)-camphor and glucose (each 0.5 g L^{-1}, B) and (+)-borneol (C) as carbon source. Y-axis: *OD*-values at 600 nm; x-axis: time [h]; black triangle: wt; grey square: Δ*camE*$_{25\text{-}2}$ Δ*camE*$_{25\text{-}1}$ mutant; Error bars represent the standard deviation of triplicates.

Next, conversion of (-)- and (+)-camphor and (-)-and (+)-borneol respectively was analyzed by GC-MS using glucose grown stationary cells of the wt and the mutant (chapter 2.2.1.3). For the amount and composition of the intermediates no differences were observed. This

confirmed the results from the growth curves where the mutant strain and the wt showed a similar behavior.

Taken these results together it was possible to knock out the desired genes for both 2,5-DKCMOs. Nevertheless, the resulting Δ*camE*$_{25\text{-}2}$ Δ*camE*$_{25\text{-}1}$ mutant strain was still able to grow on all substrates and could not be used for the conversion of camphor towards 2,5-diketocamphane.

3.6 Production of lactones

Lactones are interesting starting materials for the synthesis of polymers as they could be easily polymerized by ring opening polymerization. In order to obtain camphor-based lactones three different BVMOs were recombinantly expressed in *P. putida* KT2440 and analyzed for their conversion of different substrates within this work by *Rehberger et al.* (Figure 39).[160] Furthermore, the role of CamH within the camphor degradation pathway and if the deletion of *camH* would yield a mutant strain for the production of 5-oxo-1,2-campholide, which could be a precursor for polyesters, was investigated.

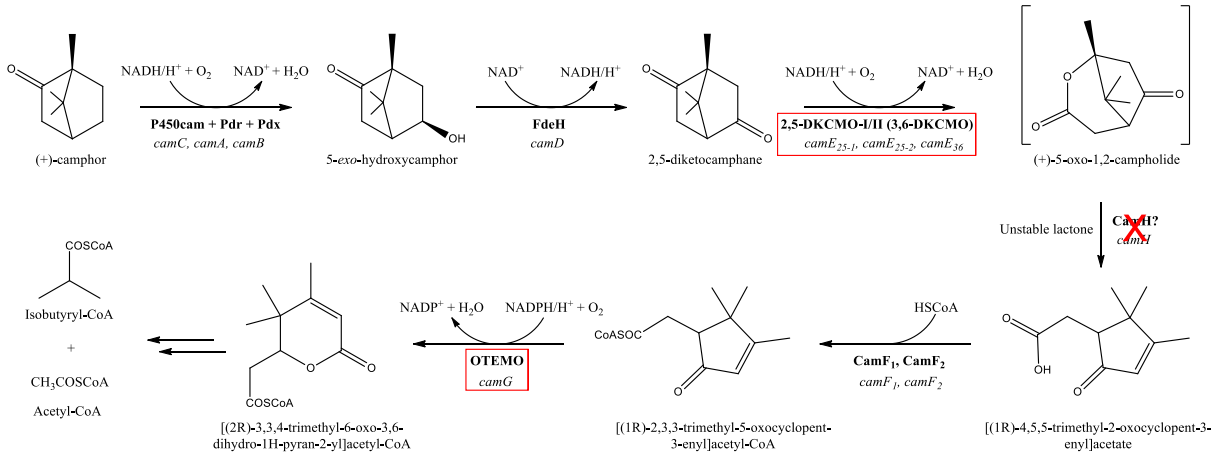

Figure 39: Biodegradation of (+)-camphor to isobutyryl-CoA and acetyl-CoA by the CAM plasmid of *P. putida* ATCC17453. Recombinant expression of three BVMOs (2,5-DKCMO-I, 3,6-DKCMO and OTEMO) in *P. putida* KT2440 to obtain different strains for the synthesis of lactones (red boxes). Clarification if CamH is involved in the camphor degradation pathway by recombinant expression in *P. putida* KT2440 and gene deletion (red cross). Enzymes are displayed in bold, corresponding genes in italic.

3.6.1 Characterization of CamH

The gene sequence of CamH (*camH*) is located on the CAM plasmid near the camphor degrading operon *camDCAB*. Chromosomal and plasmid DNA were isolated (chapter 2.2.2.2) from *P. putida* ATCC17453 cultivated with camphor as a sole carbon source and the gene was amplified using specific primers to add restriction sites (NotI, NcoI) as well as an N- and C-terminal his-tag respectively (chapter 2.2.2.6). For the expression in *E. coli* BL21(DE3) the pET28a expression vector was digested with the same enzymes and after ligation the successful cloning was confirmed by sequencing. Afterwards, the constructs were transferred into *E. coli* BL21(DE3) and used for an expression test by varying the expression temperatures and the amount of inductor (chapter 2.2.3.1). In Figure 40 an exemplary SDS-PAGE analysis is shown.

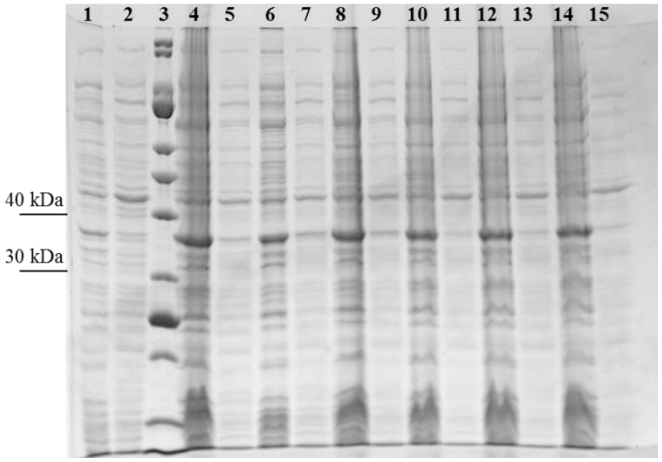

Figure 40: SDS-PAGE analysis of *E. coli* BL21(DE3) pET28a::*camH*-N-his expression test after 4 h of induction at 30 °C (lane 4 – 9) and 37 °C (lane 10 – 15). Lane 1: negative control, 0.1 mM IPTG, pellet; lane 2: negative control, 0.1 mM IPTG, supernatant; lane 3: protein standard; lane 4: 0.1 mM IPTG, pellet; lane 5: 0.1 mM IPTG supernatant; lane 6: 0.5 mM IPTG, pellet; lane 7: 0.5 mM IPTG, supernatant; lane 8: 1.0 mM IPTG, pellet; lane 9: 1.0 mM IPTG, supernatant; lane 10: 0.1 mM IPTG, pellet; lane 11: 0.1 mM IPTG supernatant; lane 12: 0.5 mM IPTG, pellet; lane 13: 0.5 mM IPTG, supernatant; lane 14: 1.0 mM IPTG, pellet; lane 15: 1.0 mM IPTG, supernatant.

All test cultures showed the expected band around 39 kDa in the pellet fraction and also a weak band at the same height in the supernatant. The negative control (lane 1 and 2) itself did not show a protein overexpression at the height of CamH. No big differences were observed

by varying the expression parameters as SDS-PAGE analysis of the other cultures gave similar results.

Next, an expression culture was harvested and CamH was purified in order to provide the pure enzyme for activity assays (chapter 2.2.3.4). The elution fractions of peak 1 and 2 were combined and after buffer exchange the purity of the enzyme was analyzed by SDS-PAGE (Figure 41). Compared to the negative control (lane 1 and 2) a clear band for the expression of CamH-C-his was observed in the pellet and supernatant (lane 3 and 4). A small amount of target enzyme was also detectable in the flow-through whereas no enzyme was lost by the washing step. Both elution peaks showed distinct bands for the desired CamH-C-his at the expected height. A higher purity was obtained for peak 2 compared to peak 1 and small amounts of enzyme were lost by the buffer exchange step. Although SDS-PAGE analysis showed some impurities for elution peak 1, protein concentration of both peaks were determined by UV absorbance measurement at 280 nm, which resulted in 3.1 mg of protein for peak 1 and 1.0 mg of protein for peak 2 or a total yield of 0.90 $mg_{protein}/g_{pellet}$, respectively.

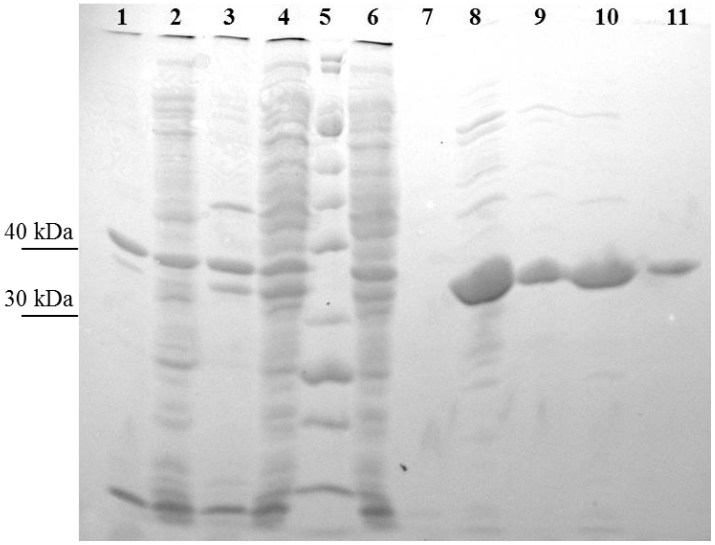

Figure 41: SDS-PAGE analysis of the purification of CamH-C-his expressed in *E. coli* BL21(DE3) over night at 16 °C using 0.5 mM IPTG. Lane 1: negative control pellet, lane 2: negative control supernatant; lane 3: CamH-C-his pellet; lane 4: CamH-C-his supernatant; lane 5: protein standard; lane 6: flow-through; lane 7: washing fraction; lane 8: peak 1 before buffer exchange; lane 9: peak 1 after buffer exchange; lane 10: peak 2 before buffer exchange; lane 11: peak 2 after buffer exchange.

The purified enzymes as well as the crude cell extract, the supernatant and a negative control (pellet and crude cell extract) were used for an activity assay (chapter 2.2.3.14). As the natural substrate ((+)-5-oxo-1,2-campholide) is not available, camphor lactone and ε-caprolactone were used as substrates. After incubation over 2 d none of the samples showed the conversion of any substrate and also no difference compared to the negative controls was observed.

Next, the natural substrate 5-oxo-1,2-campholide should be produced by a biotransformation using camphor lactone as a substrate and the strain *P. putida* KT2440 pBBr122::*camDCAB*, which carries the enzymes for the hydroxylation of camphor and its further oxidation (chapter 2.2.3.13). The conversion of camphor lactone was followed by GC-MS analysis (Figure 42).

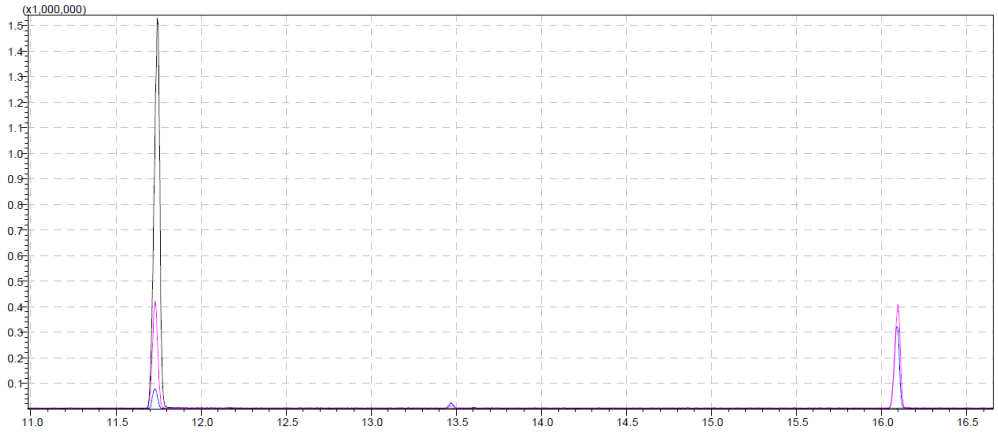

Figure 42: GC-MS analysis of the conversion of camphor lactone conversion by *P. putida* KT2440 pBBr122::*camDCAB* after 0, 3 and 5 h of incubation. Y-axis: intensity; x-axis: retention time [min]; black: after 0 h; pink: after 3 h; blue: after 5 h; t_r(camphor lactone) ~ 11.75 min; t_r(5-oxo-1,2-campholide) ~ 16.10 min.

A distinct decrease in the substrate peak of camphor lactone was obtained, and a minor product peak was detectable by GC-MS analysis. The product peak did not increase with the complete degradation of the substrate. This could be an indication for an unstable product formation where the 5-oxo-1,2-campholide opens by an elimination reaction. As the free acid is not detectable with GC-MS analysis, HPLC-MS analysis was performed using the aqueous phase of the samples (Figure 43, chapter 2.2.5.2).

Compared to the negative control (red) the chromatogram of the conversion of camphor lactone by *P. putida* KT2440 pBBr122::*camDCAB* showed a peak with a retention time of 2.91 min (black). The masses obtained from the MS spectrum fit with the masses expected for the [(1R)-4,5,5-trimethyl-2-oxocyclopent-3-enyl]acetate, the opened version of (-)-5-oxo-1,2-campholide (chapter 7.4).

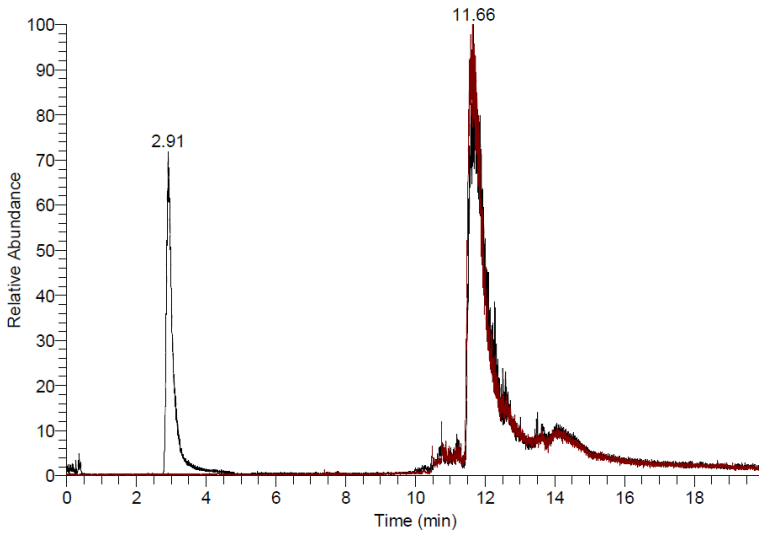

Figure 43: HPLC-MS analysis of the conversion of camphor lactone by *P. putida* KT2440 pBBr122::*camDCAB*. Y-axis: relative abundance; x-axis: retention time [min]; red: negative control; black: aqueous sample of the conversion; t_r([(1R)-4,5,5-trimethyl-2-oxocyclopent-3-enyl]acetate) ~ 2.91 min.

3.6.2 Mutant Δ*camH*

In order to confirm that CamH is not part of the camphor degradation pathway in *P. putida* ATCC17453 the corresponding gene on the CAM plasmid should be deleted. The mutant strain was produced using the method according to *Martinez-Garcia et al.*[73] and successful gene deletion was confirmed by PCR using specific primers for the amplification of *camH* (Figure 44, chapter 2.2.2.9).

The PCR of the wt showed the expected band with a size of about 3.9 kbp (lane 1), which was absent in both Δ*camH* mutant strains (lane 2 and 3). The desired PCR product with a size of 2.9 kbp for the successful gene deletion was obtained for both of the tested mutant strains. Several side-products of the PCR were obtained, but they were present in both, wt and mutant strains. Additionally, the seamless gene knockout was confirmed by sequencing.

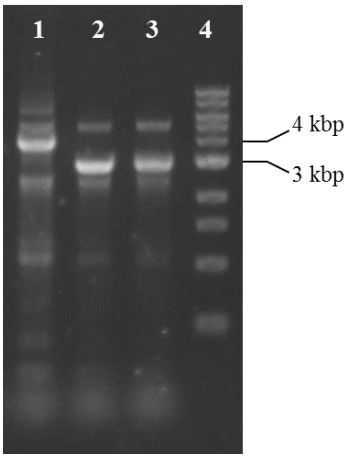

Figure 44: Phusion PCR using isolated DNA from the *P. putida* ATCC17453 Δ*camH* mutant strain and wt. Size of the expected PCR products: wt ~ 3.9 kbp; Δ*camH* mutant: ~ 2.9 kbp. Lane 1: wt; lane 2 and 3: mutant; lane 4: DNA standard.

Next, growth curves of the Δ*camH* mutant strain and the wt were obtained by following the OD_{600} values (chapter 2.2.1.3). In order to identify any difference in camphor metabolism, (+)-camphor was used as a single carbon source. The Δ*camH* mutant and wt strain showed a similar growth behavior (Figure 45).

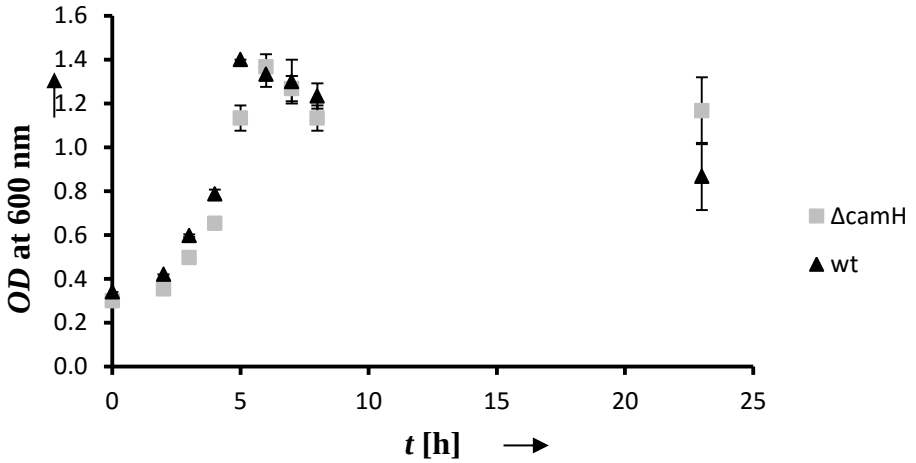

Figure 45: Growth curves of wt *P. putida* ATCC17453 and *P. putida* ATCC17453 Δ*camH* mutant strain in minimal medium using 0.5 g L^{-1} of (+)-camphor as a single carbon source. Y-axis: *OD*-values at 600 nm; x-axis: time [h]; black triangle: wt; grey square: Δ*camH* mutant. Error bars represent the standard deviation of triplicates.

Additionally, GC-MS samples were taken during the growth of both strains and the analysis revealed a similar distribution of the different intermediates for the wt and the Δ*camH* mutant.

If CamH is part of the camphor degradation pathway and responsible for the opening of the (-)-5-oxo-1,2-campholide the deletion of the gene should at least yield a strain with a reduced growth on camphor compared to the wt or even no growth. Furthermore, the (-)-5-oxo-1,2-campholide should accumulate in the Δ*camH* mutant strain, which could not be confirmed by GC-MS analysis. These results revealed that the Δ*camH* mutant strain is still able to metabolize (+)-camphor. For that reason it could be assumed that CamH is not absolutely necessary for the degradation of (+)-camphor and may not be part of the camphor degradation pathway.

4 Discussion

4.1 (+)-Bornyl pyrophosphate synthase

The recombinant expression of the (+)-BPPS in *P. putida* KT2440 should yield a strain able to synthesize (+)-borneol based on its precursors IPP and DMAPP, which are built in the end of the MEP pathway present in *Pseudomonas*. In 1976 the formation of borneol based on neryl pyrophosphate during the biosynthesis of camphor in *Salvia officinalis* was reported for the first time by *Croteau et al.* analyzing the soluble enzyme preparation of the plant leaves.[161] Later the same group isolated the responsible enzyme for the formation of borneol, the (+)-BPPS and demonstrated that geranyl pyrophosphate is the preferred substrate of the enzyme.[162]

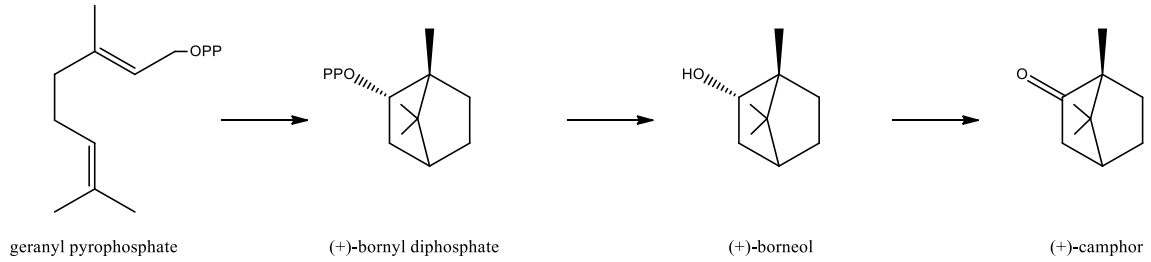

Figure 46: Biosynthesis of camphor in *S. officinalis* according to *Croteau et al.*.[163]

In nature the (+)-BPPS represents one of the key enzymes for the biosynthesis of camphor in *S. officinalis* whereby (+)-borneol is formed as an intermediate.[164] The native enzyme is present as a homodimer with a molecular mass of about 120 kDa and bornyl diphosphate is released as the major product (~ 75 %).[165] The remaining 25 % are a mixture of a series of olefins whereby (+)-camphene (~ 9.5 %) represents the major side-product.[165]

The expression of plant monoterpene synthases in prokaryotes often is problematic due to host codon usage and formation of inclusion bodies.[166] For that reason, a codon-optimized synthetic gene for the target organism *Pseudomonas* was used for the expression of the (+)-BPPS, but the successful expression of the enzyme could not be confirmed, neither by SDS-PAGE nor by western blot analysis (chapter 3.1.1). In order to exclude any problems for the expression caused by the organism *Pseudomonas* itself the gene was cloned into the vector pET28a, but also the expression in *E. coli* BL21(DE3) was not successful. Many plant

monoterpene synthases harbor a transit sequence for the transport to certain compartments in the cell often found at the N-terminus of the enzyme. These transit sequences could hinder the expression of the enzyme as they show a tight association with bacterial chaperones.[166] *Williams et al.* reported the truncation of the (-)-4S-limonene synthase of spearmint directly upstream the highly conserved R58R59 motif, which is necessary for enzyme activity.[166] The expression of the truncated enzyme resulted in a higher yield of the enzyme and even showed a higher catalytic efficiency compared to the native species.[166] The highly conserved arginine motif is also present in the (+)-BPPS (R55R56) and in combination with the aspartate-rich motif DDIYD (starting at D351) it may be responsible for substrate stabilization and the binding and coordination of magnesium ions.[155] As many other monoterpene synthases the (+)-BPPS harbors a transit sequence directly upstream of the arginine motif (aas 1 – 50).[165] After the transfer into the plastids the transit sequence is proteolytically cleaved off and the mature form of the enzyme is processed.[165] *Whittington et al.* could show the expression of an active pseudomature version of the (+)-BPPS truncated at E50 in *E. coli* BLR(DE3) yielding ~ 15 mg of pure enzyme per liter of bacterial cell culture.[155] Consequently, the E50 truncated version of the enzyme was cloned into the vectors pBBr122 and pET28a for the expression in *P. putida* KT2440 and *E. coli* BL21(DE3). In contrast to *Whittington et al.*, the successful expression of the enzyme was not detectable via SDS-PAGE, western blot analysis and activity assays (chapter 3.1.1, 3.1.2). The main difference in this work compared to *Whittington et al.* is the host organism as *P. putida* KT2440 was used instead of *E. coli* BLR(DE3). One reason could be a defective enzyme expression in the organism due to the lack of protein folding chaperones, which could lead to its degradation directly after the expression.[167] Hence, the mRNA level of (+)-BPPS should be determined to clarify if the enzyme is transcribed. If an appropriate mRNA level could be determined the folding and stability of the enzyme within *Pseudomonas* has to be further increased. In order to improve the expression of (+)-BPPS chaperones such like GroESL could be co-expressed as it was shown to increase the solubility, activity and amount of enzyme for the recombinant expression in *E. coli*.[168] Furthermore, the folding of the enzyme could be increased by its expression as a fusion protein. For *E. coli* it was shown that the folding of expressed enzymes in the bacterial cytoplasm could be improved if the desired enzyme is for example fused to a maltose-

binding protein (MBP) from *E. coli*.[169] Moreover, the fusion to *Staphylococcus* protein A (SPA) could also increase the folding and solubility of the enzyme in bacterial organisms.[169] These approaches could also improve the expression and folding of (+)-BPPS in *P. putida* KT2440. Besides the (+)-BPPS the substrates DMAPP and IPP are required for the formation of borneol. Formation of the precursors DMAPP and IPP via the MEP pathway is limited by the bottleneck enzymes Dxs and Idi.[170] For the production of carotenoids via the MEP pathway in *E. coli* it was demonstrated that overexpression of these two enzymes in combination with enzymes responsible for the carotenoid biosynthesis could enhance the overall yield up to 10 times for lycopene and 50 times for astaxanthin, respectively.[171],[172] *Beuttler et al.* constructed a plasmid for the production of zeaxanthin in *P. putida* KT2440.[173] The plasmid harbors six enzymes responsible for the biosynthesis of zeaxanthin and encodes for the overexpression of Dxs and Idi to enhance the formation of the precursors.[173] With this plasmid the group could increase the yield of zeaxanthin by a factor of 4.7 in *P. putida* KT2440.[173] In order to exclude false negative results based on too low amounts of the precursors the genes coding for the biosynthesis of zeaxanthin were exchanged by the truncated *(+)-bpps* gene yielding a plasmid (pJH14), which still codes for the overexpression of the bottleneck enzymes Dxs and Idi. But also with this construct it was not possible to detect any borneol by GC-MS analysis or any expression of the (+)-BPPS in SDS-PAGE and western blot analysis (chapter 3.1.1). As the functionality of the plasmid has been proven for *P. putida* KT2440, which is the same host for the expression in the present work, the unsuccessful enzyme expression may be attributed to the gene sequence. In order to show the active expression of the (+)-BPPS further expression tests could be performed using hosts, which are more related to plants for example yeast strains such as *S. cerevisiae*. For the successful production of terpene-based monomers it was subsequently focused on the biotransformation by recombinant expression of enzymes and the knockout of different genes on the CAM plasmid, respectively.

4.2 Modification of the CAM plasmid

4.2.1 Engineering molecular biological methods for *Pseudomonas*

Before the quantification of the CAM plasmid an appropriate method for the PCR using the isolated plasmid had to be developed. First attempts using the Taq and Phusion polymerase and the recommend PCR protocol of the supplier resulted in no PCR product formation. Various parameters could influence the outcome of a PCR such as the composition of the PCR mixture, the kind of polymerase, the temperature program and also the presence of inhibitors within the sample. As a cofactor for many polymerases the concentration of Mg^{2+} ions is one of the key factors for the success of PCR product amplification.[174] However, the primers and also DNA template both of which are negatively charged could chelate the Mg^{2+} ions and may reduce the amount of free ions for the polymerase, which would result in decreased PCR product formation. Furthermore, any kind of inhibitor present within the sample due to the sample preparation procedure would also negatively influence the yield of the PCR.[175] For that reason the amount of template DNA was decreased by several dilutions. As a result, on the one hand more free Mg^{2+} ions are available for the polymerase and on the other hand the concentration of any inhibitor is decreased and its influence towards the PCR reduced. With the dilution of the template DNA the PCR protocol could be further improved as the signal strength for all PCR products could be increased with an optimal template DNA concentration of 0.2 ng μL^{-1}. Afterwards, the optimal annealing temperature for the PCR on the CAM plasmid (+ 3 °C of the primer with the lower T_m) was obtained by a temperature gradient in the range of ± 10 °C of the T_m. Further improvement by the addition of enhancers such as DMSO, which could enhance the solubility of the template DNA did not influence the product yield (chapter 3.2.1).

Next, an appropriate method for the transformation of *Pseudomonas* had to be developed. For that reason, different methods including chemical transformation, electroporation and conjugation were analyzed using different conditions. The most essential components for chemical competence are divalent cations.[176] The method is based on the formation of small pores (zones of adhesion for the DNA) caused by the divalent cations, which induce a reorganization of the LPS structure and solidification of the inner and outer membrane of the target organism.[176] The chemical transformation of *P. putida* ATCC17453 yielded a high

amount of false-positive clones. In order to reduce the background of false-positive clones, the selective pressure was increased by increasing the antibiotic concentration (gentamycin). The transformation efficiency should be further increased by using Mn^{2+} ions instead of Mg^{2+} for the preparation of the competent cells as it was shown that the cation species itself influences the transformation efficiency in the following order: $Mn^{2+} > Ca^{2+} > Ba^{2+} > Sr^{2+} > Mg^{2+}$.[177] In contrast to the first transformation, this time no clones grew on the selective LB agar plates. As the chemical transformation was not successful for *P. putida* ATCC174534 next transformation experiments were carried out using electroporation. This method is also based on the generation of pores due to the depolarization of the cell membrane allowing the entry of the DNA induced by a high intensity electric field.[178],[179] First attempts for the electroporation resulted in false-positive clones or no clones at increased antibiotic concentration. *Cho et al.* could show that different parameters such as the origin of the DNA, sample volume, electric field strength and the buffer could influence the transformation efficiency for *P. putida* KT2440.[180] By the variation of the different parameters this group showed an improved method for the electroporation of *P. putida* KT2440, which was used for the experiments with *P. putida* ATCC17453, but even with this method no positive clones could be observed (chapter 3.2.1). Finally, the transformation using conjugation was analyzed. In contrast to the chemical transformation and electroporation where the DNA is in the surrounding of the cells, the bacterial conjugation is based on the DNA transfer between two or more organisms. In Gram-negative bacteria the direct contact between the donor cell and the recipient is absolutely necessary. The mechanism is based on the formation of a cell-envelope-spanning translocation channel and a pilus, which is an assembly of a type IV secretion system, called the transferosome.[181],[182] *Martinez-Garcia et al.* could show the successful transfer of DNA towards *P. putida* KT2440 by a tri-parental mating experiment using *E. coli* DH5α λpir with the desired plasmid for the transfer and *E. coli* DH5α pRK2013 as a helper strain.[73] Consequently, the same method was used for the transfer of plasmid DNA into *P. putida* ATCC17453 and positive clones were obtained in every experiment (chapter 3.2.1).

4.2.2 Quantification of the CAM plasmid

Although different degradative plasmids in *Pseudomonas* such as the CAM, SAL, NAH, OCT or TOL plasmid have been known for more than 40 years, none of these plasmids had ever been quantified.[183] For the preparation of the calibration curve either PCR products or plasmid DNA coding for the target gene could be used as templates. It was shown that plasmid DNA is more robust and suitable especially for long term studies compared to PCR templates.[184] For that reason, the vector pBBr122::*camDCAB* harboring the genes for the conversion of camphor towards 2,5-diketocamphane on the CAM plasmid was used for the preparation of the calibration curve. The product formation of different specific primers was analyzed by agarose gel electrophoresis and best results were obtained targeting *camC*. In the first experiment a high variation in the signal strength was obtained in the amplification curves of the standard and the samples, which also resulted in an efficiency of the standard, which was not within the tolerable range for qPCR analysis (> 110 %, chapter 3.2.2). One reason could be the primer concentration, which directly affects the efficiency of the qPCR.[185] *Raso et al.* could show that the efficiency decreased when using primer concentrations below the optimal concentration and on the other hand efficiencies greater than 100 % were obtained with primer concentrations above the optimum.[185] Furthermore, melt peak analysis revealed the formation of side-products with melting temperatures in the range of 88 – 92 °C for some of the standards and the samples. Side-product formation could be due to unspecific binding of the primers, but also a too high amount of template DNA and primers would lead to unspecific products and would hamper the quantification.[185] For that reason, the concentration of the template DNA and the primers was reduced, which led to an improved efficiency within the expected range. Furthermore, the amplification curves revealed constant PCR signals and also the side-product formation could be reduced. Finally, the calculation revealed that 4 – 6 plasmids per cell are present in *P. putida* ATCC17453 (first experiment 4.31 ± 0.13 plasmids per cell, second experiment 6.07 ± 0.49, chapter 3.2.2). For an absolute quantification of the CAM plasmid and in order to confirm these results the qPCR analysis has to be repeated. Furthermore, the whole process of the quantification starting from the DNA extraction of the cultures should be performed in more detail. For that reason, different methods for the DNA extraction and quantification of the sample and standard should be tested because the method itself could have an influence on

the amount of extracted DNA and would influence the result of the qPCR.[186] Moreover, more than one culture should be used for the preparation of the DNA and also different growth stages should be analyzed. The point for this work was to know that the desired gene had to be deleted on not only a single plasmid, but a number of plasmids.

4.2.3 Seamless gene knock out on the CAM plasmid

Several methods for the seamless gene knock out in Gram-negative bacteria had been developed so far whereby the CRISPR/Cas9 methodology represents one of the most recently established methods. In this work the pEMG knockout system reported by *Martinez-Garcia et al.* in 2011 was used for different reasons. The main reason is that it was developed for *P. putida* KT2440, which on the one hand could be used as a positive control and on the other hand is in close relationship to the target organism *P. putida* ATCC17453. For that reason an easy transfer of the method was expected.[73] The method is based on the integration of a first vector (pEMG) into the genome or in this case the CAM plasmid and afterwards a double strand break (DSB) is induced by the I-SceI nuclease, which is located on a second plasmid (pSW-II, Figure 47). The highly specific endonuclease I-SceI produces the DSB at a unique 18 base pair long recognition sequence, which is introduced by the pEMG vector.[187] Subsequently, the DNA recombines via homologous recombination whereby the wt or the desired mutant strain could be formed with a theoretical chance of 50 % (Figure 47). With this method the seamless gene deletion on the CAM plasmid was successful and positive mutants for single and multiple gene deletion appeared at frequencies between 5 and 30 % of the total tested clones depending on the target gene (chapter 3.3.5). The frequencies were below the theoretical 50 %, but also *Martinez-Garcia et al.* reported a variation in the frequencies of 15 –65 % for single gene deletion and 47 – 82 % for multiple gene deletions, which might be due to specific constrains of the genome architecture of these individual regions.[73]

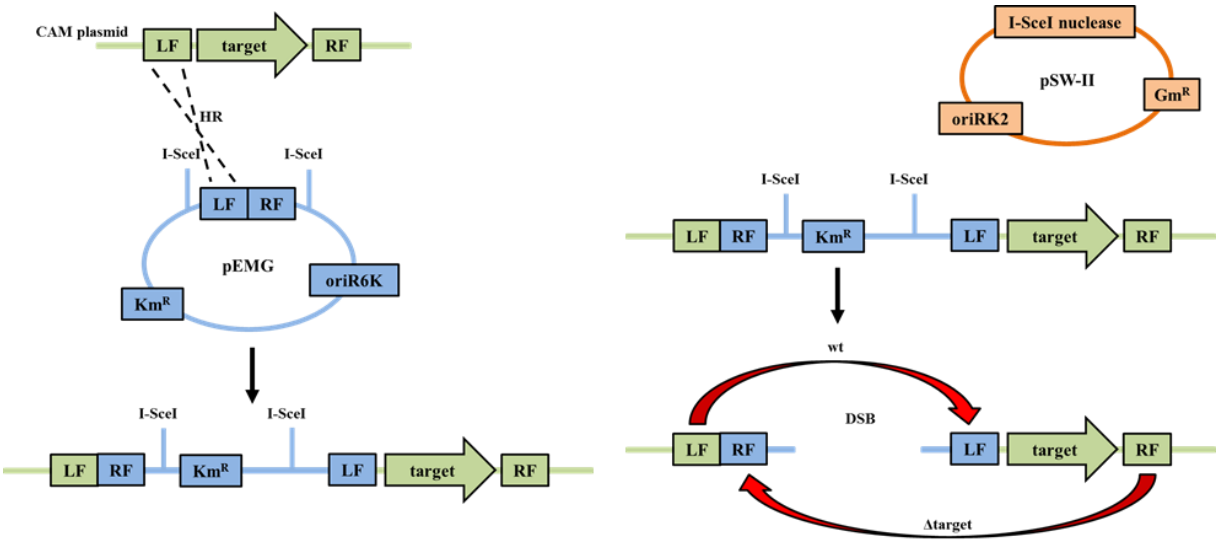

Figure 47: The pEMG knockout system developed for the seamless gene deletion in *P. putida* KT2440 according to *Martinez-Garcia et al.*.[73] Left side: Homologous regions down- and upstream of the target gene are fused together and cloned into the pEMG vector, which carries a kanamycin resistance gene and could not replicate in *Pseudomonas* species. This vector will integrate into the *Pseudomonas* genome or in this case the CAM plasmid while screening for kanamycin resistant clones. Integration could occur via the downstream and the upstream region Right: A second plasmid (pSW-II) codes for the I-SceI nuclease, which is under the control an inducible promotor (3-methyl benzoate). After the expression of the nuclease a double strand break is induced via two regions on the integrated pEMG vector. Consequently, the DSB induces a repair mechanism by homologous recombination whereby the wt and the desired deletion strain could be obtained. The pSW-II vector could be cured afterwards by passaging the cell culture in LB-medium without any antibiotic whereby the method could be used for repeated gene deletions. LF: left flank of the target gene (downstream); RF: right flank of the target gene (upstream); Km^R: kanamycin resistance gene; Gm^R: gentamycin resistance gene; oriR6K and oriRK2: origin of replication.

4.3 Production of 5-*exo*-hydroxyborneol

The first approach for the production of 5-*exo*-hydroxyborneol was the biosynthesis of (+)-borneol by the recombinant expression of (+)-BPPS from *S. officinalis* in combination with the $P450_{cam}$, Pdr and Pdx of *P. putida* ATCC17453. As the expression of (+)-BPPS was not successful the biotransformation of (-)-borneol towards 5-*exo*-hydroxyborneol was analyzed in two different approaches: (i) the deletion of the *camD* gene of *P. putida* ATCC17453 on the CAM plasmid in order to interrupt the metabolism at the stage of the hydroxylation step; (ii) recombinant expression of the $P450_{cam}$, Pdr and Pdx under the control of a constitutive promotor.

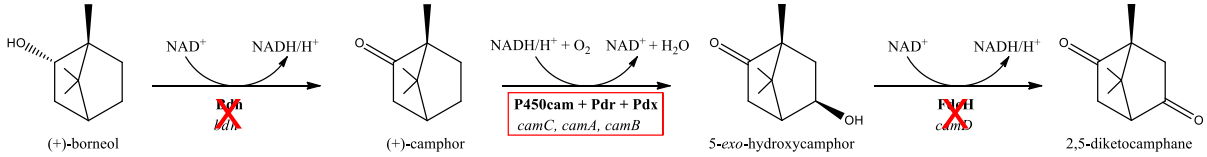

Figure 48: Relevant part of the biodegradation of (+)-borneol by the CAM plasmid of *P. putida* ATCC17453 for the production of 5-*exo*-hydroxyborneol. *Orf16* was found to be a borneol dehydrogenase (*bdh*). Two strategies for the conversion of (-)-borneol towards 5-*exo*-hydroxyborneol were analyzed: (i) recombinant expression of $P450_{cam}$, Pdr and Pdx in *P. putida* KT2440 (red box); (ii) deletion of Orf16 (*bdh*) and FdH (*camD*) to interrupt the metabolism after hydroxylation by $P450_{cam}$, Pdr and Pdx (red cross). Enzymes are displayed in bold, corresponding genes in italic.

During the analysis of the mutant strain *P. putida* ATCC17453 Δ*camD* it turned out that the strain was able to convert (-)-borneol towards camphor by a dehydrogenase encoded by *orf16*. Consequently, this dehydrogenase (Bdh) was analyzed and afterwards a double mutant was constructed by the deletion of the *orf16* gene (*bdh*) and analyzed for its conversion of (-)-borneol.

4.3.1 The borneol dehydrogenase of *P. putida* ATCC17453

The first microbial borneol dehydrogenase was discovered in 2016 by *Tsang* and coworkers analyzing *Pseudomonas* sp. strain TCU-HL1.[159] The group could show that the Bdh_{TCU} is part of the camphor degradation pathway within this strain and showed activity towards

(+)- and (-)-borneol as well as towards (±)-*iso*-borneol.[159] The k_{cat} and k_{cat}/K_M values of the microbial Bdh_{TCU} were 1,800-fold and 500-fold higher compared to the plant Bdh of lavender, which might be due to its different role in the organisms.[159] In bacteria the enzyme is absolutely necessary for the production of energy by the breakdown of borneol and therefore a high activity is of advantage. In contrast, in plants the enzyme is required for the biosynthesis of secondary plant metabolites, which are not essential for plant survival.

Pretests in this work revealed that *P. putida* ATCC17453 was also able to metabolize (+)- and (-)-borneol via the camphor degradation pathway. Sequence alignment of the Bdh_{TCU} of *Pseudomonas* TCU-HL1 and the CAM plasmid *P. putida* ATCC17453 showed a sequence identity of 82 % of the Bdh_{TCU} and the Orf16 of *P. putida* ATCC17453 on the protein level. *Tsang et al.* expressed a synthetic variant of the *orf16* gene (*bdh*) in *E. coli* BL21 and after refolding the enzyme was analyzed by trypsin digestion. Four fragments had the same amino acid sequence and molecular mass compared to the Bdh_{TCU} of *Pseudomonas* TCU-HL1, which indicates a close relation in function and activity.[159] However, *Tsang et al.* reported that the Bdh of *P. putida* ATCC17453 showed no activity against borneol and by molecular modeling and docking studies the same group suggested that the bulky amino acid residue Gln91 blocked the tunnel for the entrance of borneol to the active site of the enzyme whereby the role of the enzyme in the camphor degradation pathway still remained unclear.[159] In contrast, in this work the Bdh of *P. putida* ATCC17453 was cloned by a PCR targeting the gene sequence on the CAM plasmid and expressed in *E. coli* BL21(DE3). The induced *E. coli* cells harboring the *bdh* gene already showed the conversion of (-)-borneol (chapter 3.3.4). The sequencing results of three variants of the enzyme (native, N-terminal and C-terminal his-tag) all showed the same deletion at bp 737, which resulted in a truncated version of the enzyme lacking the last 25 amino acids at the C-terminus. Sequence alignment of the native form of the Bdh from *P. putida* ATCC17453, the truncated version expressed in this work and the Bdh_{TCU} reported from *Tsang et al.* revealed that all enzymes harbor the conserved NAD(H) binding motif G13-X-X-X-G17-X-G19 (Figure 49).[159] Furthermore, the typical SDR catalytic triade S144, Tyr157 and Ser144 was consistent in all enzymes.[159] In contrast to the report of *Tsang et al.*, neither the native Bdh of *P. putida* ATCC17453 nor the truncated version harbored the Gln91, which was thought to block the entrance of the substrate binding pocket, but Asn was present in all sequences at position 91 (Figure 49). The

next glutamine is located at position 96 in the native and truncated version of the *P. putida* ATCC17453 Bdh. At this position the Bdh_{TCU} harbors a histidine, but the Gln96 obviously did not hinder the substrate entering the binding pocket as the activity of the Bdh towards borneol was shown in this work.

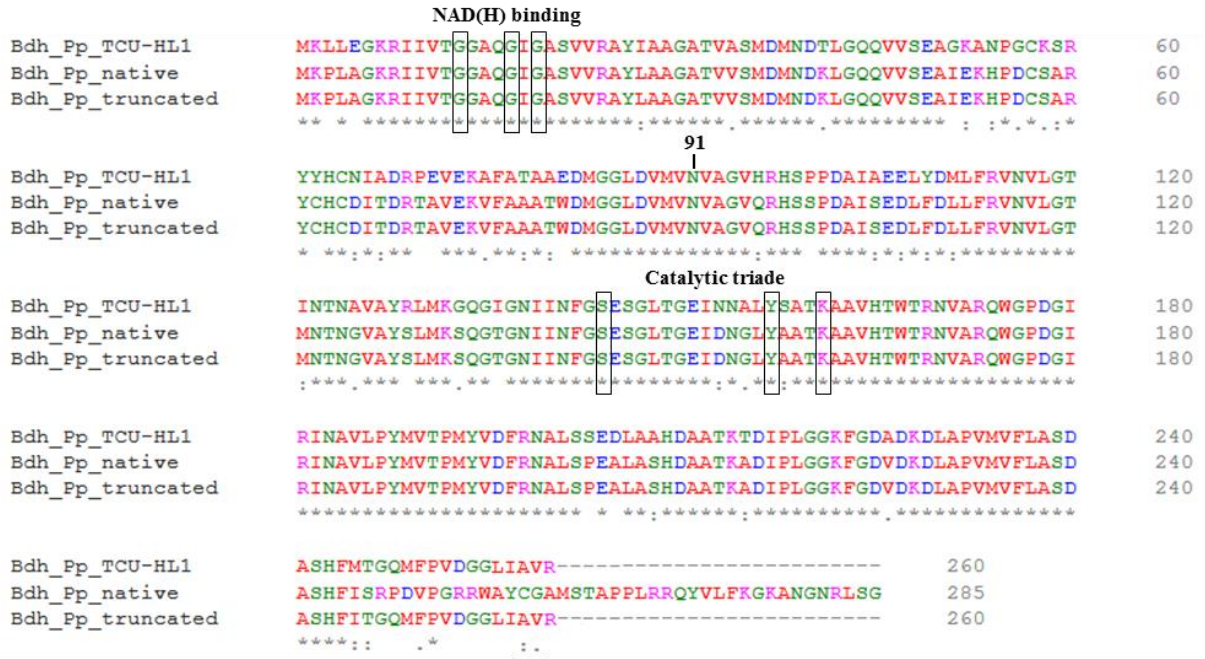

Figure 49: Sequence alignment of Bdh_{TCU} from *Pseudomonas sp.* TCU-HL1 (Bdh_Pp_TCU-HL1), native Bdh from *P. putida* ATCC17453 (Bdh_Pp_native) and the truncated Bdh from *P. putida* ATCC17453 (Bdh_Pp_truncated) expressed in this work. The sequence of the native Bdh is based on the translation of the DNA sequence reported by NCBI (NCBI reference sequence WP_032492645.1). The conserved NAD(H) binding motif G13-X-X-X-G17-X-X-G19 and the catalytic triade for short chain dehydrogenases S144, Y157 and K161 are highlighted in black boxes. Clustal Omega was used for the sequence alignment.

Moreover, the truncated Bdh showed a higher similarity compared to the Bdh_{TCU} on the protein level (sequence identity of 84 %, overall similarity of 89 %) than the reported native protein sequence. Furthermore, the truncated Bdh showed the same length of 260 amino acids as the Bdh_{TCU}. For that reason the structure of the enzyme is supposed to be similar to the Bdh_{TCU} and the tunnel towards the active site is accessible for the substrate borneol. Additionally, all three independent PCRs for the cloning of the *bdh* gene from *P. putida* ATCC17453 showed the same mutation at bp 737, which resulted in the expression of an active Bdh with a high similarity compared to the Bdh_{TCU}. Based on these results, it could be

possible that the reported DNA sequence for the Bdh on the CAM plasmid might be erroneously. Additionally, the wt itself also could convert (+)- and (-)-borneol indicating the presence of an active Bdh within the organism. Taken these results together it can be assumed that the truncated sequence could also be the native one, but to ensure this hypothesis the DNA sequence of the *bdh* gene on the CAM plasmid has to be confirmed by resequencing.

Besides (+)- and (-)-borneol the purified enzyme was also able to convert (±)-iso-borneol and 5-*exo*-hydroxyborneol in the presence of NAD^+. Interestingly, the conversion of 5-*exo*-hydroxyborneol only resulted in the formation of 5-*exo*-hydroxycamphor and no further conversion towards 2,5-diketocamphane was observed (chapter 3.3.4). This indicates a strong preference for the hydroxyl group at position C2 in the natural substrate borneol and that *camD* is absolutely necessary for the further metabolism of borneol and camphor, respectively. The site of the equilibrium of the Bdh_{TCU} was not analyzed by *Tsang et al.*, but it was investigated for the Bdh of *P. putida* ATCC17453 in this work. The equilibrium of the reaction is on the camphor product site as incubation of the purified enzyme together with (+)- or (-)-camphor and $NADH/H^+$ yielded only small amounts of borneol and an even lower amount of isoborneol after 2 d. *Croteau et al.* reported a similar product spectrum for the plant borneol dehydrogenase of *S. officinalis*.[60] Incubation of the plant Bdh with (+)-camphor and saturating concentrations of $NADH/H^+$ revealed a reduction of (+)-camphor with about 6 % of the rate of (+)-borneol oxidation.[60] The group identified (+)-borneol and (-)-isoborneol as the products of the reduction with a three times higher formation of (+)-borneol than (-)-isoborneol.[60] Nevertheless, it was possible to shift the equilibrium of the Bdh of *P. putida* ATCC17453 towards the borneol site by the addition of formate and the formate dehydrogenase of the yeast *Candida boidinii* (chapter 3.3.4). With this setup (-)-camphor could be completely converted after an incubation of 2 – 3 d into borneol and a small amount of isoborneol.

These results showed that it is absolutely necessary to delete the *bdh* gene on the CAM plasmid of *P. putida* ATCC17453 in order to obtain a strain stopping at the hydroxylation of borneol. Otherwise the Bdh would further oxidize 5-*exo*-hydroxyborneol to 5-*ex*o-hydroxycamphor and product yields would decrease.

4.3.2 Mutant strains *P. putida* ATCC17453 Δ*camD* and Δ*camD* Δ*bdh*

Both mutant strains *P. putida* ATCC17453 Δ*camD* and Δ*camD* Δ*bdh* could be generated using the pEMG vector system (chapter 3.3.5). Growth tests using (+)- or (-)-camphor as a single carbon source revealed that both strains lost their ability to utilize camphor as no growth could be obtained. Using glucose in combination with camphor as carbon source both strains were viable, but no conversion of camphor was observed (chapter 3.3.5). These results reveal that neither CamD nor Bdh are essential for the survival of *P. putida* ATCC17453. As expected the Δ*camD* mutant was able to convert borneol towards camphor whereas this ability was lost in the Δ*camD* Δ*bdh* mutant. However, only a small amount of 5-*exo*-hydroxycamphor was detectable for the Δ*camD* mutant and no conversion of either borneol or camphor was observed for the Δ*camD* Δ*bdh* mutant. When using camphor or borneol as a single carbon source this result might be expected as the cells are not able to produce enough energy for the expression of $P450_{cam}$, Pdr and Pdx. More unexpected is the fact that even when feeding glucose together with the substrates camphor or borneol no conversion was observed, because the cells showed growth and should have enough energy for the transcription of the genes necessary for the conversion of the substrates (chapter 3.3.5). In order to understand this phenomenon it is necessary to know how the expression of the cam operon is regulated *in vivo*. The key protein for the transcription of the cam operon is CamR a homodimeric protein, which negatively regulates the transcription of the cam operon (*camDCAB*) and its own gene (*camR*).[188],[189] The regulator consists of two domains, one DNA-binding domain and a regulatory domain.[188] The DNA-binding domain of CamR binds to an operator region (*camO*) between the *camR* gene and the *camDCAB* operon blocking both promotors for the transcription of *camR* and *camDCAB* (Figure 50).[190]

In the presence of low amounts of camphor the repressor still remains bound to *camO* whereas at camphor concentrations > 60 µM CamR is no longer bound to the DNA and the expression of *camR* as well as *camDCAB* is initiated.[84] The experiments in this work were performed using camphor with a concentration 0.5 g L^{-1}, which is equal to 3.28 mM (chapter 3.3.5). At these concentrations CamR should no longer be bound to *camO*, which was also confirmed by the positive control using the wt with the same camphor concentration.

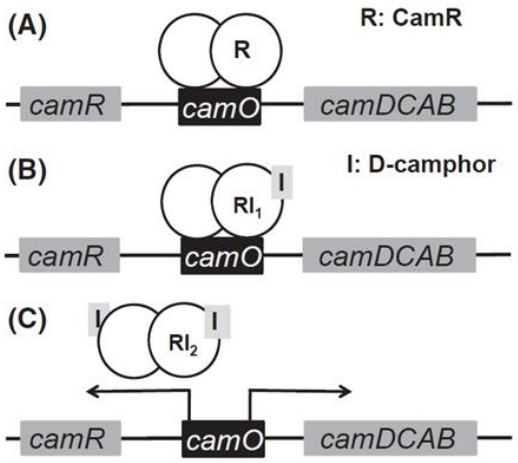

Figure 50: Model of interplay between camphor and CamR/*camO* via two-step binding according to *Aramaki et al.*.[190] A: The dimeric CamR (R) is bound to *camO* in the absence of camphor. B: The repressor (R) is still bound to *camO* at low camphor concentrations. C: The repressor is released from *camO* at higher camphor concentration and *camR* as well as *camDCAB* are expressed.

As mentioned above CamR binds upstream of *camR* and downstream of *camDCAB* thus hindering the RNA polymerase binding the DNA and initiating the transcription. One explanation for an inactive *camCAB* operon could be a disturbed interplay between CamR, *camO* and the RNA polymerase as a result of the deletion of *camD*. The exact binding region of both RNA polymerase and CamR on the DNA level is shown in Figure 51.

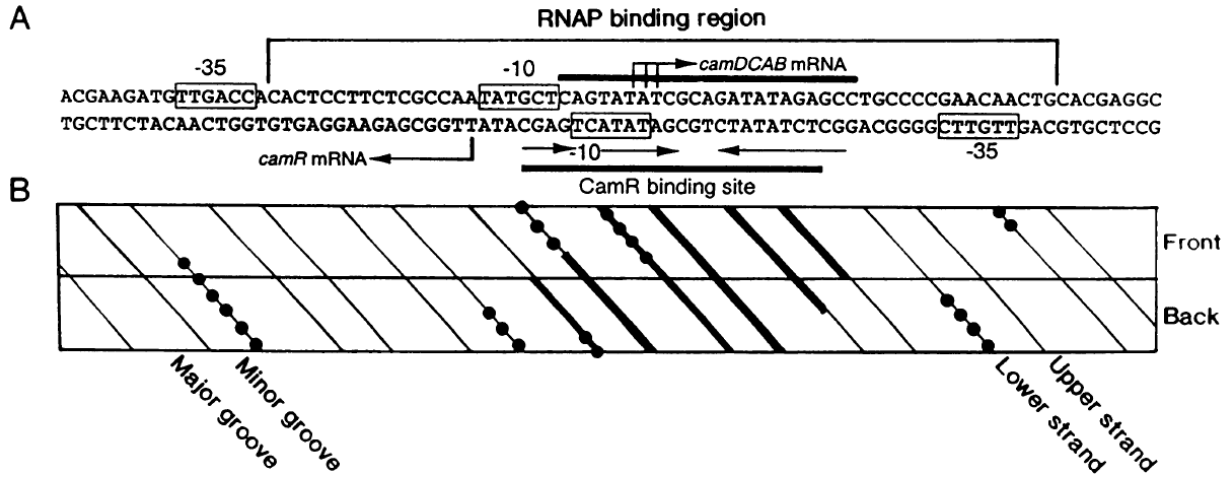

Figure 51: Nucleotide sequence of the *cam* control region (A) and its cylindrical projection (B) according to *Fujita et al.*.[191] Both promotors (*camR* and *camDCAB*) are shown in boxes and transcription start sites are indicated by arrows. Thick bars covering the strands indicate the CamR binding region. Dotted lines indicate the hexanucleotides of the - 35 and -10 promotor regions.

Both promotors (*camR* and *camDCAB*) are overlapping and the CamR binding site is directly in the RNA polymerase binding region. As many other DNA-binding proteins CamR consists of a specific helix-turn-helix region for DNA-binding.[83] The DNA of the *camO* region forms a hairpin structure with both strands connected by a loop of CCCCC and a 5'-protruding G, which is bound by CamR.[190] Assuming that the supercoiled structure of this region of the CAM plasmid is disturbed by the deletion of *camD* and reordered in a form, which CamR could not bind the DNA both *camR* and *camCAB* should be expressed constitutively in the resulting mutant Δ*camD*. As a result CamR would be overexpressed and the conversion of camphor could be prevented by the binding of the substrate to CamR. On the other hand unlike to the *camDCAB* promotor the *camR* promotor shows a low homology to the σ^{70} consensus sequence and for that reason might have a lower affinity for the binding of the RNA polymerase.[191] Furthermore, it was shown that the mRNA level of *camR* in presence of camphor is only about 40 % of that of *camDCAB* mRNA *in vivo*.[191] Thus, $P450_{cam}$, Pdr and Pdx would be present at a higher level than CamR within the cells and the hydroxylated product should be obtained.

Assuming that $P450_{cam}$, Pdr and Pdx are transcribed in both mutants the reason for their inactivity could also be on the level of translation. A *Shine-Dalgarno* (SD) sequence for the mRNA binding by the ribosome is directly located upstream of *camD* (Figure 52).[89]

The spacer between the SD sequence and the initial ATG codon consists of 7 bp. Caused by the deletion of *camD* in both mutants the SD sequence is now in front of *camC*. However, a second SD sequence for the translation of *camC* is located 10 bp upstream of the initial ATG start codon.[89] As a consequence in both mutants two SD sequences are directly located after each other in a distance of only 21 bp. The distance between the SD sequence and the initial start codon was shown to affect the translation efficiency.[192] For Gram negative organisms such as *E. coli* spacers have a typical length of 5 – 9 bp depending on the SD sequence.[192] If the spacer was further increased translation efficiencies decreased and at a distance above 17 bp no translation could be determined.[192] Under the assumption that the mRNA of the Δ*camD* mutant was bound at the SD_{camD} sequence by the ribosome the distance towards the start codon increased up to 36 bp, which could be the reason for a weak *camC* expression and hydroxylation of camphor, respectively.

Figure 52: DNA sequence of *camD* and *camC* in the wt (A) and Δ*camD* mutant (B). Both genes have their own SD sequence (SD_{camD}, SD_{camC}) upstream of the start codon ATG. By the deletion of *camD* the mRNA of *camC* consists of both SD sequences in a distance of 21 bp (B). Underlined: - 35 and - 10 region of the promoter; Bold: start and stop codons; Underlined and bold: SD sequences of *camD* and *camC*. Figure 50 A according to *Aramaki et al.*.[89]

Besides the distance of the SD sequence towards the start codon, the structure of the RNA also influences the translation efficiency, especially the presence of hairpin structures within the area of the SD sequence and the start codon.[193] If hairpin structures are formed directly downstream the start codon or are located at any position between the SD sequence and the coding region a strong inhibition of the translation could be the consequence.[193] RNA structure analysis of the wt *camD* gene revealed that the SD_{camD} sequence is easily accessible for the anti-SD region of the ribosome (Figure 53 A).

In contrast, in any Δ*camD* mutant the SD_{camD} and also SD_{camC} is involved in the formation of hairpin structures and for that reason a decrease in the translation efficiency might be the consequence as the binding of the ribosome is hindered (Figure 53 B).

As a consequence the decreased activity of $P450_{cam}$ for the hydroxylation of camphor might be the result of a disturbed expression of the enzyme caused on transcriptional or translational level as a result of the deletion of *camD*. The same behavior would be expected for the hydroxylation of (-)-borneol by the Δ*camD* Δ*bdh* mutant, but no activity of $P450_{cam}$

could be determined. The reason therefore could be the result of the weak translation of *camC* as mentioned above in combination with a possible low binding affinity of CamR towards (-)-borneol. The induction of the *camDCAB* operon by different intermediates of the camphor degradation pathway such as 5-*exo*-hydroxycamphor or 2,5-diketocamphane as well as camphor-derived structures such as norcamphor and norbornane was shown, but the binding of (-)-borneol by CamR had never been reported.[84]

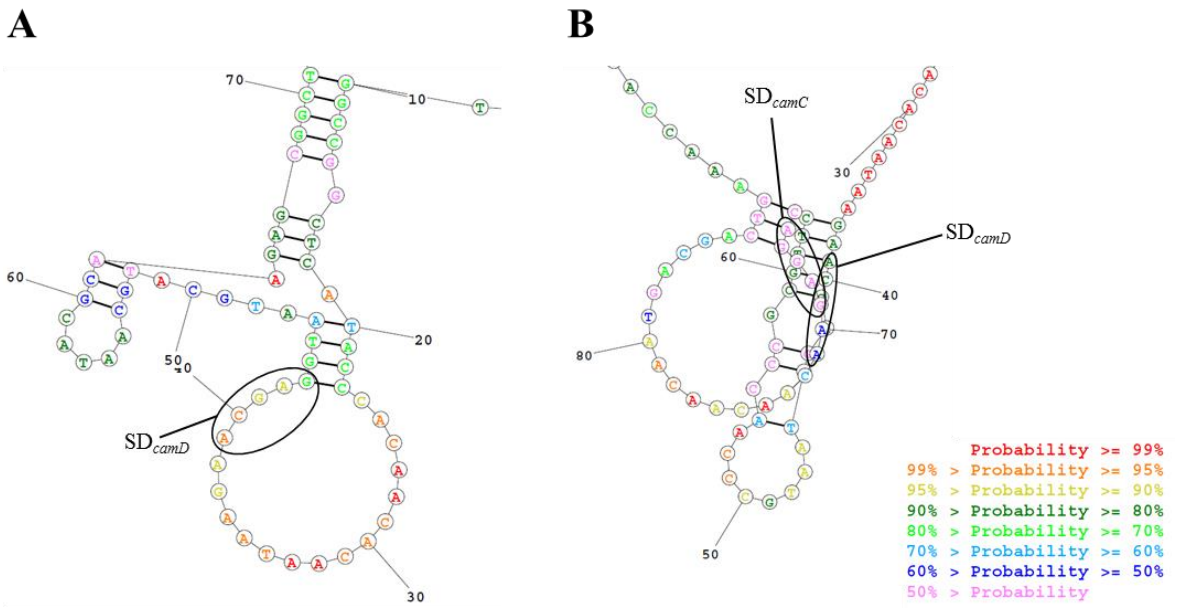

Figure 53: RNA structure comparison of wt *camD* (A) and Δ*camD* or Δ*camD* Δ*bdh* mutant *camC* (B). The segments of the SD sequences in front of the start codons are shown. Wt RNA structure of *camD* was predicted by the whole *camD* sequence and the 50 bp upstream of the start codon of *camD*. RNA structure of the Δ*camD* mutant was predicted using the same 50 bp upstream of *camD* and the complete sequence after *camD* until the stop codon of *camC*. The SD$_{camD}$ is accessible for the anti-SD region of the ribosome in the wt whereas the SD$_{camD}$ and SD$_{camC}$ are located within a hairpin structure in the Δ*camD* or Δ*camD* Δ*bdh* mutant, respectively. The RNA structures were predicted using the RNAstructure prediction web server (https://rna.urmca.rochester.edu). For the wt RNA 20 structures were predicted and all showed a similar structure for the region of SD$_{camD}$. For the Δ*camD* or Δ*camD* Δ*bdh* mutant, respectively 20 structures were predicted and 19 of the 20 showed a similar structure for the region of SD$_{camD}$ and SD$_{camC}$. The different colors of the bps show their probability for their structural position within the RNA structure of the wt and the mutant (down right).

Furthermore, no camphor lactone formation could be obtained by GC-MS analysis neither for the Δ*camD* nor for the Δ*camD* Δ*bdh* mutant, but the induction of both 2,5-DKCMOs and the 3,6-DKCMO by both camphor enantiomers had already been shown, which is another indication for the disturbance of the whole camphor degradation pathway within these mutants.[80]

In order to completely clarify if the key problem for the hydroxylation by $P450_{cam}$ is on the transcriptional or translational level the mutants have to be further analyzed. On the one hand *camR* could be deleted to analyze its impact on the $P450_{cam}$ expression within in the mutants. Additionally, a non-coding DNA sequence with the same length as *camD* could be inserted instead of *camD* in order to analyze if the insertion would restore the activity of the *camCAB* operon. Furthermore, analysis of the amount of mRNA of *camR*, *camD* and *camC* in the wt and all mutants should clarify whether the problem is on the level of transcription or translation.

4.3.3 Conversion of (-)-borneol by $P450_{cam}$, Pdr, Pdx

The enzymatic hydroxylation of (-)-borneol by $P450_{cam}$ requires molecular oxygen and $NADH/H^+$ as a cofactor. Additionally, two more enzymes Pdr and Pdx are necessary for the electron transport towards the $P450_{cam}$.[194] In order to be independent of a cofactor regeneration system the hydroxylation of (-)-borneol was performed using *P. putida* KT2440 as a whole catalyst. The conversion rate of both, enzymatic and whole catalysis is strongly linked to the conditions in the surrounding environment such as pH, buffer substance and temperature. In this work the optimal conditions for the whole cell catalytic conversion of (-)-borneol were 30 °C with a phosphate buffer at pH 6 (chapter 3.3.1). In contrast, *Michizoe et al.* could show that the stability of Pdx could be increased using Tris-HCl buffer instead of a phosphate buffer in a cell free approach.[195] Compared to a cell free conversion, in whole cell catalysis the enzymes are inside the cells and not in direct contact with the buffer or buffer substance itself. The intracellular pH of cells maintains nearly constant at a surrounding pH in the range of 6 – 8 due to ion transport processes. For that reason, the buffer mainly affects the cell growth and solubility of the substrate. In this work, the substrate solubility would not be greatly influenced by the buffer due to its unpolar character.

So, the buffer would mainly affect cell growth. *Mouri et al.* observed the best results for the conversion of camphor by the $P450_{cam}$ system at pH 7.4 also using whole cells.[196] The difference in pH might be attributed to the fact that *Mouri et al.* used *E. coli* BL21 as a host and not *P. putida* KT2440.[196] The same group reported an optimal temperature for the hydroxylation of camphor of 20 °C. The authors used inducible cells for protein expression, which were harvested, concentrated and afterwards used for the hydroxylation of 2 mM camphor.[196] In contrast, the setup for the hydroxylation of (-)-borneol reported here is different as protein expression is under the control of a constitutive promotor and cells were allowed to grow further. Therefore 30 °C seemed to be the optimal temperature for the conversion as it is also the optimal growth temperature of *P. putida*.[197]

During the optimization of the conditions for the conversion of (-)-borneol, 5-*oxo*-camphor was observed as a side-product at lower pH values and higher temperatures (chapter 3.3.1). The side-product formation could be attributed to different effects: (i) 5-*exo*-hydroxyborneol is further oxidized by $P450_{cam}$ due to unspecific oxidation as shown for camphor,[198] (ii) a high oxygen level in the medium also favors an overoxidation by $P450_{cam}$.[199] Further product oxidation should be prevented by the introduction of two phase system where the product is dissolved in the organic phase. Furthermore, the high volatility as well as insolubility of (-)-borneol in aqueous media as two major challenges could be circumvented as well. Moreover, *Pseudomonas* species are excellent candidates for the biotransformation in the presence of an organic solvent as they are highly tolerant to different organic solvents.[71],[200] For that reason, *n*-hexane and *n*-dodecane both of which could minimize toxic effects of substrate and product were analyzed (chapter 3.3.1).[201] The *STY*s for the aqueous and two phase conversion of (-)-borneol were similar ($STY_{aqueous} \sim 34$ mg L^{-1} h^{-1}, $STY_{organic} \sim 32$ mg L^{-1} h^{-1}) and are also in accordance to the ones reported for the conversion of *α*- and *β*-pinene by resting cells of *Pseudomonas* strain PIN ($STY = 22$ and 44 mg L^{-1} h^{-1}).[202]

Schewe et al. also reported the biotransformation of *α*-pinene using *E. coli* cells as a host and the $P450_{BM-3}$ monooxygenase from *Bacillus megaterium* and obtained *α*-pinene oxide as a major product with a yield of 20 mg g^{-1} cdw.[203] The conversion rates decreased after 30 min and the authors concluded that the reason was the toxicity of the substrate *α*-pinene.[203] In order to preclude any toxicity of (-)-borneol or 5-*exo*-hydroxyborneol towards *P. putida*

KT2440 the organism was incubated with both, but neither the substrate nor the product showed any toxic effect on the cells at these concentrations.

The hydroxylation of camphor by $P450_{cam}$ is reported to be highly site-specific and solely leads to the formation of 5-*exo*-hydroxycamphor without the formation of 5-*endo*-hydroxycamphor.[157],[204] Nevertheless, the orientation of the C5 hydroxyl group in the product was analyzed by NMR spectroscopy and GC-MS analysis. Both confirmed the hydroxylation of (-)-borneol in the postulated orientation of the hydroxyl group.

4.3.4 Semi-continuous batch process

The semi-continuous batch process for the production of 5-*exo*-hydroxyborneol was developed in order to improve the conversion rate, product yield and separation of the product from the cell broth. After every fresh substrate addition the conversion rates were constantly > 98 %, which confirmed the reusability of the cells as a catalyst. However, reaction times for full substrate conversion increased from 8 to 40 h within the process (chapter 3.3.2). This effect is mainly due to the concentration of the cells during the product separation and dilution through the addition of fresh medium and substrate where the cells need some time to adapt to the new conditions. Furthermore, the cells are stressed during the pumping and the cross-flow filtration, which also results in a short lag phase. These effects have also to be considered for the scale up in an industrial process. Product separation by filtration as used in the laboratory scale would be very time consuming, because of the increased volume at an industrial scale. For that reason, a batch process with centrifugation would be more suitable. A disk separator could be implemented for the continuous production of 5-*exo*-hydroxyborneol. Thereby, the filtrate could be directly used for product extraction and further purification. Additionally, the cells could be returned to the bioreactor and reused for further substrate conversion. By this separation method, the cells might also show a short lag phase caused by the stress in the disk separator. For that reason the productivity of both processes has to be analyzed to decide, which is more suitable for the production of 5-*exo*-hydroxyborneol at an industrial scale.

The product yields varied slightly with the addition of fresh substrate, but were similar to those in the preliminary tests. In each cross-flow filtration step a certain amount of medium

remained in the reactor otherwise cell densities would increase and as a consequence cells would be damaged by increased shear stress. As a result the product yields remained at approximately 80 % (chapter 3.3.2). Furthermore, there could also be some loss of substrate during the biotransformation due to the volatile nature of the substrate. Similar product yields were also reported for the hydroxylation of limonene by a *P. putida* MTCC 1072 whole cell catalyst.[205]

Compared to a batch process the semi-continuous process brought along several advantages at the laboratory scale. Due to the low water solubility of the substrate the batch process is limited to a substrate concentration of 5 mM and after the conversion the product has to be isolated from the medium, which often is time consuming. In contrast, with the semi-continuous process it was possible to convert more substrate over time thereby increasing the total product yield. Moreover, when cells are present during the extraction of the product with ethyl acetate an interphase is formed by cells and cell fragments. Hence, the product extraction after the cell removal by cross-flow filtration was more efficient.

4.4 Polymerization of 5-*exo*-hydroxyborneol

For a proof of concept 5-*exo*-hydroxyborneol was copolymerized with succinic dimethyl ester in order to obtain a completely bio-based polymer. Succinic acid could be obtained from renewable resources such as carbohydrates by fermentation of metabolically engineered bacteria and yeasts.[206],[207],[208] The resulting polymer showed a glass transition temperature of about 70 °C and a molecular weight in the range of 2,000 – 4,000 g mol^{-1} (*PDI* = 1.9, chapter 3.4).

Polycondensation of modified terpenoids is a rather underexplored area in the wide field of terpene-based polymers. Due to the chemical structure of the most abundant terpenoids such as limonene and α- and β-pinene, respectively often other polymerization procedures such as cationic polymerization, which make use of the double bonds in terpenoids, are investigated. For example *Satoh et al.* reported the cationic polymerization of poly(β-pinene), which resulted in a biopolymer with a high transparency and high molecular weights (M_n up to 50,000 g mol^{-1}).[209] Terpenoids carrying single carbonyl groups such as menthone are another group of terpenoids, which are extensively investigated for their use as monomers

are. The carbonyl group could be easily converted into lactams or lactones by chemical approaches both of which represent monomers for ring opening polymerizations. According to this strategy (-)-menthone derived polyamides (M_w = 1,700 – 3400 g mol^{-1}) and polyesters (M_n up to 90,000 g mol^{-1}) have been reported.[144],[210] Besides (-)-menthone also other terpenoid derived lactones such as carvone were reported to give homopolymers with molecular weights in a range of M_n = 700 – 10,500 g mol^{-1}.[211] Compared to these terpene-derived polymers, the novel borneol-based biopolymer represents an interesting starting point for further investigations, especially by using polycondensation as a polymerization technique, thus novel bio-based materials could be obtained.

In order to clarify the suitability of 5-*exo*-hydroxyborneol in the wide area of biopolymers its copolymerization with other monomers has to be further investigated. Furthermore, the polymerization procedure itself has to be optimized. For that reason, it is necessary to analyze the optimal temperature for the oligomerization as well as the polycondensation during the polymerization as it is known that the temperature directly affects the resulting polymer.[212] Moreover, other polymerization parameter such as (i) amount and kind of catalyst, (ii) polymerization time and (iii) pressure during the polymerization should be analyzed in order to further improve the polymerization procedure. Additionally, it would be interesting to analyze whether the orientation of the C2 hydroxyl group in borneol shows any effect towards the properties of the resulting polymer. The C2 hydroxyl group of 5-*exo*-hydroxyborneol used in this work is in axial orientation whereas the C5 hydroxyl group is equatorially orientated. Besides the bicyclic structure of the monomer the axial orientation of the C2 hydroxyl group could also hamper the polymerization as well as the order of the polymer chains and might affect the glass transition temperature of the polymer. Thus, an equatorial orientation of both hydroxyl groups might enhance the order of the polymer chains. In order to test this hypothesis (+)-isoborneol could be hydroxylated by the strain *P. putida* KT2440 pBBr122::*camCAB* and the resulting product could be used for copolymerization.

4.5 Production of 2,5-diketocamphane

The production of 2,5-diketocamphane was already reported using the purified enzymes of the *camDCAB* operon as well as using *P. putida* KT2440 as a host harboring the cam *camDCAB* operon.[95],[213],[214] In this work the genes responsible for the lactonization of 2,5-diketocamphane (*camE*$_{25\text{-}1}$ and *camE*$_{25\text{-}2}$) in *P. putida* ATCC17453 were deleted and the ability of the resulting mutant for the production of 2,5-diketocamphane was analyzed (Figure 54).

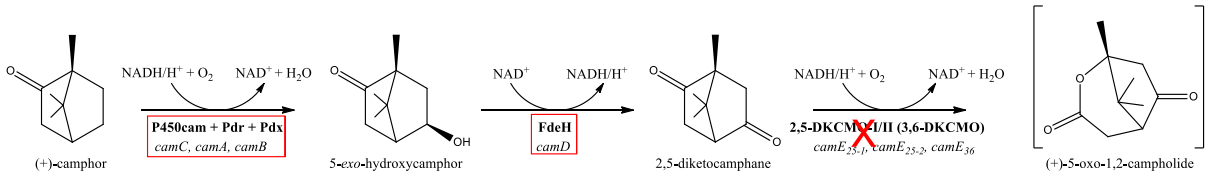

Figure 54: Relevant part of the biodegradation of (+)-camphor by the CAM plasmid of *P. putida* ATCC17453 for the production of 2,5-diketocamphane. Two strategies for the conversion of (+)-camphor towards 2,5-diketocamphane were analyzed: (i) recombinant expression of P450$_{cam}$, Pdr, Pdx and FdH in *P. putida* KT2440 (red box); (ii) deletion of 2,5-DKCMO-I and -II (*camE*$_{25\text{-}1}$, *camE*$_{25\text{-}2}$) to interrupt the metabolism (red cross). Enzymes are displayed in bold, corresponding genes in italic.

The mutant strain was still able to grow on (+)-camphor and (+)-borneol as single carbon sources indicating that the substrates could be completely metabolized. Furthermore, compared to the wt the mutant showed nearly the same growth behavior as seen in the growth curves (chapter 3.5.1). Consequently, the 2,5-diketocamphane has to be recognized by other enzymes in the mutant strain otherwise there would be no growth obtainable. It is known that the expression of both 2,5-DKCMO and the highly related 3,6-DKCMO is induced by both camphor isomers.[77],[91] The substrate specificity for the camphor isomers of the 3,6-DKCMO and also 2,5-DKCMO is discussed contradictorily in literature over the last decades. Besides the natural substrate 3,6-diketocamphane also related structures such as (R,R)-bicyclo[2.2.1]heptane-2,5-dion are recognized by the 3,6-DKCMOs and also by the OTEMO the third enzyme in the camphor degradation pathway.[79] Furthermore, the 3,6-DKCMO and the OTEMO are both able to oxidize norcamphor, which is structurally in close relation to (-)-camphor.[124],[79],[194] Additionally, the oxidation of (+)-camphor by both

2,5-DKCMOs and (-)-camphor by the 3,6-DKCMO was reported several times.[136],[215] The oxidation of (+)-camphor by the 2,5-DKCMOs and of (-)-camphor by the 3,6-DKCMO was reported to be highly specific for each of the DKCMOs.[215] In contrast, recently it was also reported that the 2,5-DKCMOs are able to convert a small amount of (-)-camphor and also the 3,6-DKCMO is able to convert (+)-camphor.[76],[91] *Balke et al.* could even show that up to 88 % of (+)-camphor were converted y the 3,6-DKCMO and up to 25 % of (-)-camphor were converted by the 2,5-DKCMO using crude cell extract.[136] The same group could also show that even the OTEMO is able to convert 44 % of (+)-camphor and 22 % of (-)-camphor, respectively.[136]

The recognition and conversion of (+)-camphor by the 3,6-DKCMO and OTEMO would also explain the growth of the *P. putida* ATCC17453 Δ*camE*$_{25-1}$Δ*camE*$_{25-2}$ mutant generated in this work using (+)-camphor as single carbon source. The hypothetical camphor degradation pathway for the Δ*camE*$_{25-1}$ Δ*camE*$_{25-2}$ mutant would be as follows (Figure 55 D). In the first step (+)-camphor is oxidized by either the 3,6-DKCMO or the OTEMO. However, it was shown that the expression of the OTEMO is not induced by the addition of any camphor enantiomer in the wt.[80] In contrast, the expression of both 2,5-DKCMOs and the 3,6-DKCMO is indeed induced by (+)- and (-)-camphor.[80] For that reason, lactonization of (+)-camphor is probably due to the expression of the 3,6-DKCMO within in Δ*camE*$_{25-1}$ Δ*camE*$_{25-2}$ mutant. The resulting (+)-camphor lactone can serve as a substrate for the hydroxylation by P450$_{cam}$, Pdr and Pdx (*camCAB*) and could be further oxidized by FdeH (*camD*).

Evidence for the recognition of the camphor lactone by the *camDCAB* operon was also made in this work and will be discussed later (chapter 4.6.1). With this pathway the Δ*camE*$_{25-1}$ Δ*camE*$_{25-2}$ mutant would still be able to metabolize (+)-camphor and would still grow on this single carbon source. In order to prove this hypothesis the gene for the 3,6-DKCMO (*camE*$_{36}$) and to analyze the influence of the OTEMO also *camG* would have to be deleted in the Δ*camE*$_{25-1}$ Δ*camE*$_{25-2}$ mutant. The resulting mutant should not be able to metabolize (+)-camphor any more, but should produce 2,5-diketocamphane. However, if the mutant still shows growth on (+)-camphor as a single carbon source more than the known enzymes of the camphor degradation pathway will be involved in its complete breakdown.

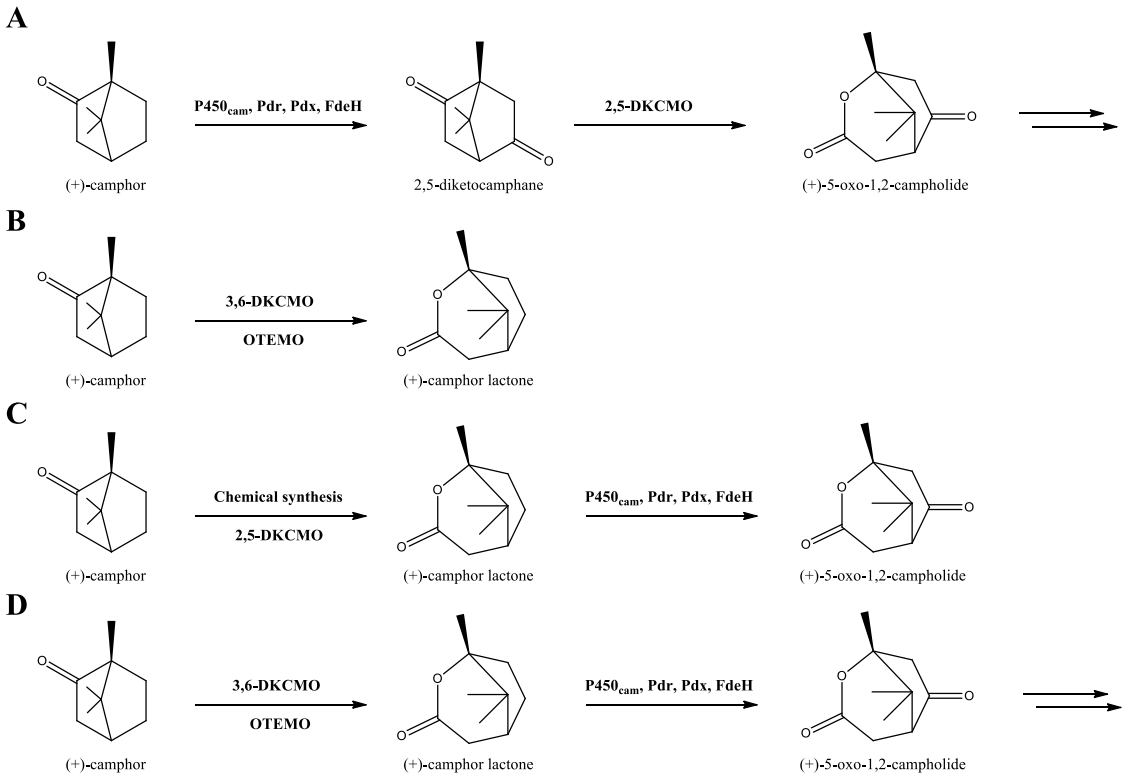

Figure 55: A: Native camphor degradation pathway in *P. putida* ATCC17453 up to the unstable (+)-5-oxo-1,2-campholide. B: Reported activity of 3,6-DKCMO and OTEMO towards (+)-camphor according to *Balke et al.*.[136] The resulting product should be a (+)-camphor lactone. C: Chemical or biological conversion using 2,5-DKCMO of (+)-camphor results in the formation of (+)-camphor lactone, which is recognized by $P450_{cam}$, Pdr, Pdx and FdeH and further converted to the unstable (+)-5-oxo-1,2-campholide (this work). D: Hypothetical (+)-camphor degradation pathway in the *P. puti*da ATCC17453 Δ*camE*$_{25\text{-}1}$ Δ*camE*$_{25\text{-}2}$ lacking both 2,5-DKCMOs. (+)-camphor is converted into (+)-camphor lactone by either 3,6-DKCMO or OTEMO. The resulting lactone could serve as a substrate for $P450_{cam}$, Pdr, Pdx and FdeH producing the unstable (+)-5-oxo-1,2-campholide which could be further metabolized. Enzymes are displayed in bold.

4.6 Production of lactones

Lactones are interesting monomers for polymers as they could be easily polymerized by ring opening polymerization. As already mentioned above BVMOs are catalyzing the formation of lactones based on ketone substrates. The camphor degradation pathway harbors several BVMOs, which were recombinantly expressed and analyzed within this work by *Rehberger et al.*.[160]

Furthermore, the role of CamH of the CAM plasmid in terms of camphor degradation was

investigated. With the deletion of *camH* in *P. putida* ATCC17453 it should be clarified whether CamH is part of the degradation pathway and additionally if it is possible to isolate the 5-oxo-campholide from the mutant strain (Figure 56).

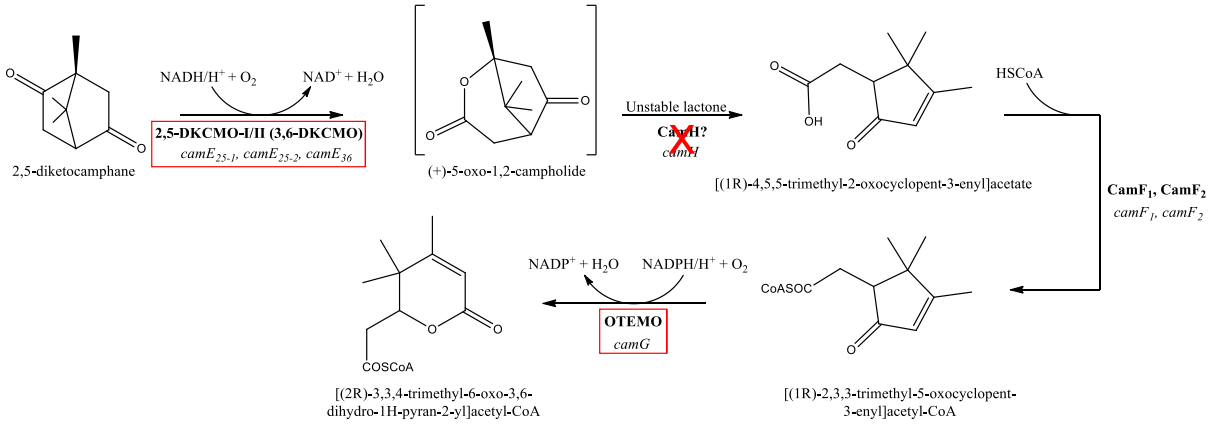

Figure 56: Relevant part of the biodegradation of (+)-camphor by the CAM plasmid of *P. putida* ATCC17453 for the production of lactones. Recombinant expression of three BVMOs (2,5-DKCMO-I, 3,6-DKCMO and OTEMO) in *P. putida* KT2440 to obtain different strains for the synthesis of lactones (red boxes). Clarification if CamH is involved in the camphor degradation pathway by recombinant expression in *P. putida* KT2440 and gene deletion (red cross). Enzymes are displayed in bold, corresponding genes in italic.

4.6.1 Characterization of CamH and the mutant *P. putida* ATCC17453 Δ*camH*

The gene sequence of CamH is directly located between one of the 2,5-DKCMOs and the repressor CamR on the CAM plasmid and might be part of the camphor degradation pathway.[194] In literature CamH is reported to be a “putative lactone hydrolase”, but the protein was neither cloned nor characterized until now.[79],[194] This hypothesis of the lactone hydrolase is reinforced by the analysis of the protein sequence using NCBI’s Conserved Domain Database (CDD).[216] The structure of the enzyme showed homology regions to conserved domains of the MBL-fold metallohydrolase superfamily. Members of this family are mainly hydrolytic enzymes mostly known for the hydrolysis of *β*-lactam antibiotics. Nevertheless, some of the MBL-fold metallohydrolases also show esterase activity and the hydrolysis and opening of lactone rings. In order to find structurally related enzymes with a similar activity, the amino acid sequence of CamH was further analyzed using the

SWISS-MODEL database (Table 23).

Table 23: List of CamH structurally related enzymes by screening via the SWISS-MODEL database. Hits are listed according to their GMQE value.

Description	Origin	GMQE	Sequence identity [%]	Sequence coverage	QMEAN
Organophosphorus hydrolase	*P. oleovorans*	0.78	60.32	0.96	-1.20
Organophosphorus hydrolase	*P. oleovorans*	0.76	59.56	0.98	-1.26
Reconstructed lactonase ancestor Anc1-MPH	Template: bacterial methyl parathion hydrolase	0.70	43.62	0.87	-0.64
Putative hydrolase	*Acinetobacter sp.*	0.70	43.97	0.86	-0.84
Methyl parathion hydrolase	*Pseudomonas sp. WBC-3*	0.69	41.58	0.89	-1.47

The top five hits for the alignment of the structure of the enzyme are listed according to the GMQE value (Global Model Quality Estimation). Besides the reconstructed lactonase from bacterial methyl parathion hydrolases the organophosphorus hydrolase from *P. oleovorans* and also the hydrolase from *Acinetobacter sp*. were reported to cleave lactone rings in substrates such as 3,4-dihydrocoumarin, δ-decanolactone and γ-nonanolactone.[217],[218]

The results of both databases reveal that CamH might show a lactone hydrolase activity. Consequently, the CamH was expressed, purified and used for substrate conversion tests. As most members of the metallohydrolase superfamily use zinc as a metal cofactor, CamH was purified in the presence of 1 mM $ZnCl_2$, but CamH did not show any activity against camphor lactone and the monocyclic ε-caprolactone (chapter 3.6.1). As one of the natural substrates of CamH could be 5-oxo-1,2-campholide this compound should be obtained by the conversion of (+)-camphor lactone by *P. putida* KT2440 pBBr122::*camCAB* (chapter 3.6.1). However, it turned out that the resulting campholide is unstable under these conditions and most probably the lactone ring opens through an elimination reaction (Figure 57).

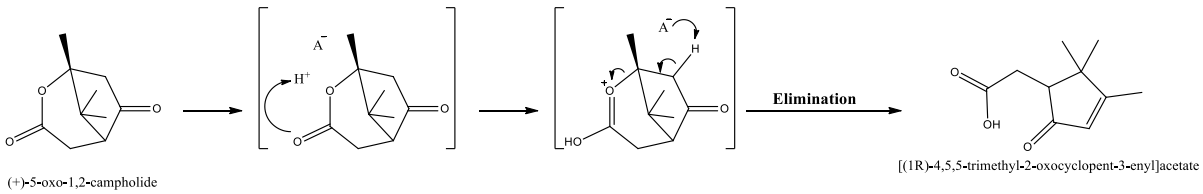

Figure 57: Elimination of the unstable 5-oxo-1,2-campholide and formation of [(1R)-4,5,5-trimethyl-2-oxocyclopent-3-enyl]acetate as a product.

The fact that CamH did not recognize (+)-camphor lactone as a substrate and that the natural 5-oxo-1,2-campholide is unstable strongly indicates that CamH is not involved in the cleavage of the lactone ring. However, CamH could be part of the camphor degradation pathway at another stage. *Iwaki et al.* suggested that CamH could also be responsible for the cleavage of the lactone ring in the OTEMO product (Figure 58).[79]

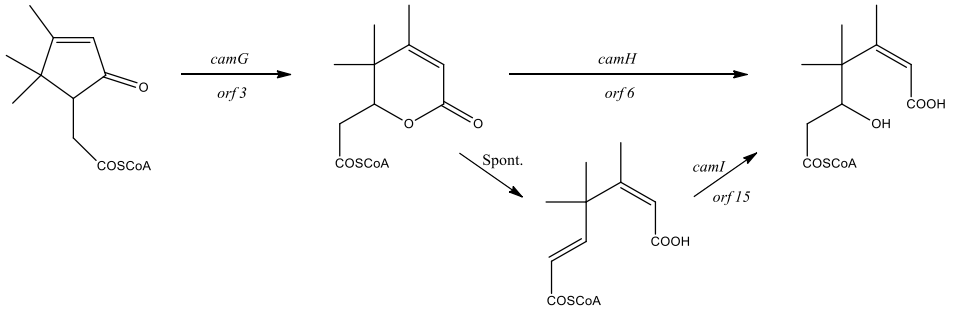

Figure 58: Proposed participation of CamH in the cleavage of the OTEMO (*camG*) product [(2R)-3,4,4-trimethyl-6-oxo-3,6-dihydro-1H-pyran-2-yl]acetyl-CoA. Figure according to *Iwaki et al.*.[79]

In order to get more details about the role of CamH in the camphor degradation pathway the gene *camH* was deleted in *P. putida* ATCC17453. The resulting mutant showed the same growth behavior compared to the wt using camphor as a single carbon source (chapter 3.6.2). Furthermore, GC-MS analysis revealed a similar composition of the different intermediates within the cells of the wt and the camH mutant.

Taken all these results together one could suggest that CamH might not be part of the camphor degradation pathway or plays a minor role. However, it was not possible to demonstrate the activity of the recombinantly expressed CamH towards any substrate and for that reason its role within the organism still remains obscure.

4.6.2 BVMOs of the CAM plasmid used in whole cell biotransformation

Within this work, *Rehberger et al*. recombinantly expressed the three BVMOs 2,5-DKCMO, 3,6-DKCMO and OTEMO from *P. putida* ATCC17453 in *P. putida* KT2440 under the control of the constitutive camphor promotor and analyzed their ability to convert (+)- and (-)-camphor and structural analogs (Figure 59).[160]

Both DKCMOs were reported to be highly selective for the corresponding enantiomer, but recently it was reported that the 2,5-DKCMO recombinantly expressed in *E. coli* was also able to convert (-)-camphor although at a lower conversion rate.[77],[91],[219]

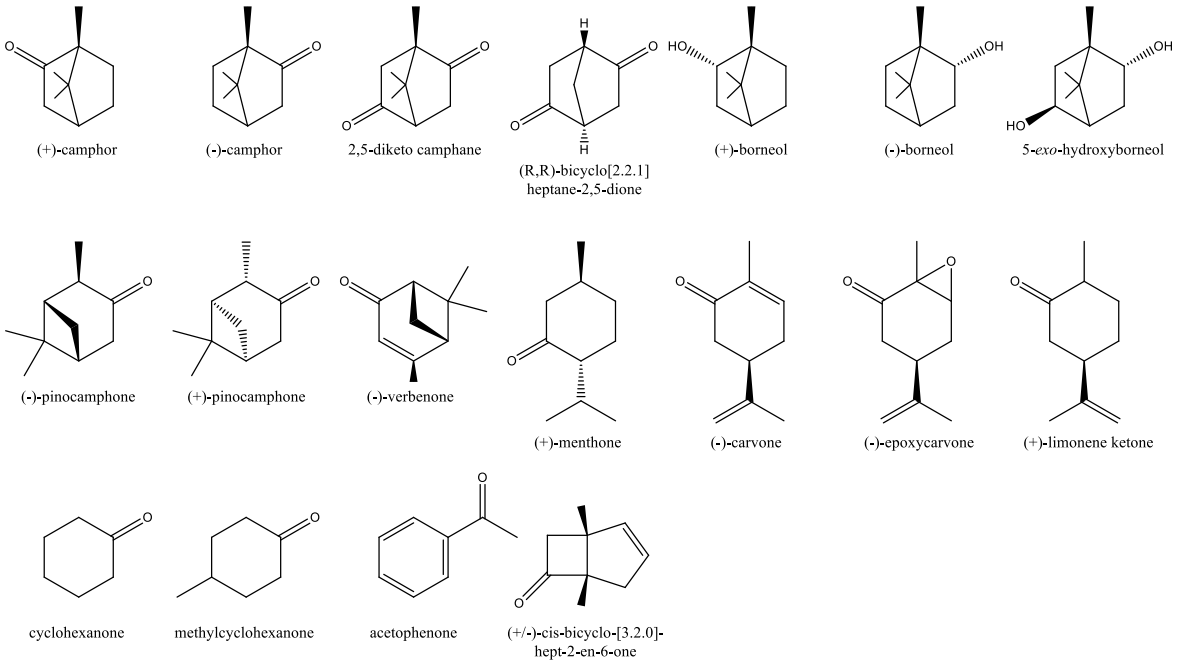

Figure 59: Different substrates analyzed by *Rehberger et al.* for the conversion by *P. putida* KT2440 harboring the different BVMOs (2,5-DKCMO-I, 3,6-DKCMO, OTEMO).[160] A: camphor derived structures; B: other terpene-based structures; C: other ketones.

The same behavior was observed by *Rehberger et al.* for the conversion of (-)-camphor by 2,5-DKCMO in whole cell catalysis.[160] Furthermore, as expected the 2,5-DKCMO was not able to convert any of the tested monocyclic lactones.[79],[91]

Analysis of the 3,6-BVMO revealed that only (-)-camphor was recognized as a substrate and converted to the corresponding lactone at low rates.[160] Contrary to the conversion of other

bicyclic ketones such as (±)-cis-bicyclo-[3,2,0]-hept-2-en-6-one and aromatic ketones such as acetophenon reported in literature, the 3,6-BVMO showed no activity towards any of these compounds.[94],[194] Gene sequence analysis of the clone revealed a mutation at bp 1126, which resulted in an elongation of the C-terminus of the enzyme from LL-PKR to LL-LSVEPQW.[160] Furthermore, in literature the enzyme activity of the 3,6-DKCMO was reported to be the lowest (0.09 mU mg^{-1}) compared to the 2,5-DKCMO and OTEMO using crude cell extracts and the preferred substrate of each BVMO.[79],[94] The low natural activity in combination with the elongation at the C-terminus of the enzyme, which could cause a structural change compared to the native one might be one of the reason for the missing activity towards the other reported bicyclic ketones.

As reported in literature the OTEMO recognized and converted the substrate (±)-cis-bicyclo-[3,2,0]-hept-2-en-6-one in high rates.[94] Furthermore, *Kadow et al.* reported the conversion of (+)- and (-)-camphor as well as cyclohexanone, acetophenone and (R,R)-bicyclo[2.2.1]hept-2,5-dione by the OTEMO.[94] However, none of these substrates were converted by the OTEMO whole cell catalyst under the conditions used by *Rehberger et al.*.[160]

As it turned out the most promising approach to obtain a bio-based lactone monomer was the conversion of (+)-camphor using *P. putida* KT2440 expressing the 2,5-DKCMO.[160] One of the key parameters in whole cell oxidation processes is the availability of molecular oxygen as it is required for the cell metabolism as well as for the desired oxidation reaction.[220] At higher cell densities the oxygen supply for the oxidation could be limited due to its competition with the metabolism.[220],[221] In order to provide enough oxygen for both the oxidation and the metabolism the conversion rate was analyzed depending on different oxygen capacities by the variation of the shaker frequencies. As expected the conversion rate was low at low shaker frequencies and increased with the increase of shaker frequencies reaching an optimum at 130 rpm .[160] *Baldwin et al.* reported a similar behavior for the conversion of bicyclo[3.2.0]hept-2-en-6-one using the cyclohexanone monooxygenase of *Acinetobacter calcoaceticus* NCIMB 9871 in recombinant *E. coli*.[222] Using the same substrate and enzyme *Hilker et al.* could confirm the effect of a higher conversion rate at higher oxygen concentrations in the medium.[223] Also at increased oxygen capacities it took 3 d for the complete conversion of 2 mM (+)-camphor by the 2,5-DKCMO.[160] For that

reason, the conversion was performed by the addition of glucose and substrate every three days and in total 9.44 g of (+)-camphor lactone could be produced with a yield of 65 %.[160] The reduced yield by complete conversion is most likely due to the binding of product to the cells, which were separated by centrifugation before the extraction. Furthermore, there could be some loss due to the volatile character of the substrate itself.

5 Outlook

***P. putida* ATCC17453 as a host for the production of terpene-based monomers**

In order to clarify whether *P. putida* ATCC17453 mutants could be hosts for the production of various terpene-based and especially camphor-derived monomers a more detailed investigation of the CAM plasmid is still necessary. In particular, understanding the role and effect of CamR towards the transcription of the *camCAB* operon in Δ*camD* and Δ*camD* Δ*bdh* mutants is of high interest. If the deletion of *camR* reveals that the resulting mutants could efficiently hydroxylate and further oxidize borneol or camphor these mutants can be used for the synthesis of 5-*exo*-hydroxyborneol and related compounds, which has to be analyzed in further studies. What is more, restoring the activity of *camCAB* in the Δ*camD* and Δ*camD* Δ*bdh* mutants by the insertion of a non-coding DNA sequence with the same length as *camD* should be investigated in future works. In this context also the influence of the deletion of *camD* towards transcription of the 2,5-DKCMO I and II and 3,6-DKCMO should be analyzed as the Δ*camD* mutant was not able to convert (+)-camphor into the corresponding lactone.

Analysis of the purified CamH and the Δ*camH* mutant indicated that the enzyme might not be responsible for the opening of the 5-oxo-1,2-campholide lactone under the conditions used in this work. Instead, it could be shown that the lactone opens by an elimination reaction. Thus, in order to obtain a strain for the lactonization of camphor it might be necessary to delete the *camDCAB* operon in further works so a stable camphor lactone is formed by both 2,5-DKCMOs and the 3,6-DKCMO. For this purpose the deletion of *camR* might not be necessary as it was shown that the expression of both 2,5-DKCMOs and the 3,6-DKCMO is induced by camphor.

The production of 2,5-diketocamphane could not be realized by the knockout of the 2,5-DKCMO I and II genes as the mutant was still able to completely metabolize (+)-camphor as a single carbon source. The reason for this might be the degradation of the diketocamphane species by the 3,6-DKCMO. Consequently, the next step would be the deletion of the $camE_{36}$ gene in the Δ$camE_{25\text{-}1}$ Δ$camE_{25\text{-}2}$ mutant. The resulting mutant should then be analyzed depending on its product formation using camphor as a substrate.

Biotransformation of terpenes using the enzymes of the CAM plasmid

Within this work the most promising method for the production of camphor-derived monomers for polymers was the expression of the corresponding enzyme under the constitutive camphor promotor in *P. putida* KT2440 instead of the metabolic engineering of *P. putida* ATCC17453. With this procedure and after the optimization of the cultivation conditions, it was possible to produce 5-*exo*-hydroxyborneol and 2,5-diketocamphane (shown earlier) in "g" scale. For both products the next step is a scale up from the laboratory conditions in order to obtain a higher amount of product.

Furthermore, the production of (+)-camphor lactone by the 2,5-DKCMO could be realized by *Rehberger et al.*.[160] Next, the ability to polymerize (+)-camphor lactone has to be analyzed using different polymerization procedures such as ring opening polymerization. In contrast to 5-*exo*-hydroxyborneol, the polymerization of (+)-camphor lactone is expected to be more challenging as the opening of the lactone would yield a tertiary alcohol, which could sterically hamper the polymerization. If a polymer with interesting properties could be obtained it would be necessary to further improve the activity of the 2,5-DKCMO in order to decrease reaction times.

Copolymerization of 5-*exo*-hydroxyborneol

The copolymerization of 5-*exo*-hydroxyborneol with succinic acid dimethyl ester could be realized by a polycondensation reaction. In the wide area of terpene-based polymers the polycondensation is a rather unexploited procedure. Thus, the procedure for the copolymerization of 5-*exo*-hydroxyborneol has to be further improved. The method was originally adopted from the polycondensation of polybutylene terephthalate. However, other polycondensation procedures and their influence on the properties of the resulting biopolymer should be analyzed. Furthermore, the polymerization parameters could be further optimized for the copolymerization of 5-*exo*-hydroxyborneol by screening different catalysts. Besides varying the amount of the catalyst also the reaction temperature and pressure should be varied and the effect towards the resulting polymer analyzed. Additionally, it would be interesting to copolymerize 5-*exo*-hydroxyborneol with dicarboxylic acids of different length in order to see any effect of the length of the side-chain towards the polymer. Moreover, the

effect of the orientation of the hydroxyl group towards the resulting polymer could be analyzed by the biotransformation of (+)-isoborneol using *P. putida* KT2440 pBBr122::*camCAB* and the copolymerization of the resulting product. Nevertheless, in the end all obtained polymers have to be analyzed in more detail to find an appropriate field for their application.

6 References

[1] M. Peplow, *Nature* **2016**, *536*.

[2] R. Geyer, J. R. Jambeck, K. L. Law, *Science advances* **2017**, *3*, e1700782.

[3] G. Gourmelon, *New Worldwatch Institute analysis explores trends in global plastic consumption and recycling. Recuperado de http://www.worldwatch. org* **2015**.

[4] A. Fivga, I. Dimitriou, *Energy* **2018**, *149*, 865-874.

[5] N. Singh, D. Hui, R. Singh, I. P. S. Ahuja, L. Feo, F. Fraternali, *Composites Part B: Engineering* **2017**, *115*, 409-422.

[6] H. Storz, K.-D. Vorlop, *Applied Agriculture and Forestry Research* **2013**, *63*, 321-332.

[7] M. A. Carus, Florence, 2017-03 ed., www.bio-based.eu/reports, **2017**.

[8] N. Hernandez, R. C. Williams, E. W. Cochran, *Organic & Biomolecular Chemistry* **2014**, *12*, 2834-2849.

[9] R. P. Babu, K. O'Connor, R. Seeram, *Progress in Biomaterials* **2013**, *2*, 8.

[10] M. Urbaniak, D. Stankowska-Walczak, **2000**.

[11] V. Flaris, G. Singh, *Journal of Vinyl and Additive Technology* **2009**, *15*, 1-11.

[12] S. Fischer, K. Thümmler, B. Volkert, K. Hettrich, I. Schmidt, K. Fischer, in *Macromolecular Symposia, Vol. 262*, Wiley Online Library, **2008**, pp. 89-96.

[13] A. Mohanty, A. Wibowo, M. Misra, L. Drzal, *Composites Part A: applied science and manufacturing* **2004**, *35*, 363-370.

[14] M. Zhang, Y. Yu, *Industrial & Engineering Chemistry Research* **2013**, *52*, 9505-9514.

[15] Y. Lin, S. Tanaka, *Applied Microbiology and Biotechnology* **2006**, *69*, 627-642.

[16] F. Koopman, N. Wierckx, J. H. de Winde, H. J. Ruijssenaars, *Bioresource Technology* **2010**, *101*, 6291-6296.

[17] E. de Jong, M. A. Dam, L. Sipos, G. J. M. Gruter, in *Biobased Monomers, Polymers, and Materials, Vol. 1105*, American Chemical Society, **2012**, pp. 1-13.

[18] A. Cukalovic, C. V. Stevens, *Green Chemistry* **2010**, *12*, 1201-1206.

[19] A. Pellis, K. Haernvall, C. M. Pichler, G. Ghazaryan, R. Breinbauer, G. M. Guebitz, *Journal of Biotechnology* **2016**, *235*, 47-53.

[20] G.-Q. Chen, *Chemical Society Reviews* **2009**, *38*, 2434-2446.

[21] Y. Poirier, C. Nawrath, C. Somerville, *Nature biotechnology* **1995**, *13*, 142.

[22] M. Zinn, B. Witholt, T. Egli, *Advanced Drug Delivery Reviews* **2001**, *53*, 5-21.

[23] A. J. Pieja, K. H. Rostkowski, C. S. Criddle, *Microbial Ecology* **2011**, *62*, 564-573.

[24] K. Bohmert, I. Balbo, J. Kopka, V. Mittendorf, C. Nawrath, Y. Poirier, G. Tischendorf, R. N. Trethewey, L. Willmitzer, *Planta* **2000**, *211*, 841-845.

[25] K. D. Snell, O. P. Peoples, *Metabolic Engineering* **2002**, *4*, 29-40.

[26] R. Carpine, F. Raganati, G. Olivieri, K. J. Hellingwerf, A. Pollio, P. Salatino, A. Marzocchella, *Algal Research* **2018**, *29*, 49-60.

[27] Z. Katerova, D. Todorova, K. Tasheva, I. Sergiev, *Influence of ultraviolet radiation on plant secondary metabolite production, Vol. 2*, **2012**.

[28] J. Gershenzon, N. Dudareva, *Nature Chemical Biology* **2007**, *3*, 408.

[29] L. Janssens, H. L. De Pooter, N. M. Schamp, E. J. Vandamme, *Process Biochemistry* **1992**, *27*, 195-215.

[30] S. G. Griffin, S. G. Wyllie, J. L. Markham, D. N. Leach, *Flavour and Fragrance Journal* **1999**, *14*, 322-332.

[31] K. A. Hammer, C. F. Carson, T. V. Riley, *Journal of Applied Microbiology* **2003**, *95*, 853-860.

[32] B. C. Clark, T. S. Chamblee, in *Developments in Food Science, Vol. 28* (Ed.: G. Charalambous), Elsevier, **1992**, pp. 229-285.

[33] J. Hirschberg, *Current opinion in plant biology* **2001**, *4*, 210-218.

[34] H. T. Gordon, J. C. Bauernfeind, T. E. Furia, *C R C Critical Reviews in Food Science and Nutrition* **1983**, *18*, 59-97.

[35] M. D. Leavell, D. J. McPhee, C. J. Paddon, *Current Opinion in Biotechnology* **2016**, *37*, 114-119.

[36] M. Aqil, A. Ahad, Y. Sultana, A. Ali, *Drug Discovery Today* **2007**, *12*, 1061-1067.

[37] I. Gubelmann, H. W. Elley, *Industrial & Engineering Chemistry* **1934**, *26*, 589-594.

[38] A. I. Allahverdiev, G. Gündüz, D. Y. Murzin, *Industrial & Engineering Chemistry Research* **1998**, *37*, 2373-2377.

[39] F. Rohdich, W. Eisenreich, J. Wungsintaweekul, S. Hecht, C. A. Schuhr, A. Bacher, *European Journal of Biochemistry* **2001**, *268*, 3190-3197.

[40] A. X. Cheng, Y. G. Lou, Y. B. Mao, S. Lu, L. J. Wang, X. Y. Chen, *Journal of Integrative Plant Biology* **2007**, *49*, 179-186.

[41] N. L. Brock, J. S. Dickschat, in *Natural Products: Phytochemistry, Botany and Metabolism of Alkaloids, Phenolics and Terpenes* (Eds.: K. G. Ramawat, J.-M. Mérillon), Springer Berlin Heidelberg, Berlin, Heidelberg, **2013**, pp. 2693-2732.

[42] V. J. Martin, D. J. Pitera, S. T. Withers, J. D. Newman, J. D. Keasling, *Nature biotechnology* **2003**, *21*, 796.

[43] J. Yang, G. Zhao, Y. Sun, Y. Zheng, X. Jiang, W. Liu, M. Xian, *Bioresource technology* **2012**, *104*, 642-647.

[44] E. Vranová, D. Coman, W. Gruissem, *Annual review of plant biology* **2013**, *64*, 665-700.

[45] C. Yang, X. Gao, Y. Jiang, B. Sun, F. Gao, S. Yang, *Metabolic engineering* **2016**, *37*, 79-91.

[46] H. M. Miziorko, *Archives of Biochemistry and Biophysics* **2011**, *505*, 131-143.

[47] E. I. Wilding, J. R. Brown, A. P. Bryant, A. F. Chalker, D. J. Holmes, K. A. Ingraham, S. Iordanescu, C. Y. So, M. Rosenberg, M. N. Gwynn, *Journal of bacteriology* **2000**, *182*, 4319-4327.

[48] A. Banerjee, T. Sharkey, *Natural product reports* **2014**, *31*, 1043-1055.

[49] M. A. Phillips, P. León, A. Boronat, M. Rodríguez-Concepción, *Trends in Plant Science* **2008**, *13*, 619-623.

[50] W. N. Hunter, *Journal of Biological Chemistry* **2007**, *282*, 21573-21577.

[51] W. Eisenreich, F. Rohdich, A. Bacher, *Trends in Plant Science* **2001**, *6*, 78-84.

[52] H. K. Lichtenthaler, *Biochemical Society Transactions* **2000**, *28*, 785-789.

[53] W. Eisenreich, A. Bacher, D. Arigoni, F. Rohdich, *Cellular and Molecular Life Sciences CMLS* **2004**, *61*, 1401-1426.

[54] D. Tholl, *Current opinion in plant biology* **2006**, *9*, 297-304.

[55] M. Rodrıguez-Concepción, A. Boronat, *Plant physiology* **2002**, *130*, 1079-1089.

[56] D. M. Martin, J. Fäldt, J. Bohlmann, *Plant physiology* **2004**, *135*, 1908-1927.

[57] F. Beran, P. Rahfeld, K. Luck, R. Nagel, H. Vogel, N. Wielsch, S. Irmisch, S. Ramasamy, J. Gershenzon, D. G. Heckel, T. G. Köllner, *Proceedings of the National Academy of Sciences* **2016**, *113*, 2922-2927.

[58] F. Chen, D. Tholl, J. Bohlmann, E. Pichersky, *The Plant Journal* **2011**, *66*, 212-229.

[59] L. Pazouki, Ü. Niinemets, *Frontiers in Plant Science* **2016**, *7*.

[60] R. Croteau, C. Lee Hooper, M. Felton, *Archives of Biochemistry and Biophysics* **1978**, *188*, 182-193.

[61] J. Bohlmann, C. I. Keeling, *The Plant Journal* **2008**, *54*, 656-669.

[62] K. N. Timmis, *Environmental Microbiology* **2002**, *4*, 779-781.

[63] I. Poblete-Castro, J. Becker, K. Dohnt, V. M. Dos Santos, C. Wittmann, *Applied microbiology and biotechnology* **2012**, *93*, 2279-2290.

[64] V. M. Dos Santos, S. Heim, E. Moore, M. Strätz, K. Timmis, *Environmental Microbiology* **2004**, *6*, 1264-1286.

[65] J. I. Jiménez, B. Miñambres, J. L. García, E. Díaz, *Environmental microbiology* **2002**, *4*, 824-841.

[66] P. A. Williams, J. R. Sayers, *Biodegradation* **1994**, *5*, 195-217.

[67] L. P. Wackett, Nature Publishing Group, **2003**.

[68] L. M. Blank, G. Ionidis, B. E. Ebert, B. Bühler, A. Schmid, *The FEBS journal* **2008**, *275*, 5173-5190.

[69] B. E. Ebert, F. Kurth, M. Grund, L. M. Blank, A. Schmid, *Applied and environmental microbiology* **2011**, AEM. 05588-05511.

[70] J. L. Ramos, E. Duque, M.-T. Gallegos, P. Godoy, M. I. Ramos-Gonzalez, A. Rojas, W. Terán, A. Segura, *Annual Reviews in Microbiology* **2002**, *56*, 743-768.

[71] J.-L. Ramos, M. Sol Cuenca, C. Molina-Santiago, A. Segura, E. Duque, M. R. Gómez-García, Z. Udaondo, A. Roca, *FEMS microbiology reviews* **2015**, *39*, 555-566.

[72] J. R. Elmore, A. Furches, G. N. Wolff, K. Gorday, A. M. Guss, *Metabolic Engineering Communications* **2017**, *5*, 1-8.

[73] E. Martínez-García, V. de Lorenzo, *Environmental Microbiology* **2011**, *13*, 2702-2716.

[74] K. Nelson, C. Weinel, I. Paulsen, R. Dodson, H. Hilbert, V. M. dos Santos, D. Fouts, S. Gill, M. Pop, M. Holmes, *Environmental microbiology* **2002**, *4*, 799-808.

[75] W. H. Bradshaw, H. E. Conrad, E. J. Corey, I. C. Gunsalus, D. Lednicer, *Journal of*

the American Chemical Society **1959**, *81*, 5507-5507.

[76] M. Kadow, K. Balke, A. Willetts, U. T. Bornscheuer, J.-E. Bäckvall, *Applied microbiology and biotechnology* **2014**, *98*, 3975-3986.

[77] K. H. Jones, R. T. Smith, P. W. Trudgill, *Microbiology* **1993**, *139*, 797-805.

[78] J. G. Rheinwald, A. M. Chakrabarty, I. C. Gunsalus, *Proceedings of the National Academy of Sciences of the United States of America* **1973**, *70*, 885-889.

[79] H. Iwaki, S. Grosse, H. Bergeron, H. Leisch, K. Morley, Y. Hasegawa, P. C. Lau, *Applied and environmental microbiology* **2013**, AEM. 03958-03912.

[80] A. Willetts, P. Masters, C. Steadman, *Microorganisms* **2018**, *6*, 41.

[81] M. Wheelis, *Annual Reviews in Microbiology* **1975**, *29*, 505-524.

[82] H. Koga, H. Aramaki, E. Yamaguchi, K. Takeuchi, T. Horiuchi, I. Gunsalus, *Journal of bacteriology* **1986**, *166*, 1089-1095.

[83] H. Aramaki, Y. Sagara, K. Takeuchi, H. Koga, T. Horiuchi, *Biochimie* **1994**, *76*, 63-70.

[84] H. Aramaki, Y. Sagara, H. Kabata, N. Shimamoto, T. Horiuchi, *Journal of bacteriology* **1995**, *177*, 3120-3127.

[85] H. Aramaki, Y. Sagara, M. Hosoi, T. Horiuchi, *Journal of bacteriology* **1993**, *175*, 7828-7833.

[86] B. Unger, I. Gunsalus, S. Sligar, *Journal of Biological Chemistry* **1986**, *261*, 1158-1163.

[87] S. A. Hollingsworth, T. L. Poulos, *Protein Science* **2015**, *24*, 49-57.

[88] I. F. Sevrioukova, C. Garcia, H. Li, B. Bhaskar, T. L. Poulos, *Journal of Molecular Biology* **2003**, *333*, 377-392.

[89] H. Aramaki, H. Koga, Y. Sagara, M. Hosoi, T. Horiuchi, *Biochimica et Biophysica Acta (BBA)-Gene Structure and Expression* **1993**, *1174*, 91-94.

[90] M. N. Isupov, E. Schröder, R. P. Gibson, J. Beecher, G. Donadio, V. Saneei, S. A. Dcunha, E. J. McGhie, C. Sayer, C. F. Davenport, *Acta Crystallographica Section D: Biological Crystallography* **2015**, *71*, 2344-2353.

[91] M. Kadow, S. Saß, M. Schmidt, U. T. Bornscheuer, *AMB express* **2011**, *1*, 13.

[92] A. Willetts, D. R. Kelly, *Microbiology* **2014**, *160*, 1783-1794.

[93] D. G. Taylor, P. W. Trudgill, *Journal of bacteriology* **1986**, *165*, 489-497.

[94] M. Kadow, K. Loschinski, S. Saß, M. Schmidt, U. T. Bornscheuer, *Applied microbiology and biotechnology* **2012**, *96*, 419-429.

[95] M. Hofer, H. Strittmatter, V. Sieber, *ChemCatChem* **2013**, *5*, 3351-3357.

[96] J. Zhao, H. Schlaad, in *Bio-synthetic Polymer Conjugates* (Ed.: H. Schlaad), Springer Berlin Heidelberg, Berlin, Heidelberg, **2013**, pp. 151-190.

[97] M. Firdaus, M. A. R. Meier, U. Biermann, J. O. Metzger, *European Journal of Lipid Science and Technology* **2014**, *116*, 31-36.

[98] J. Lu, M. Kamigaito, M. Sawamoto, T. Higashimura, Y.-X. Deng, *Macromolecules* **1997**, *30*, 27-31.

[99] S. Sharma, A. K. Srivastava, *European Polymer Journal* **2004**, *40*, 2235-2240.

[100] M. Bähr, A. Bitto, R. Mülhaupt, *Green Chemistry* **2012**, *14*, 1447-1454.

[101] M. Firdaus, M. A. Meier, *Green Chemistry* **2013**, *15*, 370-380.

[102] S. L. Kristufek, K. T. Wacker, Y.-Y. T. Tsao, L. Su, K. L. Wooley, *Natural product reports* **2017**, *34*, 433-459.

[103] M. Winnacker, J. Sag, *Chemical Communications* **2018**.

[104] S. Kobayashi, C. Lu, T. R. Hoye, M. A. Hillmyer, *Journal of the American Chemical Society* **2009**, *131*, 7960-7961.

[105] K. Yakabi, T. Mathieux, K. Milne, E. M. López-Vidal, A. Buchard, C. Hammond, *ChemSusChem* **2017**, *10*, 3652-3659.

[106] H. C. Quilter, M. Hutchby, M. G. Davidson, M. D. Jones, *Polymer Chemistry* **2017**, *8*, 833-837.

[107] M. Winnacker, J. Sag, A. Tischner, B. Rieger, *Macromolecular rapid communications* **2017**, *38*.

[108] M. Winnacker, M. Neumeier, X. Zhang, C. M. Papadakis, B. Rieger, *Macromolecular rapid communications* **2016**, *37*, 851-857.

[109] A. Behr, L. Johnen, A. Wintzer, A. Gümüş Çetin, P. Neubert, L. Domke, *ChemCatChem* **2016**, *8*, 515-522.

[110] W. Schwab, C. Fuchs, F. C. Huang, *European journal of lipid science and technology* **2013**, *115*, 3-8.

[111] V. B. Urlacher, S. Lutz-Wahl, R. D. Schmid, *Applied microbiology and biotechnology* **2004**, *64*, 317-325.

[112] D. J. Cook, J. D. Finnigan, K. Cook, G. W. Black, S. J. Charnock, in *Advances in Protein Chemistry and Structural Biology, Vol. 105* (Ed.: C. Z. Christov), Academic Press, **2016**, pp. 105-126.

[113] B. Meunier, S. P. de Visser, S. Shaik, *Chemical reviews* **2004**, *104*, 3947-3980.

[114] D. Werck-Reichhart, R. Feyereisen, *Genome biology* **2000**, *1*, reviews3003. 3001.

[115] E. G. Hrycay, S. M. Bandiera, in *Monooxygenase, Peroxidase and Peroxygenase Properties and Mechanisms of Cytochrome P450* (Eds.: E. G. Hrycay, S. M. Bandiera), Springer International Publishing, Cham, **2015**, pp. 1-61.

[116] J. A. McIntosh, C. C. Farwell, F. H. Arnold, *Current Opinion in Chemical Biology* **2014**, *19*, 126-134.

[117] B. A. Halkier, *Phytochemistry* **1996**, *43*, 1-21.

[118] V. B. Urlacher, S. Eiben, *Trends in Biotechnology* **2006**, *24*, 324-330.

[119] K. A. Vespermann, B. N. Paulino, M. C. Barcelos, M. G. Pessôa, G. M. Pastore, G. Molina, *Applied microbiology and biotechnology* **2017**, *101*, 1805-1817.

[120] F. M. Schempp, L. Drummond, M. Buchhaupt, J. Schrader, *Journal of agricultural and food chemistry* **2017**.

[121] J.-W. de Kraker, M. Schurink, M. C. Franssen, W. A. König, A. de Groot, H. J. Bouwmeester, *Tetrahedron* **2003**, *59*, 409-418.

[122] A. Baeyer, V. Villiger, *Berichte der deutschen chemischen Gesellschaft* **1899**, *32*, 3625-3633.

[123] M. Marko D., M. Bernhard, S. Peter, *European Journal of Organic Chemistry* **2002**, *2002*, 3711-3730.

[124] S. M. Roberts, P. W. H. Wan, *Journal of Molecular Catalysis B: Enzymatic* **1998**, *4*, 111-136.

[125] M. A. Delgove, M. T. Elford, K. V. Bernaerts, S. M. De Wildeman, *Journal of Chemical Technology & Biotechnology* **2018**, *93*, 2131-2140.

[126] D. E. Torres Pazmiño, H. M. Dudek, M. W. Fraaije, *Current Opinion in Chemical Biology* **2010**, *14*, 138-144.

[127] G. J. ten Brink, I. W. C. E. Arends, R. A. Sheldon, *Chemical Reviews* **2004**, *104*, 4105-4124.

[128] M. W. Fraaije, N. M. Kamerbeek, W. J. H. van Berkel, D. B. Janssen, *FEBS Letters* **2002**, *518*, 43-47.

[129] H. Leisch, K. Morley, P. C. K. Lau, *Chemical Reviews* **2011**, *111*, 4165-4222.

[130] W. J. H. van Berkel, N. M. Kamerbeek, M. W. Fraaije, *Journal of Biotechnology* **2006**, *124*, 670-689.

[131] R. Orru, H. M. Dudek, C. Martinoli, D. E. T. Pazmiño, A. Royant, M. Weik, M. W. Fraaije, A. Mattevi, *Journal of Biological Chemistry* **2011**, *286*, 29284-29291.

[132] R. Orru, D. E. T. Pazmiño, M. W. Fraaije, A. Mattevi, *Journal of Biological Chemistry* **2010**, *285*, 35021-35028.

[133] D. Sheng, D. P. Ballou, V. Massey, *Biochemistry* **2001**, *40*, 11156-11167.

[134] I. Polyak, M. T. Reetz, W. Thiel, *Journal of the American Chemical Society* **2012**, *134*, 2732-2741.

[135] G. de Gonzalo, M. D. Mihovilovic, M. W. Fraaije, *ChemBioChem* **2010**, *11*, 2208-2231.

[136] K. Balke, M. Kadow, H. Mallin, S. Saß, U. T. Bornscheuer, *Organic & biomolecular chemistry* **2012**, *10*, 6249-6265.

[137] M. O. Carmody, W. H. Carmody, *Journal of the American Chemical Society* **1937**, *59*, 1312-1312.

[138] H. Panda, *Handbook on Oleoresin and Pine Chemicals (Rosin, Terpene Derivatives, Tall Oil, Resin & Dimer Acids)*, ASIA PACIFIC BUSINESS PRESS Inc., **2008**.

[139] R. T. Mathers, M. A. Meier, *Green Polymerization Methods: Renewable Starting Materials, Catalysis and Waste Reduction*, John Wiley & Sons, **2011**.

[140] M. N. Belgacem, A. Gandini, *Monomers, Polymers and Composites from Renewable Resources*, Elsevier Science, **2011**.

[141] H. J. Endres, A. Siebert-Raths, *Technische Biopolymere: Rahmenbedingungen, Marktsituation, Herstellung, Aufbau und Eigenschaften*, Carl Hanser Verlag GmbH & Company KG, **2019**.

[142] S. Koltzenburg, M. Maskos, O. Nuyken, R. Mülhaupt, *Polymere: Synthese, Eigenschaften und Anwendungen*, Springer Berlin Heidelberg, **2013**.

[143] Y. Zhu, C. Romain, C. K. Williams, *Nature* **2016**, *540*, 354.

[144] M. Winnacker, B. Rieger, *ChemSusChem* **2015**, *8*, 2455-2471.

[145] A. Llevot, P. K. Dannecker, M. von Czapiewski, L. C. Over, Z. Soeyler, M. A. Meier, *Chemistry–A European Journal* **2016**, *22*, 11510-11521.

[146] P. A. Wilbon, F. Chu, C. Tang, *Macromolecular rapid communications* **2013**, *34*, 8-37.

[147] P. Sarkar, A. K. Bhowmick, *Rsc Advances* **2014**, *4*, 61343-61354.

[148] R. Ciriminna, M. Lomeli-Rodriguez, P. D. Cara, J. A. Lopez-Sanchez, M. Pagliaro, *Chemical Communications* **2014**, *50*, 15288-15296.

[149] A. Gandini, T. M. Lacerda, *Progress in Polymer Science* **2015**, *48*, 1-39.

[150] J. Sambrook, D. W. Russell, D. W. Russell, *Molecular cloning: a laboratory manual (3-volume set), Vol. 999*, Cold spring harbor laboratory press New York, **2001**.

[151] K. Kleppe, E. Ohtsuka, R. Kleppe, I. Molineux, H. G. Khorana, *Journal of Molecular Biology* **1971**, *56*, 341-361.

[152] C. Aaij, P. Borst, *Biochimica et Biophysica Acta (BBA) - Nucleic Acids and Protein Synthesis* **1972**, *269*, 192-200.

[153] U. K. Laemmli, *Nature* **1970**, *227*, 680-685.

[154] H. Towbin, T. Staehelin, J. Gordon, *Proceedings of the National Academy of Sciences* **1979**, *76*, 4350-4354.

[155] D. A. Whittington, M. L. Wise, M. Urbansky, R. M. Coates, R. B. Croteau, D. W. Christianson, *Proceedings of the National Academy of Sciences* **2002**, *99*, 15375-15380.

[156] S. Roth, I. Funk, M. Hofer, V. Sieber, *ChemSusChem* **2017**, *10*, 3574-3580.

[157] M. H. Gelb, D. C. Heimbrook, P. Malkonen, S. G. Sligar, *Biochemistry* **1982**, *21*, 370-377.

[158] Y. A. G. P. Gunawardana, G. A. Cordell, I. R. C. Bick, *Journal of Natural Products* **1988**, *51*, 142-144.

[159] H.-L. Tsang, J.-L. Huang, Y.-H. Lin, K.-F. Huang, P.-L. Lu, G.-H. Lin, A. A. Khine, A. Hu, H.-P. Chen, *Applied and Environmental Microbiology* **2016**, *82*, 6378-6385.

[160] J. Rehberger, **2017**.

[161] R. Croteau, F. Karp, *Biochemical and Biophysical Research Communications* **1976**, *72*, 440-447.

[162] R. Croteau, F. Karp, *Archives of Biochemistry and Biophysics* **1979**, *198*, 512-522.

[163] R. Croteau, M. Felton, F. Karp, R. Kjonaas, *Plant Physiology* **1981**, *67*, 820-824.

[164] W. Schwab, D. C. Williams, E. M. Davis, R. Croteau, *Archives of Biochemistry and Biophysics* **2001**, *392*, 123-136.

[165] M. L. Wise, T. J. Savage, E. Katahira, R. Croteau, *Journal of Biological Chemistry* **1998**, *273*, 14891-14899.

[166] D. C. Williams, D. J. McGarvey, E. J. Katahira, R. Croteau, *Biochemistry* **1998**, *37*, 12213-12220.

[167] Y. Lin, X. Sun, Q. Yuan, Y. Yan, *Metabolic Engineering* **2013**, *18*, 69-77.

[168] M. J. Weickert, D. H. Doherty, E. A. Best, P. O. Olins, *Current Opinion in Biotechnology* **1996**, *7*, 494-499.

[169] E. R. LaVallie, J. M. McCoy, *Current Opinion in Biotechnology* **1995**, *6*, 501-506.

[170] P. K. Ajikumar, W.-H. Xiao, K. E. J. Tyo, Y. Wang, F. Simeon, E. Leonard, O. Mucha, T. H. Phon, B. Pfeifer, G. Stephanopoulos, *Science* **2010**, *330*, 70-74.

[171] P. D. Matthews, E. T. Wurtzel, *Applied Microbiology and Biotechnology* **2000**, *53*, 396-400.

[172] C.-W. Wang, M.-K. Oh, J. C. Liao, *Biotechnology and Bioengineering* **1999**, *62*, 235-241.

[173] H. Beuttler, J. Hoffmann, M. Jeske, B. Hauer, R. D. Schmid, J. Altenbuchner, V. B. Urlacher, *Applied Microbiology and Biotechnology* **2011**, *89*, 1137-1147.

[174] M. F. Kramer, D. M. Coen, *Current Protocols in Molecular Biology* **2001**, *56*, 15.11.11-15.11.14.

[175] K. H. Roux, *Cold Spring Harbor Protocols* **2009**, *2009*, pdb.ip66.

[176] D. Hanahan, F. R. Bloom, *Escherichia coli and Salmonella: cellular and molevular biologi. American Society for Microbiology, Washington, DC* **1996**, 2449-2459.

[177] T. E. V. Aune, F. L. Aachmann, *Applied Microbiology and Biotechnology* **2010**, *85*, 1301-1313.

[178] J. M. Diver, L. E. Bryan, P. A. Sokol, *Analytical Biochemistry* **1990**, *189*, 75-79.

[179] S. Fiedler, R. Wirth, *Analytical Biochemistry* **1988**, *170*, 38-44.

[180] J.-H. Cho, E.-K. Kim, J.-S. So, *Biotechnology Techniques* **1995**, *9*, 41-44.

[181] I. Chen, P. J. Christie, D. Dubnau, *Science* **2005**, *310*, 1456-1460.

[182] F. De La Cruz, L. S. Frost, R. J. Meyer, E. L. Zechner, *FEMS Microbiology Reviews* **2010**, *34*, 18-40.

[183] A. Chakrabarty, *Annual review of genetics* **1976**, *10*, 7-30.

[184] S. Dhanasekaran, T. M. Doherty, J. Kenneth, *Journal of Immunological Methods* **2010**, *354*, 34-39.

[185] A. Raso, S. Mascelli, P. Nozza, E. Ugolotti, I. Vanni, V. Capra, R. Biassoni, *Journal of Clinical Laboratory Analysis* **2011**, *25*, 389-394.

[186] T. Demeke, G. R. Jenkins, *Analytical and Bioanalytical Chemistry* **2010**, *396*, 1977-1990.

[187] L. T. Fernández-Martínez, M. J. Bibb, *Scientific Reports* **2014**, *4*, 7100.

[188] K. Maenaka, K. Fukushi, H. Aramaki, Y. Shirakihara, *Acta Crystallographica Section F* **2005**, *61*, 796-798.

[189] H. Aramaki, M. Fujita, Y. Sagara, A. Amemura, T. Horiuchi, *FEMS Microbiology Letters* **1994**, *123*, 49-54.

[190] H. Aramaki, H. Kabata, S. Takeda, H. Itou, H. Nakayama, N. Shimamoto, *Genes to Cells* **2011**, *16*, 1200-1207.

[191] M. Fujita, H. Aramaki, T. Horiuchi, A. Amemura, *Journal of Bacteriology* **1993**, *175*, 6953-6958.

[192] E. Jay, H. Chen, R. Kumar, M. Bjerknes, *Nucleic Acids Research* **1994**, *22*, 4953-4957.

[193] I. A. Osterman, S. A. Evfratov, P. V. Sergiev, O. A. Dontsova, *Nucleic Acids Research* **2012**, *41*, 474-486.

[194] H. Leisch, R. Shi, S. Grosse, K. Morley, H. Bergeron, M. Cygler, H. Iwaki, Y. Hasegawa, P. C. K. Lau, *Applied and Environmental Microbiology* **2012**, *78*, 2200-2212.

[195] J. Michizoe, H. Ichinose, N. Kamiya, T. Maruyama, M. Goto, *Journal of Bioscience and Bioengineering* **2005**, *99*, 12-17.

[196] T. Mouri, N. Kamiya, M. Goto, *Biotechnology Letters* **2006**, *28*, 1509-1513.

[197] P. Fonseca, R. Moreno, F. Rojo, *Environmental Microbiology Reports* **2011**, *3*, 329-339.

[198] O. Sibbesen, J. J. De Voss, P. R. O. de Montellano, *Journal of Biological Chemistry* **1996**, *271*, 22462-22469.

[199] B. Prasad, D. J. Mah, A. R. Lewis, E. Plettner, *PLOS ONE* **2013**, *8*, e61897.

[200] Y. Sardessai, S. Bhosle, *Research in Microbiology* **2002**, *153*, 263-268.

[201] F. van Keulen, C. N. Correia, M. M. R. da Fonseca, *Journal of Molecular Catalysis B: Enzymatic* **1998**, *5*, 295-299.

[202] S. K. Yoo, D. F. Day, *Process Biochemistry* **2002**, *37*, 739-745.

[203] H. Schewe, B.-A. Kaup, J. Schrader, *Applied Microbiology and Biotechnology* **2008**, *78*, 55-65.

[204] P. V. Gould, M. H. Gelb, S. G. Sligar, *Journal of Biological Chemistry* **1981**, *256*, 6686-6691.

[205] T. Chatterjee, D. Bhattacharyya, *Applied Microbiology and Biotechnology* **2001**, *55*, 541-546.

[206] I. Bechthold, K. Bretz, S. Kabasci, R. Kopitzky, A. Springer, *Chemical Engineering & Technology* **2008**, *31*, 647-654.

[207] S. J. Lee, D.-Y. Lee, T. Y. Kim, B. H. Kim, J. Lee, S. Y. Lee, *Applied and Environmental Microbiology* **2005**, *71*, 7880-7887.

[208] T. V. Yuzbashev, E. Y. Yuzbasheva, T. I. Sobolevskaya, I. A. Laptev, T. V. Vybornaya, A. S. Larina, K. Matsui, K. Fukui, S. P. Sineoky, *Biotechnology and Bioengineering* **2010**, *107*, 673-682.

[209] K. Satoh, A. Nakahara, K. Mukunoki, H. Sugiyama, H. Saito, M. Kamigaito, *Polymer Chemistry* **2014**, *5*, 3222-3230.

[210] M. Winnacker, A. Tischner, M. Neumeier, B. Rieger, *RSC Advances* **2015**, *5*, 77699-77705.

[211] J. R. Lowe, M. T. Martello, W. B. Tolman, M. A. Hillmyer, *Polymer Chemistry* **2011**, *2*, 702-708.

[212] Y. Xin, H. Uyama, *Journal of Polymer Research* **2012**, *19*, 15.

[213] K. Stahl, *Master Thesis* **2013**.

[214] S. Roth, *Bachelor Thesis* **2015**.

[215] A. Willetts, D. Kelly, *Microorganisms* **2016**, *4*, 38.

[216] A. Marchler-Bauer, Y. Bo, L. Han, J. He, C. J. Lanczycki, S. Lu, F. Chitsaz, M. K. Derbyshire, R. C. Geer, N. R. Gonzales, M. Gwadz, D. I. Hurwitz, F. Lu, G. H. Marchler, J. S. Song, N. Thanki, Z. Wang, R. A. Yamashita, D. Zhang, C. Zheng, L. Y. Geer, S. H. Bryant, *Nucleic acids research* **2017**, *45*, D200-D203.

[217] X.-J. Luo, X.-D. Kong, J. Zhao, Q. Chen, J. Zhou, J.-H. Xu, *Biotechnology and Bioengineering* **2014**, *111*, 1920-1930.

[218] J. Chen, X.-J. Luo, Q. Chen, J. Pan, J. Zhou, J.-H. Xu, *Bioresources and Bioprocessing* **2015**, *2*, 39.

[219] I. C. Gunsalus, V. P. Marshall, D. W. Ribbons, *CRC Critical Reviews in Microbiology* **1971**, *1*, 291-310.

[220] J. B. van Beilen, W. A. Duetz, A. Schmid, B. Witholt, *Trends in Biotechnology* **2003**, *21*, 170-177.

[221] H. E. M. Law, C. V. F. Baldwin, B. H. Chen, J. M. Woodley, *Chemical Engineering Science* **2006**, *61*, 6646-6652.

[222] C. V. F. Baldwin, J. M. Woodley, *Biotechnology and Bioengineering* **2006**, *95*, 362-369.

[223] I. Hilker, C. Baldwin, V. Alphand, R. Furstoss, J. Woodley, R. Wohlgemuth, *Biotechnology and Bioengineering* **2006**, *93*, 1138-1144.

7 Appendix

7.1 NMR analysis of 5-*exo*-hydroxyborneol

The ^{13}C NMR analysis of 5-*exo*-hydroxyborneol is shown in Figure 60.

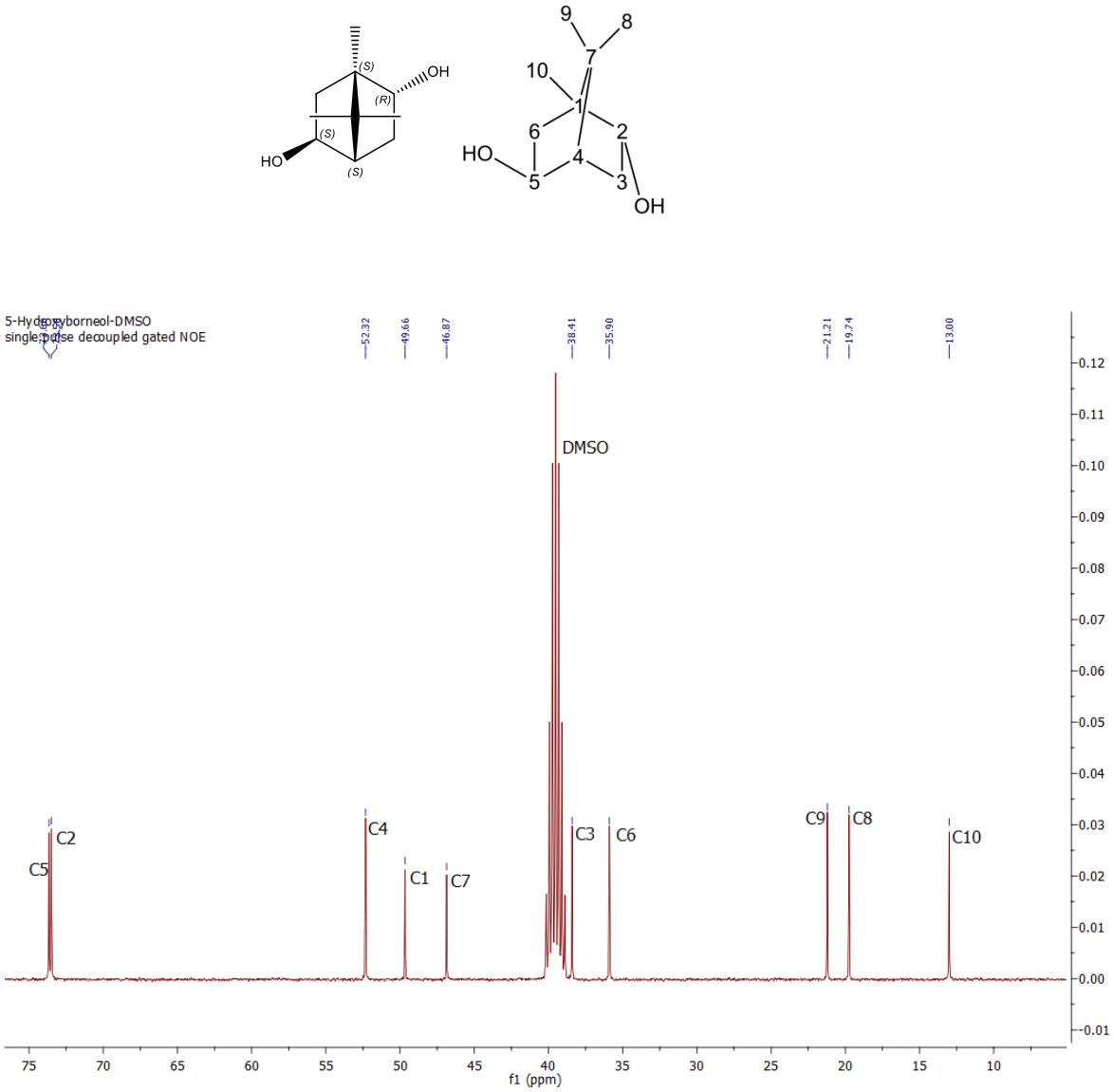

Figure 60: ^{13}C NMR chromatogram of 5-*exo*-hydroxyborneol in *d*-DMSO. Y-axis: intensity; x-axis: Chemical shifts with reference to tetramethylsilane [ppm]. All peaks were assigned to the corresponding H-atoms. ^{13}C NMR (101 MHz,) δ 73.7, 73.5, 52.3, 49.7, 46.9, 38.4, 35.9, 21.2, 19.7, 13.0.

7.2 Gel permeation chromatography

The calibration curve obtained for GPC analysis of the polymerization of 5-*exo*-hydroxyborneol using the ReadyCal-Kit Poly(methyl methacrylate) low from PSS is shown in Figure 61 (chapter 2.2.5.4).

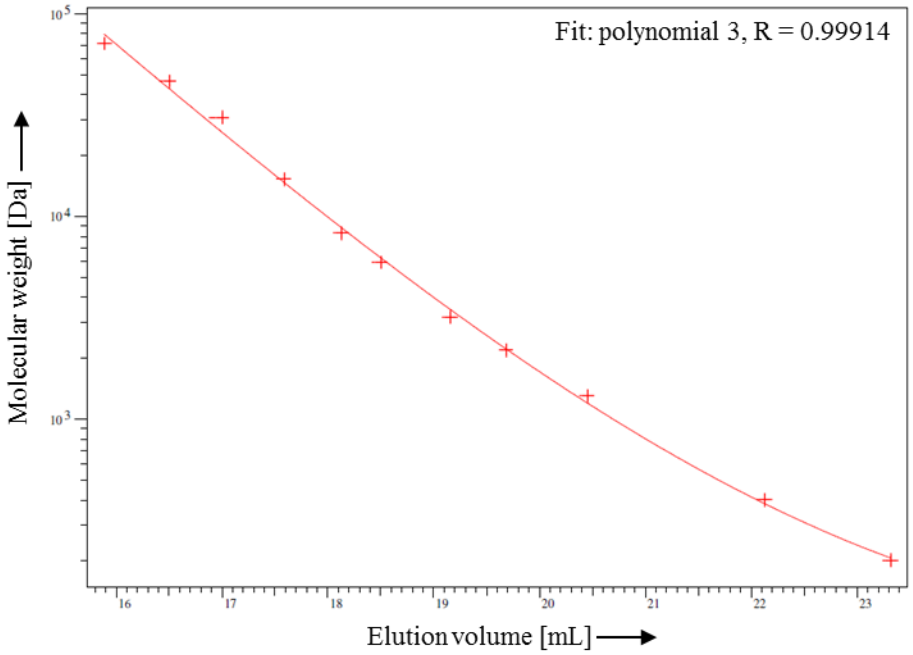

Figure 61: Calibration curve for GPC analysis using the ReadyCal-Kit Poly(methyl methacrylate) low from PSS. Y-axis: molecular weight [Da]; x-axis: elution volume [mL].

Based on the calibration curve the molecular weight of a reference (Vestodur) and the polymers obtain from the polymerization of 5-*exo*-hydroxyborneol and succinic acid dimethyl ester were calculated (Table 24).

Table 24: Calculated molecular weight of the polymer samples of the polymerization of 5-*exo*-hydroxyborneol and succinic acid dimethyl ester based on the results of the calibration curve.

	Vestodur	Sample 1	Sample 2	Sample 3
M_W [g mol^{-1}] 1. run	56,244	2,796	4,037	2,266
M_W [g mol^{-1}] 2. run	56,484	2,792	4,089	2,272
M_W [g mol^{-1}] mean	56,364 ± 170	2,794 ± 2.8	4,063 ± 36.8	2,269 ± 4.2

7.3 Glucose assay

For the calibration curve glucose concentrations in the range of 0 – 90 mg L^{-1} were analyzed (Figure 62).

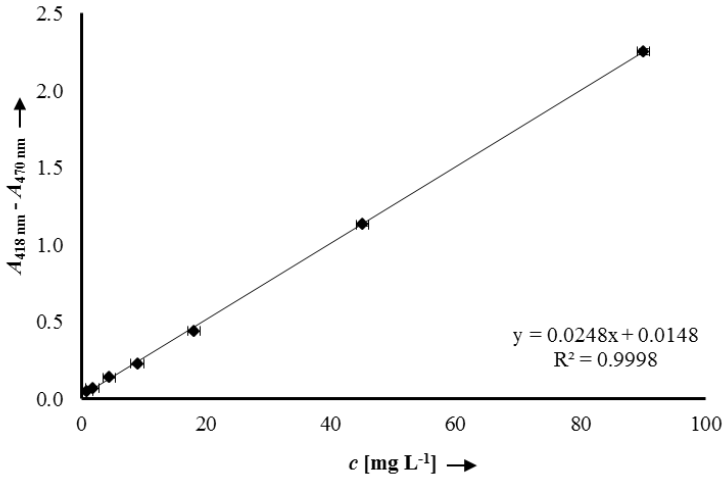

Figure 62: Calibration curve for the glucose assay. Y-axis: $A_{418\ nm} - A_{470\ nm}$; x-axis: concentration [mg L^{-1}]. Standards were analyzed in triplicates.

The amount of glucose during the cultivation of the *P. putida* ATCC17453 wt and the different mutants was calculated based on the calibration curve (Figure 63).

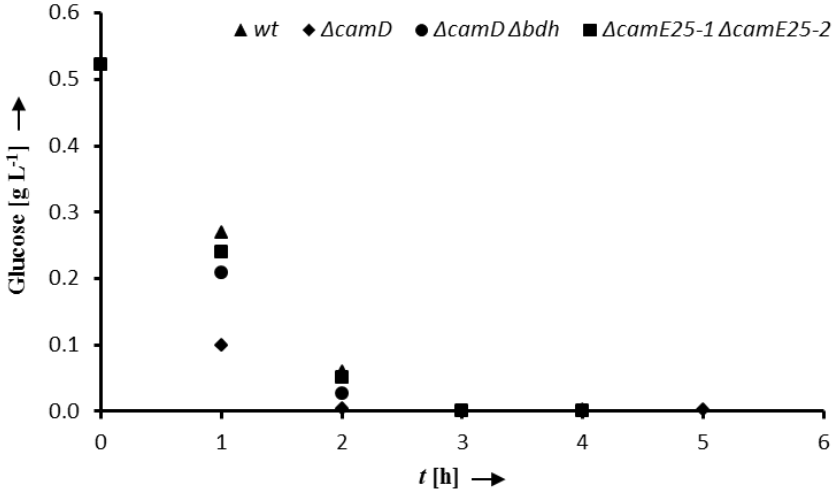

Figure 63: Amount of glucose during the cultivation of *P. putida* ATCC17453 wt (black triangle), Δ*camD* mutant (black diamond), Δ*camD* Δ*bdh* mutant (black dot) and Δ$camE_{25\text{-}1}$ Δ$camE_{25\text{-}2}$. Y-axis: glucose concentration [g L^{-1}]; x-axis: *t* [h]. Samples were analyzed in triplicates.

7.4 HPLC-MS

The conversion of (+)-camphor lactone was followed by HPLC-MS analysis (chapter 2.2.5.2). Figure 64 shows the chromatogram for the conversion after 4 h (A) and 0 h (B) compared to a reference standard (C).

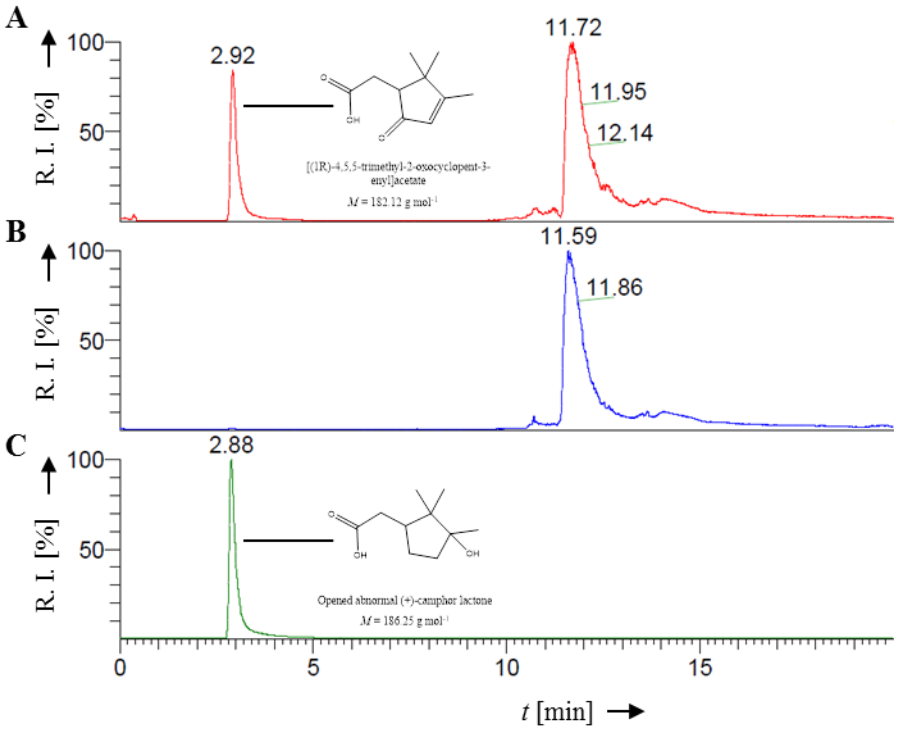

Figure 64: HPLC chromatogram for the conversion of (+)-camphor lactone by *P. putida* KT2440 pBBr122::*camDCAB* at 30 °C and 135 rpm after 4 h (A, red) and 0 h (B, blue). The abnormal (+)-camphor lactone was opened and used as a reference (C, green). Y-axis: relative intensity; x-axis: time [min].

The structure of the reference standard is in close relation to the opened 5-oxo-1,2-campholide and both eluted at similar retention times (t_R ~ 2.9 min) . In Figure 65 the MS spectrum of both peaks is shown. Both structures could be identified by their M-H mass peaks as indicated.

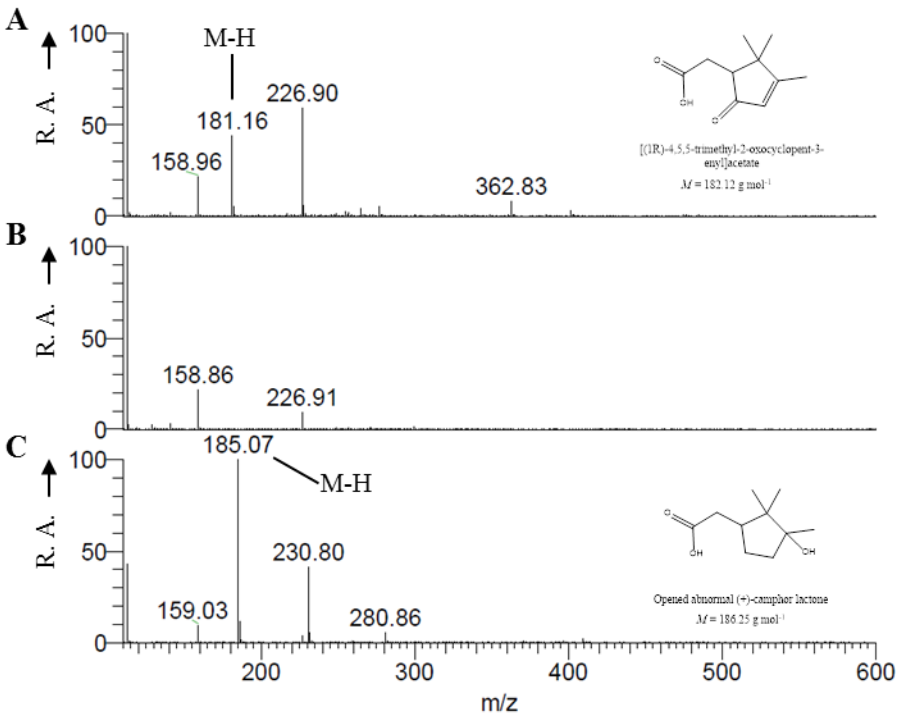

Figure 65: MS spectrum of the signal obtained at 2.91 min retention time for the conversion of (+)-camphor lactone by *P. putida* KT2440 pBBr122::*camDCAB* at 30 °C and 135 rpm after 4 h (A) and 0 h (B). The abnormal (+)-camphor lactone was opened and used as a reference (C). Y-axis: relative abundance; x-axis: m/z.

7.5 Semi-continuous batch process

The conversion of 5 mM (-)-borneol using the semi-continuous batch process is shown in Figure 66 and Table 25.

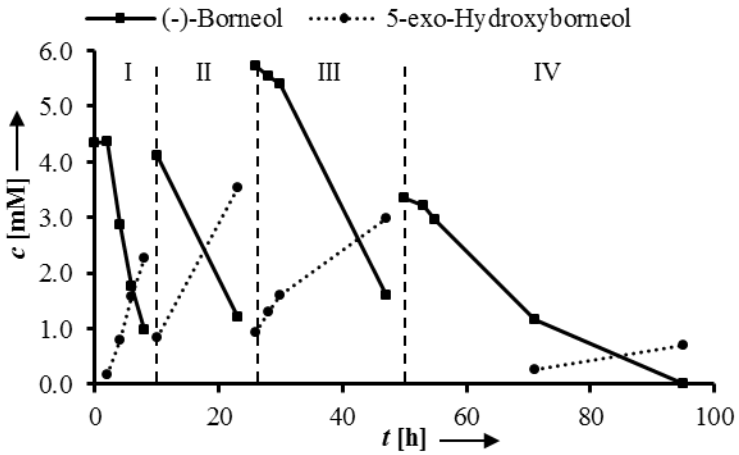

Figure 66: Substrate conversion and product formation during the biotransformation of (-)-borneol by *P. putida* KT2440 pBBr122::*camCAB* with cell recycling. Each dotted vertical line indicates the addition of fresh substrate and medium. Overall cells could be used up to four times for the conversion of (-)-borneol (Phase I - IV).

Table 25: Parameters obtained during the biotransformation of (-)-borneol by *P. putida* KT2440 pBBr122::*camCAB*. *STY*s refer to wet biomass, for calculation see experimental section.

	Phase I	Phase II	Phase III	Phase IV
t [h]	8	13	21	45
Conversion [%]	93.6	90.5	88.4	99.6
Yield [%]	52.3	85.8	52.0	20.9
STY [mg L^{-1} h^{-1}]	48	31	24	2.7
STY [mg mg^{-1} h^{-1}]	10	6.3	5.7	0.5

7.6 Gene sequences

Gene sequence (+)-BPPS (*S. officinalis*, *(+)-bpps*):

```
(+)_BPPS_S.officinalis            atgtctatcattagcatgaacgtatcgatccttagcaagccactaaattgcctccacaac      60
(+)_BPPS_optimized_Pseudomonas    ATGTCGATCATCTCGATGAATGTCTCGATCCTGTCCAAGCCGCTGAACTGCCTCCACAAC      60
                                  ***** *****    ***** ** ********   ****** ** ** ************

(+)_BPPS_S.officinalis            ttggagaggagaccttcaaaagccttgcttgtcccttgcactgcacccaccgctcgcctc      120
(+)_BPPS_optimized_Pseudomonas    CTGGAACGTCGGCCTAGTAAGGCCCTGTTGGTACCCTGTACGGCCCCAACTGCCCGCTTG      120
                                   ****  *  * ***   ** *** ** * ** ** ** ** ** ** ** ** *** *

(+)_BPPS_S.officinalis            cgggcatcttgctcctcaaaactacaagaagctcatcaaatccgacgatctggaaactac      180
(+)_BPPS_optimized_Pseudomonas    CGTGCCAGTTGTAGCAGCAAGCTGCAAGAGGCTCACCAGATCCGTCGTTCGGGTAACTAC      180
                                  ** **   ***   *   ** ** ***** ***** ** ***** ** ** ** ******

(+)_BPPS_S.officinalis            caacctgccctttgggattccaattacattcagtctctcaatactccatatacggaggag      240
(+)_BPPS_optimized_Pseudomonas    CAGCCGGCGTTGTGGGATAGCAATTACATCCAGAGCCTGAATACGCCGTATACCGAAGAA      240
                                  ** ** **  * ******  ********* ***   ** ***** ** ***** ** **

(+)_BPPS_S.officinalis            aggcacttggatagaaaagcagagctgattgtgcaagtgaggatactgctaaaggaaaaa      300
(+)_BPPS_optimized_Pseudomonas    CGCCATCTGGACCGGAAGGCAGAGCTGATCGTCCAAGTGCGCATCCTGCTGAAAGAGAAG      300
                                   * **  ****  * ** ********** ** ****** * ** ***** ** ** **

(+)_BPPS_S.officinalis            atggagcctgttcaacaattggagttgattcatgacttgaaatatttggggctctcggat      360
(+)_BPPS_optimized_Pseudomonas    ATGGAGCCGGTACAGCAACTGGAACTGATCCACGACCTGAAGTATCTGGGCCTGAGCGAC      360
                                  ******** ** ** *** ****  **** ** *** **** *** **** **    **

(+)_BPPS_S.officinalis            ttttttcaagatgagattaaggagatcttaggtgttatatacaatgagcacaaatgcttt      420
(+)_BPPS_optimized_Pseudomonas    TTCTTCCAGGACGAAATCAAGGAGATTCTCGGCGTGATCTACAACGAGCACAAGTGCTTT      420
                                  ** ** ** ** ** ** ********  * ** ** ** ***** ******** ******

(+)_BPPS_S.officinalis            cacaataatgaagtagagaaaatggatttgtatttcacagctcttggattcagactcctc      480
(+)_BPPS_optimized_Pseudomonas    CACAACAACGAAGTGGAAAAGATGGACCTGTACTTCACCGCGTTGGGTTTTCGCTTGCTG      480
                                  ***** ** ***** ** ** *****  **** ***** **  * ** **  *  * **

(+)_BPPS_S.officinalis            agacaacatggttttaatatttcccaagatgtatttaattgtttcaagaacgagaagggt      540
(+)_BPPS_optimized_Pseudomonas    CGCCAACATGGCTTCAACATCAGCCAAGACGTGTTCAACTGCTTCAAGAACGAGAAAGGG      540
                                   * ******** ** ** **   ****** ** ** ** ** ************** **

(+)_BPPS_S.officinalis            attgatttcaaggcaagccttgctcaagatacgaagggaatgttacaactgtatgaagcg      600
(+)_BPPS_optimized_Pseudomonas    ATCGACTTCAAAGCGAGCCTGGCCCAGGACACCAAAGGCATGCTGCAGCTCTACGAAGCC      600
                                  ** ** ***** ** ***** ** ** ** ** ** ** ** *** * ** ** ** *****

(+)_BPPS_S.officinalis            tctttccttttgagaaaaggtgaagatacattggagcttgcaagagaatttgccacaaaa      660
(+)_BPPS_optimized_Pseudomonas    AGCTTTCTGCTGCGGAAAGGCGAGGATACTCTGGAGCTGGCCCGGGAGTTCGCAACCAAA      660
                                     ** **  ** * ***** ** *****  ******* **  * ** ** ** ** ***

(+)_BPPS_S.officinalis            tgtctgcagaaaaaacttgatgaaggtggtaatgaaattgatgagaatctattattgtgg      720
(+)_BPPS_optimized_Pseudomonas    TGCCTGCAGAAGAAGCTGGACGAAGGCGGCAACGAAATTGATGAGAACTTGCTGCTGTGG      720
                                  ** ******** ** ** ** ***** ** ** **************  *  *  *****

(+)_BPPS_S.officinalis            attcgccactctttggatcttcctctccactggaggattcaaagtgtagaggcaagatgg      780
(+)_BPPS_optimized_Pseudomonas    ATTCGCCATAGCCTGGATTTGCCCCTGCACTGGCGCATCCAGAGCGTCGAAGCACGCTGG      780
                                  ********     ***** * ** ** ****** * ** ** ** ** ** ** *** * ***

(+)_BPPS_S.officinalis            ttcatagatgcttatgcgagaaggccagacatgaatccacttatttttcgagcttgccaaa      840
(+)_BPPS_optimized_Pseudomonas    TTCATCGACGCGTATGCTCGCCGTCCTGACATGAACCCGCTGATCTTTGAGCTGGCCAAG      840
                                  ***** ** ** *****  *  * ** ******** ** ** ** ** ***** *****

(+)_BPPS_S.officinalis            ctcaacttcaatattattcaagcaacacatcaacaagaactgaaagatctctcgaggtgg      900
(+)_BPPS_optimized_Pseudomonas    CTCAACTTCAACATCATCCAAGCCACGCATCAGCAGGAACTGAAGGACCTGAGCCGTTGG      900
                                  ********** ** ** ***** ** ***** ** ******** ** **     * ***

(+)_BPPS_S.officinalis            tggagtagattatgcttccctgaaaagctcccatttgtgagggataggctcgttgaatcc      960
(+)_BPPS_optimized_Pseudomonas    TGGAGCCGCCTGTGCTTCCCAGAGAAGCTCCCGTTCGTTCGCGATCGCCTGGTTGAGTCG      960
                                  *****  *  * ******** ** ******** ** **  * *** * ** ***** **

(+)_BPPS_S.officinalis            ttcttttgggcggttgggatgtttgagccacatcaacatggatatcagagaaaaatggcc     1020
(+)_BPPS_optimized_Pseudomonas    TTCTTCTGGGCCGTCGGCATGTTCGAACCGCATCAGCACGGCTACCAGCGCAAGATGGCC     1020
                                  ***** ***** ** ** ***** ** ** ***** ** ** ** *** * ** ******

(+)_BPPS_S.officinalis            gccacaattattgttttagcaacagttatagatgatatttacgatgtgtatggtacacta     1080
(+)_BPPS_optimized_Pseudomonas    GCGACGATTATCGTCCTGGCGACCGTGATCGACGACATCTACGACGTGTACGGGACGCTG     1080
                                  ** ** ***** **  * ** ** ** ** ** ** ** ***** ***** ** ** **

(+)_BPPS_S.officinalis            gatgaactagaactatttacagacacgtttaagagatgggatactgaatcaataacccga     1140
(+)_BPPS_optimized_Pseudomonas    GATGAACTGGAACTCTTTACCGACACCTTCAAGCGCTGGGATACCGAGTCCATCACCCGG     1140
                                  ******** ***** ***** ***** ** *** * ******** ** ** ** *****

(+)_BPPS_S.officinalis            cttccttattacatgcaattatgttattggggtgtccacaactatatttccgatgcagca     1200
(+)_BPPS_optimized_Pseudomonas    CTGCCTTACTACATGCAGCTGTGCTACTGGGGCGTCCACAACTACATCTCCGATGCCGCG     1200
                                  ** ***** ********  * ** ** ***** ********** ** ******** **

(+)_BPPS_S.officinalis            tatgatattctcaaagaacatggtttcttttgtctccaatatctccggaaatcggtggta     1260
(+)_BPPS_optimized_Pseudomonas    TATGACATCCTGAAGGAGCACGGCTTCTTTTGCCTGCAGTACCTGCGCAAAAGCGTGGTG     1260
                                  ***** ** ** ** ** ** ** ******** ** ** ** ** ** ***   *****
```

```
(+)_BPPS_S.officinalis            gatttggttgaagcatattttcacgaggcaaagtggtaccacagcggttatacaccaagc       1320
(+)_BPPS_optimized_Pseudomonas    GACTTGGTGGAGGCCTACTTCCACGAAGCGAAATGGTATCACTCGGGGTACACCCCGAGC       1320
                                  ** ***** ** ** ** ** ***** ** ** ***** ***   ** ** ** ** ***

(+)_BPPS_S.officinalis            ctggatgaatatctcaacatcgccaagatttcagtggcgtctcctgcaataatatcccca       1380
(+)_BPPS_optimized_Pseudomonas    CTGGATGAGTACCTCAACATCGCCAAGATTTCCGTAGCCAGTCCGGCCATCATCTCGCCC       1380
                                  ******** ** ********************* ** **   *** ** ** ** ** **

(+)_BPPS_S.officinalis            acctatttcacattcgcaaacgcgtctcatgacacagcagtcatcgacagcttgtaccaa       1440
(+)_BPPS_optimized_Pseudomonas    ACCTACTTCACCTTCGCCAATGCGTCGCATGACACCGCTGTGATTGACAGCCTGTACCAG       1440
                                  ***** ***** ***** ** ***** ******** ** ** ** ****** *******

(+)_BPPS_S.officinalis            tatcatgacatactttgcctagcaggaattattttgaggcttcccgacgatcttgggaca       1500
(+)_BPPS_optimized_Pseudomonas    TACCACGACATCCTGTGCCTGGCAGGCATCATCTTGCGCTTGCCGGATGACCTGGGCACC       1500
                                  ** ** ***** ** ***** ***** ** ** *** *  * ** ** ** ** ** ** **

(+)_BPPS_S.officinalis            tcatattttgagctggcgagaggcgacgtgccgaaaacaatccagtgctacatgaaggaa       1560
(+)_BPPS_optimized_Pseudomonas    AGCTATTTCGAACTGGCTCGCGGTGACGTGCCGAAAACCATTCAGTGCTACATGAAGGAA       1560
                                     ***** ** *****  * ** ************** ** ******************

(+)_BPPS_S.officinalis            acaaatgctagtgaggaggaggcggtggagcacgtgaagtttctgataagggaggcgtgg       1620
(+)_BPPS_optimized_Pseudomonas    ACCAATGCAAGCGAGGAAGAAGCCGTCGAGCATGTCAAGTTCCTCATTCGCGAAGCGTGG       1620
                                  ** ***** ** ***** ** ** ** ***** ** ***** ** **  * ** ******

(+)_BPPS_S.officinalis            aaggatatgaacacggccatagcagccggttatccgtttccggatggtatggtggcgggc       1680
(+)_BPPS_optimized_Pseudomonas    AAGGACATGAACACCGCCATCGCCGCTGGCTATCCCTTCCCAGACGGCATGGTGGCCGGT       1680
                                  ***** ******** ***** ** ** ** ***** ** ** ** ** ******** **

(+)_BPPS_S.officinalis            gcagctaatattgggcgcgtggcgcagtttatttatctccacggagatgggtttggcgtg       1740
(+)_BPPS_optimized_Pseudomonas    GCAGCCAACATCGGCCGCGTTGCGCAGTTCATTTACCTGCACGGTGATGGGTTCGGCGTG       1740
                                  ***** ** ** ** ***** ******** ***** ** ***** ******** ******

(+)_BPPS_S.officinalis            caacactcgaaaacgtacgagcatatcgccggcctactgttcgagccttatgcatga   1797
(+)_BPPS_optimized_Pseudomonas    CAGCATTCCAAGACCTATGAGCACATCGCGGGCCTGCTCTTTGAGCCCTACGCCTGA   1797
                                  ** ** ** ** ** ** ** ***** ***** ***** ** ** ***** ** ** ***
```

Gene sequence $P450_{cam}$ (*P. putida* ATCC17453, *camC*):

ATGACGACTGAAACCATACAAAGCAACGCCAATCTTGCCCCTCTGCCACCCCATGTGCCAGAGCACCTGGTAT
TCGACTTCGACATGTACAATCCGTCGAATCTGTCTGCCGGCGTGCAGGAGGCCTGGGCAGTTCTGCAAGAATC
AAACGTACCGGATCTGGTGTGGACTCGCTGCAACGGCGGACACTGGATCGCCACTCGCGGCCAACTGATCCG
TGAGGCCTATGAAGATTACCGCCACTTTTCCAGCGAGTGCCCGTTCATCCCTCGTGAAGCCGGCGAAGCCTAC
GACTTCATTCCCACCTCGATGGATCCGCCCGAGCAGCGCCAGTTTCGTGCGCTGGCCAACCAAGTGGTTGGCA
TGCCGGTGGTGGATAAGCTGGAGAACCGGATCCAGGAGCTGGCCTGCTCGCTGATCGAGAGCCTGCGCCCGC
AAGGACAGTGCAACTTCACCGAGGACTACGCCGAACCCTTCCCGATACGCATCTTCATGCTGCTCGCAGGTCT
ACCGGAAGAAGATATCCCGCACTTGAAATACCTAACGGATCAGATGACCCGTCCGGATGGCAGCATGACCTT
CGCAGAGGCCAAGGAGGCGCTCTACGACTATCTGATACCGATCATCGAGCAACGCAGGCAGAAGCCGGGAAC
CGACGCTATCAGCATCGTTGCCAACGGCCAGGTCAATGGGCGACCGATCACCAGTGACGAAGCCAAGAGGAT
GTGTGGCCTGTTACTGGTCGGCGGCCTGGATACGGTGGTCAATTTCCTCAGCTTCAGCATGGAGTTCCTGGCC
AAAAGCCCGGAGCATCGCCAGGAGCTGATCGAGCGTCCCGAGCGTATTCCAGCCGCTTGCGAGGAACTACTC
CGGCGCTTCTCGCTGGTTGCCGATGGCCGCATCCTCACCTCCGATTACGAGTTTCATGGCGTGCAACTGAAGA
AAGGTGACCAGATCCTGCTACCGCAGATGCTGTCTGGCCTGGATGAGCGCGAAAACGCCTGCCCGATGCACG
TCGACTTCAGTCGCCAAAAGGTTTCACACACCACCTTTGGCCACGGCAGCCATCTGTGCCTTGGCCAGCACCT
GGCCCGCCGGGAAATCATCGTCACCCTCAAGGAATGGCTGACCAGGATTCCTGACTTCTCCATTGCCCCGGGT
GCCCAGATTCAGCACAAGAGCGGCATCGTCAGCGGCGTGCAGGCACTCCCTCTGGTCTGGGATCCGGCGACT
ACCAAAGCGGTATAA

Gene sequence Pdr (*P. putida* ATCC17453, *camA*):

GTGAACGCAAACGACAACGTGGTCATCGTCGGTACCGGACTGGCTGGCGTTGAGGTCGCCTTCGGCCTGCGC
GCCAGCGGCTGGGAAGGCAATATCCGGTTGGTGGGGGATGCGACGGTAATTCCCCATCACCTACCACCGCTA
TCCAAAGCTTACTTGGCCGGCAAAGCCACAGCGGAAAGCCTGTACCTGAGAACCCCAGATGCCTATGCAGCG
CAGAACATCCAACTACTCGGAGGCACACAGGTAACGGCTATCAACCGCGACCGACAGCAAGTAATCCTATCG
GATGGCCGGGCACTGGATTACGACCGGCTGGTATTGGCTACCGGAGGGCGTCCAAGACCCCTACCGGTGGCC
AGTGGCGCAGTTGGAAAGGCGAACAACTTTCGATACCTGCGCACACTCGAGGACGCCGAGTGCATTCGCCGG
CAGCTGATTGCGGATAACCGTCTGGTGGTGATTGGTGGCGGCTACATTGGCCTTGAAGTGGCTGCCACCGCCA
TCAAGGCGAACATGCACGTCACCCTGCTTGATACGGCAGCCCGGGTTCTGGAGCGGGTTACCGCCCCGCCGGT
ATCGGCCTTTTACGAGCACCTACACCGCGAAGCCGGCGTTGACATACGAACCGGCACGCAGGTGTGCGGGTT
CGAGATGTCGACCGACCAACAGAAGGTTACCGCCGTCCTCTGCGAGGACGGCACAAGGCTGCCAGCGGATCT
GGTAATCGCCGGGATTGGCCTGATACCAAACTGCGAGTTGGCCAGTGCGGCCGGCCTGCAGGTTGATAACGG
CATCGTGATCAACGAACACATGCAGACCTCTGATCCCTTGATCATGGCCGTCGGCGACTGTGCCCGATTTCAC
AGTCAGCTCTATGACCGCTGGGTGCGTATCGAATCGGTGCCCAATGCCTTGGAGCAGGCACGAAAGATCGCC
GCCATCCTCTGTGGCAAGGTGCCACGCGATGAGGCGGCGCCCTGGTTCTGGTCCGATCAGTATGAGATCGGAT
TGAAGATGGTCGGACTGTCCGAAGGGTACGACCGGATCATTGTCCGCGGCTCTTTGGCGCAACCCGACTTCAG
CGTTTTCTACCTGCAGGGAGACCGGGTATTGGCGGTCGATACAGTGAACCGTCCAGTGGAGTTCAACCAGTCA
AAACAAATAATCACGGATCGTTTGCCGGTTGAACCAAACCTACTCGGTGACGAAAGCGTGCCGTTAAAGGAA
ATCATCGCCGCCGCCAAAGCTGAACTGAGTAGTGCCTGA

Gene sequence Pdx (*P. putida* ATCC17453, *camB*):

ATGTCTAAAGTAGTGTATGTGTCACATGATGGAACGCGTCGCGAACTGGATGTGGCGGATGGCGTCAGCCTGA
TGCAGGCTGCAGTCTCCAATGGTATCTACGATATTGTCGGTGATTGTGGCGGCAGCGCCAGCTGTGCCACCTG
CCATGTCTATGTGAACGAAGCGTTCACGGACAAGGTGCCCGCCGCCAACGAGCGGGAAATCGGCATGCTGGA
GTGCGTCACGGCCGAACTGAAGCCGAACAGCAGGCTCTGCTGCCAGATCATCATGACGCCCGAGCTGGATGG
CATCGTGGTCGATGTTCCCGATAGGCAATGGTAA

Gene sequence CamH (*P. putida* ATCC17453, *camH*):

ATGCGCAAGTTCAGATCCTTCGCCTTCCAGCTGACGCTGGTAACAGTCACTGTGGGCTGCGGCATGAACACCA
TACCTGCAATCGCTGAGCCTGCCGGCAGGCAACAACATCAAGTGCCCGGATTTTACCGCATGAACCTGGGTGA
GTTTGAAATCACGGCGCTCTATGACGGTTTTATCAAGCTTGATCCGGCATGGCTCAGCGGCATCAGTGCCGAC
AACATTCAGAGCCTGCTGGCAAAAATGTTCATCGATTCGAGCAAGGGCATTCAAACCGCAGTGAACGGCTAC
CTGATCAATACCGGCGAACACCTGGTGCTGGTCGATGCAGGCTCAGCTCAGTGCTTCGGTTCGACGTTGGGGG
TGATGCGCCGCAACCTAGAAGCGTCCGGTTATCAGGTAGAACAAGTGGATAGCGTGCTGCTGACCCACCTGC
ATCCGGATCATGCCTGCGGTCTGGCCAATGCCGATGGCACGCCAACCTACCCGAATGCCAGGGTCTACGTGCC
GCGCCAGGAAGCCGAATTCTGGCTGGATCAGGATATCGCCGCCATGCCGGAACCCAGCCAAGCGTTTTTCCTG
ATGGCCAGGGCAGCAGTCGCACCCTATGCGCAGGGGCGCCTGCTGCGCTATGAGCCTGACGCCGCATTGCTG
CCGGGCGTGGAAAGCGTGCCTACCTACGGGCATACACCTGGTCACTCAGCCTACCTCTTTACCTCTGGCGATG
AACGCCTGATGGTCTGGGGGGATCTGGTGCATAACCATGCCATTCAGTTCGCCCGGCCGGAAGTGGTTATCGA
GTTTGACGCAGACTCTGCGCAAGCCAGGAGCTCACGGCAGAGCATGCTGACGAATGCTGCAAAGGAGCATTT
TTGGGTAGCGGGTGCACATCTACCCTTTCCCGGGCTTGGCCGTGTTCGCGCGACGGATGGCGCCTACGCCTGG
GTACCCATTGAGTTTGGCCCAGTTGGAGACCACCCCTGA

Gene sequence 2,5-DKCMO (*P. putida* ATCC17453, *camE*$_{25\text{-}1}$):

ATGAAATGCGGATTTTTCCATACCCCATACAACTTGCCGACCCGTACCGCTCGGCAGATGTTCGACTGGTCCC
TCAAGCTGGCGCAGGTTTGTGACGAGGCCGGTTTCGCCGACTTCATGATCGGCGAGCATTCCACGCTGGCCTG
GGAAAATATCCCCTGCCCGGAAATCATCATCGGCGCCGCAGCACCGCTGACCAAGAACATCCGCTTTGCACC
GATGGCGCATTTGCTGCCTTACCACAACCCGGCTACCCTGGCGATCCAGATCGGCTGGCTGTCGCAGATTCTC
GAAGGCCGCTACTTCCTCGGCGTGGCGCCGGGTGGCCACCATACCGATGCCATCCTGCATGGCTTCGAAGGCA
TTGGCCCGCTACAGGAGCAGATGTTCGAATCCCTGGAGCTGATGGAAAAAATCTGGGCCCGCGAGCCCTTCAT
GGAGAAAGGCAAGTTCTTCCAGGCTGGCTTCCCCGGCCCGGACACCATGCCCGAGTACGATGTGGAGATCGC
CGACAACAGCCCCTGGGGCGGACGCGAGTCGATGGAAGTCGCGGTCACCGGCCTGACCAAGAATTCCTCGTC
GCTGAAGTGGGCGGGTGAGCGCAACTACAGTCCGATCTCCTTCTTCGGCGGTCACGAAGTCATGCGCTCGCAT
TACGACACCTGGGCGGCGGCTATGCAGTCGAAAGGCTTCACTCCCGAGCGTTCCCGCTTCCGTGTCACCCGTG
ACATCTTCATTGCCGACACCGATGCCGAAGCGAAGAAGCGTGCCAAGGCCAGTGGCCTGGGGAAAAGTTGGG
AGCACTATCTGTTCCCGATCTACAAGAAGTTCAATCTGTTCCCCGGCATCATCGCCGATGCCGGCCTCGACAT
CGATCCGAGCCAGGTGGACATGGATTTCCTCGCTGAGCATGTCTGGCTTTGTGGCTCGCCGGAAACGGTGAAA
GGCAAGATCGAGCGCATGATGGAGCGTAGCGGTGGCTGTGGGCAGATAGTCGTCTGCTCCCACGACAATATC
GACAACCCGGAACCTTATTTCGAATCGCTACAGCGCCTTGCCAGCGAAGTGTTACCGAAGGTTCGAATGGGCT
GA

Gene sequence OTEMO (*P. putida* ATCC17453, *camG*):

ATGAGCAATAGAGCAAAAAGTCCGGCACTGGATGCCGTAGTGATCGGTGCGGGCGTCACTGGTATCTATCAG
GCCTTTCTAATCAACCAGGCAGGAATGAAAGTCCTGGGTATAGAGGCTGGTGAGGACGTCGGCGGAACCTGG
TACTGGAACCGATATCCAGGCTGCAGGCTGGATACGGAAAGCTACGCTTACGGCTATTTCGCGCTGAAGGGC
ATCATTCCGGAATGGGAGTGGAGCGAAAATTTCGCTTCTCAACCGGAAATGCTCCGTTATGTCAATCGCGCGG
CCGACGCGATGGATGTGCGCAAGCACTATCGTTTCAACACACGCGTAACCGCAGCTAGGTATGTCGAGAACG
ATAGGCTCTGGGAAGTGACGCTGGACAATGAAGAAGTGGTCACCTGCCGCTTTCTTATCTCCGCAACCGGCCC
GCTCTCGGCCAGTCGCATGCCTGACATCAAGGGGATCGACAGCTTCAAGGGTGAATCCTTCCATTCCTCCCGC
TGGCCAACTGATGCCGAGGGGGCTCCCAAGGGGGTTGATTTCACCGGCAAGCGTGTGGGTGTGATCGGCACG
GGCGCGACCGGCGTCCAAATTATCCCAATTGCGGCGGAGACAGCCAAGGAACTCTATGTGTTCCAGCGGACG
CCGAACTGGTGCACACCACTTGGCAACTCGCCAATGAGCAAGGAGAAAATGGATTCTCTCCGCAATCGCTATC
CGACCATCCTCGAGTATGTGAAATCAACTGACACGGCCTTCCCTTATCACCGTGATCCCCGCAAAGGCACCGA
TGTATCGGAATCGGAACGTGACGCATTCTTCGAAGAACTGTATCGCCAACCGGGCTATGGCATCTGGCTGAGC
GGATTCCGCGACTTACTGCTGAACAAGGAATCGAACAAATTCCTTGCCGATTTCGTCGCGAAGAAAATCCGTC
AGCGCGTGAAGGATCCCGTTGTCGCTGAAAAACTGATTCCCAAGGATCATCCCTTCGGTGCTAAGCGCGTGCC
GATGGAAACCAATTATTACGAGACCTACAACCGCGATAACGTCCATCTGGTCGATATCCGTGAGGCACCGATT
CAGGAGGTCACGCCGGAAGGGATCAAAACGGCTGACGCAGCCTACGATCTTGATGTGATCATCTATGCCACG
GGCTTTGATGCGGTCACTGGTTCACTCGACCGGATCGACATCAGGGGCAAGGACAACGTCCGGCTGATCGATG
CCTGGGCTGAAGGCCCAAGCACTTATCTCGGCCTTCAGGCTCGGGGCTTCCCGAACTTCTTCACCCTTGTCGGC
CCGCACAACGGCTCGACCTTTTGCAACGTCGGTGTATGTGGAGGATTGCAGGCGGAGTGGGTGCTCCGAATGA
TCTCCTACATGAAGGATAACGGTTTCACCTATTCCGAACCGACCCAAGCAGCAGAGAACCGGTGGACCGAGG
AAGTCTATGCCGACTTCTCCCGCACTCTGCTTGCAGAGGCCAATGCCTGGTGGGTCAAGACCACGACCAAACC
GGATGGCTCGGTCGTGCGCCGCACGCTGGTGCATGTCAGTGGTGGACCGGAATACCGCAAGCGCTGCGAGCA
GGTCGCTTATAATAACTACAACGGATTTGAACTCGCCTAA

Gene sequence 3,6-DKCMO (*P. putida* ATCC17453, *camE36*):

```
3,6-DKCMO_Pp_reported      ATGGCAATGGAAACTGGTTTGATCTTCCACCCCTACATGCGCCCCGGTCGTAGCGCCAGG      60
3,6-DKCMO_Pp_this_work     ATGGCAATGGAAACTGGTTTGATCTTCCACCCCTACATGCGCCCCGGTCGTAGCGCCAGG      60
                           ************************************************************

3,6-DKCMO_Pp_reported      CAGACCTTTGACTGGGGTATTAAGAGTGCTGTTCAGGCGGACAGCGTTGGCATCGACTCC     120
3,6-DKCMO_Pp_this_work     CAGACCTTTGACTGGGGTATTAAGAGTGCTGTTCAGGCGGACAGCGTTGGCATCGACTCC     120
                           ************************************************************

3,6-DKCMO_Pp_reported      ATGATGATCTCCGAGCACGCCTCGCAGATCTGGGAAAACATCCCCAACCCTGAATTGCTG     180
3,6-DKCMO_Pp_this_work     ATGATGATCTCCGAGCACGCCTCGCAGATCTGGGAAAACATCCCCAACCCTGAATTGCTG     180
                           ************************************************************

3,6-DKCMO_Pp_reported      ATTGCCGCCGCTGCCTTGCAGACCAAGAACATCAAGTTCGCTCCGATGGCCCACCTGTTG     240
3,6-DKCMO_Pp_this_work     ATTGCCGCCGCTGCCTTGCAGACCAAGAACATCAAGTTCGCTCCGATGGCCCACCTGTTG     240
                           ************************************************************

3,6-DKCMO_Pp_reported      CCGCACCAGCACCCGGCCAAGCTGGCGACCATGATCGGTTGGCTGTCCCAGATCCTGGAG     300
3,6-DKCMO_Pp_this_work     CCGCACCAGCACCCGGCCAAGCTGGCGACCATGATCGGTTGGCTGTCCCAGATCCTGGAG     300
                           ************************************************************

3,6-DKCMO_Pp_reported      GGTCGTTACTTTCTCGGTATTGGTGCCGGGGCCTATCCGCAAGCGTCCTATATGCATGGC     360
3,6-DKCMO_Pp_this_work     GGTCGTTACTTTCTCGGTATTGGTGCCGGGGCCTATCCGCAAGCGTCCTATATGCATGGC     360
                           ************************************************************

3,6-DKCMO_Pp_reported      ATTCGCAATGCCGGTCAGTCGAATACCGCCACTGGTGGCGAAGAGACCAAGAACCTCAAC     420
3,6-DKCMO_Pp_this_work     ATTCGCAATGCCGGTCAGTCGAATACCGCCACTGGTGGCGAAGAGACCAAGAACCTCAAC     420
                           ************************************************************

3,6-DKCMO_Pp_reported      GACATGGTGCGCGAGTCGCTGTTCATCATGGAGAAGATCTGGAAGCGCGAACCCTTTTTC     480
3,6-DKCMO_Pp_this_work     GACATGGTGCGCGAGTCGCTGTTCATCATGGAGAAGATCTGGAAGCGCGAACCCTTTTTC     480
                           ************************************************************

3,6-DKCMO_Pp_reported      CACGAGGGCAAGTACTGGGATGCCGGCTATCCGGAAGAGTTGGAAGGGGAGGAGGGGGAC     540
3,6-DKCMO_Pp_this_work     CACGAGGGCAAGTACTGGGATGCCGGCTATCCGGAAGAGTTGGAAGGGGAGGAGGGGGAC     540
                           ************************************************************

3,6-DKCMO_Pp_reported      GAGCAGCACAAGCTGGCCGACTTCAGCCCATGGGGTGGCAAGGCGCCGGAAATCGCCGTG     600
3,6-DKCMO_Pp_this_work     GAGCAGCACAAGCTGGCCGACTTCAGCCCATGGGGTGGCAAGGCGCCGGAAATCGCCGTG     600
                           ************************************************************

3,6-DKCMO_Pp_reported      ACCGGCTTCAGCTACAATTCGCCGTCCATGCGCCTGGCGGGTGAGCGCAATTTCAAGCCA     660
3,6-DKCMO_Pp_this_work     ACCGGCTTCAGCTACAATTCGCCGTCCATGCGCCTGGCGGGTGAGCGCAATTTCAAGCCA     660
                           ************************************************************

3,6-DKCMO_Pp_reported      GTATCGATCTTCTCTGGCTTGGATGCGTTGAAAAGGCACTGGGAAGTCTATTCCGAGGCG     720
3,6-DKCMO_Pp_this_work     GTATCGATCTTCTCTGGCTTGGATGCGTTGAAAAGGCACTGGGAAGTCTATTCCGAGGCG     720
                           ************************************************************

3,6-DKCMO_Pp_reported      GCTATCGAAGCTGGCCATACGCCGGATCGTTCGCGTCATGCAGTGTCCCATACGGTGTTC     780
3,6-DKCMO_Pp_this_work     GCTATCGAAGCTGGCCATACGCCGGATCGTTCGCGTCATGCAGTGTCCCATACGGTGTTC     780
                           ************************************************************

3,6-DKCMO_Pp_reported      TGCGCAGACACCGACAAGGAAGCCAAGCGCCTGGTGATGGAAGGGCCTATCGGTTATTGC     840
3,6-DKCMO_Pp_this_work     TGCGCAGACACCGACAAGGAAGCCAAGCGCCTGGTGATGGAAGGGCCTATCGGTTATTGC     840
                           ************************************************************

3,6-DKCMO_Pp_reported      TTCGAGCGCTATCTGATTCCGATCTGGCGTCGTTTCGGCATGATGGATGGCTACGCCAAG     900
3,6-DKCMO_Pp_this_work     TTCGAGCGCTATCTGATTCCGATCTGGCGTCGTTTCGGCATGATGGATGGCTACGCCAAG     900
                           ************************************************************

3,6-DKCMO_Pp_reported      GATGCGGGGATCGATCCGGTCGATGCTGATCTCGAGTTCCTGGTCGACAACGTGTTCCTG     960
3,6-DKCMO_Pp_this_work     GATGCGGGGATCGATCCGGTCGATGCTGATCTCGAGTTCCTGGTCGACAACGTGTTCCTG     960
                           ************************************************************

3,6-DKCMO_Pp_reported      GTCGGCTCGCCGGATACCGTGACGGAGAAGATCAACGCCCTTTTCGAAGCCACAGGCGGC    1020
3,6-DKCMO_Pp_this_work     GTCGGCTCGCCGGATACCGTGACGGAGAAGATCAACGCCCTTTTCGAAGCCACAGGCGGC    1020
                           ************************************************************

3,6-DKCMO_Pp_reported      TGGGGGACGCTGCAGGTGGAGGCGCATGATTACTACGATGATCCTGCGCCTTGGTTCCAG    1080
3,6-DKCMO_Pp_this_work     TGGGGGACGCTGCAGGTGGAGGCGCATGATTACTACGATGATCCTGCGCCTTGGTTCCAG    1080
                           ************************************************************

3,6-DKCMO_Pp_reported      TCGTTGGAACTGATCTCCAAAGAGGTAGCGCCAAAGATTCTCCTGCCTAAGCGTTGA---    1137
3,6-DKCMO_Pp_this_work     TCGTTGGAACTGATCTCCAAAGAGGTAGCGCCAAAGATTCTCCTGCTAAGCGTTGAACCA    1140
                           ********************************************  *    *  *

3,6-DKCMO_Pp_reported      ---------   1137
3,6-DKCMO_Pp_this_work     CAATGGTAA   1149
```

Gene sequence Bdh (*P. putida* ATCC17453, *orf16*, *bdh*):

```
bdh_Pp_reported      ATGAAACCGCTAGCAGGTAAAAGAATCATCGTCACTGGTGGAGCACAGGGTATCGGAGCG      60
bdh_Pp_this_work     ATGAAACCGCTAGCAGGTAAAAGAATCATCGTCACTGGTGGAGCACAGGGTATCGGAGCG      60
                     ************************************************************

bdh_Pp_reported      TCAGTCGTGCGCGCCTACCTGGCCGCGGGCGCAACTGTAGTGTCAATGGACATGAACGAC      120
bdh_Pp_this_work     TCAGTCGTGCGCGCCTACCTGGCCGCGGGCGCAACTGTAGTGTCAATGGACATGAACGAC      120
                     ************************************************************

bdh_Pp_reported      AAACTGGGGCAACAGGTCGTCTCCGAGGCCATTGAGAAACACCCCGACTGCAGCGCCCGC      180
bdh_Pp_this_work     AAACTGGGGCAACAGGTCGTCTCCGAGGCCATTGAGAAACACCCCGACTGCAGCGCCCGC      180
                     ************************************************************

bdh_Pp_reported      TACTGCCATTGCGACATTACTGATCGCACTGCAGTGGAAAAGGTTTTCGCCGCGGCGACC      240
bdh_Pp_this_work     TACTGCCATTGCGACATTACTGATCGCACTGCAGTGGAAAAGGTTTTCGCCGCGGCGACC      240
                     ************************************************************

bdh_Pp_reported      TGGGACATGGGCGGCCTGGACGTCATGGTCAACGTAGCGGGTGTACAGCGCCATAGCTCT      300
bdh_Pp_this_work     TGGGACATGGGCGGCCTGGACGTCATGGTCAACGTAGCGGGTGTACAGCGCCATAGCTCT      300
                     ************************************************************

bdh_Pp_reported      CCAGACGCCATATCGGAAGATCTGTTCGACTTACTGTTCCGCGTCAACGTACTAGGCACC      360
bdh_Pp_this_work     CCAGACGCCATATCGGAAGATCTGTTCGACTTACTGTTCCGCGTCAACGTACTAGGCACC      360
                     ************************************************************

bdh_Pp_reported      ATGAACACCAACGGCGTGGCCTATTCGCTGATGAAATCCCAGGGCACAGGCAATATCATC      420
bdh_Pp_this_work     ATGAACACCAACGGCGTGGCCTATTCGCTGATGAAATCCCAGGGCACAGGCAATATCATC      420
                     ************************************************************

bdh_Pp_reported      AACTTCGGCTCCGAATCGGGCTTAACAGGCGAGATCGACAACGGCCTATATGCCGCAACC      480
bdh_Pp_this_work     AACTTCGGCTCCGAATCGGGCTTAACAGGCGAGATCGACAACGGCCTATATGCCGCAACC      480
                     ************************************************************

bdh_Pp_reported      AAGGCCGCGGTACATACCTGGACTCGCAATGTGGCTCGCCAATGGGGCCCTGACGGCATC      540
bdh_Pp_this_work     AAGGCCGCGGTACATACCTGGACTCGCAATGTGGCTCGCCAATGGGGCCCTGACGGCATC      540
                     ************************************************************

bdh_Pp_reported      CGCATCAATGCCGTTCTGCCCTACATGGTCACCCCTATGTACGTCGACTTCCGCAATGCC      600
bdh_Pp_this_work     CGCATCAATGCCGTTCTGCCCTACATGGTCACCCCTATGTACGTCGACTTCCGCAATGCC      600
                     ************************************************************

bdh_Pp_reported      CTGTCACCAGAAGCGCTTGCCTCCCATGACGCCGCCACCAAGGCCGACATACCGCTAGGC      660
bdh_Pp_this_work     CTGTCACCAGAAGCGCTTGCCTCCCATGACGCCGCCACCAAGGCCGACATACCGCTAGGC      660
                     ************************************************************

bdh_Pp_reported      GGAAAATTTGGCGATGTCGACAAGGACTTGGCACCAGTGATGGTCTTCCTCGCCAGCGAC      720
bdh_Pp_this_work     GGAAAATTTGGCGATGTCGACAAGGACTTGGCACCAGTGATGGTCTTCCTCGCCAGCGAC      720
                     ************************************************************

bdh_Pp_reported      GCCTCCCACTTCATCAGCCGGCCAGATGTTCCCGGTAGACGGTGGGCTTATTGCGGTGCG      780
bdh_Pp_this_work     GCCTCCCACTTCATCAC-CGGCCAGATGTTCCCGGTAGACGGTGGGCTTATTGCGGTGCG      779
                     ****************  *****************************************

bdh_Pp_reported      ATGAGTACGGCCCCGCCCCTGAGGAGGCAATATGTTCTTTTCAAAGGAAAAGCAAACGGC      840
bdh_Pp_this_work     ATGAGTACGGCCCCGCCCCTGAGGAGGCAATATGTTCTTTTCAAAGGAAAAGCAAACGGC      839
                     ************************************************************

bdh_Pp_reported      AATCGATTGTCTGGTTGA        858
bdh_Pp_this_work     AATCGATTGTCTGGTTGA        857
                     ******************
```

7.7 Amino acid sequences

Amino acid sequence (+)-BPPS (*S. officinalis*, *(+)-bpps*):

MSIISMNVSILSKPLNCLHNLERRPSKALLVPCTAPTARLRASCSSKLQEAHQIRRS
GNYQPALWDSNYIQSLNTPYTEERHLDRKAELIVQVRILLKEKMEPVQQLELIHD
LKYLGLSDFFQDEIKEILGVIYNEHKCFHNNEVEKMDLYFTALGFRLLRQHGFNIS
QDVFNCFKNEKGIDFKASLAQDTKGMLQLYEASFLLRKGEDTLELAREFATKCLQ
KKLDEGGNEIDENLLLWIRHSLDLPLHWRIQSVEARWFIDAYARRPDMNPLIFEL
AKLNFNIIQATHQQELKDLSRWWSRLCFPEKLPFVRDRLVESFFWAVGMFEPHQH
GYQRKMAATIIVLATVIDDIYDVYGTLDELELFTDTFKRWDTESITRLPYYMQLC
YWGVHNYISDAAYDILKEHGFFCLQYLRKSVVDLVEAYFHEAKWYHSGYTPSLD
EYLNIAKISVASPAIISPTYFTFANASHDTAVIDSLYQYHDILCLAGIILRLPDDLGT
SYFELARGDVPKTIQCYMKETNASEEEAVEHVKFLIREAWKDMNTAIAAGYPFPD
GMVAGAANIGRVAQFIYLHGDGFGVQHSKTYEHIAGLLFEPYA

Amino acid sequence $P450_{cam}$ (*P. putida* ATCC17453, *camC*):

MTTETIQSNANLAPLPPHVPEHLVFDFDMYNPSNLSAGVQEAWAVLQESNVPDLV
WTRCNGGHWIATRGQLIREAYEDYRHFSSECPFIPREAGEAYDFIPTSMDPPEQRQ
FRALANQVVGMPVVDKLENRIQELACSLIESLRPQGQCNFTEDYAEPFPIRIFMLL
AGLPEEDIPHLKYLTDQMTRPDGSMTFAEAKEALYDYLIPIIEQRRQKPGTDAISI
VANGQVNGRPITSDEAKRMCGLLLVGGLDTVVNFLSFSMEFLAKSPEHRQELIER
PERIPAACEELLRRFSLVADGRILTSDYEFHGVQLKKGDQILLPQMLSGLDERENA
CPMHVDFSRQKVSHTTFGHGSHLCLGQHLARREIIVTLKEWLTRIPDFSIAPGAQI
QHKSGIVSGVQALPLVWDPATTKAV

Amino acid sequence Pdr (*P. putida* ATCC17453, *camA*):

MNANDNVVIVGTGLAGVEVAFGLRASGWEGNIRLVGDATVIPHHLPPLSKAYLA
GKATAESLYLRTPDAYAAQNIQLLGGTQVTAINRDRQQVILSDGRALDYDRLVLA
TGGRPRPLPVASGAVGKANNFRYLRTLEDAECIRRQLIADNRLVVIGGGYIGLEV
AATAIKANMHVTLLDTAARVLERVTAPPVSAFYEHLHREAGVDIRTGTQVCGFE
MSTDQQKVTAVLCEDGTRLPADLVIAGIGLIPNCELASAAGLQVDNGIVINEHMQ
TSDPLIMAVGDCARFHSQLYDRWVRIESVPNALEQARKIAAILCGKVPRDEAAPW
FWSDQYEIGLKMVGLSEGYDRIIVRGSLAQPDFSVFYLQGDRVLAVDTVNRPVEF
NQSKQIITDRLPVEPNLLGDESVPLKEIIAAAKAELSSA

Amino acid sequence Pdx (*P. putida* ATCC17453, *camB*):

MSKVVYVSHDGTRRELDVADGVSLMQAAVSNGIYDIVGDCGGSASCATCHVYVN
EAFTDKVPAANEREIGMLECVTAELKPNSRLCCQIIMTPELDGIVVDVPDRQW

Amino acid sequence CamH (*P. putida* ATCC17453, *camH*):

MRKFRSFAFQLTLVTVTVGCGMNTIPAIAEPAGRQQHQVPGFYRMNLGEFEITAL
YDGFIKLDPAWLSGISADNIQSLLAKMFIDSSKGIQTAVNGYLINTGEHLVLVDAG
SAQCFGSTLGVMRRNLEASGYQVEQVDSVLLTHLHPDHACGLANADGTPTYPNA
RVYVPRQEAEFWLDQDIAAMPEPSQAFFLMARAAVAPYAQGRLLRYEPDAALLP
GVESVPTYGHTPGHSAYLFTSGDERLMVWGDLVHNHAIQFARPEVVIEFDADSAQ
ARSSRQSMLTNAAKEHFWVAGAHLPFPGLGRVRATDGAYAWVPIEFGPVGDHP

Amino acid sequence 2,5-DKCMO (*P. putida* ATCC17453, *camE*$_{25\text{-}1}$):

MKCGFFHTPYNLPTRTARQMFDWSLKLAQVCDEAGFADFMIGEHSTLAWENIPC
PEIIIGAAAPLTKNIRFAPMAHLLPYHNPATLAIQIGWLSQILEGRYFLGVAPGGHH
TDAILHGFEGIGPLQEQMFESLELMEKIWAREPFMEKGKFFQAGFPGPDTMPEYD
VEIADNSPWGGRESMEVAVTGLTKNSSSLKWAGERNYSPISFFGGHEVMRSHYDT
WAAAMQSKGFTPERSRFRVTRDIFIADTDAEAKKRAKASGLGKSWEHYLFPIYKK
FNLFPGIIADAGLDIDPSQVDMDFLAEHVWLCGSPETVKGKIERMMERSGGCGQI
VVCSHDNIDNPEPYFESLQRLASEVLPKVRMG

Amino acid sequence OTEMO (*P. putida* ATCC17453, *camG*):

MSNRAKSPALDAVVIGAGVTGIYQAFLINQAGMKVLGIEAGEDVGGTWYWNRYP
GCRLDTESYAYGYFALKGIIPEWEWSENFASQPEMLRYVNRAADAMDVRKHYRF
NTRVTAARYVENDRLWEVTLDNEEVVTCRFLISATGPLSASRMPDIKGIDSFKGE
SFHSSRWPTDAEGAPKGVDFTGKRVGVIGTGATGVQIIPIAAETAKELYVFQRTPN
WCTPLGNSPMSKEKMDSLRNRYPTILEYVKSTDTAFPYHRDPRKGTDVSESERDA
FFEELYRQPGYGIWLSGFRDLLLNKESNKFLADFVAKKIRQRVKDPVVAEKLIPK
DHPFGAKRVPMETNYYETYNRDNVHLVDIREAPIQEVTPEGIKTADAAYDLDVII
YATGFDAVTGSLDRIDIRGKDNVRLIDAWAEGPSTYLGLQARGFPNFFTLVGPHN
GSTFCNVGVCGGLQAEWVLRMISYMKDNGFTYSEPTQAAENRWTEEVYADFSRT
LLAEANAWWVKTTTKPDGSVVRRTLVHVSGGPEYRKRCEQVAYNNYNGFELA

Amino acid sequence 3,6-DKCMO (*P. putida* ATCC17453, *camE36*):

```
3,6-DKCMO_Pp_reported       MAMETGLIFHPYMRPGRSARQTFDWGIKSAVQADSVGIDSMMISEHASQIWENIPNPELL      60
3,6-DKCMO_Pp_this_work      MAMETGLIFHPYMRPGRSARQTFDWGIKSAVQADSVGIDSMMISEHASQIWENIPNPELL      60
                            ************************************************************

3,6-DKCMO_Pp_reported       IAAAALQTKNIKFAPMAHLLPHQHPAKLATMIGWLSQILEGRYFLGIGAGAYPQASYMHG      120
3,6-DKCMO_Pp_this_work      IAAAALQTKNIKFAPMAHLLPHQHPAKLATMIGWLSQILEGRYFLGIGAGAYPQASYMHG      120
                            ************************************************************

3,6-DKCMO_Pp_reported       IRNAGQSNTATGGEETKNLNDMVRESLFIMEKIWKREPFFHEGKYWDAGYPEELEGEEGD      180
3,6-DKCMO_Pp_this_work      IRNAGQSNTATGGEETKNLNDMVRESLFIMEKIWKREPFFHEGKYWDAGYPEELEGEEGD      180
                            ************************************************************

3,6-DKCMO_Pp_reported       EQHKLADFSPWGGKAPEIAVTGFSYNSPSMRLAGERNFKPVSIFSGLDALKRHWEVYSEA      240
3,6-DKCMO_Pp_this_work      EQHKLADFSPWGGKAPEIAVTGFSYNSPSMRLAGERNFKPVSIFSGLDALKRHWEVYSEA      240
                            ************************************************************

3,6-DKCMO_Pp_reported       AIEAGHTPDRSRHAVSHTVFCADTDKEAKRLVMEGPIGYCFERYLIPIWRRFGMMDGYAK      300
3,6-DKCMO_Pp_this_work      AIEAGHTPDRSRHAVSHTVFCADTDKEAKRLVMEGPIGYCFERYLIPIWRRFGMMDGYAK      300
                            ************************************************************

3,6-DKCMO_Pp_reported       DAGIDPVDADLEFLVDNVFLVGSPDTVTEKINALFEATGGWGTLQVEAHDYYDDPAPWFQ      360
3,6-DKCMO_Pp_this_work      DAGIDPVDADLEFLVDNVFLVGSPDTVTEKINALFEATGGWGTLQVEAHDYYDDPAPWFQ      360
                            ************************************************************

3,6-DKCMO_Pp_reported       SLELISKEVAPKILLPKR----      378
3,6-DKCMO_Pp_this_work      SLELISKEVAPKILLLSVEPQW      382
                            ***************
```

Amino acid sequence Bdh (*P. putida* ATCC17453, *orf16*, *bdh*):

```
Bdh_Pp_reported       MKPLAGKRIIVTGGAQGIGASVVRAYLAAGATVVSMDMNDKLGQQVVSEAIEKHPDCSAR      60
Bdh_Pp_this_work      MKPLAGKRIIVTGGAQGIGASVVRAYLAAGATVVSMDMNDKLGQQVVSEAIEKHPDCSAR      60
                      ************************************************************

Bdh_Pp_reported       YCHCDITDRTAVEKVFAAATWDMGGLDVMVNVAGVQRHSSPDAISEDLFDLLFRVNVLGT      120
Bdh_Pp_this_work      YCHCDITDRTAVEKVFAAATWDMGGLDVMVNVAGVQRHSSPDAISEDLFDLLFRVNVLGT      120
                      ************************************************************

Bdh_Pp_reported       MNTNGVAYSLMKSQGTGNIINFGSESGLTGEIDNGLYAATKAAVHTWTRNVARQWGPDGI      180
Bdh_Pp_this_work      MNTNGVAYSLMKSQGTGNIINFGSESGLTGEIDNGLYAATKAAVHTWTRNVARQWGPDGI      180
                      ************************************************************

Bdh_Pp_reported       RINAVLPYMVTPMYVDFRNALSPEALASHDAATKADIPLGGKFGDVDKDLAPVMVFLASD      240
Bdh_Pp_this_work      RINAVLPYMVTPMYVDFRNALSPEALASHDAATKADIPLGGKFGDVDKDLAPVMVFLASD      240
                      ************************************************************

Bdh_Pp_reported       ASHFISRPDVPGRRWAYCGAMSTAPPLRRQYVLFKGKANGNRLSG     285
Bdh_Pp_this_work      ASHFITGQMFPVDGGLI-----AVR--------------------     260
                      *****:   .*          :.
```

Abbreviation and symbols

aa	Amino acid
ABTS	2,2'-azino-bis(3-ethylbenzothiazoline-6-sulphonic acid)
Amp	Ampicillin
APS	Ammonium persulfate
BCIP	5-Bromo-4-chloro-3-indoxylphosphate
BLAST	Basic Local Alignment Search Tool
bp	Base pair
BSA	Bovine serum albumin
BVMO	Baeyer-Villiger monooxygenase
c	Concentration [mol L^{-1}]
$CaCO_3$	Calcium carbonate
$CoSO_4$	Cobalt sulfate
$CuSO_4$	Copper sulfate
CV	Column volume
d	Day
Da	Dalton
DKCMO	Diketocamphor monooxygenase
DMSO	Dimethyl sulfoxide
DTT	Dithiothreitol
E. coli	*Escherichia coli*
EDTA	Ethylenediaminetetraacetic acid
EtOH	Ethanol
FAD	Flavin adenine dinucleotide
$FeSO_4$	Iron sulfate
FMN	Flavin mononucleotide
fmol	Femto mole
Gent	Gentamycin
Gly	Glycine
h	Hour
HBO_3	Bromic acid
HCl	Hydrochloric acid

HFIP	Hexafluoro-2-propanol
IPTG	Isopropyl-*β*-D-thiogalactopyranoside
kbp	Kilo base pairs
kDa	Kilo dalton
Km	Kanamycin
KH_2PO_4	Monopotassium phosphate
LB	Lysogenic broth
m	Mass [g]
mA	Milli ampere
MeOH	Methanol
min	Minute
ms	Millisecond
$MgCl_2$	Magnesium chloride
MgO	Magnesium oxide
$MnCl_2$	Manganese chloride
$MnSO_4$	Manganese sulfate
mS cm^{-1}	Milli siemens per cm
MOPS	3-(N-morpholino)propanesulfonic acid
MTP	Multi titer plate
MWCO	Molecular Weight Cut Off
NaCl	Sodium chloride
$NAD^+/NADH/H^+$	Oxidized and reduced nicotinamide adenine dinucleotide
$NADP^+/NADPH^+$	Oxidized and reduced nicotinamide adenine dinucleotide phosphate
NaH_2PO_4	Monosodium phosphate
Na_2HPO_4	Disodium phosphate
NaOH	Sodium hydroxide
NaTFA	Sodium trifluoroacetic acid
NBT	3,3′-(3,3′-Dimethoxy-4,4′-biphenylylen)-bis-[2-(4-nitro-phenyl)-5-phenyl-2*H*-tetrazoliumchloride]
ng	Nano gram
$(NH_4)_2SO_4$	Ammonium sulfate
nm	Nano meter

OD_{600}	Optical density at 600 nm
OTEMO	(2,2,3-Trimethyl-5-oxocyclopent-3-enyl)acetyl-CoA 1,5-monooxygenase
Pdr	Putidaredoxin reductase
Pdx	Putidaredoxin
rpm	Rounds per minute
RT	Room temperature
s	Second
SDS-PAGE	Sodium dodecyl sulfate-polyacrylamide gel electrophoresis
Tet	Tetracycline
TRIS	Tris(hydroxymethyl) aminomethane
o/V	Over night
V	Volume [L]
v/v	Volume per volume
wt	Wild type
w/v	Weight per volume
$ZnSO_4$	Zinc sulfate
A	Absorbance
°C	Degree Celsius
κ	Conductivity [mS cm^{-1}]
xg	Gravitation
µL	Micro liter
µm	Micro meter

List of figures

Figure 1: Global primary plastic production (in million metric tons) according to polymer type from 1950 to 2015. PP: polypropylene; PUR: poly urethane; PET: polyethylene terephthalate; PVC: polyvinyl chloride; PS: polystyrene; HDPE: high density polyethylene; LDPE: low density polyethylene (Source: *Geyer et al.*).[2] 1

Figure 2: Classification of biopolymers and conventional polymers regarding degradability and resource. (Source: lfbb-Hannover) 3

Figure 3: Principal routes to bio-based plastics according to *Storz et al.*[6] and *Flaris et al.*.[11] 4

Figure 4: Common representatives for acyclic, monocyclic and bicyclic terpenes and terpenoids. 7

Figure 5: Biosynthesis of isopentenyl diphosphate as a precursor for terpenes via the MVA pathway. Involved enzymes are displayed in bold. Figure according to *Miziorko et al.*.[46] 8

Figure 6: Biosynthesis of IPP and DMAPP as terpene precursors via the MEP pathway. Involved enzymes are displayed in bold. Dxs: 1-deoxy-D-xylulose-5-phosphate synthase; Dxr: 1-deoxy-D-xylulose-5-phosphate reductoisomerase; IspD: 4-diphosphocytidyl-2-C-methylerythritol synthase; IspE: 4-(cytidine-5´-diphospho)-2-C-methyl-D-erythritol kinase; IspF: 2-C-methyl-D-erythritol-2,4-cyclodiphosphate synthase; IspG: 4-hydroxy-3-methyl-but-2-enyl-diphosphate synthase; IspH: 4-hydroxy-3-methylbut-2-enyl-diphosphate reductase. (Source: *Banerjee et al.*[48], *Phillips et al.*[49]) 9

Figure 7: Reaction mechanism of the monoterpene synthase AtTPS-Cin from *Arabidopsis* as an example for a multi-product TPS. Different intermediates lead to various terpene products (in dashed boxes). Figure according *to Chen et al.*.[58] 11

Figure 8: Biodegradation of (+)-camphor to isobutyryl-CoA and acetyl-CoA by the CAM plasmid of *P. putida* ATCC17453. Enzymes are displayed in bold, responsible genes in italic. Same enzymes are required for the degradation of (-)-camphor with one exception. Instead of the 2,5-DKCMO-I+II, the diketocamphane species of (-)-camphor is converted by 3,6-DKCMO (Source: *Iwaki et al.*).[79] 14

Figure 9: Different strategies to obtain terpene-based monomers for polymers by chemical modification of double bonds. A: Conversion of (+)-limonene via thiol-ene addition according to *Firdaus et al*. to obtain monomers for polyamides;[101] B: 2-Step conversion of *β*-pinene to the corresponding oxime and further conversion via Beckmann rearrangement. The resulting lactam serves as a monomer for polyamides (*Winnacker et al.*);[103] C: Ring-closing metathesis of myrcene leads to a terpene-based monomer for polymers (*Kobayashi et al.*);[104] D: Ozonolysis of *β*-pinene followed by hydrogenation with Wilkinsons's catalyst and lactonization. The resulting lactone could be a monomer for polyesters. 17

Figure 10: The prosthetic group of cysteinato-heme enzymes. The iron(III) is coordinated by four nitrogen atoms of the protoporphyrin IX and linked to the enzyme by a proximal cysteine ligand (*Meunier et al.*).[113] 20

Figure 11: Hydroxylation mechanism for P450 enzymes. The heme of the enzyme is represented by squares. In the resting state of the enzyme the sixth ligand is a water molecule (1). The water molecule is released when the substrate enters the binding pocket (2). After two electron transfers and protonation events the enzyme forms a high-valent iron-oxo intermediate also known as compound I (6), where in the last step the substrate is hydroxylated. Figure according to *Urlacher et al.*.[111] 20

Figure 12: Reaction mechanism for chemical Baeyer-Villiger oxidation. The carbonyl group of the ketone substrate is attacked by a peroxyacid and consequently the tetrahedral *Criegee* intermediate is formed. The intermediate rearranges to form the corresponding ester or lactone (*Roberts et al.*).[124] 22

Figure 13: Reaction mechanism for enzyme-catalyzed Baeyer-Villiger oxidation. The mechanism is based on the investigation of the cyclohexanone monooxygenase (CHMO) from *Acinetobacter calcoaceticus* NCIMB 9871 according to *Mihovilovic et al.*.[124] 23

Figure 14: Terpenes in the polymer industry. For example, camphor is used as an additive for the production of table tennis balls, whereas the homopolymers of isoprene, *cis*-1,4-polyisoprene is used in the automobile industry. (+)-*β*-Pinene currently represents one of the most investigated terpene for terpene-based biopolymers. A suitable polymerization technique for the industry as well as its potential application is still to be figured out. 25

Figure 15: Different strategies to obtain terpene-based monomers for novel biopolymers. (i): Recombinant expression of (+)-BPPS from *S. officinalis* and $P450_{cam}$, Pdr, Pdx from *P. putida* ATCC17453 for the *de novo* synthesis of hydroxyborneol using *P. putida* KT2440 as a host organism. (ii): Deletion of different genes on the CAM plasmid of *P. putida* ATCC17453 yield different mutant strains for the production of different terpene-based monomers. (iii): Biotransformation of (-)-borneol by recombinant expression of P450cam, Pdr and Pdx from *P. putida* ATCC17453 using *P. putida* KT2440 as a host organism. 28

Figure 16: Formation of (+)-borneol diphosphate by recombinant expression of (+)-BPPS in *P. putida* KT2440. After dephosphorylation and further modification suitable monomers for terpene-based biopolymers are obtained. 71

Figure 17: Results of the qPCR for the quantification of the copy number of the CAM plasmid. A: Amplification chromatogram. Y-axis: reaction forming units; x-axis: cycles of the PCR; green: standards in the range of $1.03 \times 10^3 – 1.03 \times 10^7$ copies in double determination; red: 0.01, 0.1 and 1 ng of sample DNA in double determination; blue: no template control in double determination. B: Standard curve for the quantification. Y-axis: c_q-value; x-axis: starting quantity in logarithmic scale; triangle: standards; X: samples. 75

Figure 18: Melt curve and melt peak analysis of the PCR products obtained by qPCR of the CAM plasmid. A: Melt curve of the PCR products. Y-axis: reaction forming units; x-axis: temperature [°C]; B: Melt peak analysis of the PCR products. Y-axis: derivative reaction forming units on temperature; x-axis: temperature [°C]; green: standards in the range of $1.03 \times 10^6 – 1.03 \times 10^8$ copies in double determination; red: 0.1, 1.0 and 10 ng of sample DNA in double determination; blue: no template control in double determination. 76

Figure 19: Biodegradation of (+)-borneol to isobutyryl-CoA and acetyl-CoA by the CAM plasmid of *P. putida* ATCC17453. *Orf16* was found to be a borneol dehydrogenase (*bdh*). Two strategies for the conversion of (-)-borneol towards 5-*exo*-hydroxyborneol were analyzed: (i) recombinant expression of $P450_{cam}$, Pdr and Pdx in *P. putida* KT2440 (red box); (ii) deletion of Orf16 (*bdh*) and FdH (*camD*) to interrupt the metabolism after hydroxylation by $P450_{cam}$, Pdr and Pdx (red cross). Enzymes are displayed in bold, responsible genes in italic. 78

Figure 20: Conversion of (-)-borneol and yield of 5-*exo*-hydroxyborneol at different temperatures after 5 h of reaction time using $P450_{cam}$ enzymes in recombinant *P. putida* KT2440 as a whole-cell catalytic system. Error bars represent standard deviation of triplicates. . 80

Figure 21: Flow chart of the biotransformation process of (-)-borneol. Biotransformation was performed in a 1.5 L air-flushed stirred tank reactor (1). After complete conversion, the product is separated from the cells by cross-flow filtration (2) and subsequently extracted with an organic solvent (3), whereas the cells were returned to the reactor and used for further biotransformations after addition of fresh media and substrate. 81

Figure 22: Substrate conversion and product formation during the biotransformation of (-)-borneol by *P. putida* KT2440 pBBr122::*camCAB* with cell recycling. Each dotted vertical line indicates the addition of fresh substrate and medium. Overall cells could be used up to four times for the conversion of (-)-borneol (Phase I - IV). Figure according to *Roth et al.*. Experiments were carried out together with Irina Funk. For conversion of 5 mM (-)-borneol see chapter 7.5. 82

Figure 23: GC-MS analysis of a mixture of (-)-borneol and (-)-*iso*-borneol in ethyl acetate. Y-axis: intensity; x-axis: retention time [min]; t_r((-)-*iso*-borneol) ~ 7.65 min; t_r((-)-borneol) ~ 7.80 min. 84

Figure 24: ^{1}H NMR chromatogram of (-)-borneol (B), (-)-*iso*-borneol (C) and a mixture of both in *d*-DMSO. Y-axis: The different ^{1}H NMR chromatograms; x-axis: Chemical shifts with reference to tetramethylsilane [ppm]. The peak for the hydroxyl group of (-)-borneol is highlighted in a green box, the one for (-)-iso-borneol in a red box. In the mixture both diastereoisomers could be separately detected. 85

Figure 25: ^{1}H NMR chromatogram of 5-*exo*-hydroxyborneol in *d*-DMSO. Y-axis: intensity; x-axis: Chemical shifts with reference to tetramethylsilane [ppm]. Above: structure of 5-*exo*-hydroxyborneol (left); the different C-atoms were numerated from 1 – 10 according to *Gunawardana et al.* (right).[157] All peaks were assigned to the corresponding H-atoms. ^{1}H NMR (400 MHz) δ 4.57 (s, 1H), 4.38 (s, 1H), 3.65 (d, *J* = 9.4 Hz, 1H), 3.61 (dd, *J* = 8.0, 3.3 Hz, 1H), 2.22 (dd, *J* = 12.9, 8.0 Hz, 1H), 2.06 (ddd, *J* = 13.3, 9.7, 5.2 Hz, 1H), 1.52 (d, *J* = 5.1 Hz, 1H), 1.15 – 1.07 (m, 1H), 1.01 (s, 3H), 0.76 (2s, overlap, 6H), 0.62 (dd, *J* = 13.2, 3.2 Hz, 1H). Two chemical shifts for the *endo*- and *exo*-hydroxyl group of 5-*exo*-hydroxyborneol were obtained at the same ratio. 86

Figure 26: SDS-PAGE analysis of *E. coli* BL21(DE3) pET28a::*orf16* expression test after 16 h of induction at 16 °C (lane 4 – 9) and after 4 h at 30 °C (lane 10 – 15). Lane 1: protein standard; lane 2: before induction, pellet; lane 3: before induction, supernatant; lane 4: 0.1 mM IPTG, pellet; lane 5: 0.1 mM IPTG, supernatant; lane 6: 0.5 mM IPTG, pellet; lane 7: 0.5 mM IPTG, supernatant; lane 8: 1.0 mM IPTG; pellet; lane 9: 1.0 mM IPTG, supernatant; lane 10: 0.1 mM IPTG, pellet; lane 11: 0.1 mM IPTG, supernatant; lane 12: 0.5 mM IPTG, pellet; lane 13: 0.5 mM IPTG, supernatant; lane 14: 1.0 mM IPTG; pellet; lane 15: 1.0 mM IPTG, supernatant. 88

Figure 27: GC-MS analysis of the conversion of (-)-borneol by *E. coli* BL21(DE) pET28a::*orf16* after 0, 1 and 2 h of incubation. Y-axis: intensity; x-axis: retention time [min]; black: after 0 h; pink: after 1 h; blue: after 2 h; brown: negative control after 0 h; green: negative control after 1 h; t_r(camphor) ~ 7.45 min; t_r((-)-borneol) ~ 7.75 min. 89

Figure 28: SDS-PAGE analysis of the purification of Orf16-N-his expressed in *E. coli* BL21(DE3) for 4 h at 30 °C using 1.0 mM IPTG. Lane 1: protein standard; lane 2: before induction, supernatant; lane 3: crude extract; lane 4: pellet; lane 5: supernatant; lane 6: flow-through; lane 7: washing step; lane 8: elution peak 1 (10 % elution buffer); lane 9: elution peak 2 (60 % elution buffer). 89

Figure 29: The equilibrium for the reduction of (-)-camphor by the Bdh could be shifted towards the borneol product side by a coupled enzyme reaction using the Fdh of *Candida boidinii* and potassium formate as a substrate. CO_2 is released as a product and could not be used for the back reaction due to its volatile nature. Enzymes are displayed in bold. 90

Figure 30: GC-MS analysis of the conversion of (-)-camphor by the purified Bdh (N-His) after 1 h, 1 d and 2 d of incubation. Y-axis: intensity; x-axis: retention time [min]; black: after 1 h; pink: after 1 d; blue: after 2 d; t_r((-)-camphor) ~ 7.45 min; t_r(isoborneol) ~ 7.65 min; t_r(borneol) ~ 7.75 min. 91

Figure 31: Phusion PCR using isolated DNA of the mutant strains *P. putida* ATCC17453 Δ*camD* (A) and *P. putida* ATCC17453 Δ*camD* Δ*bdh* (B). Size of the expected PCR products: Δ*camD* mutant ~ 3.0 kbp; Δ*camD* Δ*bdh* mutant ~ 2.4 kbp. A: Lane 1, 2, 3 and 5: different mutants of *P. putida* ATCC17453 Δ*camD*; lane 4: DNA standard; B: Lane 1 and 2: different mutants of *P. putida* ATCC17453 Δ*camD* Δ*bdh*; lane 3: DNA standard. 92

Figure 32: Growth curves of *P. putida* ATCC17453 wt, *P. putida* ATCC17453 Δ*camD* and *P. putida* ATCC17453 Δ*camD* Δ*bdh* in minimal medium using 0.5 g L^{-1} of (+)-camphor (A and B), (+)-camphor and glucose (each 0.5 g L^{-1}, C and D) or (-)-borneol (E and F) as carbon source, respectively. Y-axis: *OD*-values at 600 nm; x-axis: time [h]; black triangle: wt; grey square: Δ*camD* mutant; grey dots: Δ*camD* Δ*bdh* mutant. Error bars represent the standard deviation of triplicates. 94

Figure 33: GC-MS chromatogram using (+)-borneol as a substrate and stationary grown cells of *P. putida* ATCC17453 wt (brown), Δ*camD* mutant (pink) and Δ*camD* Δ*bdh* mutant (blue). Y-axis: intensity; x-axis: retention time [min]; t_r(camphor) ~ 7.8 min; t_r((+)-borneol) ~ 8.1 min; t_r(2,5-diketocamphane) ~ 9.8 min. 95

Figure 34: The novel terpene-based biopolymer (left) in comparison to polybutylene terephthalate (right). The amber-colored biopolymer showed a high transparency compared to the white PBT. 96

Figure 35: Differential scanning calorimetry of the terpene-based biopolymer after removal of the residual monomers. Y-axis: Heat flow [W g^{-1}]; x-axis: temperature [°C]. The second scan of the sample is shown and glass transition temperature was calculated by integration. 97

Figure 36: Biodegradation of (+)-camphor to isobutyryl-CoA and acetyl-CoA by the CAM plasmid of *P. putida* ATCC17453. Two strategies for the conversion of (+)-camphor towards 2,5-diketocamphane were analyzed: (i) recombinant expression of $P450_{cam}$, Pdr, Pdx and FdH in *P. putida* KT2440 (red box); (ii) deletion of 2,5 DKCMO-I and -II (*camE*$_{25-1}$, *camE*$_{25-2}$) to interrupt the metabolism (red cross). Enzymes are displayed in bold, corresponding genes in italic. 97

Figure 37: Phusion PCR using isolated DNA of the *P. putida* ATCC17453 wt and Δ*camE*$_{25-2}$ mutant. Size of the expected PCR products: wt ~ 3.3 kbps; Δ*camE*$_{25-2}$ mutant ~ 2.2 kbp. Lane 1 and 23: DNA standard; lane 2: wt control; lane 3 – 22: different clones for the gene knockout. 98

Figure 38: Growth curves of *P. putida* ATCC17453 wt (same data Figure 32) and *P. putida* ATCC17453 Δ*camE*$_{25-2}$ Δ*camE*$_{25-1}$ in minimal medium using 0.5 g L^{-1} of (+)-camphor (A), (+)-camphor and glucose (each 0.5 g L^{-1}, B) and (+)-borneol (C) as carbon source. Y-axis: *OD*-values at 600 nm; x-axis: time [h]; black triangle: wt; grey square: Δ*camE*$_{25-2}$ Δ*camE*$_{25-1}$ mutant; Error bars represent the standard deviation of triplicates. 99

Figure 39: Biodegradation of (+)-camphor to isobutyryl-CoA and acetyl-CoA by the CAM plasmid of *P. putida* ATCC17453. Recombinant expression of three BVMOs (2,5-DKCMO-I, 3,6-DKCMO and OTEMO) in *P. putida* KT2440 to obtain different strains for the synthesis of lactones (red boxes). Clarification if CamH is involved in the camphor degradation pathway by recombinant expression in *P. putida* KT2440 and gene deletion (red cross). Enzymes are displayed in bold, corresponding genes in italic. 100

Figure 40: SDS-PAGE analysis of *E. coli* BL21(DE3) pET28a::*camH*-N-his expression test after 4 h of induction at 30 °C (lane 4 – 9) and 37 °C (lane 10 – 15). Lane 1: negative control, 0.1 mM IPTG, pellet; lane 2: negative control, 0.1 mM IPTG, supernatant; lane 3: protein standard; lane 4: 0.1 mM IPTG, pellet; lane 5: 0.1 mM IPTG supernatant; lane 6: 0.5 mM IPTG, pellet; lane 7: 0.5 mM IPTG, supernatant; lane 8: 1.0 mM IPTG, pellet; lane 9: 1.0 mM IPTG, supernatant; lane 10: 0.1 mM IPTG, pellet; lane 11: 0.1 mM IPTG supernatant; lane 12: 0.5 mM IPTG, pellet; lane 13: 0.5 mM IPTG, supernatant; lane 14: 1.0 mM IPTG, pellet; lane 15: 1.0 mM IPTG, supernatant. 101

Figure 41: SDS-PAGE analysis of the purification of CamH-C-his expressed in *E. coli* BL21(DE3) over night at 16 °C using 0.5 mM IPTG. Lane 1: negative control pellet, lane 2: negative control supernatant; lane 3: CamH-C-his pellet; lane 4: CamH-C-his supernatant; lane 5: protein standard; lane 6: flow-through; lane 7: washing fraction; lane 8: peak 1 before buffer exchange; lane 9: peak 1 after buffer exchange; lane 10: peak 2 before buffer exchange; lane 11: peak 2 after buffer exchange. 102

Figure 42: GC-MS analysis of the conversion of camphor lactone conversion by *P. putida* KT2440 pBBr122::*camDCAB* after 0, 3 and 5 h of incubation. Y-axis: intensity; x-axis: retention time [min]; black: after 0 h; pink: after 3 h; blue: after 5 h; t_r(camphor lactone) ~ 11.75 min; t_r(5-oxo-1,2-campholide) ~ 16.10 min. 103

Figure 43: HPLC-MS analysis of the conversion of camphor lactone by *P. putida* KT2440 pBBr122::*camDCAB*. Y-axis: relative abundance; x-axis: retention time [min]; red: negative control; black: aqueous sample of the conversion; t_r([(1R)-4,5,5-trimethyl-2-oxocyclopent-3-enyl]acetate) ~ 2.91 min. 104

Figure 44: Phusion PCR using isolated DNA from the *P. putida* ATCC17453 Δ*camH* mutant strain and wt. Size of the expected PCR products: wt ~ 3.9 kbp; Δ*camH* mutant: ~ 2.9 kbp. Lane 1: wt; lane 2 and 3: mutant; lane 4: DNA standard. 105

Figure 45: Growth curves of wt *P. putida* ATCC17453 and *P. putida* ATCC17453 Δ*camH* mutant strain in minimal medium using 0.5 g L^{-1} of (+)-camphor as a single carbon source. Y-axis: *OD*-values at 600 nm; x-axis: time [h]; black triangle: wt; grey square: Δ*camH* mutant. Error bars represent the standard deviation of triplicates. 105

Figure 46: Biosynthesis of camphor in *S. officinalis* according to *Croteau et al.*.[162] 107

Figure 47: The pEMG knockout system developed for the seamless gene deletion in *P. putida* KT2440 according to *Martinez-Garcia et al.*.[73] Left side: Homologous regions down- and upstream of the target gene are fused together and cloned into the pEMG vector, which carries a kanamycin resistance gene and could not replicate in *Pseudomonas* species. This vector will integrate into the *Pseudomonas* genome or in this case the CAM plasmid while screening for kanamycin resistant clones. Integration could occur via the downstream and the upstream region Right: A second plasmid (pSW-II) codes for the I-SceI nuclease, which is under the control an inducible promotor (3-methyl benzoate). After the expression of the nuclease a double strand break is induced via two regions on the integrated pEMG vector. Consequently, the DSB induces a repair mechanism by homologous recombination whereby the wt and the desired deletion strain could be obtained. The pSW-II vector could be cured afterwards by passaging the cell culture in LB-medium without any antibiotic whereby the method could be used for repeated gene deletions. LF: left flank of the target gene (downstream); RF: right flank of the target gene (upstream); Km^R: kanamycin resistance gene; Gm^R: gentamycin resistance gene; oriR6K and oriRK2: origin of replication. 114

Figure 48: Relevant part of the biodegradation of (+)-borneol by the CAM plasmid of *P. putida* ATCC17453 for the production of 5-*exo*-hydroxyborneol. *Orf16* was found to be a borneol dehydrogenase (*bdh*). Two strategies for the conversion of (-)-borneol towards 5-*exo*-hydroxyborneol were analyzed: (i) recombinant expression of $P450_{cam}$, Pdr and Pdx in *P. putida* KT2440 (red box); (ii) deletion of Orf16 (*bdh*) and FdH (*camD*) to interrupt the metabolism after hydroxylation by $P450_{cam}$, Pdr and Pdx (red cross). Enzymes are displayed in bold, corresponding genes in italic. 115

Figure 49: Sequence alignment of Bdh_{TCU} from *Pseudomonas sp.* TCU-HL1 (Bdh_Pp_TCU-HL1), native Bdh from *P. putida* ATCC17453 (Bdh_Pp_native) and the truncated Bdh from *P. putida* ATCC17453 (Bdh_Pp_truncated) expressed in this work. The sequence of the native Bdh is based on the translation of the DNA sequence reported by NCBI (NCBI reference sequence WP_032492645.1). The conserved NAD(H) binding motif G13-X-X-X-G17-X-X-G19 and the catalytic triade for short chain dehydrogenases S144, Y157 and K161 are highlighted in black boxes. Clustal Omega was used for the sequence alignment. 117

Figure 50: Model of interplay between camphor and CamR/*camO* via two-step binding according to *Aramaki et al.*.[189] A: The dimeric CamR (R) is bound to *camO* in the absence of camphor. B: The repressor (R) is still bound to *camO* at low camphor concentrations. C: The repressor is released from *camO* at higher camphor concentration and *camR* as well as *camDCAB* are expressed. 120

Figure 51: Nucleotide sequence of the *cam* control region (A) and its cylindrical projection (B) according to *Fujita et al.*.[190] Both promotors (*camR* and *camDCAB*) are shown in boxes and transcription start sites are indicated by arrows. Thick bars covering the strands indicate the CamR binding region. Dotted lines indicate the hexanucleotides of the - 35 and -10 promotor regions. 120

Figure 52: DNA sequence of *camD* and *camC* in the wt (A) and Δ*camD* mutant (B). Both genes have their own SD sequence (SD_{camD}, SD_{camC}) upstream of the start codon ATG. By the deletion of *camD* the mRNA of *camC* consists of both SD sequences in a distance of 21 bp (B). Underlined: - 35 and - 10 region of the promoter; Bold: start and stop codons; Underlined and bold: SD sequences of *camD* and *camC*. Figure 50 A according to *Aramaki et al.*.[89] 122

Figure 53: RNA structure comparison of wt *camD* (A) and Δ*camD* or Δ*camD* Δ*bdh* mutant *camC* (B). The segments of the SD sequences in front of the start codons are shown. Wt RNA structure of *camD* was predicted by the whole *camD* sequence and the 50 bp upstream of the start codon of *camD*. RNA structure of the Δ*camD* mutant was predicted using the same 50 bp upstream of *camD* and the complete sequence after *camD* until the stop codon of *camC*. The SD_{camD} is accessible for the anti-SD region of the ribosome in the wt whereas the SD_{camD} and SD_{camC} are located within a hairpin structure in the Δ*camD* or Δ*camD* Δ*bdh* mutant, respectively. The RNA structures were predicted using the RNAstructure prediction web server (https://rna.urmca.rochester.edu). For the wt RNA 20 structures were predicted and all showed a similar structure for the region of SD_{camD}. For the Δ*camD* or Δ*camD* Δ*bdh* mutant, respectively 20 structures were predicted and 19 of the 20 showed a similar structure for the region of SD_{camD} and SD_{camC}. The different colors of the bps show their probability for their structural position within the RNA structure of the wt and the mutant (down right). 123

Figure 54: Relevant part of the biodegradation of (+)-camphor by the CAM plasmid of *P. putida* ATCC17453 for the production of 2,5-diketocamphane. Two strategies for the conversion of (+)-camphor towards 2,5-diketocamphane were analyzed: (i) recombinant expression of $P450_{cam}$, Pdr, Pdx and FdH in *P. putida* KT2440 (red box); (ii) deletion of 2,5-DKCMO-I and -II (*camE*$_{25-1}$, *camE*$_{25-2}$) to interrupt the metabolism (red cross). Enzymes are displayed in bold, corresponding genes in italic. 129

Figure 55: A: Native camphor degradation pathway in *P. putida* ATCC17453 up to the unstable (+)-5-oxo-1,2-campholide. B: Reported activity of 3,6-DKCMO and OTEMO towards (+)-camphor according to *Balke et al.*.[136] The resulting product should be a (+)-camphor lactone. C: Chemical or biological conversion using 2,5-DKCMO of (+)-camphor results in the formation of (+)-camphor lactone, which is recognized by $P450_{cam}$, Pdr, Pdx and FdeH and further converted to the unstable (+)-5-oxo-1,2-campholide (this work). D: Hypothetical (+)-camphor degradation pathway in the *P. puti*da ATCC17453 Δ*camE*$_{25-1}$ Δ*camE*$_{25-2}$ lacking both 2,5-DKCMOs. (+)-camphor is converted into (+)-camphor lactone by either 3,6-DKCMO or OTEMO. The resulting lactone could serve as a substrate for $P450_{cam}$, Pdr, Pdx and FdeH producing the unstable (+)-5-oxo-1,2-campholide which could be further metabolized. Enzymes are displayed in bold. 131

Figure 56: Relevant part of the biodegradation of (+)-camphor by the CAM plasmid of *P. putida* ATCC17453 for the production of lactones. Recombinant expression of three BVMOs (2,5-DKCMO-I, 3,6-DKCMO and OTEMO) in *P. putida* KT2440 to obtain different strains for the synthesis of lactones (red boxes). Clarification if CamH is involved in the camphor degradation pathway by recombinant expression in *P. putida* KT2440 and gene deletion (red cross). Enzymes are displayed in bold, corresponding genes in italic. 132

Figure 57: Elimination of the unstable 5-oxo-1,2-campholide and formation of [(1R)-4,5,5-trimethyl-2-oxocyclopent-3-enyl]acetate as a product. 134

Figure 58: Proposed participation of CamH in the cleavage of the OTEMO (*camG*) product [(2R)-3,4,4-trimethyl-6-oxo-3,6-dihydro-1H-pyran-2-yl]acetyl-CoA. Figure according to *Iwaki et al.*.[79] 134

Figure 59: Different substrates analyzed by *Rehberger et al.* for the conversion by *P. putida* KT2440 harboring the different BVMOs (2,5-DKCMO-I, 3,6-DKCMO, OTEMO).[159] A: camphor derived structures; B: other terpene-based structures; C: other ketones. 135

Figure 60: ^{13}C NMR chromatogram of 5-*exo*-hydroxyborneol in *d*-DMSO. Y-axis: intensity; x-axis: Chemical shifts with reference to tetramethylsilane [ppm]. All peaks were assigned to the corresponding H-atoms. ^{13}C NMR (101 MHz,) δ 73.7, 73.5, 52.3, 49.7, 46.9, 38.4, 35.9, 21.2, 19.7, 13.0. 151

Figure 61: Calibration curve for GPC analysis using the ReadyCal-Kit Poly(methyl methacrylate) low from PSS. Y-axis: molecular weight [Da]; x-axis: elution volume [mL]. 152

Figure 62: Calibration curve for the glucose assay. Y-axis: $A_{418\,nm} - A_{470\,nm}$; x-axis: concentration [mg L^{-1}]. Standards were analyzed in triplicates. 153

Figure 63: Amount of glucose during the cultivation of *P. putida* ATCC17453 wt (black triangle), Δ*camD* mutant (black diamond), Δ*camD* Δ*bdh* mutant (black dot) and Δ*camE*$_{25-1}$ Δ*camE*$_{25-2}$. Y-axis: glucose concentration [g L^{-1}]; x-axis: *t* [h]. Samples were analyzed in triplicates. 153

Figure 64: HPLC chromatogram for the conversion of (+)-camphor lactone by *P. putida* KT2440 pBBr122::*camDCAB* at 30 °C and 135 rpm after 4 h (A, red) and 0 h (B, blue). The abnormal (+)-camphor lactone was opened and used as a reference (C, green). Y-axis: relative intensity; x-axis: time [min]. 154

Figure 65: MS spectrum of the signal obtained at 2.91 min retention time for the conversion of (+)-camphor lactone by *P. putida* KT2440 pBBr122::*camDCAB* at 30 °C and 135 rpm after 4 h (A) and 0 h (B). The abnormal (+)-camphor lactone was opened and used as a reference (C). Y-axis: relative abundance; x-axis: m/z. 155

Figure 66: Substrate conversion and product formation during the biotransformation of (-)-borneol by *P. putida* KT2440 pBBr122::*camCAB* with cell recycling. Each dotted vertical line indicates the addition of fresh substrate and medium. Overall cells could be used up to four times for the conversion of (-)-borneol (Phase I - IV). 156

List of tables

Table 1: Classification of terpenes according to the number of isoprene units.[27, 36] 6
Table 2: List of the chemicals used within this work and their supplier. 29
Table 3: List of the enzymes used within this work and their supplier. 33
Table 4: Composition of the different media. 34
Table 5: Composition of buffers, staining solutions and antibiotics. 35
Table 6: Different microorganisms used in this work. 38
Table 7: Constructed plasmids used in this work. 38
Table 8: Oligonucleotides used for the cloning of (+)-BPPS. Sequences are listed in 5'-3' direction. 40
Table 9: Oligonucleotides used for the cloning of 2,5-DKCMO-I, 3,6 DKCMO, OTEMO, CamH and Bdh. Sequences are listed in 5'-3' direction. 41
Table 10: Oligonucleotides used for the knockout of *camD*, *camH*, *bdh*, $camE_{25\text{-}1}$ and $camE_{25\text{-}2}$. Sequences are listed in 5'-3' direction. 42
Table 11: Oligonucleotides used for the quantification of the CAM plasmid. Sequences are listed in 5'-3' direction. 43
Table 12: Setup for the transformation by electroporation of *P. putida* KT2440, *E. coli* DH10B and *E. coli* BL21(DE3) respectively. 51
Table 13: Composition and program for the PCR reaction using the phusion HF polymerase. 52
Table 14: Composition and program for the PCR reaction using the Taq polymerase. 53
Table 15: Composition and program for the qPCR reaction using the Q5 HF polymerase. 53
Table 16: Composition of a Gibson Assembly. 54
Table 17: Composition of the separating and stacking gel for SDS-PAGE analysis for two gels. 61
Table 18: Composition of the master mix for the glucose oxidase assay. 62
Table 19: Screening for suitable PCR conditions targeting the CAM plasmid of *P. putida* ATCC17453. For standard protocol see chapter 2.2.2.6. The results for the confirmation of the successful knockout of *camD* and $camE_{25\text{-}1}$ together with the wt control are shown exemplarily. 74
Table 20: The copy number of the CAM plasmid per cell was calculated based on the qPCR results. The quantity per mL was calculated based on the amount of the sample DNA and the starting quantity. Referred to the cells per mL the quantity per cell and the mean quantity per cell were calculated. 77
Table 21: (-)-Borneol substrate consumption and 5-*exo*-hydroxyborneol product formation depending on different buffer systems and pH values after 6 h at 30 °C. Selectivity is calculated based on conversion and yield. 79
Table 22: Parameters obtained during the biotransformation of (-)-borneol by *P. putida* KT2440 pBBr122::*camCAB*. *STY*s refer to wet biomass, for calculation see experimental section. Table according to *Roth et al.*. Experiments were carried out together with Irina Funk. For conversion of 5 mM (-)-borneol see chapter 7.5. 83
Table 23: List of CamH structurally related enzymes by screening via the SWISS-MODEL database. Hits are listed according to their GMQE value. 133
Table 24: Calculated molecular weight of the polymer samples of the polymerization of 5-*ex*o-hydroxyborneol and succinic acid dimethyl ester based on the results of the calibration curve. 152
Table 25: Parameters obtained during the biotransformation of (-)-borneol by *P. putida* KT2440 pBBr122::*camCAB*. *STY*s refer to wet biomass, for calculation see experimental section. 156